Investigations on Maximum Power Point Tracking Techniques for Solar Photovoltaic Systems under Partially Shaded Conditions

Submitted in partial fulfillment of the requirements
for the award of the degree of

Doctor of Philosophy

By
Dileep Krishna Mathi
(Roll No. 717113)

Supervisor
Dr. Ramulu Chinthamalla
Assistant Professor

Department of Electrical Engineering
National Institute of Technology
Warangal

March - 2021

Dedicated to

My beloved parents **M. Venkata Satyanarayana & M.Lakshmi Annapoornamma**

and to my wife **M. Jaya Naga Lakshmi**

and to my daughters **M. Hanshitha & M. Punarvita**

APPROVAL SHEET

This thesis entitled **"Investigations on Maximum Power Point Tracking Techniques for Solar Photovoltaic Systems under Partially Shaded Conditions"** by **Dileep Krishna Mathi** is approved for the degree of Doctor of Philosophy.

Examiners

.....

.....

.....

Supervisor

Dr. Ramulu Chinthamalla

Assistant Professor,

Department of Electrical Engineering, NIT Warangal.

Chairman

Dr. M. Sailaja Kumari

Professor & Head,

Department of Electrical Engineering, NIT Warangal.

Date:.....

Department of Electrical Engineering
National Institute of Technology Warangal
Warangal - 506004, Telangana State, India.

DEPARTMENT OF ELECTRICAL ENGINEERING

NATIONAL INSTITUTE OF TECHNOLOGY WARANGAL

WARANGAL-506004

CERTIFICATE

This is to certify that the thesis entitled **"Investigations on Maximum Power Point Tracking Techniques for Solar Photovoltaic Systems under Partially Shaded Conditions"**, which is being submitted by **Mr. Dileep Krishna Mathi** (Roll No: 717113), is a bonafide work submitted to National Institute of Technology Warangal in partial fulfillment of the requirements for the award of the degree of **Doctor of Philosophy** in Department of Electrical Engineering. To the best of my knowledge, the work incorporated in this thesis has not been submitted elsewhere for the award of any degree.

Date:
Place: NIT-Warangal

Dr. Ramulu Chinthamalla
(Supervisor)
Assistant Professor
Department of Electrical Engineering
National Institute of Technology Warangal
Warangal - 506004

DECLARATION

This is to certify that the work presented in the thesis entitled **"Investigations on Maximum Power Point Tracking Techniques for Solar Photovoltaic Systems under Partially Shaded Conditions"** is bonafide work done by me under the supervision of **Dr. Ramulu Chinthamalla**, Assistant Professor, Department of Electrical Engineering, National Institute of Technology, Warangal, India and was not submitted elsewhere for the award of any degree.

I declare that this written submission represents my ideas in my own words and where others ideas or words have been included, I have adequately cited and referenced the original sources. I also declare that I have adhered to all principles of academic honesty and integrity and have not misrepresented or fabricated or falsified any idea/date/fact/source in my submission. I understand that any violation of the above will be cause for disciplinary action by the institute and can also evoke penal action from the sources which have thus not been properly cited or from whom proper permission has not been taken when needed.

Date:
Place: NIT-Warangal

Dileep Krishna Mathi
(Roll no: 717113)

ACKNOWLEDGMENTS

It gives me immense pleasure to express my deep sense of gratitude and thanks to my supervisor **Dr. Ramulu Chinthamalla**, Assistant Professor, Department of Electrical Engineering, National Institute of Technology Warangal, for his invaluable guidance, support, and suggestions. His knowledge, suggestions, and discussions helped me to become a capable researcher. He has shown me the imaginative side of this wonderful and potential research area. His encouragement helped me to overcome the difficulties encountered in research as well in my life.

I am very much thankful to **Prof. M. Sailaja Kumari,** Head, Department of Electrical Engineering, for her constant encouragement, support, and cooperation.

I take this opportunity to thank all my Doctoral Scrutiny Committee members, **Dr. S. Srinivasa Rao,** Professor, Department of Electrical Engineering, **Dr. D. Swathi,** Assistant Professor, Department of Electrical Engineering, and **Dr. P. Venkata Subba Reddy,** Assistant Professor, Department of Computer Science, for their detailed review, constructive suggestions, and excellent advice during the progress of this research work. I would like to thank **Dr. M. Raja Viswanathan,** Assistant Professor, Department of Humanities & Social Science, for their valuable suggestions, support, and cooperation.

I also appreciate the encouragement from teaching and non-teaching members of the Department of Electrical Engineering of NIT Warangal. They have always been encouraging and supportive.

I wish to express my sincere thanks to **Prof. N. V. Ramana Rao,** Director, NIT Warangal, for his support and encouragement.

I convey my special thanks to contemporary Research Scholars Dr. K. Ramsha, Dr. Venu, Dr. Phanendra Babu N V, Dr. L. Suresh, Dr. Harish, Mr. K. Hemasundara Rao, Mr. Bhaskar, Mr. K. Chinna, Mr. Madhu, Mr. P. Hema Kumar, Mr. Kusma Eshwar, Dr. K. M. Ravi Eswar, Mr. Ramesh Babu, Mr. Narendra Reddy, and Mr. Rambabu for being with me during my research journey.

I acknowledge my gratitude to all my teachers and colleagues at various places to support

and cooperate with me to complete the work. I gratefully acknowledge my best friend, **Mr. M. Ravi Shankar** for continuous support and encouragement throughout my life.

I express my deep sense of gratitude and reverence to my beloved parents **Shri. M. Venkata Satyanarayana** & **Smt. M. Lakshmi Annapoornamma**, my wife **M. Jaya Naga Lakshmi,** and her parents **Shri. N. Surya Prakasa Rao** & **Smt. N. Durga**, my daughters **M. Hanshitha and M. Punarvita**, grandfather **M. Nanchariaha**, maternal grandmother **P. Allivalu Mangamma**, and my well-wisher **K. Kavitha** for their sincere prayers, blessings, constant encouragement, shouldering the responsibilities, and moral support rendered to me throughout my life, without which my research work would not have been possible. I heartily acknowledge all my relatives and friends for their love and affection towards me.

Above all, I express my deepest regards and gratitude to "ALMIGHTY," whose divine light and warmth showered upon me the perseverance, inspiration, faith, and enough strength to keep the momentum of work high even at tough moments of research work.

Dileep Krishna Mathi

ABSTRACT

The abundant solar energy is an alternative to fossil fuels to produce green and clean electricity for high energy demands. The popularity of solar energy is limited by its high initial costs and lower conversion efficiency of photovoltaic (PV) modules. The PV system's maximum energy yield at any atmospheric conditions is essential to get back the high initial costs. For this purpose, several maximum power point tracking (MPPT) techniques are widely used. The output of PV panels is adversely affected due to atmospheric conditions like partially shaded conditions (PSC), and even these can physically damage the PV cell. Hence, to protect the PV panels from damage, the traditional method is connecting a bypass diode across the group of cells. But, this leads to multi-peak power versus voltage (P-V) curve, which becomes difficult to track the maximum power point (MPP) with conventional MPPT techniques. Hence, advanced optimization techniques are used to find the optimum value on the multi-peak P-V curve under PSC. However, these techniques fail to track GMPP due to improper algorithm design, which leads to high energy losses. In this thesis, MPPT techniques for PV systems under PSC are investigated, and new control strategies are proposed for efficient MPPT tracking. In this thesis, new fast-tracking global maximum power point tracking (GMPPT) techniques; enhanced leader adaptive velocity PSO (ELAVPSO), and adaptive butterfly PSO (ABF-PSO) are investigated for a PV string under partially shaded conditions. The proposed ELAVPSO GMPPT technique has the advantages of two PSO techniques: leader PSO (LPSO) and adaptive velocity PSO (AVPSO). The proposed ELAVPSO GMPPT technique overcomes conventional PSO limitations such as premature convergence and difficulty in parameter tuning. To reduce the power oscillations in PSO-based GMPPT technique and to improve the tracking speed, first GP region is easily identified with adaptive sensitivity parameter of the ABF-PSO algorithm and in the region identified, GMPP tracking is continued with P&O algorithm with variable length perturbations to avoid the unnecessary exploration of search space even after reaching GP region.

The PSO-based GMPPT technique's performance largely depends on the three control parameters, which are more complex to tune. A bio-inspired salp swarm algorithm (SSA) based soft computing technique is easy to implement with a single control parameter dependent

on maximum iteration count. Wrongly estimated maximum iteration count may results in the unnecessary exploration of search space even after reaching the GP region, which is the main cause for the slow-tracking of GMPP by conventional SSA. Hence, in this thesis, modified SSA-based MPPT techniques are investigated with an adaptive control parameter. Further, to achieve faster tracking of GMPP, adaptive SSA (ASSA) is used only to identify the GP region, and in that region, variable step size P&O continues tracking. To improve the accuracy of ASSA, a new hybrid GMPPT technique is proposed with the integration of SSA, differential evolution (DE), and P&O algorithms. Direct duty ratio calculation is adapted without reinitializing the GP region identification stage during load changes in an off-grid PV system. The robustness of the proposed method is tested with complex shading conditions and load variations.

Efficient hybrid tracking technology for both stand-alone and grid-connected PV systems found in the literature uses conventional P&O-based MPPT technique under uniform irradiance conditions and soft computing (SC) technique under PSC. Hence, to get the optimal performance, a simple, fast, and accurate shade detection scheme is proposed in this thesis using a curve scan with a new steady output P&O (SO-P&O). Further, the proposed curve scan can find the active power limit required for implementing flexible power point tracking (FPPT) in an on-grid PV system. A novel hybrid GMPPT technique is proposed by combining the best features of self-adaptive SSA and DE, which helps in faster convergence and exact GMPP Tracking. Hence, this work's main contributions, shade and active power limit detection, adaptive FPPT, self-adaptive SSA-DE, and SO-P&O are combined to get a faster and efficient hybrid tracking technique in an on-grid PV system. The proposed MPPT techniques are validated with simulation models and hardware prototypes developed. Finally, the simulation and experimentally obtained results to support the analysis are provided in this thesis.

Contents

List of Figures

List of Tables

Abbreviations & Symbols

ADC	Analog to digital converter
AI	Artificial intelligence
ASSA	Adaptive salp swarm algorithm
AVPSO	Adaptive velocity PSO
BF-PSO	Butterfly PSO
DE	Differential evolution
ELAVPSO	Enhanced leader adaptive velocity PSO
ELPSO	Enhanced leader PSO
FPPT	Flexible power point tracking
GMPP	Global maximum power point
GMPPT	Global maximum power point tracking
GP	Global peak
GWO	Grey wolf optimization
INC	Incremental conductance
LMPP	Local maximum power point
MPP	Maximum power point
MPPT	Maximum power point tracking
MSSA	Memetic salp swarm algorithm

PSC	Partially shaded conditions
PSO	Particle swarm optimization
PV	Photovoltaic
P&O	Perturb and observe
SC	Soft computing
SI	Swarm intelligence
SO-P&O	Steady output P&O
SSA	Salp swarm algorithm
UIC	Uniform irradiance conditions
VS-P&O	Variable step P&O
WO	Whale optimization
α_k	Time-varying probability coefficient
Δd^k	Duty ratio perturbation
$\Delta d_{critical}$	Critical value of duty ratio perturbation
η_{static}	Static MPPT efficiency
ρ	Crossover probability
σ^2	Variance
ξ	Scale factor of mutation
a	Diode ideality factor
c_1	Cognitive factor
c_2	Social factor

C_{in}	Input buffer capacitance
C_{out}	Output capacitance
d	Duty ratio
$D_i^{'}(G)$	Child vector
d_j^k	Duty ratio after perturbation
d_j^{k-1}	Duty ratio before perturbation
$D_{i1}(G)$	Target or parent vectors
dP	Difference in power
dV	Difference in voltage
F	Food source
f_s	Switching Frequency
$fitness(gbest_k)$	Fitness of global best in the k^{th} iteration
$fitness(lbest_k)$	Fitness of local best in the k^{th} iteration
h	Standard deviation
i	Particle number
I_0	Diode saturation current
I_{mp}	Current at maximum Power
I_{ph}	Photo-current
I_{pv}	Panel current
I_{sc}	Short-circuit current
ITR_k	k^{th} iteration count

ITR_{max}	Maximum iteration count
k	Present iteration
L	Inductance
l	Current iteration number
lb	Lower bound of search space
M	Multiplying factor
N_s	Number of cells in series
o	Mean of all particles in the present iteration
p_k	Probability of k^{th} iteration
P_{mp}	Maximum power
r_1	Random number
r_2	Random number
R_s	Series resistance
R_{in}	PV input resistance
R_{load}	Load resistance
R_{mp}	PV resistance at MPP
R_{sh}	Shunt resistance
$randc_i$	Cauchy distribution
$randn_i$	Normal distribution
s	Scaling parameter
S_f	Scaling factor

s_k	Sensitivity of k^{th} iteration
$U_i(G)$	Trial vector
ub	Upper bound of search space
V_T	Diode thermal voltage
V_{mp}	Voltage at maximum Power
V_{oc}	Open-circuit voltage
V_{pv}	Panel terminal voltage
vel_{max}	Maximum velocity
w	Weight factor
X^1	Position of the first salp
X^i	Position of follower salps
X_{g1}	Global best after Gaussian mutation
X_{g2}	Global best after Cauchy mutation
X_{g3}	Global best after Scaling mutation
X_{gb}	Global best
X_{lb_i}	Local best of i^{th} particle
X_{max}	Maximum value of control variable
X_{min}	Minimum value of control variable

Chapter 1

Introduction

Chapter 1

Introduction

1.1 General

In recent years, the electrical energy demand has sharply increased due to the urban and industrialization in most countries. International energy agency's (IEA) annual energy outlook 2018 has predicted significant shifts in the energy demand throughout the world and demand growing faster in developing countries. Nowadays, increasing concern about global warming and the depletion of fossil fuels increases the use of renewable energy sources. Hence, to meet this increase in demand use of renewable energy sources is vital. Renewable energy perspectives in specific about India, which is a 5^{th} leading renewable energy player, are as follows: To meet the energy demands of the country with an already installed renewable power capacity of 78 GW, India targets 175 GW of energy through renewable sources by the year 2022 and 275 GW by 2027. Because of abundant solar energy in the form of direct normal irradiance, most of the regions of the country receiving energy, which ranges 4-7 KWh/sq.mt/day [1, 2]. Hence, solar energy becomes the major renewable energy source in this country, helping in sustainable development and combating climate change.

The main reasons for the popularity of solar energy among other renewable energy sources are plenty of free and abundant solar energy. Converting it to electrical energy with photovoltaic (PV) panels is simple and leads to the absence of moving or rotating parts [3, 4] as shown in Figure 1.1. It is possible to generate power from solar energy in remote areas where the expansion of the grid is not feasible. PV systems are most popular for converting solar energy into electrical energy using PV panels/modules [5]. PV systems are classified as grid-connected and stand-alone PV systems based on the connected load.

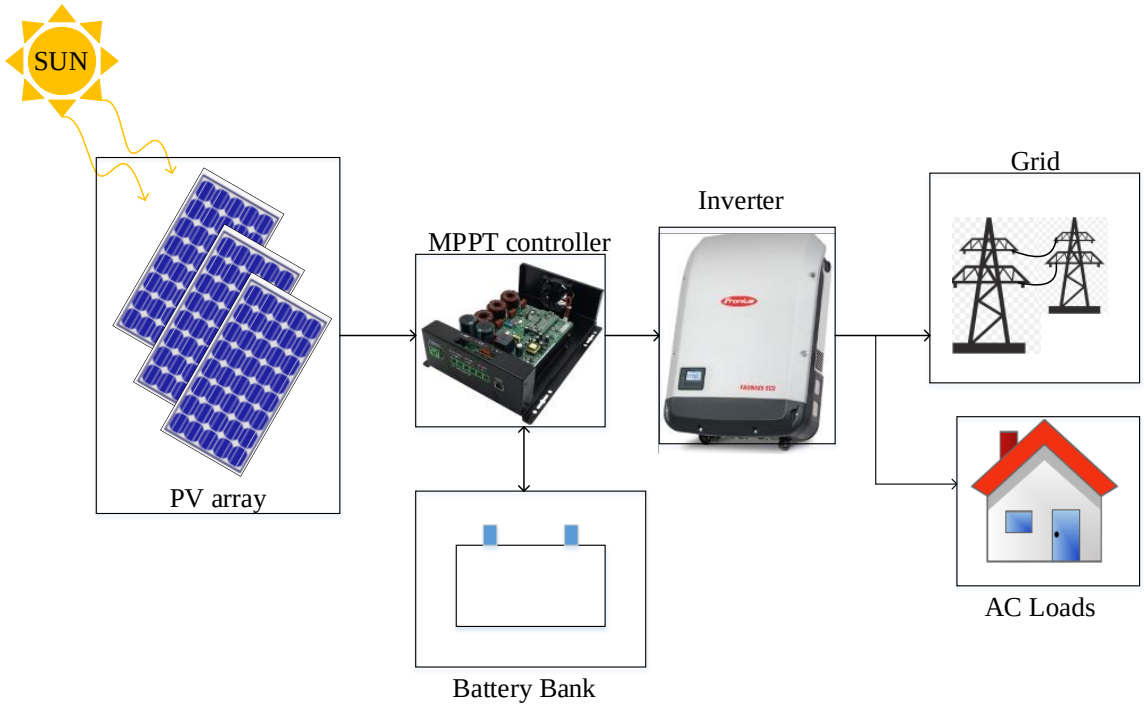

Figure 1.1: Block diagram of a PV system.

1.2 Model description of PV source

PV panels/modules are used to convert photon energy into electrical energy. PV cell is the basic building block of PV panel/ module. The PV module's mathematical model is given by (1.1), and each cell in the module can be represented with a single diode electrical equivalent circuit as shown in Figure 1.2 [6].

$$I_{pv} = I_{ph} - I_0 \times \left(e^{\left(\frac{V_{pv} + I_{pv} \times R_s}{N_s * a * V_T} \right)} - 1 \right) - \frac{V_{pv} + I_{pv} \times R_s}{R_{sh}} \tag{1.1}$$

where I_{pv} is the panel current, I_{ph} is the photo-current, I_0 is the diode saturation current, V_{pv} is the panel terminal voltage, R_s is the series resistance, N_s is the number of cells in series, a is the diode ideality factor, V_T is the diode thermal voltage, and R_{sh} is the shunt resistance.

Based on the system's voltage requirement, several modules are connected in a series arrangement known as a string. Several strings are connected in parallel to get the required power output from the PV system, making the PV array as shown in Figure 1.3. For example, a 300 W PV system can be formed with 50 W solar panels manufactured by solar power mart

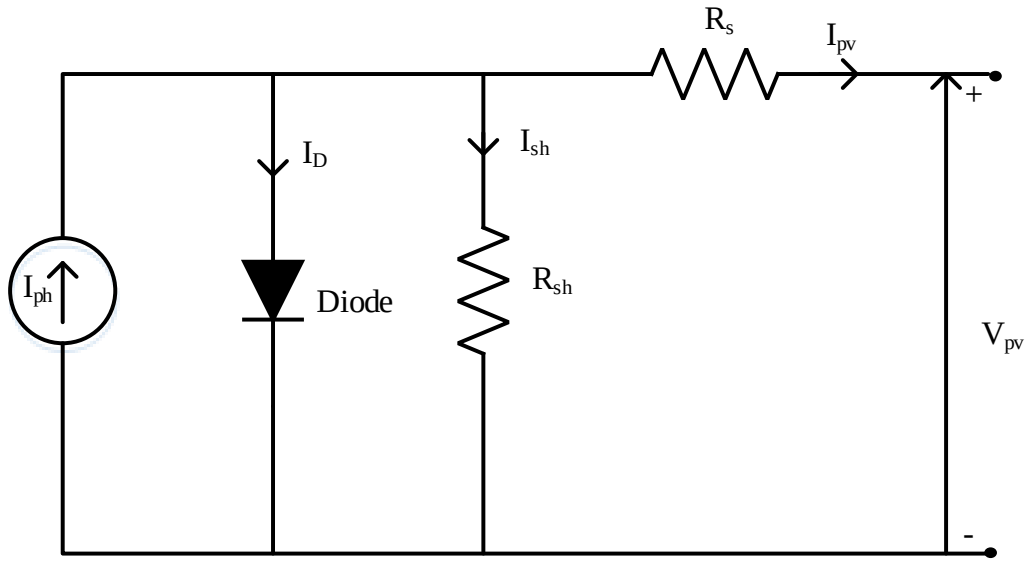

Figure 1.2: Electrical equivalent circuit diagram of PV panel by using single diode model.

SPM-50M model. Its electrical characteristics are given in Table 1.1, with six panels connected in either six series one parallel (6S-1P long String) or two 3-panel strings connected in parallel (3S-2P short string) as shown in Figure 1.4. To get the higher voltage level at the PV terminals number of modules in the series string is more. The electrical equivalent circuit parameters of the given solar panels are extracted using an analytical method proposed in [7] and values obtained are series resistance $R_s = 0.24\ \Omega$, shunt resistance $R_{sh} = 613.6\ \Omega$ and diode saturation current $I_0 = 8.46 \times 10^{-10}\ A$.

The popularity of the PV systems is limited by the intermittent nature of PV source during low insolation periods, i.e., during nights or under partially shaded conditions (PSC) and nonlinear current versus voltage (I-V) characteristics which leads to the single maximum power point (MPP) where optimum power can be extracted. Other drawbacks of PV systems are the high initial cost and low conversion efficiency of the solar panels [8]. It is imperative to extract the maximum possible power from the PV system under varying atmospheric conditions to get the profit or the high initial cost of the PV system. These atmospheric conditions are classified as uniform and nonuniform based on the irradiance at each panel of the PV array, as shown in Figure 1.5

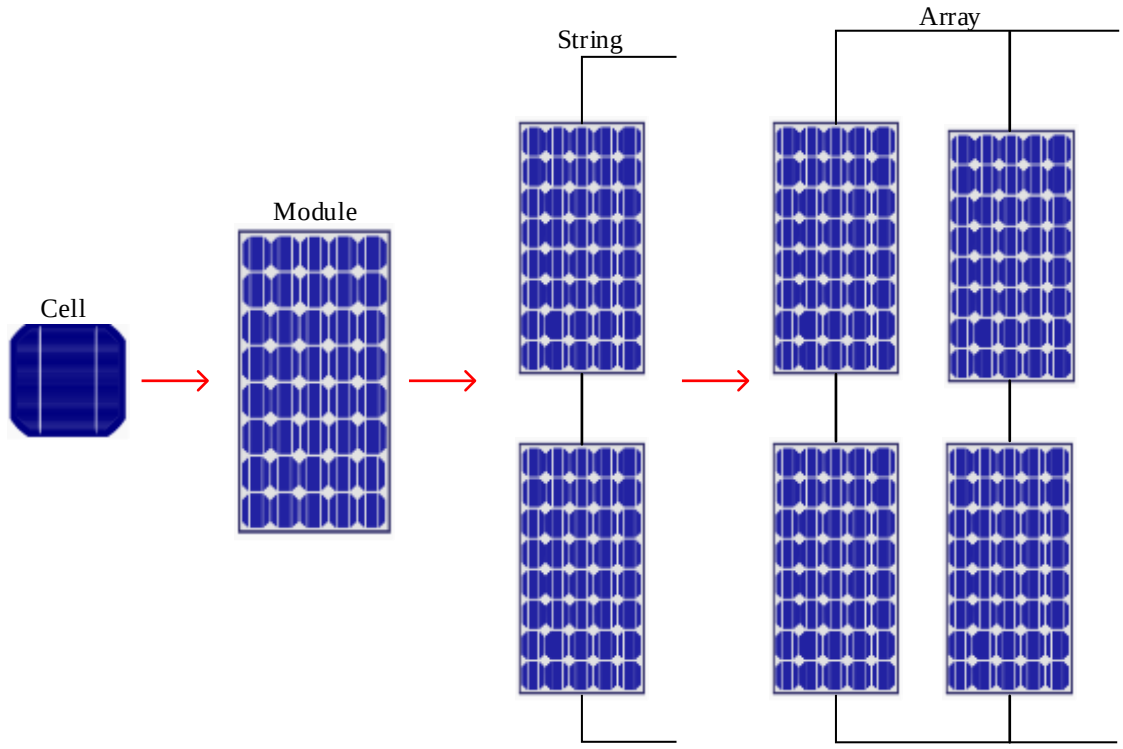

Figure 1.3: PV cell to array configuration.

Table 1.1: Electrical characteristics of solar power mart SPM-050M model 50 WP PV panel at standard test conditions AM 1.5.

S.NO	Parameter	Value
1	Maximum Power P_{mp}(W)	50
2	Voltage at Maximum Power V_{mp} (V)	18.68
3	Current at Maximum Power I_{mp} (A)	2.68
4	Open-Circuit Voltage V_{oc} (V)	22.32
5	Short-Circuit Current I_{sc} (A)	2.86
6	Temperature Coefficient of P_{mp} $(\%^{\circ}C)$	-0.45 ± 0.05

1.3 Partial shading and its effects

The PV modules of string may receive different irradiances due to the shade of buildings, trees, clouds, ice formation, bird droppings, and dust formation, as shown in Figure 1.6, which

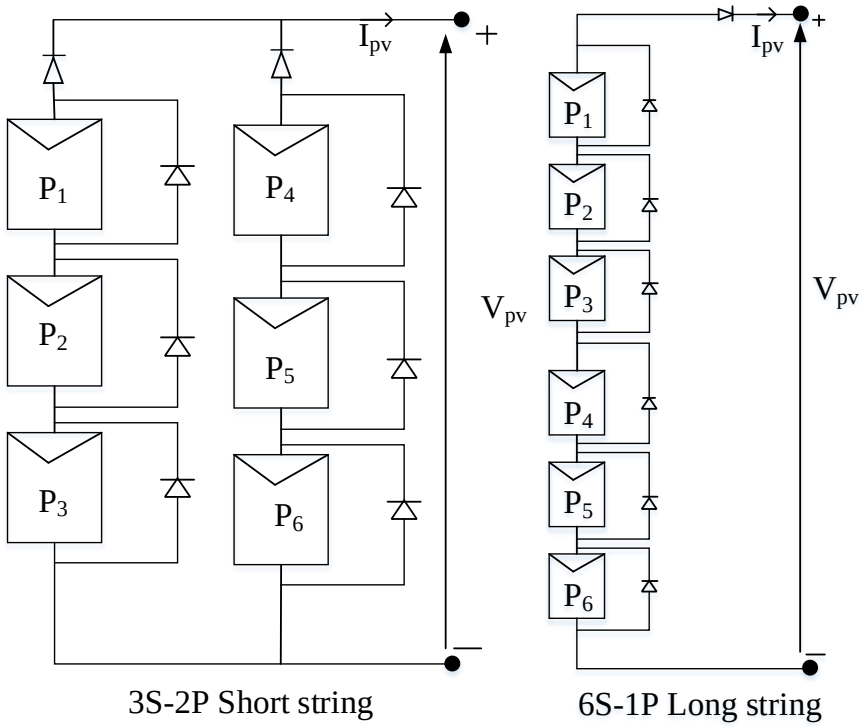

Figure 1.4: SPM-50M model PV panels P1-P6 connected in string arrangement.

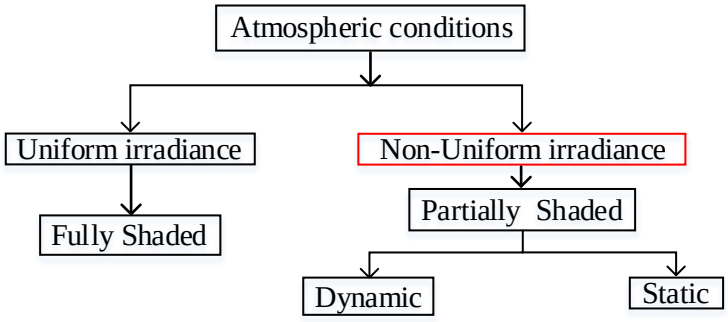

Figure 1.5: Classification of atmospheric conditions across PV system based on irradiance.

is treated as a shading condition. The photocurrent generated in the shaded cell is reduced by 20% of un-shaded cells. Hence, under PSC, shaded modules affect the string's total power, and power loss due to shading is as high as 40% [6]. Since the I-V curve of the shaded cell is extended to the negative voltage region to operate at a higher current level of an unshaded cell in the module, these cells dissipate power and are damaged permanently due to hot-spots.

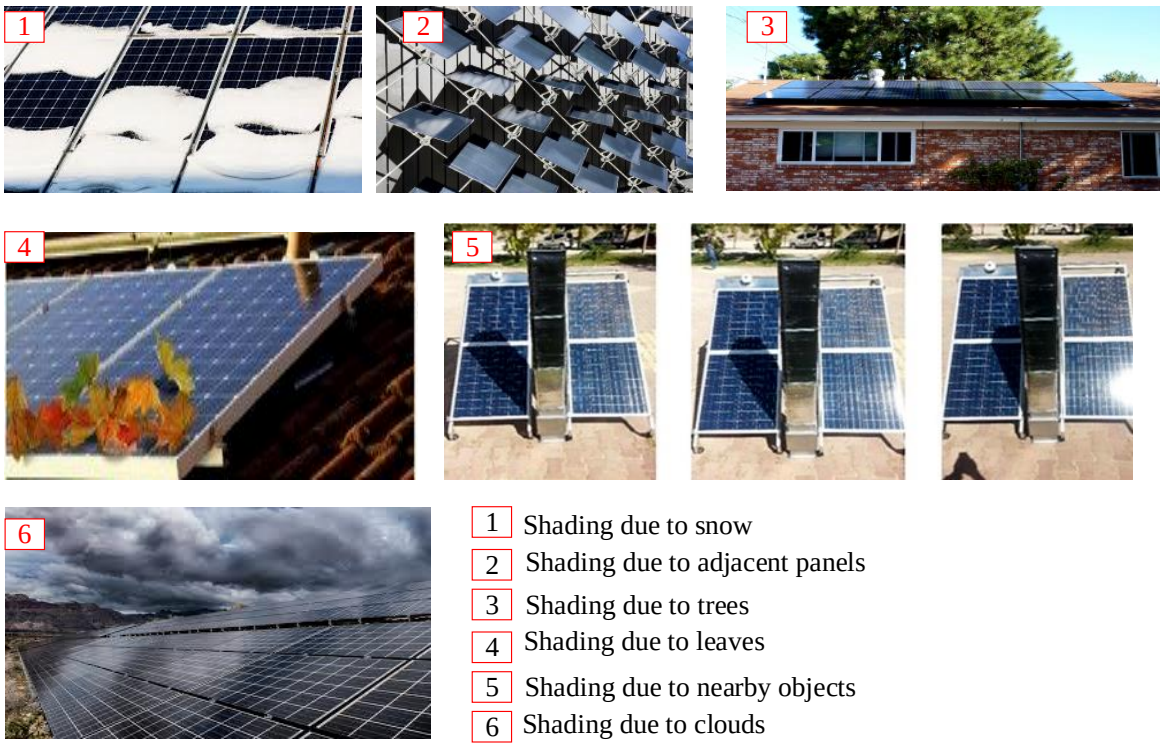

Figure 1.6: Partial shading due to various atmospheric conditions.

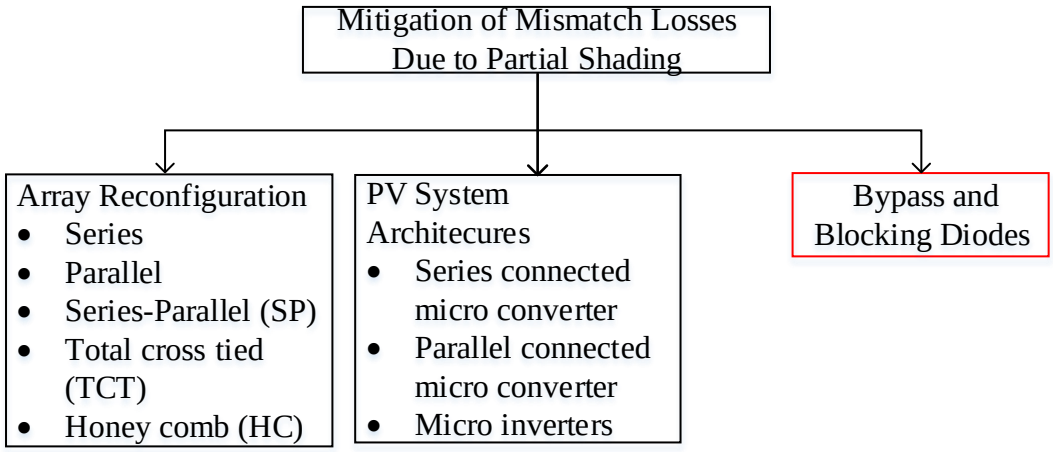

Figure 1.7: Methods found in the literature for the mitigation of mismatch losses due to partial shading.

For mitigating the power loss due to partial shading, the following methods as shown in Figure 1.7 are found in the literature. PV array reconfiguration and PV system architectures

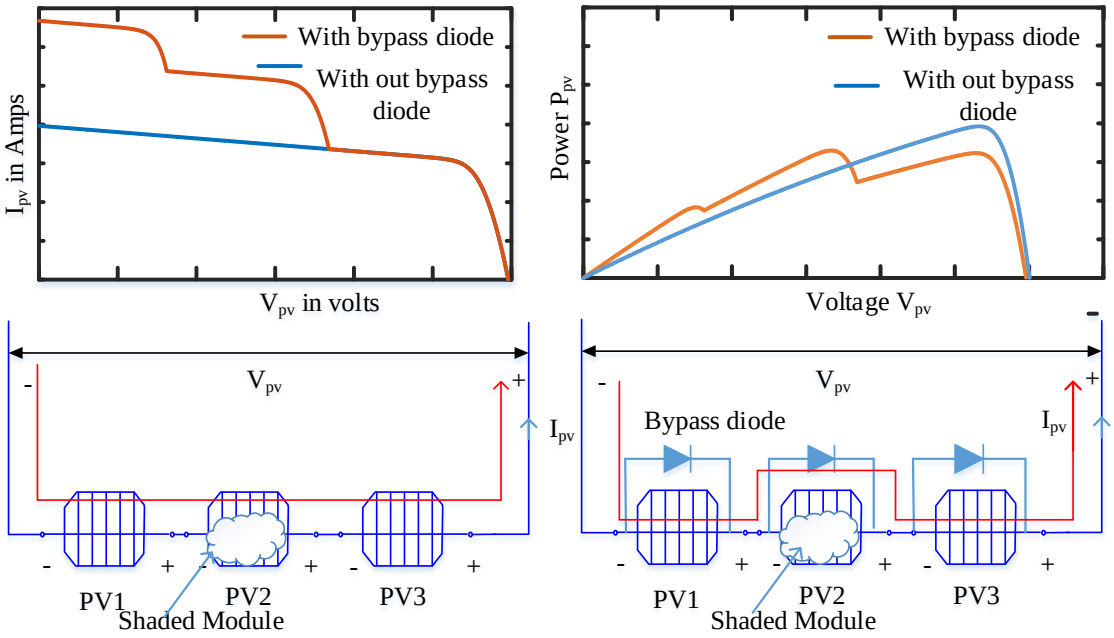

Figure 1.8: Current flow in a shaded module without and with bypass diodes.

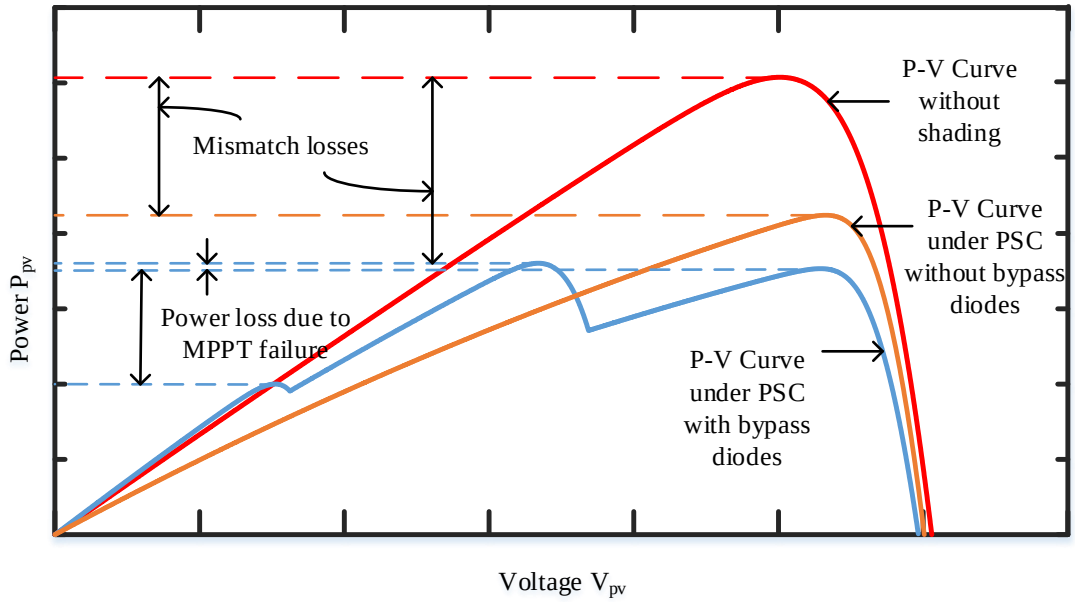

Figure 1.9: Power losses due to shading.

are costly and complex in nature. The easiest solution is connecting the bypass diode across the group of cells in the module, which bypasses the string current when it is more than the

maximum current rating of the shaded module, as shown in Figure 1.8. Since the power produced in the shaded module is bypassed, this loss is considered mismatch losses, as shown in Figure 1.9. When several modules are connected in series or parallel arrangement in an array to get the required current and voltage, the power versus voltage (P-V) curve becomes multi-peak under PSC, which has a single global peak (GP) and multiple local peaks. Whereas under uniform irradiance conditions (UIC), the P-V curve obtained is a single peak curve. Most of the conventional maximum power point tracking (MPPT) techniques are best suited for single peak P-V curves, whereas it is difficult to track the global peak of the multi-peak P-V curve under PSC with the same techniques. If the MPPT technique fails to track the GP, the power loss is considered as power loss due to MPPT failure.

1.4 Model description of MPPT controller

In 1954, Fuller et al. had proposed a practical PV system in which DC load can be connected directly to the PV panel, as shown in Figure. 1.10, it will not ensure the operating at MPP, which varies dynamically with the change in insolation and temperature. Hence, researchers later propose the maximum power point tracker, which is a power electronic converter for medium and high power rated PV systems [9]. By considering the low conversion

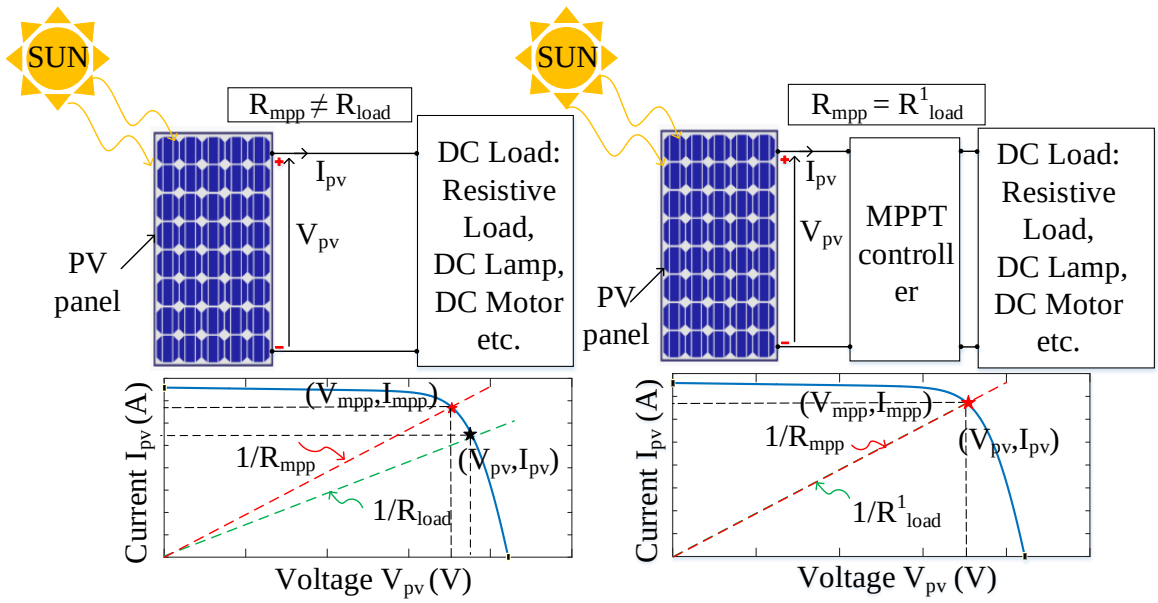

Figure 1.10: PV panel connected to load.

efficiency of PV panels, it is important to increase the efficiency of the PV system. The use of maximum power point trackers increases the PV system efficiency by 30% as compared to the system without MPPT. In recent years, new grid codes also impose maximum power point tracking for all grid-connected systems to get maximum energy yield and active power limit control to maintain stability under peak power production periods, i.e., during sunny days [10]. Hence, stand-alone and grid-connected PV systems should have the MPPT controller to extract the optimum power under all dynamic weather conditions.

The MPPT converter is a power electronic converter that adjusts the effective load resistance at PV array terminals by varying the switches' control signals. In general DC-DC converter act as an MPPT converter in a two-stage power conversion system, whereas the inverter itself acts as an MPPT converter in a single-stage power conversion system. In this thesis, the main objective is to verify the performance of various MPPT techniques; only DC-DC conversion stage of a two-stage power conversion system is used, as shown in Figure 1.11. Based on the load voltage requirement, a proper DC-DC converter is used among the basic DC-DC converter types, i.e., buck, boost, and buck-boost. In the case of battery charging application, the PV input voltage should be scale down to the battery voltage level. Hence, a buck DC-DC converter is used as an MPPT converter for battery charging applications. For the system independent on-line PV MPPT, voltage and current at the terminals of the PV are sensed and given as input to the MPPT algorithm, as shown in Figure 1.12. Based on the logic used in the algo-

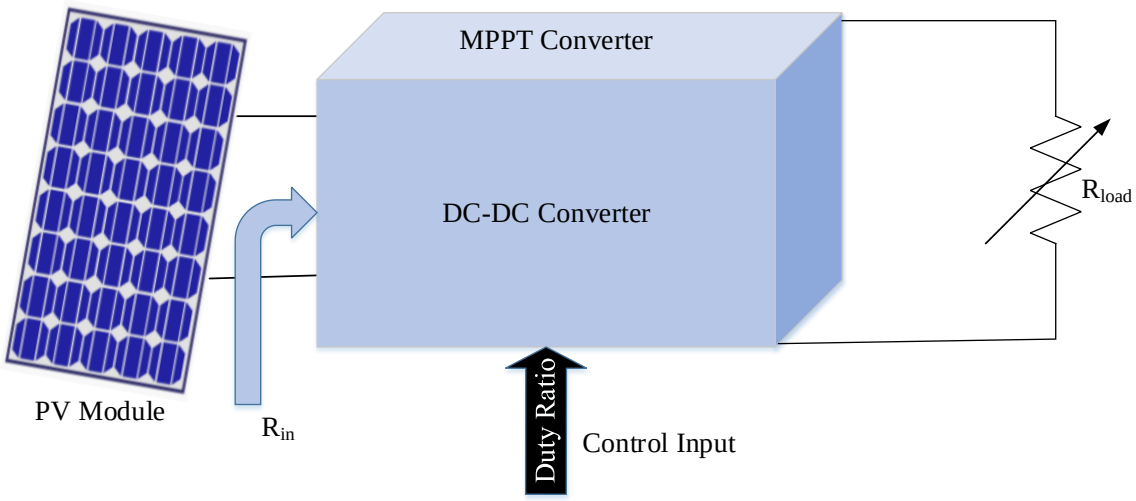

Figure 1.11: DC-DC converter as an MPPT converter.

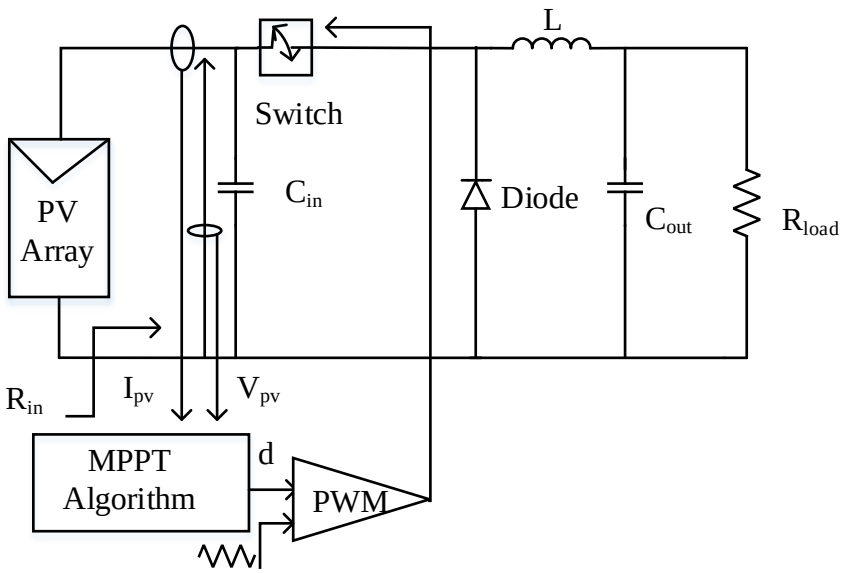

Figure 1.12: DC-DC buck converter as an MPPT converter.

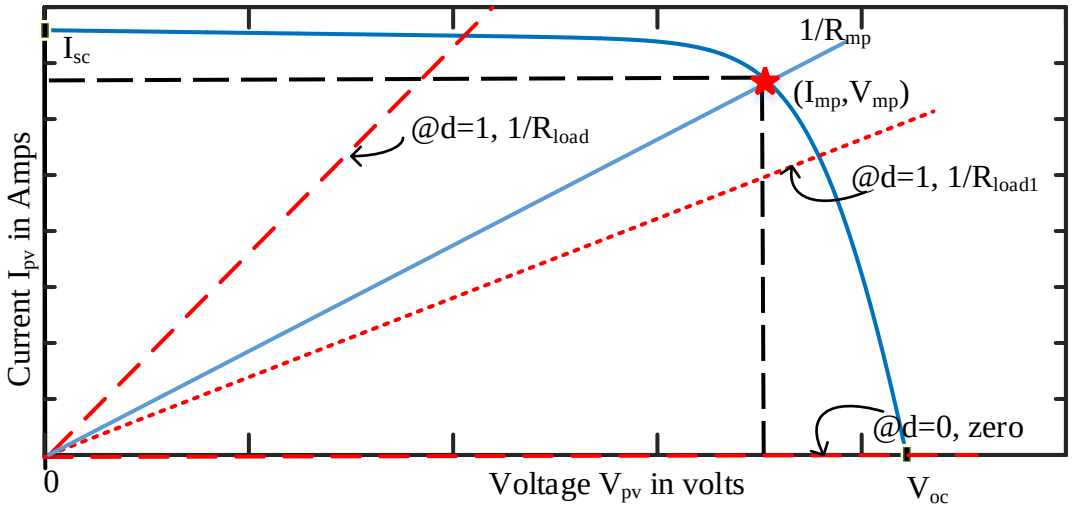

Figure 1.13: Operating region of DC-DC buck converter.

rithm, it generates the control signal. Input resistance seen at the PV array terminals is given by (1.2).

$$R_{in} = \frac{R_{load}}{d^2} \tag{1.2}$$

where R_{in} is the PV input resistance, R_{load} is the load resistance, and d is the duty ratio. The operating characteristics of the buck converter are shown in Figure 1.13. When duty ratio (d) ranges from 0 to 1, R_{in} varies from infinity to R_{load}. As per maximum power transfer principle, when $R_{mp} = R_{load}$, maximum power is transferred to the load. Where $R_{mp} = \frac{V_{mp}}{I_{mp}}$ is the PV resistance at the maximum power point. If the load resistance is greater than R_{mp}, MPP will not be covered in the operating region of the buck converter. Hence, R_{load} should be smaller than R_{mp} to track the MPP with a buck converter.

To boost the low input PV voltage to a higher level, a boost converter is used as an MPPT converter, as shown in Figure 1.14. In the case of a grid-connected solar PV system, the PV input voltage should be scaled up to the required dc-link voltage. Hence, a boost converter is used as an MPPT converter for the grid-connected PV system. Input resistance seen at the PV array terminals is given by (1.3)

$$R_{in} = R_{load} \times (1-d)^2 \tag{1.3}$$

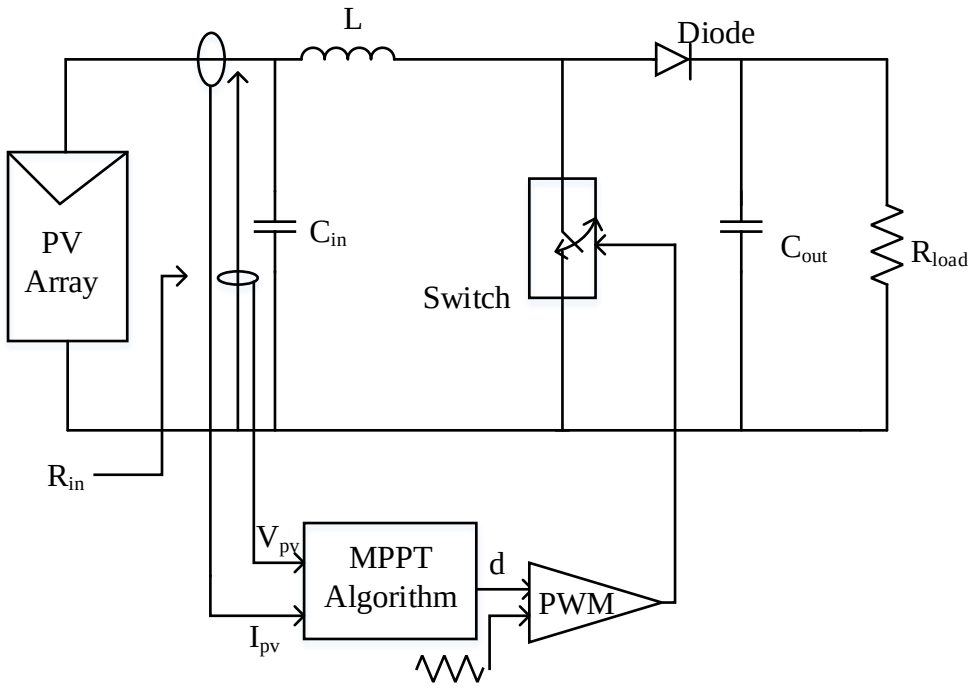

Figure 1.14: Boost converter as an MPPT converter.

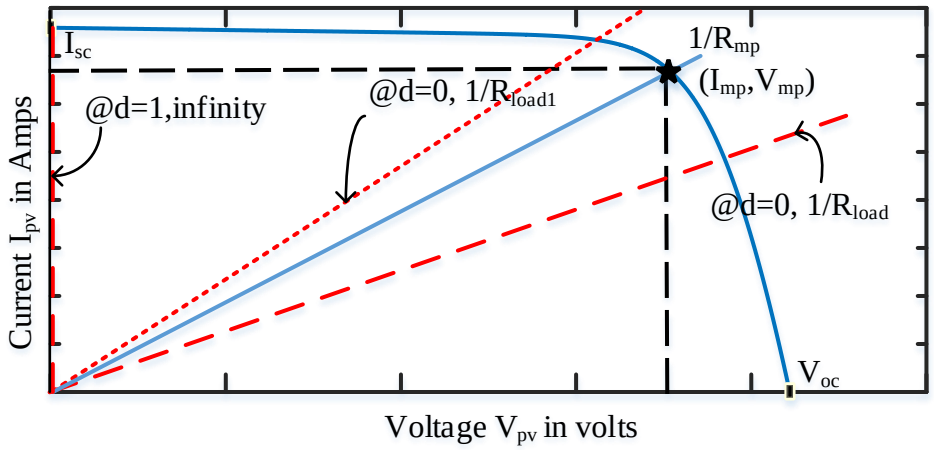

Figure 1.15: Operating region of a boost converter.

The operating characteristics of the boost converter are shown in Figure 1.15. When duty ratio (d) ranges from 0 to 1, R_{in} varies from R_{load} to zero. As per maximum power transfer principle, when $R_{mp} = R_{load}$ maximum power is transferred to the load. If the load resistance is smaller than R_{mp}, MPP will not be covered in the operating region of the boost converter. Hence, R_{load} should be grater than R_{mp} to track the MPP with boost converter.

To get the MPP tracking without independent of load value, a buck-boost converter is used as an MPPT converter as shown in Figure 1.16. Input resistance seen at the PV array terminals is given by (1.4)

$$R_{in} = R_{load} \times \left(\frac{1-d}{d}\right)^2 \tag{1.4}$$

When duty ratio (d) ranges from 0 to 1, R_{in} varies from infinity to zero. As per maximum power transfer principle, when $R_{mp} = R_{load}$ maximum power is transferred to the load. There is no restriction in choosing the load resistance value.

1.5 Overview of MPPT techniques for solar photovoltaic systems

The MPPT controller uses an algorithm to generate the control pulses based on the inputs of the controller. Initially, Fox et al. in 1979 had introduced the MPPT to the scientific

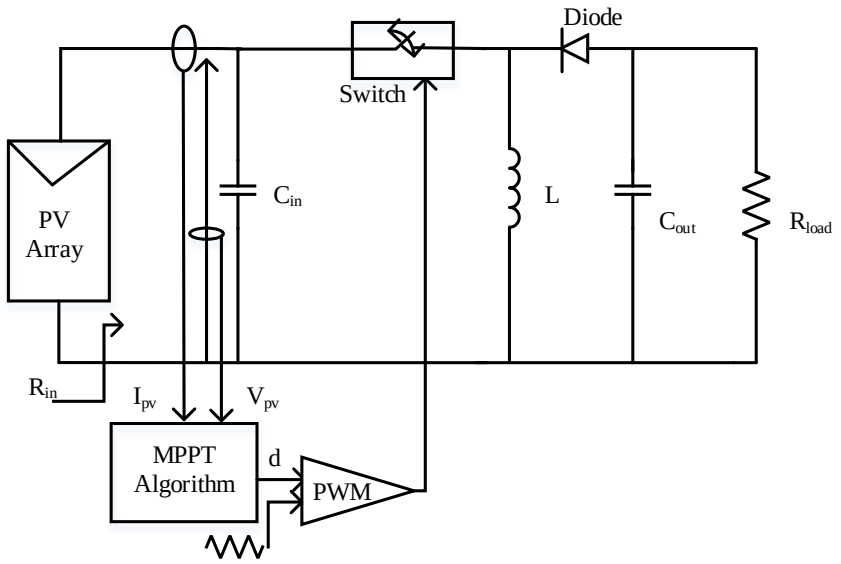

Figure 1.16: Buck-boost converter as an MPPT converter.

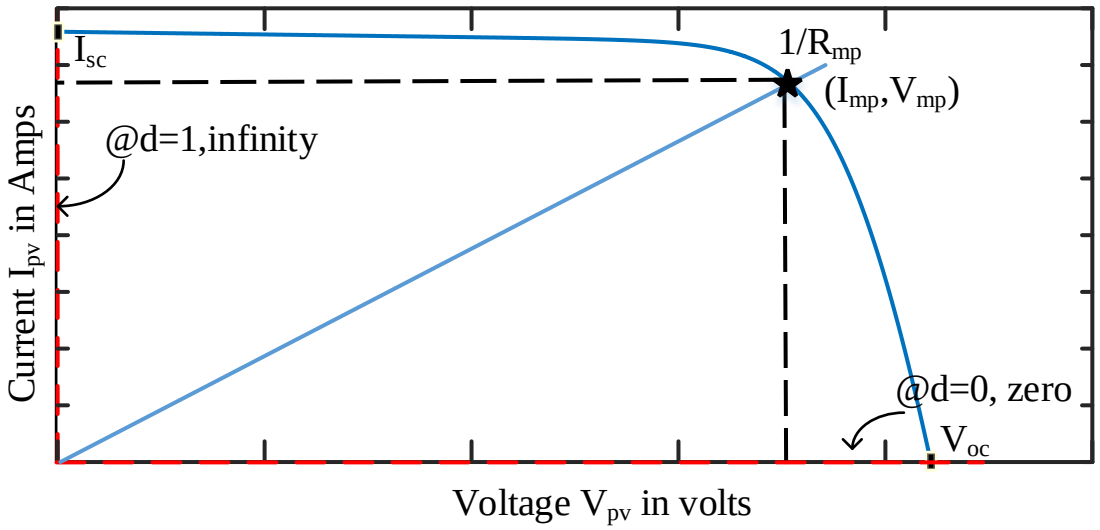

Figure 1.17: Operating region of a buck-boost converter.

world, and it is followed by a high number of research articles on MPPT, which focus on the improvement of tracking time and MPPT efficiency [11, 12]. The main objective of the MPPT technique is to extract the optimal power from the PV source. The researcher's main focus is to design efficient tracking technology that maximizes energy yield at any atmospheric condition

by using evolutionary and soft computing techniques. The following are the main features of an efficient MPPT technique found in the literature:

- √ Accurate and faster tracking of maximum power point
- √ High steady-state and dynamic efficiency
- √ Zero power oscillations during transient and steady-state
- √ Lower complexity of design and implementation
- √ Low cost
- √ System independent design

Even though several MPPT techniques are proposed in the literature, performance optimization is the major challenge in the field of PV MPPT. While designing an efficient MPPT algorithm, the important aspects of the PV system which need to be considered are given in Figure. 1.18.

The MPPT control of single-peak P-V curve requires simple algorithms like fixed voltage or current method, perturb and observe (P&O), and incremental conductance (INC). However, the presence of multi-peak P-V curves under PSC degrades these algorithms' effectiveness [9]. The conventional gradient-based techniques are popular for tracking MPP of single

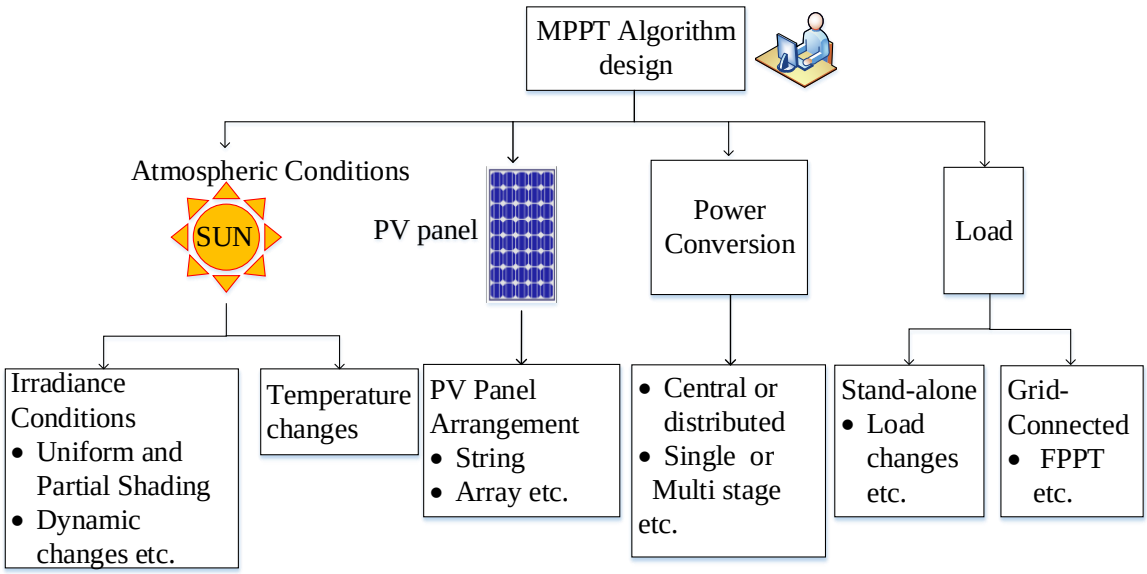

Figure 1.18: MPPT algorithm design considerations.

peak curves, but these may fail to track the GP of multi-peak P-V curve due to their hill-climbing nature, and it may cause for reduction of output power up to 40%. Under PSC, the power loss due to tracking wrong MPP and mismatch losses causes a total loss of 54% [6]. Hence, there is a need to develop suitable MPPT algorithms to accurately track the GP of the multi-peak P-V curve under PSC, which ensures maximum energy yield from the PV system under varying atmospheric conditions.

1.6 Working principles of MPPT techniques

Many techniques are available in the literature to solve the photovoltaic MPPT problem. These techniques are classified into off-line and on-line methods. The off-line method requires anyone or more system-dependent parameters such as open-circuit voltage, short-circuit current, temperature, and irradiation at each PV panel. Whereas on-line search methods are model-independent methods and generate a control signal based on instantaneous PV voltage and current.

MPPT techniques are search methods in the defined search space. These techniques are classified as single and multi-search agent methods based on the number of searching agents used. Single search agent methods mostly use the gradient information of the P-V or I-V curve, which are classified as gradient-based MPPT techniques. Whereas multi-search agent methods use more than one searching agent, exploration of the search space is derived from nature. Bio-inspired optimization algorithms, which comes under soft computing technique, are popular in multi-agent search methods because of the system independent search.

1.6.1 Gradient-based MPPT techniques

Among the conventional gradient-based MPPT techniques, P&O, INC are popular because of the simplicity and ease of implementation. P&O and INC use the single search agent, which is the control variable of the MPPT converter (duty ratio or voltage). Searching MPP starts from the initial value, and the direction of the search is based on the change in power in each perturbation, as shown in Figure 1.19. Perturbations to the control variable are continued even after reaching the MPP, which is required for finding the new MPP for any irradiance changes. However, these continuous perturbations to the control variable, even after reaching

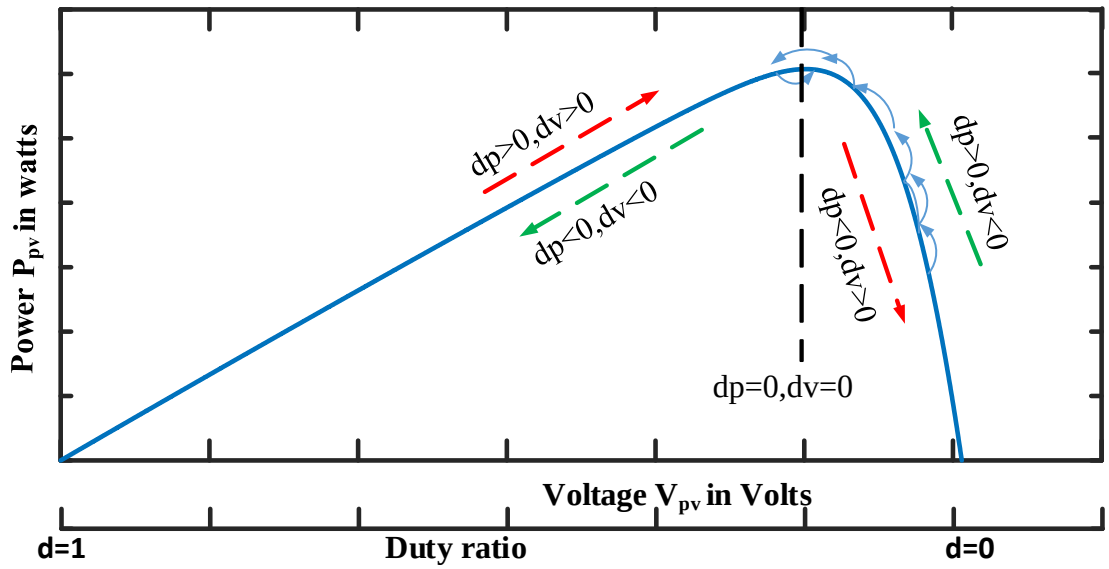

Figure 1.19: Working principle of P&O MPPT technique.

MPP, leads to power oscillations in the steady-state tracking. The speed of tracking MPP depends upon the perturbation step size. If a larger perturbation step size is chosen, it leads to faster tracking and high power oscillations in the steady-state. Whereas a smaller perturbation step size results in slower tracking and low power oscillations in the steady-state. Hence, proper step size is required to balance the tracking time and power oscillations in the steady-state [13]. Under irradiance changes, P&O is able to track the first immediate peak from the initial position of tracking, and it may fail to track the global peak of the multi-peak P-V curve under PSC due to the hill-climbing nature, as shown in Figure. 1.20. Therefore, the gradient-based MPPT techniques are best suited for single peak P-V curves, i.e., under uniform irradiance, and these may fail to track GP under PSC.

1.6.2 Soft computing-based MPPT techniques

The soft computing (SC) based MPPT techniques are multi-search agent methods. The process of exploring the search space is known as exploration, and finding the optimum after satisfying the convergence criteria is known as exploitation. In the bio-inspired SC technique, the exploration and exploitation are inherited from either animal's or bird's natural searching

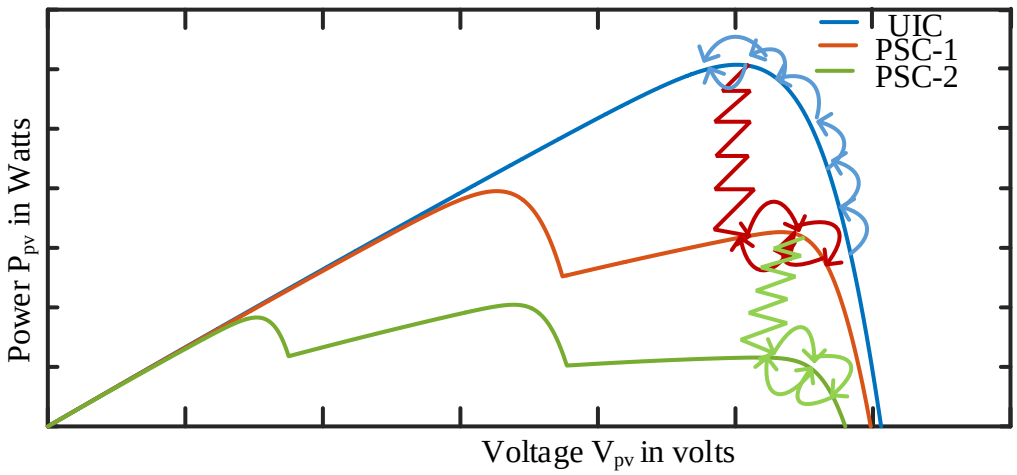

Figure 1.20: Working principle of P&O MPPT technique under irradiance changes.

strategies. In a well balanced optimization algorithm, both exploration and exploitation processes should be strong. When these SC techniques are applied in the field of MPPT to optimize the nonlinear multi-peak P-V or single peak P-V curve, the objective function is maximizing the PV power. Therefore, the problem formulation for the PV MPPT is given in (1.5). The constraint in the problem formulation is the control variable limits of the MPPT controller.

$$Maximize\ P_{pv}(d) \tag{1.5}$$

$$Subject\ to\ d_{min} < d < d_{max} \tag{1.6}$$

For example, when meta-heuristic techniques like particle swarm optimization (PSO) is applied to the on-line PV MPPT problem, the exploration of the search space is explained as follows [23]. First, the exploration of search space starts with the selection of the number of search agents (particles) and initialization of the particles (duty ratios) in the search space. For better understanding exploration phase of PSO in one iteration is explained as shown in Figure 1.21. The current position of the particle $X_i^k = 0.6$ duty ratio changes its position to $X_i^{k+1} = 0.5$ based on the (1.7) which is derived from birds flocking nature in the swarm. The current position of the particle moves more towards the $G_{best_i} = 0.35$.

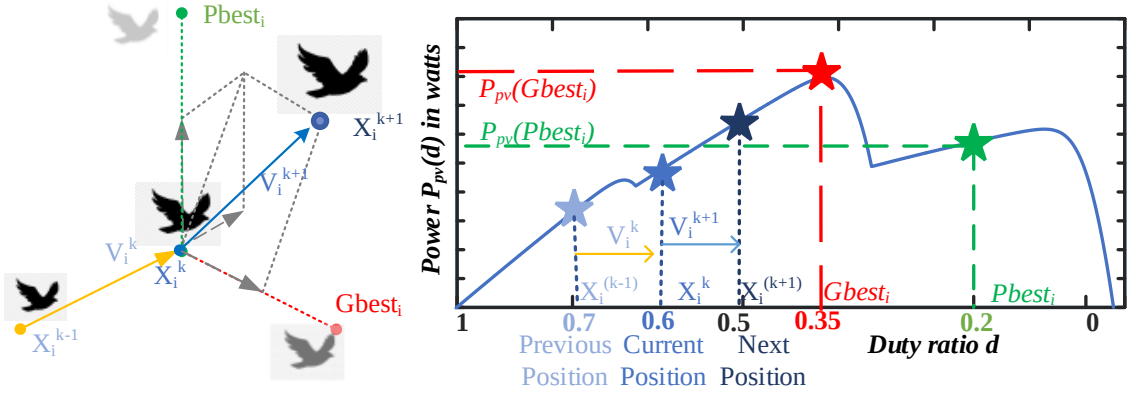

Figure 1.21: Working principle of PV MPPT technique based on PSO.

Therefore, the next position of the next particle is $X_i^{k+1} = 0.5$ with the assumed velocity $vel_i^{k+1} = 0.1$, which can be calculated with (1.8).

$$X_i^{k+1} = X_i^k + vel_i^{k+1} \tag{1.7}$$

$$vel_i^{k+1} = w \times vel_i^k + c_1 \times r_1 \times \left(P_{best_i} - X_i^k\right) + c_2 \times r_2 \times \left(G_{best_i} - X_i^k\right) \tag{1.8}$$

where i indicates particle number, k indicates the present iteration, w is weight factor which ranges from 0.4 to 0.9, c_1 is a cognitive factor which ranges from 0.1 to 2, c_2 is social factor ranges from 0.1 to 2, r_1 and r_2 are random numbers $\in$ R (0,1). In general, c_2 is greater than c_1 to move the particle position more towards the global best.

1.7 Conclusion

In this chapter, a brief introduction to solar PV systems, partial shading, and MPPT techniques has been presented. A model description of the various elements in the PV system is given. To avoid the adverse effects of partial shading like physical damage of solar cells, bypass diodes are connected across the group of cells. However, this bypassing of shaded cells/panels cause the multi-peak P-V curves. The overview and basic working principles of MPPT techniques are given. The conventional gradient-based methods like P&O fail to track the global peak of the multi-peak P-V curve under PSC due to the hill-climbing nature.

Chapter 2

Literature overview

Chapter 2

Literature overview

2.1 Introduction

In recent years, research on maximum power point tracking of the PV system is focused on extracting maximum available power during all dynamic conditions of weather like PSC and optimal performance of the tracking technique. To get maximum power from a nonlinear PV source under all weather conditions, several MPPT techniques are proposed in the literature, which include gradient and advanced SC-based MPPT techniques [14–16] as shown in Figure 2.1. Further, these MPPT techniques are classified as direct and indirect techniques based on the PV parameters considered for the design of the algorithm. Based on the data and sensors required for algorithm implementation, these techniques are further classified as on-line and off-line PV MPPT techniques.

To improve the tracking speed and power oscillations of the conventional gradient-based MPPT techniques (P&O and INC) under varying weather conditions, the combination of conventional gradient and artificial intelligence (AI)-based hybrid MPPT techniques are implemented in the literature [16, 17]. However, these hybrid techniques are complex because of the fuzzy logic controllers used, and implementation requires high-cost advanced digital controllers [18]. AI-based MPPT techniques include neural networks, and fuzzy logic shows rapid convergence under different weather conditions. However, these techniques require a huge amount of off-line training [19]. These techniques are system-dependent, which require irradiance, temperature, open-circuit voltage, and short-circuit current of each panel in the PV array. Hence, the sensors become more, and the cost of the system increases.

Since finding GP on a multi-peak nonlinear P-V curve within a defined search space is an optimization problem, SC techniques based on swarm intelligence (SI) are used for obtaining optimum solutions by using exploration and exploitation phases. In the literature, swarm-based algorithms like PSO, grey wolf optimization (GWO), whale optimization (WO), and evolu-

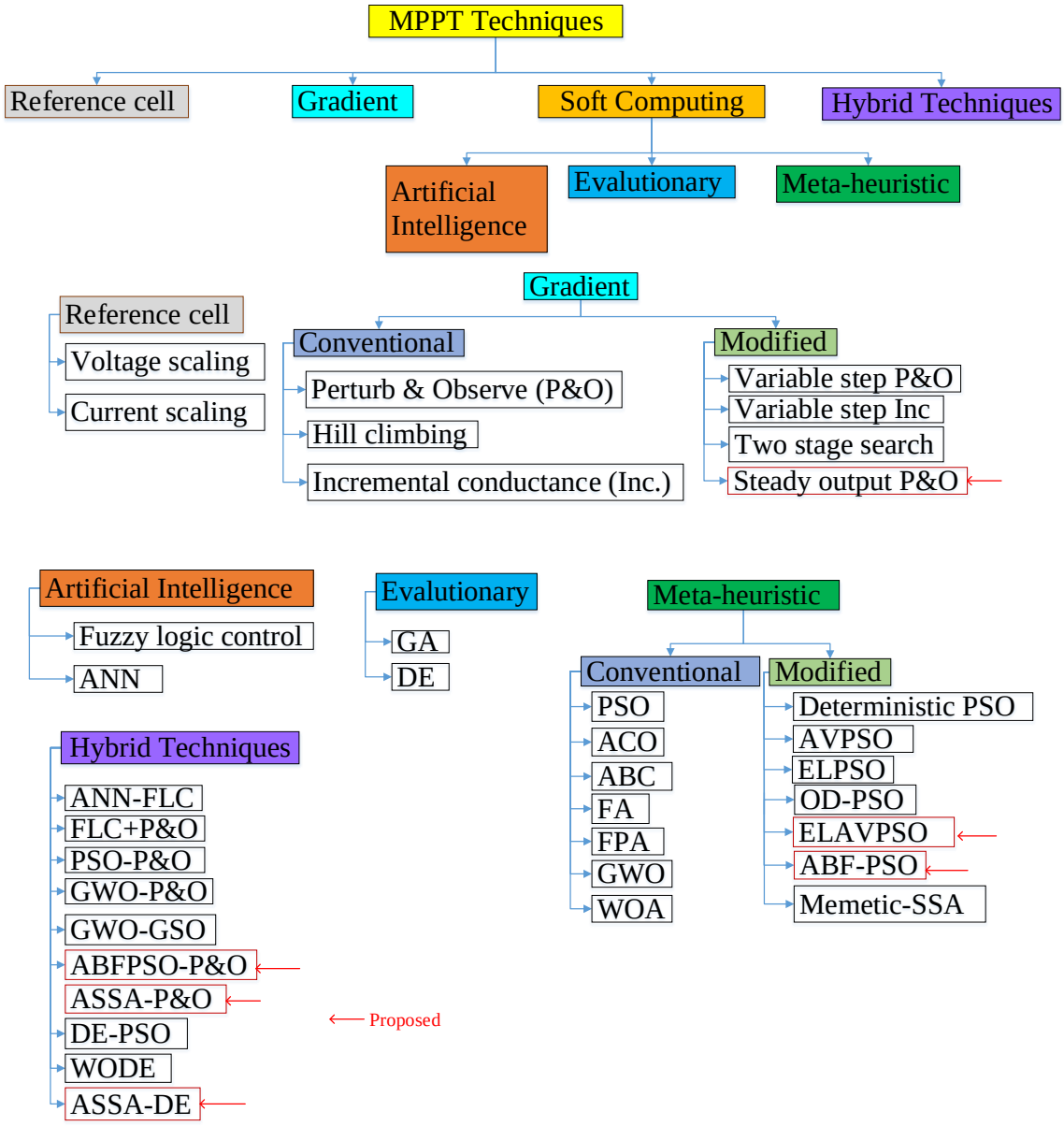

Figure 2.1: Classifications of MPPT techniques.

tionary algorithms like differential evolution (DE) are much explored for PV MPPT. The main advantage of SI techniques are:

√ Ability to track GMPP under PSC.

√ Zero steady-state oscillations.

√ High steady-state efficiency.

√ Lower complexity of design and implementation as compared to other AI techniques.

√ System independent design.

However, the major drawbacks are:

× Premature convergence.

× Parameter tuning for varying atmospheric conditions.

× Higher power oscillations during the exploration phase.

× Slow tracking of MPP as compared to conventional P&O and INC.

An adverse effect of the above drawbacks on PV MPPT is high energy loss. Hence, overall PV system conversion efficiency is decreased.

2.2 Literature overview

2.2.1 Gradient-based MPPT techniques

Traditional gradient-based MPPT techniques like P&O and INC are popular because of their simplicity and easy implementation. Under UIC, since the P-V curve is a single peak curve, conventional MPPT algorithms like P&O and incremental conductance tracks the MPP accurately. However, these techniques' performance is degraded under non-uniform irradiance conditions and large irradiance changes [20]. Another disadvantage of these methods is the continuous perturbations after reaching maximum power point results in power and voltage oscillations in the steady-state tracking [21]. Hence, to improve the performance of conventional algorithms (P&O and INC), the combination of conventional and AI techniques is implemented in the literature. The AI techniques are used to find the optimum value of perturbation step size for the dynamic atmospheric conditions. However, these hybrid techniques also fail to track the PSC's multi-peak P-V curve's global peak due to the hill-climbing nature of gradient-based techniques. The failure to track GP of multi-peak P-V curve causes power loss in addition to mismatch loss of PV system, which may cause an overall reduction of output power up to 54%. Therefore, the main limitation of the conventional gradient based MPPT techniques is failure to track the GP of multi-peak P-V curve which may cause for reduction of output power and

net energy yield. This is mainly due to tracking only the first immediate peak from the starting point of tracking because of hill climbing nature. Hence, to avoid the failure to track the GP of the multi-peak P-V curve under PSC and achieve faster and accurate MPP tracking with low power oscillations, conventional gradient-based MPPT techniques are combined with SC-based MPPT techniques.

2.2.2 Soft computing-based MPPT techniques

SC techniques can optimize the multiple maxima power curve under PSC, and these are also called global maximum power point tracking (GMPPT) techniques [22]. PV model-independent and zero steady-state power and voltage oscillations are the main advantages of SC techniques [23]. However, these techniques suffer from large initial power oscillations during tracking due to the spread of search throughout the power curve in the exploration phase. Improper algorithm control parameters result in premature convergence, causing high energy loss due to the wrong optimum found. The frequent, continuous, and rapid change in irradiance can cause for failure of the GMPPT algorithm in the form of a local optimum. Hence, there is a need to derive modified MPPT techniques, which can reduce the drawbacks like complex parameter tuning, initial power oscillations, and MPP tracking failure under dynamic irradiance conditions. Among all SI techniques, PSO is most popular in solving PV MPPT problem because of its simple structure and easy implementation. However, three fixed control parameters of the PSO are not best suited for varying atmospheric conditions. These may degrade the tracking performance of PSO, which may cause premature convergence, i.e., failing to track global peak. Hence, parameter tuning is essential for better performance of any soft computing technique, and these are known as adaptive techniques. The conventional PSO algorithm needs to be modified to match the requirements of efficient PV MPPT.

In [24, 25], PSO-based GMPPT techniques are proposed for the partially shaded PV system, and these are off-line search methods. These off-line techniques require irradiance and temperature sensors to measure irradiation and temperature at each PV panel, which are costly. PSO-based on-line PV MPPT techniques are evolved as popular GMPPT techniques because of their simplicity and lower cost of implementation [23]. However, there is a need to investigating PSO-based techniques for PV MPPT to get faster and accurate MPP tracking with low power

oscillations during exploration.

In [26], the PSO algorithm parameters are made adaptive to decrease power oscillations after reaching GMPP, and velocity is limited to avoid skipping any local MPP, which helps avoid premature convergence. A variable step P&O algorithm is used to maintain GMPP and to identify irradiance changes. In this method, feedback from the search, which is a distance from the position of global best to the position of particles, is used to tune the parameters adaptively. Overall, two parameters are made adaptive by keeping one parameter constant. On account of parameter control and limited velocity, faster convergence is achieved without premature convergence, and power oscillations in the GP region are minimized. Since the global best particle velocity is zero in adaptive velocity PSO (AVPSO), the present leader position is not updated in the next iteration. However, full tracking of global maximum power point (GMPP) is done only with the AVPSO, which involves unnecessary exploration of search space even after reaching the GP region.

In [27], an enhanced leader PSO (ELPSO) method is proposed in which mutations are applied to global best in each iteration to avoid premature convergence. This paper's main idea is that the best leader results in better particles in the exploration and mutations to avoid stagnation problem at a local peak. However, parameters of PSO algorithm which balance the exploration and exploitation are not tuned and are considered as constants. Since MPPT is an on-line/hardware-based search process, the five mutations applied to global best are nothing but increasing population size, and it causes more tracking time in on-line PV MPPT.

In [28], a deterministic PSO algorithm is proposed in which the velocity equation of the PSO algorithm is made deterministic. However, the deterministic nature of the PSO algorithm is derived by removing the control parameters in the velocity update equation. This can degrade the searching capability of the PSO algorithm.

In [29], the overall distribution PSO algorithm is used to rapidly search the area near the global maximum power point, which is further integrated with PSO to improve the accuracy of MPPT. However, the parameters of PSO are considered constant.

In [30], butterfly swarm intelligence is used for the exploration and exploitation of the PSO algorithm to avoid the limitations like premature convergence and weak exploration capability. The sensitivity feature of the butterfly PSO (BF-PSO) algorithm can be used to identify GP region. In the BF-PSO method, sensitivity and weight factors are tuned deterministically

and are dependent on the maximum iteration count. When this method is used as a PV MPPT algorithm, the number of iterations required to reach the convergence criterion is unknown initially since it is an on-line/hardware-based search process. If the estimated number of iterations for convergence is high, it results in the unnecessary exploration of search space even after reaching optimum value and results in more tracking time.

In [31], a bio-inspired optimizer for engineering design problems, a salp swarm algorithm (SSA) is proposed. It is simple and easy to implement as compared to PSO, which consists of three control parameters. However, the single control parameter in SSA is dependent on the maximum iteration count. It results in the unnecessary exploration of search space even after reaching the GP region in an on-line search process like PV MPPT.

In [32], different metaheuristic techniques are proposed for mitigating the power loss due to the wrong optimum found during PSC of PV systems in which SSA is simple and easy. The superiority of SSA over other methods lies in the efficiency of extracting GMPP. However, the convergence speed and tracking time of the conventional SSA-based MPPT technique is poor compared to other MPPT methods based on GWO, hybrid method (PSO-GSA).

A memetic salp swarm algorithm (MSSA) based MPPT is proposed in [33], which improves the searching ability and convergence stability by using multiple salp chains. Even this technique also suffers from slow convergence or slow tracking of GMPP due to dependency of control parameter on maximum iteration count. Since there are more salps in the form of multiple salp chains, it results in slower tracking of MPP in an on-line PV MPPT.

Therefore, the main limitations of SI techniques are large initial power oscillations, premature convergence, improper parameter setting, and slow tracking. These limitations results in low enrgy yield from the system. To overcome the large initial power oscillations, the velocity of the particles must be controlled and exploration phase should be limited only to find GP region, which can give fast tracking also. To overcome the premature convergence, algorithm parameters needs to be tuned properly.

2.2.3 Hybrid MPPT techniques

To improve the performance of standard versions of SI techniques like faster and more accurate tracking of MPP, several modified versions or hybrid MPPT techniques are proposed

for the PV systems under dynamic weather conditions [34]. Hybrid tracking techniques can be formed by combining two or more conventional or modified SC and gradient-based MPPT techniques. The complexity of the algorithm is increased with hybridization. However, the essential need to track global maximum power point under all dynamic weather conditions encourages the researchers to investigate more on the advanced hybrid tracking techniques.

Under dynamic atmospheric conditions, hybrid MPPT techniques, combining artificial intelligence and conventional gradient-based MPPT techniques, are proposed [35, 36]. But, these hybrid techniques are sophisticated in implementation and require large off-line training.

In the literature, several hybrid tracking techniques are proposed for PV systems under PSC, which are classified as follows. In the first category, conventional gradient-based methods are used to find all local maximum power points (LMPP) in the first-stage, and in the second-stage, these MPPs are sorted to get GMPP [4, 29]. These two-stage techniques guarantee an accurate GMPP. However, traversing all the curve peaks imposes a long tracking time, which is not a good feature to meet the requirements of an efficient PV MPPT technique.

In the second-category, the SC technique is used to identify the GP region in the first-stage, and in the second-stage, the tracking is continued with the conventional P&O technique [37, 38]. These techniques can track the GMPP much faster than the first-category. However, the exact GP region identification with SC technique and power oscillations in the steady-state are major challenges of these methods. In most of these methods found in the literature, the GP region identification is made with an unjustified predetermined number of iterations.

In [39], a hybrid GMPPT method based on PSO and P&O algorithms is proposed. To identify the type of shading, predefined rules based on the change in current, voltage, and power are used. Only on the onset of PSC, the PSO algorithm is employed and under uniform irradiance conditions, the P&O algorithm with a fixed-step is applied. Because of fixed control parameters of PSO, there is a high probability for premature convergence and unnecessary exploration even after reaching a global peak region. Whereas fixed-step P&O results in more power oscillations in the steady-state tracking.

In [40], a scheme is proposed to identify the global peak region by using enhanced leader PSO and the conventional algorithm is used in the region so that P&O can track the GMPP. But basic PSO is becoming more complex by introducing mutations to the leader, and it involves tuning of more parameters.

In [37], a hybrid MPPT method based on PSO and P&O is proposed for more accurate tracking of GMPP. First GP region is identified with PSO with deterministically tuned control parameters, and thereon tracking is continued with a fixed-step P&O technique. Since the control parameters of PSO in this method are dependent on the unknown value of the maximum iteration count, it causes slow convergence to identify the GP region. In this method, three control variables must be tuned, and PSO needs to be re-initialized for change in insolation as well as for the load variations while the velocity of particles is not limited, which creates high initial power oscillations during tracking.

In [38], a gray wolf assisted P&O based MPPT is proposed for fast-tracking of MPP. GWO algorithm requires two parameters that are to be tuned. The parameters are dependent on maximum iteration count, which causes slow convergence in identifying the GP region. The fixed-step P&O algorithm is used in the global peak region, which causes the power oscillations in the steady-state. The step-size of fixed-step P&O algorithm needs to be selected properly to get the reduced power oscillations.

In the third-category, two or more soft computing techniques are combined to enhance the exploration and exploitation of the main SC technique [41–43]. In [41], a hybrid MPPT technique is proposed for dynamic conditions of partially shaded PV systems. To enhance the performance of WO, evolutionary algorithm DE is combined in series with WO. The WO algorithm parameters are sensitive to maximum iteration count, which is unknown initially. The whole algorithm needs to be reinitialized for any system changes due to either load or insolation change.

In [42], a hybrid evolutionary algorithm DEPSO is proposed in which PSO is applied in odd iterations, and DE is operated in even iterations to get the fast-tracking and to improve the performance of standard PSO. However, in this method, a total of six parameters needs to be tuned.

In [43], a dual algorithm is proposed in which golden selection search optimization (GSO) is used to reduce unnecessary oscillations in the global peak region by GWO algorithm. Even though a new reinitialization judgment is proposed for the sudden changes in power, the algorithm needs to be reinitialized for both changes in insolation and load.

In this category, the optimum solution obtained in each iteration of the main SC technique is enhanced by another SC technique, which may be evolutionary or swarm-based. The

accuracy of the solution obtained will be more than the case of a single SC technique is used. However, the number of algorithm parameters to be tuned is more and complex. To avoid the power oscillations due to the irregular searching of the SC technique, tracking MPP with P&O in the UIC and SC technique during PSC is ideal. The second and third-category methods should rely on the SC technique for tracking MPP of both UIC and PSC due to a lack of partial shading identification methodology.

In the fourth-category, shade detection is enabled in the first-stage to find a uniform or PSC. In the second-stage, the SC technique is used only to identify the GP region of the PSC, and P&O is used in the steady-state and UIC, so that the use of the SC technique can be limited to PSC only. An accurate shade detection helps to improve the performance of these hybrid tracking technologies [39]. The main challenges of fourth-category methods that need to be investigated more are fast and accurate tracking of maximum power point, accurate shade detection, low power oscillations in the steady-state tracking, easy parameter tuning, and proper shifting of algorithms, which comes under optimizing the performance of the hybrid tracking techniques [44]. Hence, performance optimization of the hybrid tracking technique is most important and challenging for the researchers in the field of PV MPPT.

In the third and fourth category hybrid MPPT techniques, the major limitations are use of either conventional or SI technique with out improper parameters can cause for failure in tracking MPP, and the improper judgment for the shifting the algorithms can cause for delayed MPP tracking. Hence, modified or hybrid SI techniques can be the best solution for finding accurate GP region. Adaptive parameters of the algorithm can be used to avoid unjustified algorithm shifts.

2.2.4 Performance optimization of hybrid tracking technique

With the increase in rooftop grid-connected solar PV systems, penetration of medium and high-rated PV systems connected to the grid are increased. With the high penetration of PV systems, the power injected into the grid may become more than the demand during sunny or peak production periods, which may cause instability and overload [45]. Therefore, the grid-connected PV system should have the flexibility to deliver the active power within the power limit known as flexible power point tracking (FPPT) [46]. The new grid codes impose MPPT

for all grid-connected systems to get maximum energy yield and active power limit control to maintain stability under peak power production periods. Hence, the MPPT tracking algorithm should have maximum power point tracking under all dynamic weather conditions and active power limit control in the form of FPPT, which is a cost-effective solution for active power control.

In stand-alone PV systems, the sudden change in load causes the change in operating point from the maximum power point. The change in load causes the reinitialization of SI technique which results in large power oscillations due to exploration phase. This reinitialization of SI technique is best suited only for insolation changes where global peak changes. Whereas for load change, only operating point is changing but not the global peak.

2.3 Motivation

Literature review of the MPPT techniques under partial shading conditions leads to the following motivations.

To mitigate the partial shading effects, connecting bypass diode across the group of cells in a module is cost-effective. However, the resulted multi-peak P-V curve becomes a limitation for the popular conventional gradient-based MPPT techniques like P&O and Inc. The failure of GP tracking resulted in power loss in addition to mismatch loss. The power loss due to wrong optimum found by the GMPPT technique results in less energy yield under PSC. Hence, the overall PV system conversion efficiency decreases. The author of this thesis is motivated to investigate more on the MPPT techniques of solar PV systems under partial shading conditions and proposed efficient tracking technologies for the solar PV systems, which gives optimum energy yield under PSC.

Even though PSO-based GMPPT techniques are evolved as popular GMPPT technique among SI based MPPT techniques, it has the drawbacks like complex parameter tuning, initially large power oscillations, and premature convergence. Hence, modified PSO-based MPPT techniques are proposed in the literature to get faster and accurate tracking of GMPP. Under dynamic weather conditions, identifying GMPP with less probability of premature convergence is a major challenge for all GMPPT techniques. The large initial power oscillations due to exploration of PSO algorithm should be limited in on-line PV MPPT. Hence, there is a need for further investigations on PSO-based MPPT techniques to get fast and accurate tracking of

GMPP under PSC with less power oscillations. To avoid the major drawbacks of PSO: weak exploration and more number parameters (three) to be tuned, there is a need for a simple GMPPT technique with fewer parameters tuning.

Salp swarm algorithm is a bio-inspired soft computing technique, already proved to be a simple and efficient optimization algorithm with one control parameter for most of the engineering design problems which also matches with requirement of fewer control parameters and more efficient tracking of PV MPPT. The slow convergence or tracking GMPP is primarily due to the dependence of the deterministically tuned control parameter, which depends on the maximum iteration count. In an on-line search process like PV MPPT, the wrongly estimated maximum iteration count results in the unnecessary exploration of the search process even after reaching the GP region, which delays the convergence. Hence, there is a necessity of deriving the control parameter, which is independent of the iteration count, and avoiding unnecessary exploration of search space in the GP region to get faster tracking with SSA-based MPPT technique. The essential need to track global maximum power point under all dynamic weather conditions encourages the researchers to investigate more on the advanced hybrid tracking techniques.

Even though GMPPT techniques are able to identify the GP under PSC, to avoid the power oscillations of these techniques under uniform irradiance conditions use of conventional gradient-based MPPT techniques is ideal. Henceforth, fourth category hybrid tracking technologies are found by the researchers in which shading detection is vital. There is a need for an exact shade detection scheme in these hybrid tracking technologies. The new grid codes demand other features like flexible power point tracking. Hence, there is a need for proper shade and active power limit detection in an on-grid PV system. The combined study of FPPT, GMPPT, and shade detection has not been investigated in the literature. To get the performance of hybrid GMPPT technique which is the major challenge for the PV MPPT researchers, the inclusion of hybrid SI techniques in the two-stage search method is essential, which is not explored yet in the literature. Whereas in a stand-alone system, load changes demand the tracking GMPP without large power oscillations. Hence, exact load change detection and rapid tracking of GMPP under load changes are essential. The main challenges of hybrid tracking techniques that need to be investigated more are :

- Fast and accurate tracking of maximum power point

- Accurate shading detection
- Low power oscillations in the steady-state tracking
- Easy parameter tuning and proper shifting of algorithms

Hence, performance optimization of the hybrid tracking technique is most important and challenging for researchers in the field of solar PV MPPT.

2.4 Thesis Objectives

With the above motivations in the MPPT techniques, the following research objectives are designed for the research work presented in this thesis.

1) Maximum energy yield from the PV system under partially shaded conditions by eliminating power loss due to wrong MPP found with the MPPT controller.

2) Optimum use of GMPPT technique under dynamic partial shading conditions.

3) Development of an efficient hybrid MPPT technique to get faster tracking with reduced power oscillations.

4) Reduction of parameter tuning complexity in the hybrid tracking techniques.

5) Investigation of hybrid MPPT techniques in the stand-alone PV system to get maximum power under both irradiance and load changes.

6) Investigation of hybrid MPPT techniques in the grid-connected PV system to get the optimal performance.

2.5 Contribution

This thesis main aim is to propose efficient GMPPT techniques that can overcome the limitations of state-of-art MPPT techniques for the PV systems under partially shaded conditions. The main focus of the present thesis work is to get the proposed tracking techniques' optimal performance. Hence, optimum energy yield from the PV system under partially shaded conditions is ensured.

Various control strategies proposed in this research work are

Control strategy - 1

To overcome the stagnation of search at local maximum and slower convergence in a PSO-based on-line PV MPPT technique:

1) A new fast-tracking PSO-based GMPPT technique (Enhanced leader adaptive velocity PSO (ELAVPSO)) with adaptive parameter tuning and enhanced leader features is proposed.

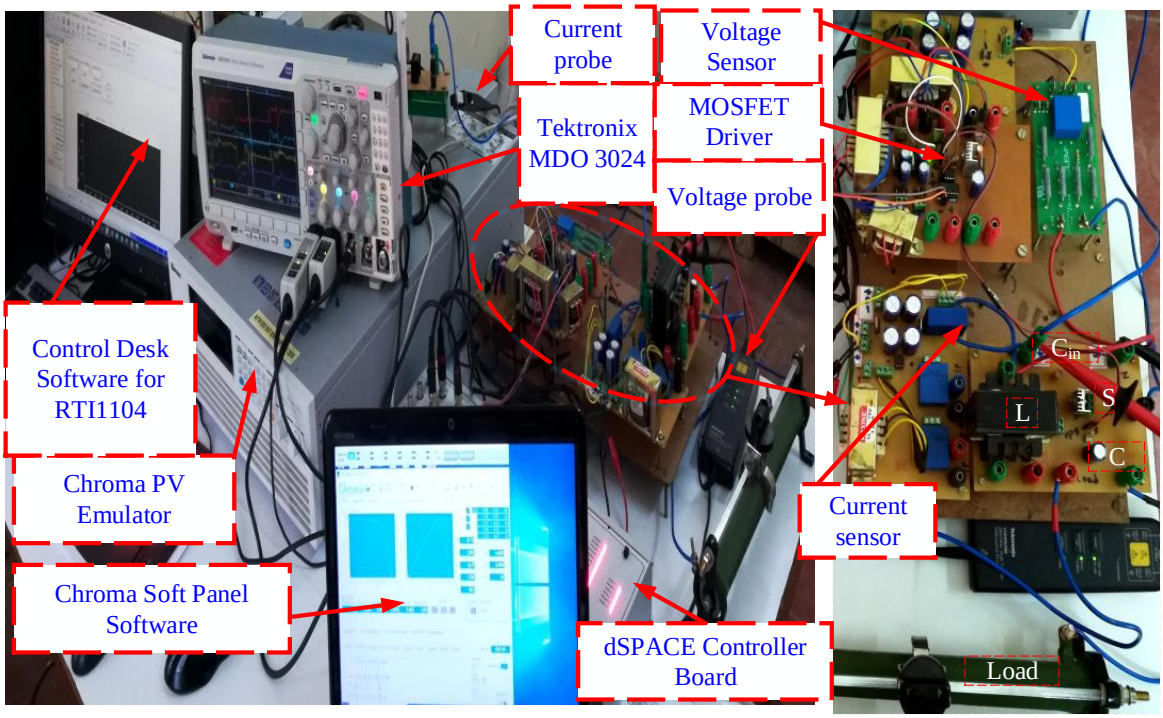

Figure 2.2: Experimental setup.

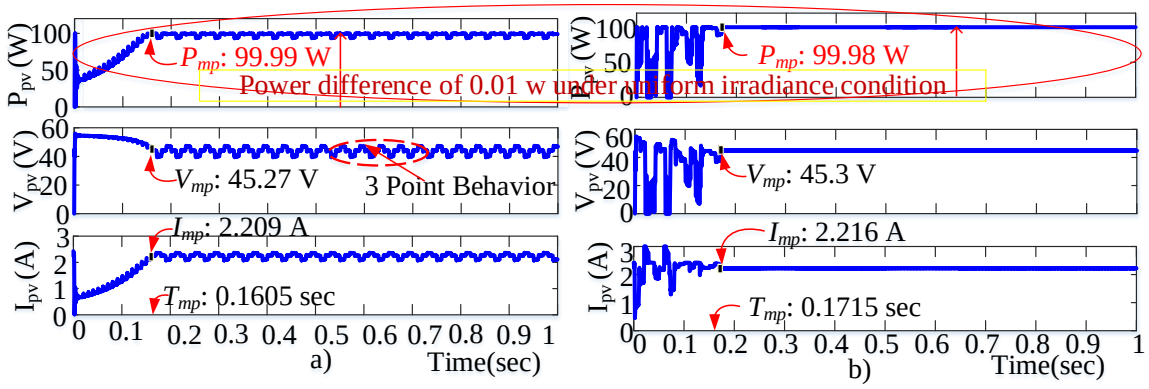

Figure 2.3: Simulation results of MPPT techniques under uniform irradiance a) P&O, b) ELAVPSO.

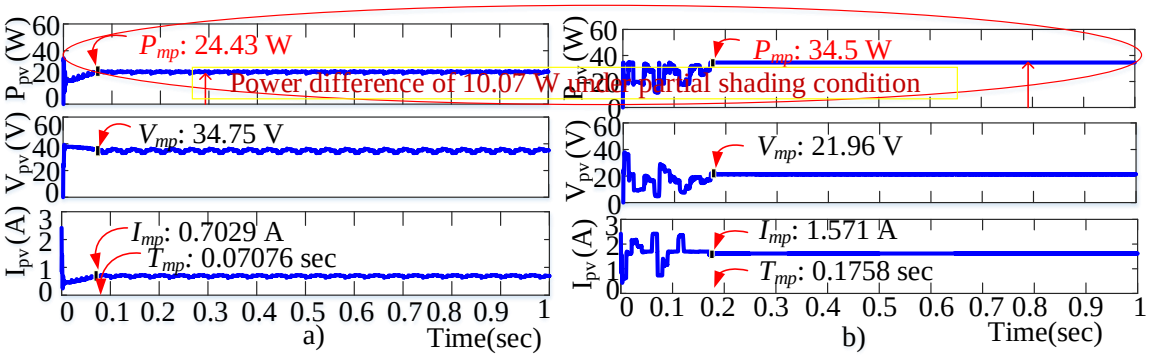

Figure 2.4: Simulation results of MPPT techniques under partial shading condition a) P&O, b) ELAVPSO.

The proposed technique is tested on 100 W PV experimental setup shown in Figure 2.2 and results are shown in Figures 2.3 and 2.4. From the simulation results, it is evident that the P&O and the proposed ELAVPSO MPPT technique results in almost same results under uniform irradiance. However, under PSC, only the proposed method tracks the GMPP, i.e., $P_{mp} = 34.5\ W$.

2) A new shading detection technique to identify the type of shading based on variable step P&O is proposed to limit the GMPPT technique only to PSC. Hence, power oscillations due to the GMPPT technique under uniform irradiance can be avoided. The results of the proposed shading detection are shown in Figure 2.5. From the simulation and experimental results, it is evident that the proposed shading detection accurately identifies the uniform

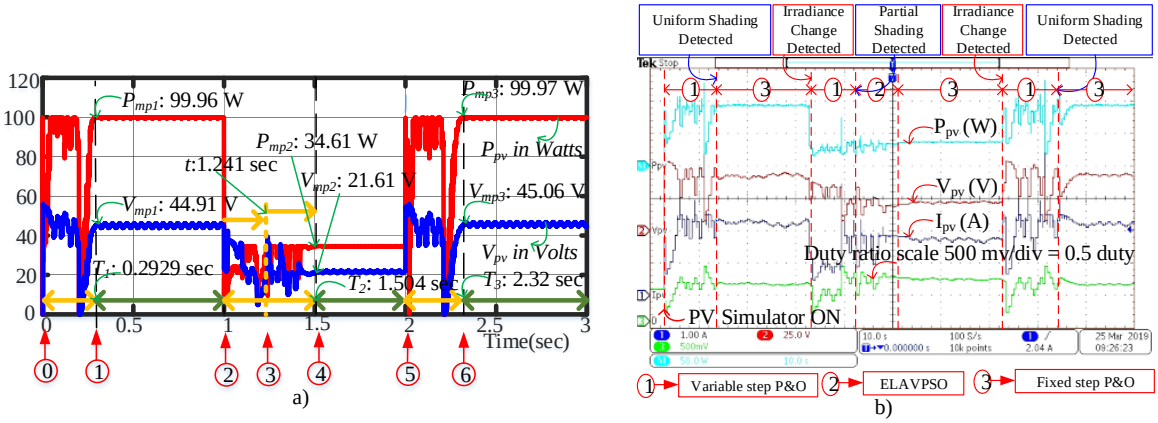

Figure 2.5: Proposed shading detection technique results in a) Simulation, b) Experimental.

and PSC conditions and allows the use of ELAVPSO GMPPT technique only under the occurance of PSC.

In ELAVPSO, mainly premature convergence and parameter tuning are minimized. However, the other drawback of PSO-based GMPPT technique is that high power oscillations during the exploration phase remain when ELAVPSO is used alone without shading detection.

Control strategy - 2

To overcome the limitations of PSO-based MPPT methods: high power oscillations during the exploration phase, stagnation of search at local maximum, and slower convergence in a PSO-based on-line PV MPPT technique:

1) A hybrid GMPPT method based on butterfly PSO (BF-PSO) and P&O algorithms for a PV system under partially shaded conditions is proposed. The experimental verification is done with the setup shown in Figure 2.2 and the results are shown in Figure 2.6. From the experimental results, it is evident that the proposed hybrid GMPPT technique results in tracking MPP less than 2.4 sec.

2) A new reinitialization method based on the previous history of tracking GP region under both medium and severe nonuniformity in irradiance changes is proposed. From the exper-

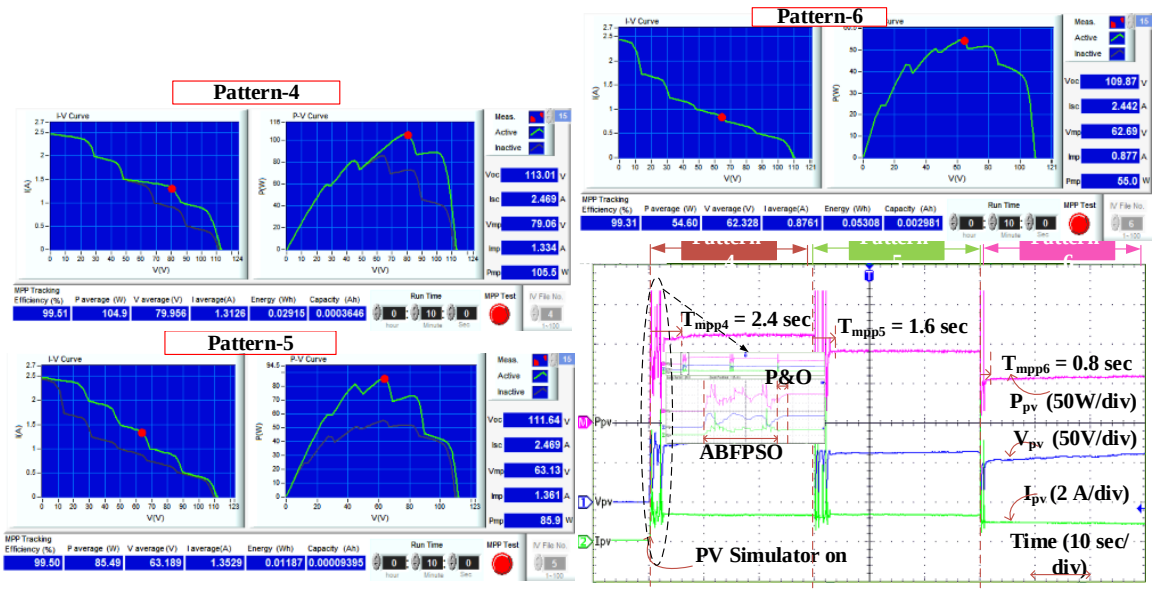

Figure 2.6: Experimentally obtained results of the proposed ABFPSO-P&O MPPT technique.

imental results shown in Figure 2.6, it is evident that the proposed reintialization method results in faster and accurate tracking, i.e., $T_{mpp5} = 1.6\ sec$ and $T_{mpp6} = 0.8\ sec$ under irradiance changes.

In adaptive BF-PSO, mainly premature convergence, parameter tuning, and power oscillations during tracking are minimized. Further, the reinitialization of particles under irradiance changes improves the tracking speed as well as limits the power oscillations during tracking. However, there are more parameters, i.e., three to be tuned in PSO-based MPPT techniques.

Control strategy - 3

The global maximum power point tracking technique based on adaptive salp swarm algorithm and P&O technique for a PV string under partially shaded conditions is proposed to reduce parameter tuning complexity. The experimental verification is done with setup shown in Figure 2.2 and results are shown in Figure 2.7. From the experimental results it is evident that the proposed GMPPT technique results in faster and accurate tracking of MPP with single control parameter.

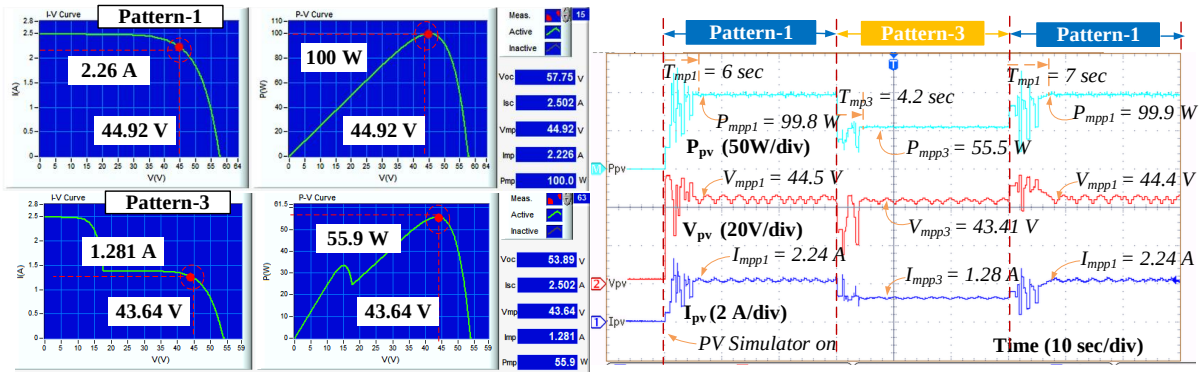

Figure 2.7: Experimentally obtained results of the proposed ASSA-P&O MPPT technique.

In ASSA-P&O, the number of parameters to be tuned and power oscillations during tracking are minimized. However, slower tracking of GP region identification in hybrid MPPT techniques (formed with SC and gradient MPPT techniques) is mainly due to the least fitness particles. When these techniques are applied to off-grid PV systems, reinitialization of the GP

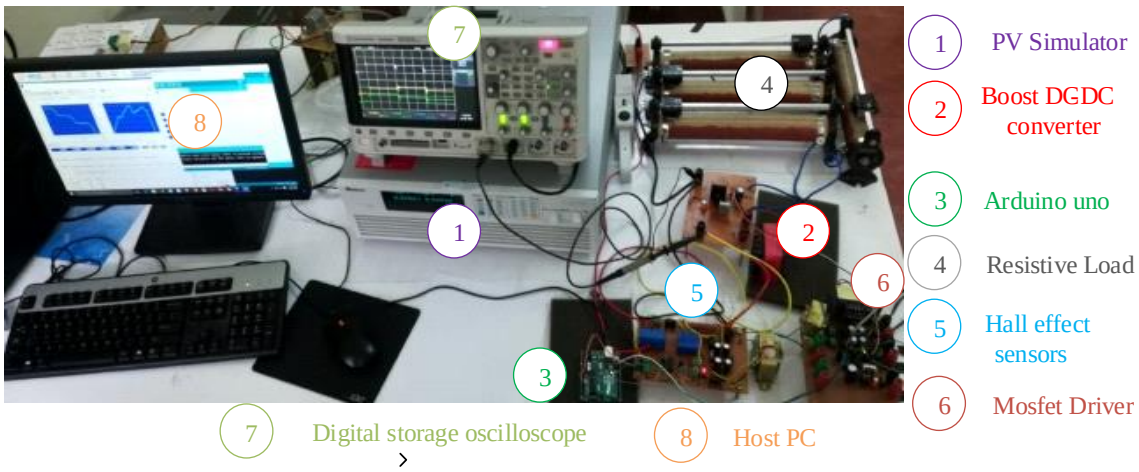

Figure 2.8: Experimental setup.

region identification stage for load changes degrades hybrid MPPT techniques' performance.

Control strategy - 4

In this control strategy, the least fitness particle is accelerated more towards the leader to get faster GP region identification. The leader salp is enhanced in the food source region to get better accuracy. In an off-grid PV system, reinitialization of GP region identification only for irradiance change and direct duty ratio calculation for load change is adopted. Hence, in this contribution,

1) A hybrid global maximum power point tracking of the partially shaded PV system under load variation using adaptive salp swarm algorithm and differential evolution – perturb and observe technique is proposed. The proposed technique is experimentally validated on the setup shown in Figure 2.8 and the results are shown in Figure 2.9. From the experimental results, it is evident that the proposed hybrid MPPT technique results in faster and accurate MPP tracking, where as direct duty ratio calculation helps in identifying GMPP with in a short time 0.1 sec without reinitializing the SI technique.

ASSADE-P&O based GMPPT technique with direct duty ratio calculation under load changes has established as a favorable method for the off-grid PV system. However, for a grid-connected PV system, the hybrid tracking technique's performance optimization must meet

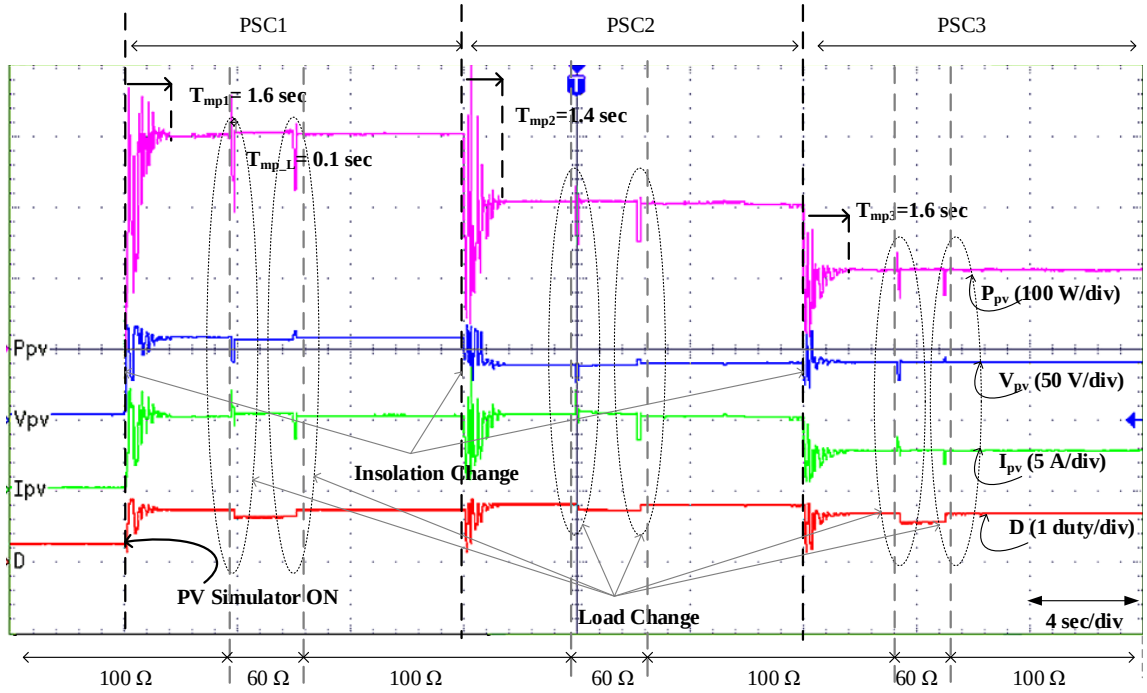

Figure 2.9: Experimentally obtained results of the proposed ASSADE-P&O MPPT technique under load changes.

the grid standards like active power limit control.

Control strategy - 5

Since partial shading is quite a common phenomenon in the grid-connected system and grid code also demands active power control, MPPT with flexible and global maximum power point tracking with hybrid tracking technology and shade detection is vital. Hence, in this contribution,

1) Optimal performance of hybrid tracking technique for maximum and flexible power point tracking of grid-connected PV system under partially shaded conditions is proposed.

2) A simple, fast, and accurate shade detection scheme is proposed using a curve scan with a new steady output P&O (SO-P&O). The proposed technique is experimentally validated by using setup shown in Figure 2.8 and the results are shown in Figure 2.10. From the experimental results, it is evident that the proposed shade detection results in accurate shade and active power limit control to activate FPP mode or MPP mode. self adaptive parameter

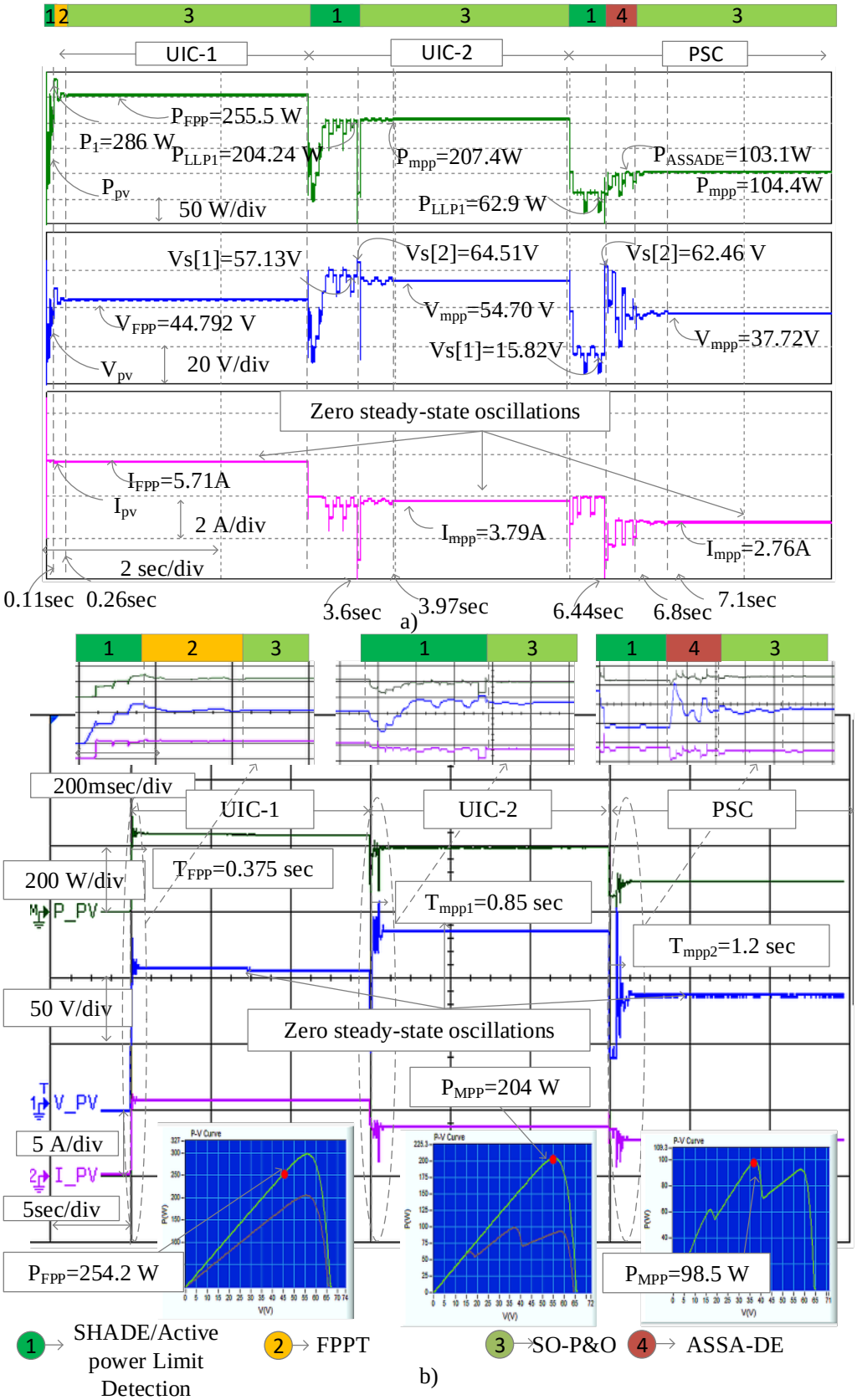

Figure 2.10: Optimal performance of proposed hybrid tracking technique a) Simulation, b) Experimental.

tuning results in accurate tracking of MPP under PSC. SO-P&O technique results in zero steady-state oscillations.

The hybrid tracking technique's proposed optimal performance guarantees both faster and accurate FPP and GMPP tracking with zero steady-state oscillations in a grid-connected PV system.

2.6 Thesis organization

The thesis has been structured into seven chapters, which are organized as explained below:

Chapter 1 briefly introduces an overview of solar photovoltaic systems and maximum power point tracking techniques for photovoltaic systems under partially shaded conditions.

Chapter 2 explores the relevant literature overview of the proposed research work.

Chapter 3 describes the modified PSO-based maximum power point tracking techniques for PV system under partial shading conditions.

Chapter 4 addresses the global maximum power point tracking of partially shaded PV system with adaptive hybrid salp swarm algorithms.

Chapter 5 describes the performance optimization of hybrid tracking techniques for an on-grid PV system.

Chapter 6 presents the comparison of the proposed MPPT techniques with the state-of-art techniques in the literature.

Finally, **Chapter 7** summarizes the main findings of the research work reported in this thesis and suggests the scope for future work.

2.7 Conclusion

In this chapter, a comprehensive bibliographical review on maximum power point tracking techniques of solar PV systems under partial shading conditions has been presented. The shortcomings of all existing approaches have been discussed. Finally, the motivation and contribution to research have been presented. The main contributions and thesis organization are presented.

Chapter 3

Modified PSO-based maximum power point tracking techniques for PV system under partially shaded conditions

Chapter 3

Modified PSO-based maximum power point tracking techniques for PV system under partially shaded conditions

3.1 Introduction

Under uniform irradiance conditions, since the P-V curve is a single-peak curve, conventional MPPT algorithms like P&O and incremental conductance tracks the MPP accurately. But under PSC, the P-V curve is a multi-peak curve, and because of the hill-climbing nature of P&O [4, 47], it may be struck at a local peak. Hence to find the GMPP on multi-peak P-V curve, soft computing techniques like PSO are used. PSO-based GMPPT technique becomes very popular because of its strong exploitation capability. But its popularity is limited due to weak exploration, because of which there could be premature convergence. The weak exploration is due to the attraction of all particles more towards the swarm leader in conventional PSO, as discussed in [48,49]. To balance the exploration and exploitation of the PSO algorithm, control parameters need to be tuned, these being problem-specific. This parameter setting or tuning affects the convergence speed of the PSO algorithm. In the case of PV MPPT, tracking speed depends on the convergence rate of the PSO algorithm [39, 50, 51]. Hence, to get faster tracking of GMPP using the PSO algorithm, parameter control pertaining to the PSO algorithm is essential. In the conventional PSO-based GMPPT technique, power oscillations at the beginning of the exploration process are high due to the high velocity of particles, and this may cause skipping of any local peak. To avoid this, the velocity of particles should be limited. Power oscillations due to the long exploration process of PSO GMPPT technique can be reduced by limiting search space.

Hence, to improve the performance of the basic PSO algorithm, in recent years, several modified versions of conventional PSO algorithm have been proposed for PV MPPT problem [26,27,52] in which the main objective is to avoid premature convergence. In [27], a leader PSO-based GMPPT is proposed in which the global best found in each iteration is enhanced by

using five mutations to the leader or global best. The main idea of authors of this paper [27] is that the best leader results in better particles in the exploration and mutations to avoid stagnation problem at a local peak. However, parameters of PSO algorithm which balance the exploration and exploitation are not tuned and are considered as constants. In [26, 52], an AVPSO-based GMPPT is proposed to control the parameters adaptively during the search. The adaptive parameter control updates the values of inertia factor 'w' and cognitive factor 'c_1' adaptively based on distance from the global best position. On account of parameter control and limited velocity, faster convergence is achieved without premature convergence, and power oscillations during exploration are minimized. Since the global best particle velocity is zero in AVPSO, the present leader position is not updated in the next iteration. The enhanced leader feature of LPSO helps us to explore the global region further to find the best leader. By adding this feature to the exploration process of AVPSO, faster convergence and faster tracking of GMPP can be achieved. In [39], PSO and P&O based GMPPT technique is proposed in which the main idea is to apply P&O algorithm in uniform irradiance conditions and to apply PSO algorithm only in the occurrence of PSC. Using the proposed scheme, unnecessary power oscillations of PSO-based GMPPT in uniform irradiance can be avoided. To detect the occurrence of PSC, change in voltage, current, and power at the instant of irradiance change is considered. However, the window-based search reduces the search space of PSO while control parameters are not tuned to avoid premature convergence.

With the aforementioned advantages of enhanced leader and parameter tuning, an enhanced leader adaptive velocity PSO-based GMPPT technique is proposed. The proposed algorithm uses the advantages of LPSO and AVPSO so that the leader is enhanced in each iteration and parameters of PSO algorithm are tuned adaptively. Furthermore, a new shading detection scheme is proposed in which P-V curve is scanned for multi-peak with variable step P&O (VS-P&O) algorithm. Only in PSC, the proposed GMPPT method with limited search space may be used to find GMPP; From that point onwards, tracking is continued with P&O algorithm. Therefore, the main contributions of this work are: (a) a new fast-tracking PSO based GMPPT technique with adaptive parameter tuning and enhanced leader features. (b) a new shading detection technique to identify the type of shading.

Contributions of this chapter are

- Premature convergence and parameter tuning of most popular PSO based GMPPT techniques are minimized with ELAVPSO.
- High power oscillations during exploration phase of PSO based MPPT techniques are minimized with ABF-PSO P&O hybrid GMPPT technique.
- A new shading detection scheme is proposed, which accurately finds the type of shading from P-V curve scanning.
- A new reintialization method is proposed.

3.2 Proposed MPPT technique based on ELAVPSO algorithm

PSO is a meta-heuristic optimization algorithm to solve nonlinear objective functions. It is mostly used soft computing technique to solve MPPT problems [39] because of its simplicity in implementation. The proposed ELAVPSO algorithm is derived from conventional PSO algorithm and its variants ELPSO and AVPSO algorithms.

3.2.1 Conventional PSO algorithm

PSO is used to find the global maximum in a given search space by using the exploration and exploitation process. It involves the following steps to find the global best.
Step 1: Initialization of the particles.
Step 2: Find the fitness of each particle and updating local best and global best.
Step 3: Find the velocity of each particle by using (3.1).
Step 4: Update the position of each particle by using (3.2) and repeat the steps 2 to 4 until the convergence criteria are reached.

$$vel_i^{k+1} = w \times vel_i^k + c_1 \times r_1 \times \left(X_{lb\_i} - X_i^k\right) + c_2 \times r_2 \times \left(X_{gb} - X_i^k\right) \tag{3.1}$$

$$X_i^{k+1} = X_i^k + vel_i^{k+1} \tag{3.2}$$

where i indicates particle number, k indicates the present iteration, w is weight factor which ranges from 0.4 to 0.9, c_1 is a cognitive factor which ranges from 0.1 to 2, c_2 is social factor ranges from 0.1 to 2, r_1 and r_2 are random numbers $\in$ R (0,1). In general, c_2 is greater than c_1 to move the particle position towards the global best.

3.2.2 Enhanced leader PSO algorithm

In the conventional PSO algorithm, the initial velocity of particles is high and decreases as the global maximum is reached. The initial high velocity of particles may move the particle position out of the search space or may cause skipping of any local peak. Hence, there is a chance for skipping the global peak also, resulting in premature convergence. One of the methods to avoid premature convergence is the enhancement of global best by using mutations so that particles do not struck at any local maxima [27]. In this work, mainly three mutations are applied, which are categorized into a short jump and long jump mutations. They are 1) Gaussian mutation, 2) Cauchy mutation, and 3) Scaling mutation. The first two are used to enhance the role of the leader in the local best region while the third one used for enhancement in the region far away from local best so that the tendency of movement of all particles towards global best does not cause premature convergence. Following are the steps to implement enhanced leader PSO (ELPSO) algorithm.

Step 1: Initialization of the particles.

Step 2: Find the fitness of each particle and updating local best and global best.

Step 3:

[i] Apply Gaussian mutation to the leader by using (3.3). If the fitness value of the leader is more than previous, update the leader.

[ii] Apply Cauchy mutation to the leader by using (3.4). If the fitness value of the leader is more than previous, update the leader.

[iii] Apply Scaling mutation to the leader by using (3.6). If the fitness value of the leader is more than previous, update the leader.

Step 4: Find the velocity of each particle by using (3.1), update the position of each particle by using (3.2) and repeat the step 2 to 4 until the convergence criteria are reached.

$$X_{g1} = X_{gb} + (X_{max} - X_{min}) \times Gaussian\,(o,h) \tag{3.3}$$

where X_{g1} is the global best after Gaussian mutation, X_{gb} is the global best, X_{max} and X_{min} are maximum and minimum values of the control variable, $Gaussian(o,h)$ is the Gaussian distribution function where 'o' is the mean of all particles in the present iteration, and 'h' is the standard deviation. If the fitness of X_{g1} is higher than the fitness of X_{gb}, replace X_{gb} with X_{g1}.

$$X_{g2} = X_{gb} + (X_{max} - X_{min}) \times Cauchy\,(o,s) \tag{3.4}$$

where X_{g2} is the global best after Cauchy mutation, X_{max} and X_{min} are maximum and minimum values of control variable, $Cauchy(o,s)$ is the Cauchy distribution function where 'o' is the mean of all particles in the present iteration and 's' is the scaling parameter which decreases linearly as the iteration number increases to improve the exploitation capability. If the fitness of X_{g2} is higher than the fitness of X_{gb}, replace X_{gb} with X_{g2}.

$$s\,(k+1) = s(k) - \left[\frac{1}{t_{max}}\right] \tag{3.5}$$

$$X_{g3} = X_{gb} + S_f \times \left(X_i^k - X_j^k\right) \tag{3.6}$$

where X_{g3} is the global best after scaling mutation, X_i^k and X_j^k are two random particles in the present iteration, and 'S_f' is the scaling factor. If the fitness of X_{g3} is higher than the fitness of X_{gb}, replace X_{gb} with X_{g3}.

3.2.3 Adaptive velocity PSO algorithm

The velocity equation of both conventional PSO and ELPSO algorithms is same, and weight factor w is constant. It causes the oscillations of global best even after reaching the region of the global peak and slower convergence. In [39] cognitive factor c_1 and social factor

c_2 range from 0 to 2, w and c_1 are kept constant which causes for high velocity of particles at the beginning of the search process, and velocity of the particles is not limited. Even though the ELPSO algorithm can avoid premature convergence by mutations, the parameters need to be tuned for better performance. The present AVPSO algorithm is derived from [26, 52] for direct duty ratio control of the MPPT controller. In the AVPSO algorithm, an adaptive velocity equation is derived based on the distance from the present particle to the global best particle.

3.2.3.1 Selection of adaptive weight factor

The weight factor is selected based on the distance from the present global best to particle position. Thus the oscillations in the vicinity of the global peak decreased.

$$w = \left| X_{gb} - X_i^k \right| \tag{3.7}$$

where X_{gb} is the global best position in the present iteration, and X_i^k is the present particle position.

3.2.3.2 Selection of adaptive cognitive factor

In general, c_2 is greater than c_1 to make the velocity of the particle more towards the global best. In the AVPSO algorithm, c_2 is fixed and ranges (0-2). The c_1 is made adaptive and changes according to the difference in the global best position and local best position of the particle as given in (3.8). Factor 0.5 is taken to make the cognitive term less than social term under all conditions.

$$c_1 = \frac{0.5 \times c_2}{1 + round\left[\frac{\left|X_{gb} - X_{lb\_i}\right|}{vel_{max}}\right]} \tag{3.8}$$

where X_{lb_i} is the local best of i^{th} particle, and vel_{max} is the maximum velocity. The velocity of each particle should be limited to avoid the skipping of any peak of the multi-peak P-V curve. The velocity of a particle is nothing but a change in duty ratio Δd. Hence, velocity should

satisfy the relation $0 < vel < vel_{max}$ and

$$vel_{max} = \frac{(X_{max} - X_{min})}{m}, m>n \tag{3.9}$$

where vel_{max} is the maximum velocity, X_{max} and X_{min} are the maximum and minimum values of duty ratio, and n is the number of modules in the string. With the minimal value of maximum velocity, it takes more time to reach the global maximum and converge. By considering all weather conditions and aging of modules $m>n$ is justified. With all these considerations, the adaptive velocity equation is derived as follows:

$$vel_i^{k+1} = \left|X_{gb} - X_i^k\right| \times vel_i^k + \left\{\frac{0.5 \times c_2}{1 + round\left[\frac{|X_{gb} - X_{lb\_i}|}{Vel_{max}}\right]}\right\} \times r_1 \times \left(X_{lb\_i} - X_i^k\right) + c_2 \times r_2 \times \left(X_{gb} - X_i^k\right) \tag{3.10}$$

where r_1 and r_2 are the random variables and $r_1 = r_2 = random\ (0,\ 1)$. In [52] AVPSO based GMPPT technique, to control the voltage changes during the start of the search process, particles are sorted in the sequence of ascending order followed by descending order and then to the ascending order of the particle positions in the search space. Hence voltage regulation during the tracking of global maximum is improved. The implementation of AVPSO algorithm involves the following steps:

Step 1: Find maximum velocity by using (3.9). Initialization of the particles by using the following expression.

$$X_i = X_{i\_min} + rand(0,1) \times vel_{max}, i = 1,2,3,4 \tag{3.11}$$

Step 2: Find the fitness of each particle and updating local best and global best.

Step 3: Find the velocity of each particle by using (3.10).

Step 4: Update the position of each particle by using (3.2).

Step 5: Sort the particles and repeat steps 2 to 4 until the convergence criteria are reached.

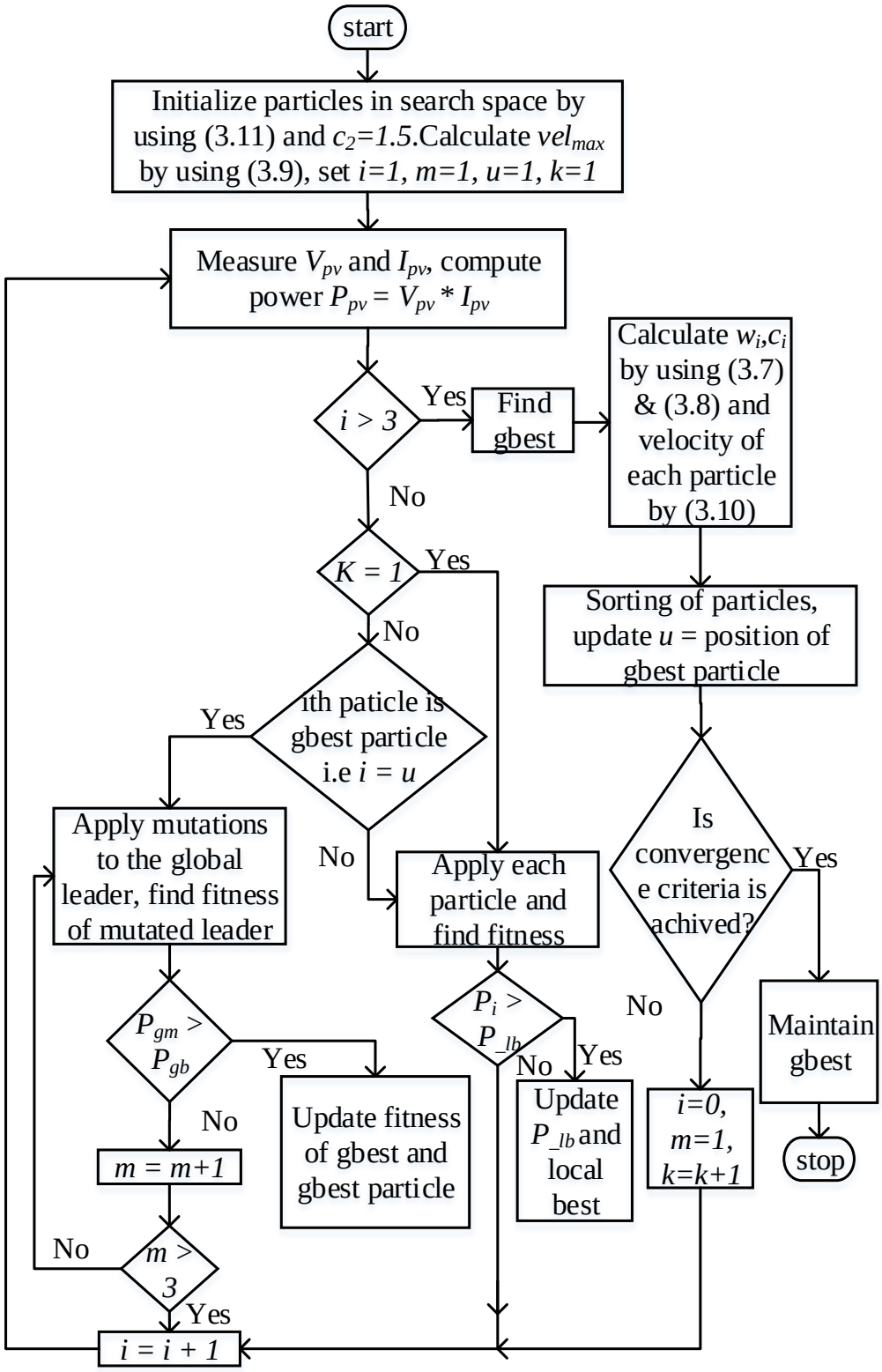

Figure 3.1: Flowchart of the proposed ELAVPSO algorithm.

3.2.4 Proposed enhanced leader adaptive velocity PSO algorithm

An adaptive velocity equation is derived based on the distance from the present particle to the global best particle to tune the parameters of PSO adaptively in AVPSO algorithm. Even though AVPSO has adaptive parameter tuning, there is a chance for further improving convergence speed by enhanced leader feature. By considering all advantages of both ELPSO and AVPSO, a new efficient fast-tracking algorithm is proposed with the dynamic leader and adaptive velocity features. The proposed ELAVPSO algorithm uses the same mutations discussed in section 3.2.2 and the velocity of each particle found from (3.10). The advantage of the dynamic leader as the best leader is that it always results in better performance of other particles and adaptive velocity guaranties parameter tuning of PSO for all dynamic conditions. ELAVPSO starts from the initialization of particles by using (3.11). The proposed algorithm uses three randomly chosen particles in the search space, and the other three particles are based on the knowledge of global best and generated by mutations. The maximum velocity is found from (3.9). Fitness of the global best position is calculated by applying Gaussian, Cauchy, and Scaling mutations. The flowchart of the proposed algorithm is shown in Figure 3.1.

3.2.5 Proposed shading detection technique with variable step P&O

The main idea of the shading detection technique is to apply a conventional algorithm to uniform shading conditions and GMPPT algorithm to non-uniform shading conditions after detecting the type of P-V characteristics under present weather conditions [53–55]. For both conditions, the P-V curve is different and the hill-climbing nature of P&O algorithm is used to identify the occurrence of a single-peak P-V or multi-peak P-V curve. Variable step P&O algorithm uses the variable value of perturbation Δd, and its value is large during the initial tracking process and small in the vicinity of maximum power point. This feature is used to identify the peaks of the P-V curve. The proposed detection scheme scans the P-V curve by using three duty ratios d_1, d_2 *and* d_3, where $d_1 = d_{min}, d_2 = \frac{(d_1+d3)}{2}, d_3 = d_{max}$ and d_{min}, d_{max} are the minimum and maximum values of the search space. After applying each duty ratio, perturbations to the duty ratio are applied by using (3.13).

$$d_j^k = d_j^{k-1} \pm \Delta d^k, where\ j = 1,2\ and\ 3 \tag{3.12}$$

where d_j^k is the duty ratio after perturbation, and d_j^{k-1} is the duty ratio before perturbation.

$$\Delta d^k = M \times \left| \frac{dP}{dV} \right| \tag{3.13}$$

where Δd^k is the perturbation step size, M is a multiplying factor, dP is the difference in power $(P_k - P_{k-1})$, dV is the difference in the voltage $(V_k - V_{k-1})$.

$$\Delta d \leqslant \Delta d_{critical} \tag{3.14}$$

where $\Delta d_{critical}$ is the duty ratio perturbation required for the three-point behavior of the P&O algorithm is given in [13]. Whenever (3.14) is satisfied more than three times, as shown in Figure 3.2, it guarantees that the peak is reached and the corresponding value of duty ratio d_{j_final} is stored. To identify the shading type, the following conditions are to be tested.

$$\begin{aligned} (Max(d_{j\_final})) - (Min(d_{j\_final})) &\leqslant vel_{max} \Rightarrow single\ \ peak\ \ P-V\ \ curve \\ (Max(d_{j\_final})) - (Min(d_{j\_final})) &\geqslant vel_{max} \Rightarrow multi\ \ peak\ \ P-V\ \ curve \end{aligned} \tag{3.15}$$

Once the shading detection is completed, a fixed-step P&O algorithm is used for tracking MPP of a single-peak P-V curve starting from the duty ratio $d = Max(d_{j\_final})$, and in the case of multi-peak P-V curve, the proposed ELAVPSO algorithm is used for finding the global peak. Once the GMPP is found, all PSO variant's duty ratio does not change unless the particles are

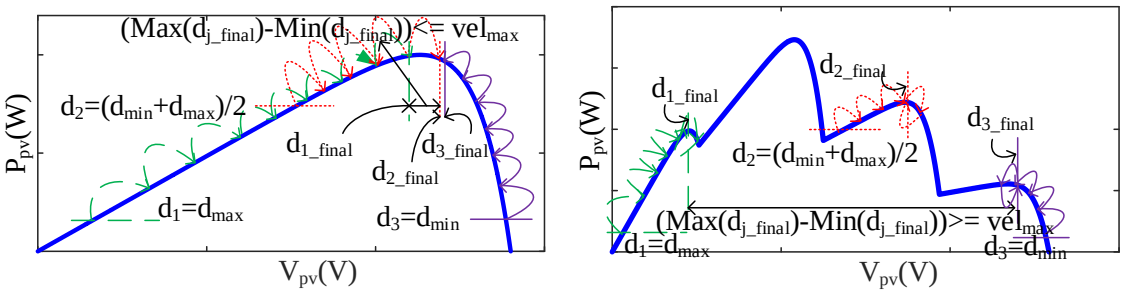

Figure 3.2: Shading detection method by using VS-P&O algorithm.

reinitialized. Hence, in the proposed shading detection scheme, if the GMPP is found, tracking is continued with a fixed-step P&O algorithm until another irradiance change is detected. With a fixed-step P&O algorithm, the operating point is maintained at GMPP even for small changes in irradiance, which cannot be detected as a change in weather conditions with the help of (3.17) & (3.18) that have been used for irradiance change detection. The value of perturbation Δd in the fixed-step P&O algorithm is smaller than $\Delta d_{critical}$ in the VS-P&O algorithm to maintain

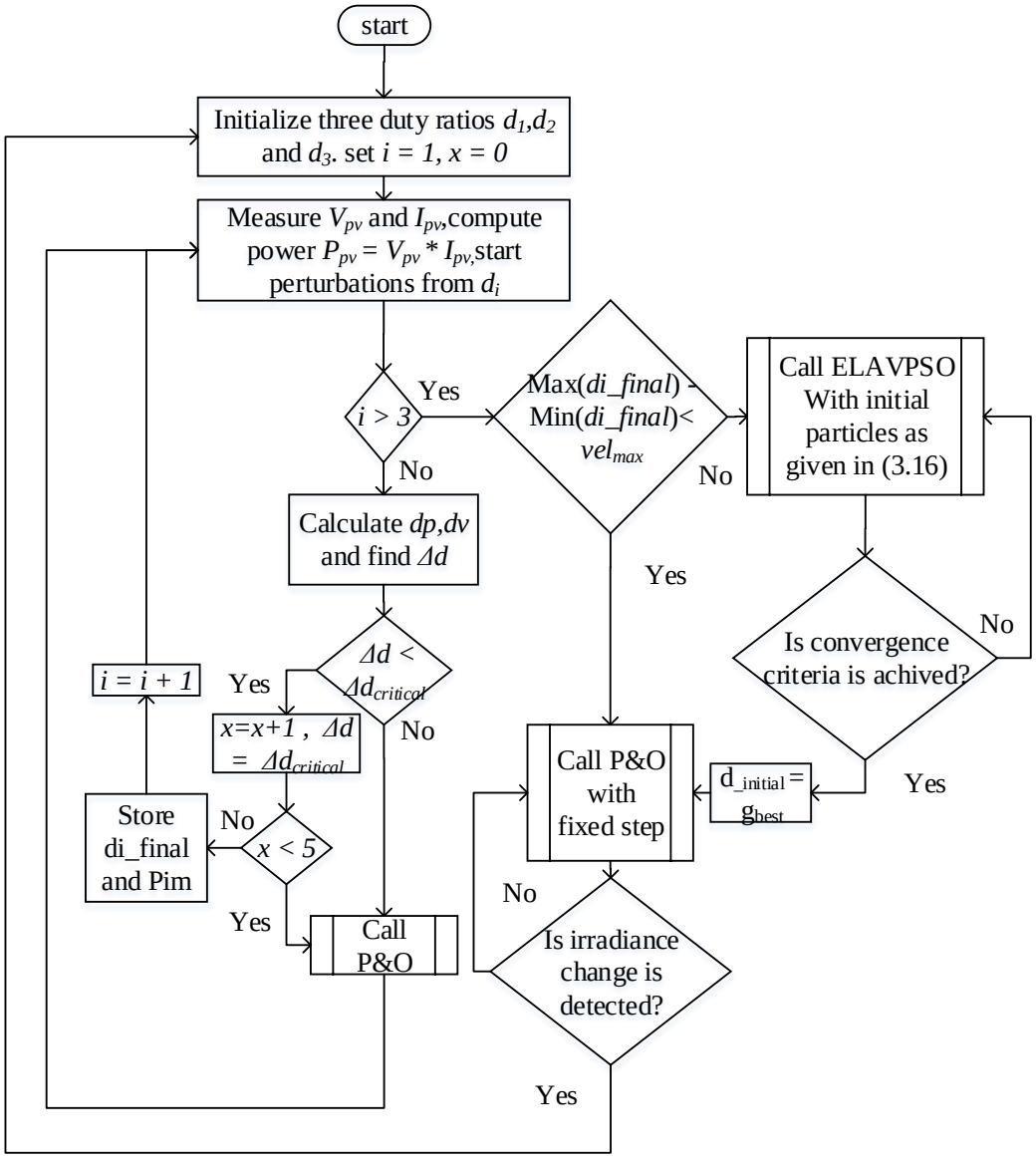

Figure 3.3: Flowchart of proposed shading detection technique.

less steady-state power oscillations. The flowchart of the proposed shading detection technique is shown in Figure. 3.3. The initial value of the population in ELAVPSO algorithm during GMPP tracking is

$$\begin{aligned} d_1 &= Min(d_{j\_final}) \\ d_2 &= \frac{d_1 + d_3}{2} \\ d_3 &= Max(d_{j\_final}) \end{aligned} \tag{3.16}$$

Irradiance change is detected by using (3.17) & (3.18).

$$\left| \frac{V_k - V_{k-1}}{V_k} \right| \geqslant 0.2 \tag{3.17}$$

$$\left| \frac{I_k - I_{k-1}}{I_k} \right| \geqslant 0.1 \tag{3.18}$$

With the proposed scheme of shading detection, MPP tracking is started with shading detection, and if uniform shading is detected, tracking is continued with fixed-step P&O algo-

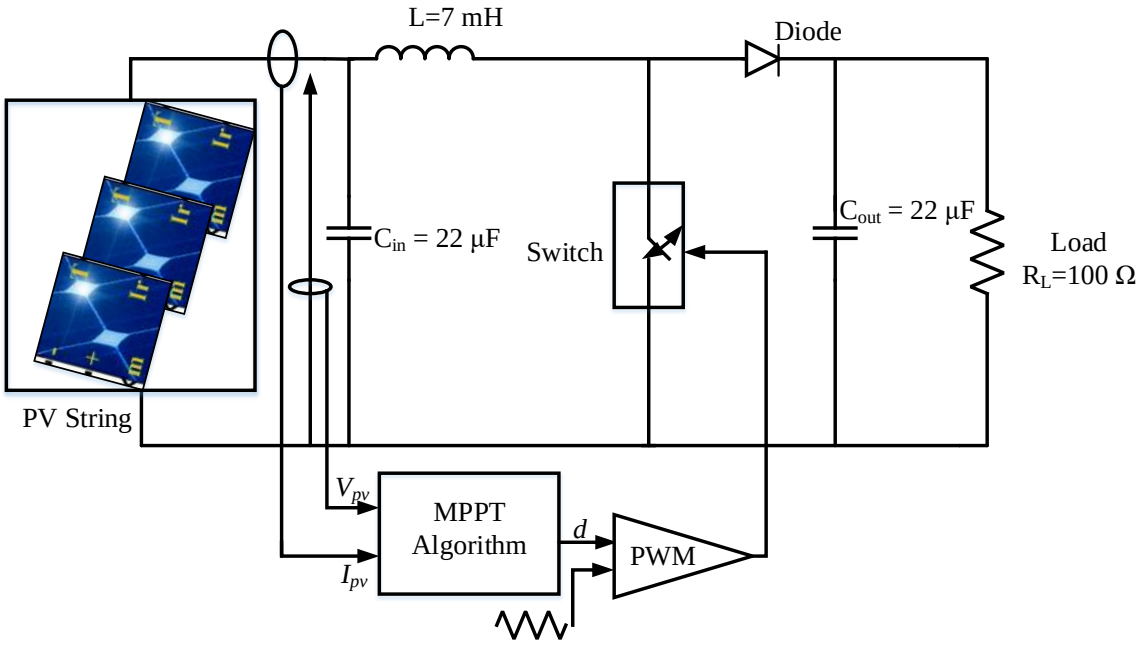

Figure 3.4: Schematic diagram of MPPT controller.

rithm, if non-uniform shading is detected, GMPP is found with ELAVPSO algorithm and from that point onwards tracking is continued further with fixed-step P&O algorithm . Hence, there is no need for the GMPPT technique for tracking MPP during the starting of the system and for uniform irradiance conditions.

3.2.6 Simulation and experimental justification

3.2.6.1 Simulation studies of the proposed algorithms

The proposed algorithms are simulated using MATLAB/ Simulink software. A boost DC-DC converter is used as an MPPT controller, and the schematic diagram is given in Figure. 3.4. Direct duty ratio control is used for generating PWM pulses to control the switch in the DC-

Table 3.1: Details of PV system used in simulation and hardware.

S.No	Parameter	Specifications
1	Number of modules in the string	4
2	Each module rating	V_{OC} = 14 V, I_{SC} = 2.5 A, V_{MPP} = 11.25 V, P_{MPP} = 25 W.

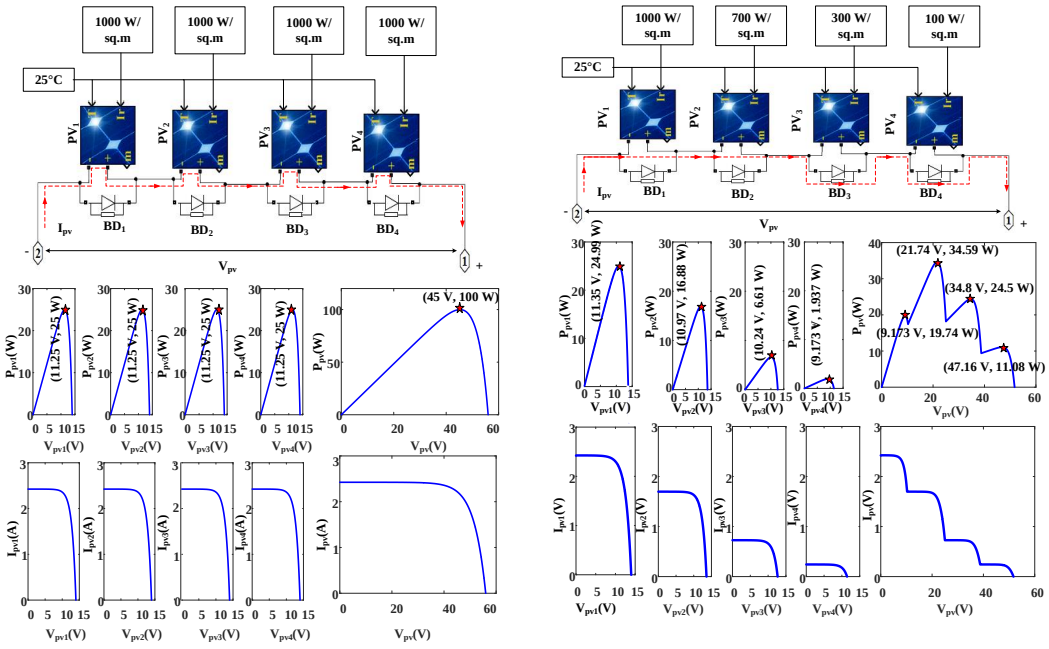

(a) (b)

Figure 3.5: P-V and I-V curve of 4 panel string a) Uniform irradiance, b) PSC.

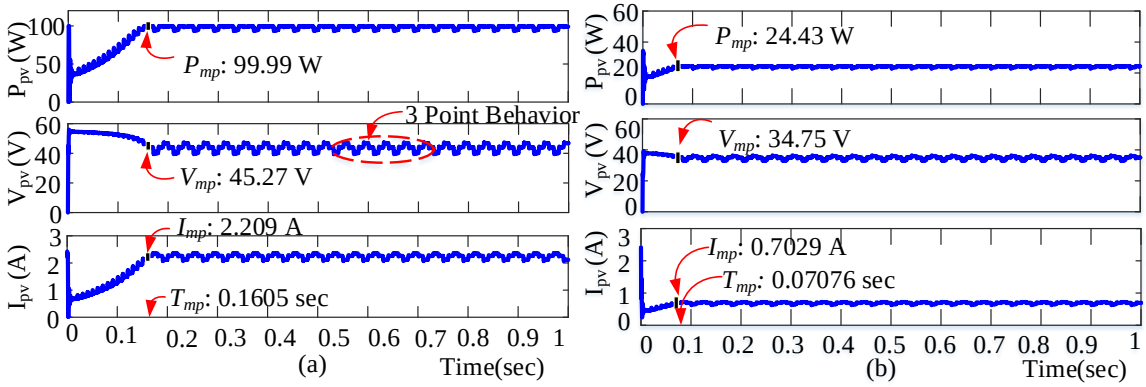

Figure 3.6: Simulation results of P&O MPPT algorithm under a) uniform irradiance, b) PSC.

DC converter. In this method, V_{pv} and I_{pv} are the inputs to the MPPT algorithm block, which generate a duty ratio that is converted to PWM pulses by using a comparator. The proposed algorithms are simulated at a sample time $T_s = 10\ msec$ and a switching frequency of $f_s = 20\ KHz$. Simulation results of the proposed algorithm under the uniform irradiance and PSC are given in Figure 3.6, Figure 3.7, and Figure 3.8.

Case (1): Under uniform irradiance conditions the irradiance is set as PV1: 1 KW/m^2, PV2: 1 KW/m^2, PV3: 1 KW/m^2, PV4: 1 KW/m^2 as shown in Figure 3.5. The P-V curve obtained with this irradiance is a single-peak curve and MPP is at $V_{pv} = 45\ V$, $I_{pv} = 2.2\ A$, $P_{pv} = 100\ W$.

P&O algorithm is simulated by using duty ratio perturbation $\Delta d = 0.03$ to get three-point behavior in the steady-state. The tracking of MPP is started from duty ratio $d_{init} = 0.1$ and under uniform irradiance conditions, P&O algorithm reaches the peak within time $T_{mp} = 0.1605\ sec$. In Fig. 3.6.a), it is observed that power, voltage and current oscillate around $P_{mp} = 99.99\ W$, $V_{mp} = 45.27\ V$ and $I_{mp} = 2.209\ A$ in steady-state. These oscillations are a drawback of conventional P&O algorithm.

Table 3.2: Parameters of PSO used in simulation and hardware.

S.No	Parameter	Specifications
1	Inertia Constant w	0.4
2	Acceleration Constants c_1, c_2	1.2,2
3	Limits of Search Space $[dmin, dmax]$	[0.1, 0.9]
4	Scaling Factor F	0.8

The conventional PSO and its variants overcome this drawback. All these algorithms are forced to run with the same parameters as given in Table 3.2. In the conventional PSO algorithm, four particles are initialized randomly in the search space, and tracking of MPP is completed at $T_{mp} = 0.402\ sec$. The tracking time of the PSO algorithm is given by $T_{mp} = (T_s \times number\ of\ particles \times iteration\ count)$. Once the GMPP is found at $V_{mp} = 45.31\ V, I_{mp} = 2.207\ A$ and $P_{mp} = 99.98\ W$ there is no further oscillations in the power. It is because the convergence criteria are satisfied and convergence criteria used for the given system is the difference in the maximum and minimum value of fitness of particles which is less than 10 percent of rated power while the difference in the maximum and minimum value of particle positions is less than 0.05.

$$\begin{aligned} Max(P) - Min(P) &< 0.1 \times P_{rated} \\ Max(d) - Min(d) &< 0.05 \end{aligned} \tag{3.19}$$

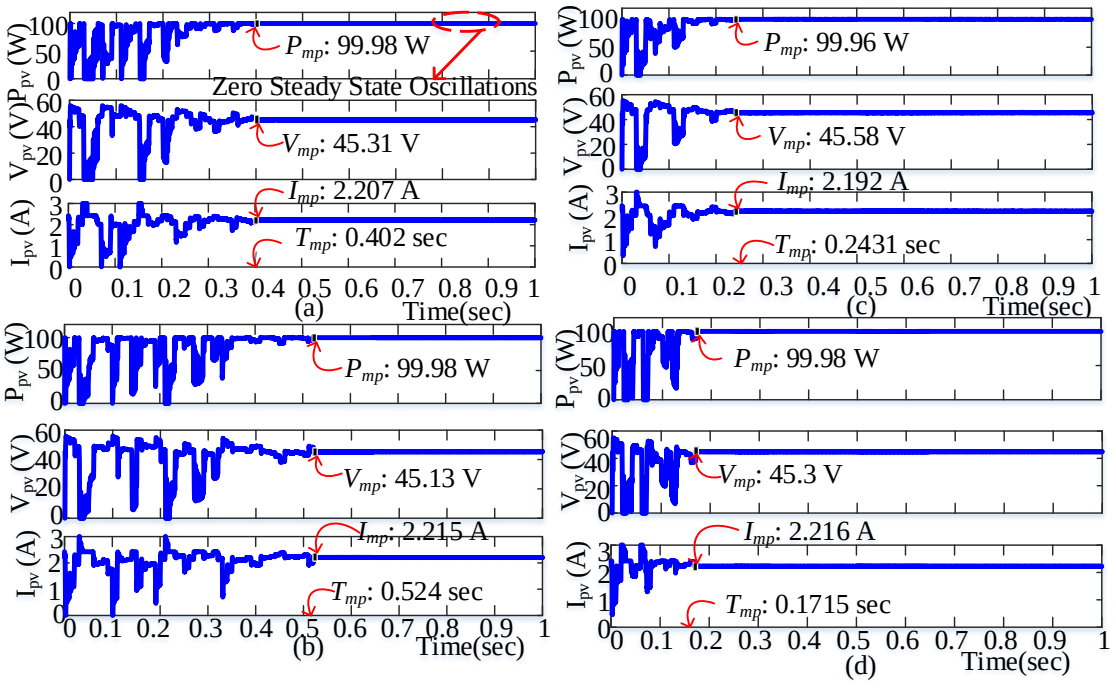

Figure 3.7: Simulation results of PSO-based GMPPT algorithms under uniform irradiance conditions a) PSO, b) ELPSO, c) AVPSO, d) ELAVPSO.

In a conventional PSO algorithm, since the velocity of each particle is not limited, and parameters of the PSO algorithm are fixed, there is a chance of premature convergence. The mutations are applied to the global leader in ELPSO algorithm to avoid premature convergence, and it takes $T_{mp} = 0.524\ sec$ to reach GMPP. It takes more time for convergence than the conventional PSO algorithm due to additional three mutations applied along with four particles. Therefore, in each iteration, the number of particles used for searching GMPP becomes seven. In the AVPSO algorithm, the same number of particles used in PSO algorithm is used with the adaptive velocity in (3.10). AVPSO algorithm parameters are made adaptive to the global best, and velocity of each particle is limited to vel_{max}. In the simulation, constant m in (3.9) is taken as five, which is greater than the number of panels (= 4) in the string. In the simulation result shown in Figure 3.7. (c), it is observed that voltage oscillations are regulated due to the sorting of particles. The AVPSO GMPPT technique reaches GMPP in time $T_{mp} = 0.2431\ sec$ and a steady-state is attained at $P_{mp} = 99.96\ W, V_{mp} = 45.58\ V$ and $I_{mp} = 2.192\ A$.

The proposed ELAVPSO algorithm uses mainly three particles, while the other three particles are generated from the mutations of the global best to search the GMPP in the given search space. Even though a total of six particles are applied in each iteration, it is observed that convergence criteria are reached quickly than AVPSO algorithm with four particles due to the combined effect of dynamic leader and adaptive velocity. It takes a tracking time $T_{mp} = 0.1715\ sec$ and steady-state operating points of $P_{mp} = 99.98\ W, V_{mp} = 45.3\ V$ and $I_{mp} = 2.216\ A$ to reach the GMPP.

Case (2): under PSC the irradiance is set as PV1: 1 KW/m^2, PV2: 0.7 KW/m^2, PV3: 0.3 KW/m^2, PV4: 0.1 KW/m^2 as shown in Figure 3.5. The P-V curve obtained with this irradiance results in multi-peak and the MPPs are at LMPP1 (9.173 V, 19.74 W), LMPP2 (21.74 V, 34.59 W), LMPP3 (34.8 V, 24.5 W), and LMPP4 (47.16 V, 11.08 W). Among the local peaks, LMPP2 is the global peak for the given PSC. Hence, all the MPPT algorithms presented in this work are tested with the multi-peak P-V curve.

From simulation results of P&O algorithm shown in Figure 3.6.b), it is observed that tracking of GMPP on multi-peak P-V curve is not possible as it may be struck at any local MPP. For the present PSC case, P&O algorithm track MPP at LMPP3, and it is not GMPP. Even though P&O algorithm and the proposed GMPPT method draw the same amount of power under uniform irradiance conditions, i.e., 99.99 W and 99.98 W respectively, the proposed

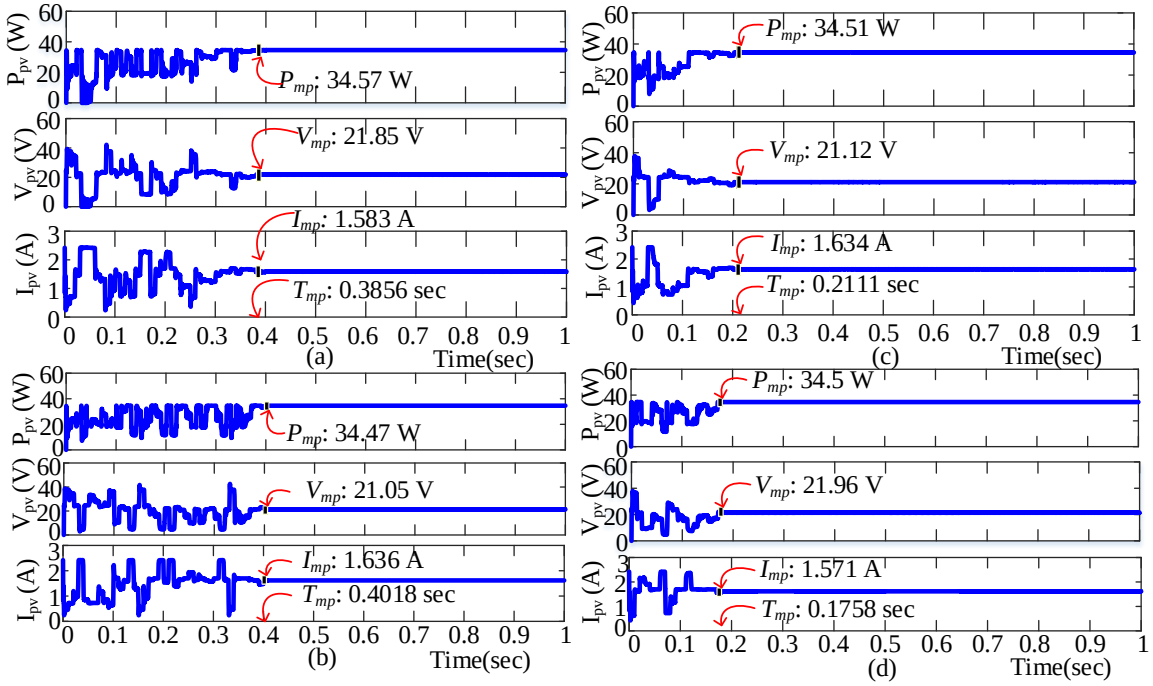

Figure 3.8: Simulation results of PSO based GMPPT algorithms under PSC a) PSO, b) ELPSO, c) AVPSO, d) ELAVPSO.

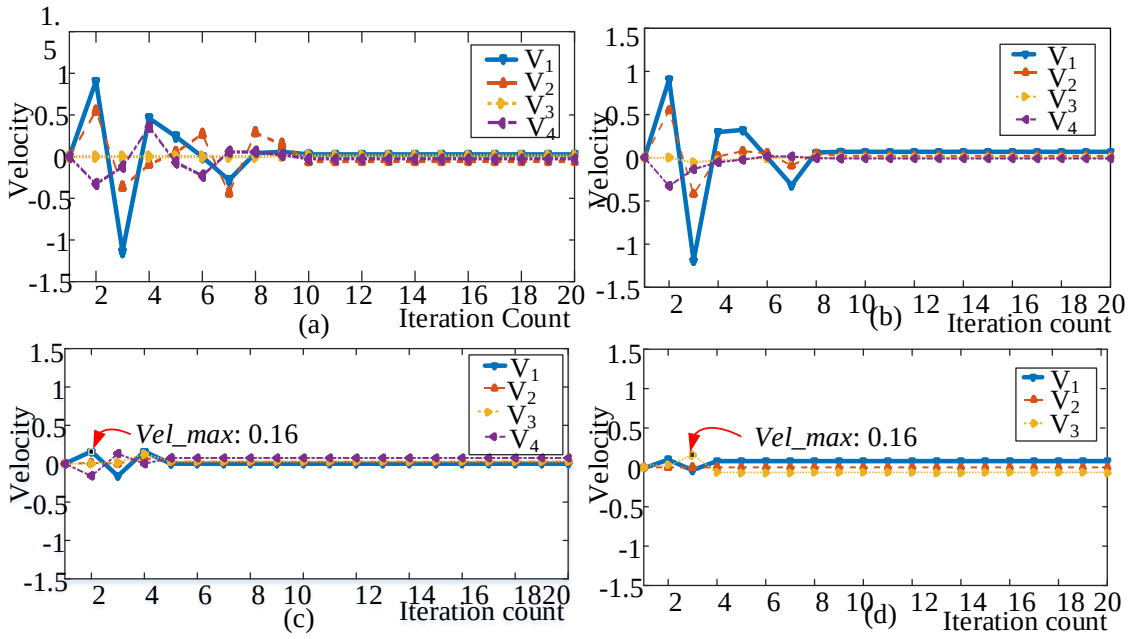

Figure 3.9: Simulation results of velocity variations of a) PSO, b) ELPSO, c) AVPSO, d) ELAVPSO GMPPT techniques.

Table 3.3: Simulation results of MPPT techniques.

	P&O			PSO			ELPSO			AVPSO			Proposed		
	T_{mp} (sec)	P_{mpp}(W)	$\%\eta_{static}$	T_{mp}(sec)	P_{mpp}(W)	$\%\eta_{static}$	T_{mp}(sec)	P_{mpp}(W)	$\%\eta_{static}$	T_{mp}(sec)	P_{mpp}(W)	$\%\eta_{static}$	T_{mp}(sec)	P_{mpp}(W)	$\%\eta_{static}$
Uniform (GMPP=100 W)	0.16	99.99	99.99	0.402	99.98	99.98	0.524	99.98	99.98	0.2431	99.96	99.96	0.1715	99.98	99.98
PSC (GMPP=34.59 W)	0.07	24.43	70.62	0.3856	34.57	99.94	0.402	34.47	99.65	0.211	34.51	99.77	0.1758	34.5	99.77

GMPPT method extracts more power under partially shaded conditions. From the simulation results shown in Figure 3.8 and Table 3.3, the P_{mp} achieved by the proposed method is 34.5 W, whereas P&O draws 24.43 W only. There is a power difference of 10.07 W between P_{mp} achieved by the proposed GMPPT method and P&O algorithm. All the PSO GMPPT algorithms can reach GMPP; among all algorithms, ELAVPSO GMPPT algorithm takes the lowest time and iterations to reach the global peak. Further, the P&O MPPT technique has an advantage over PSO GMPPT methods, such as fewer power oscillations during transient part of MPPT in uniform irradiance conditions, and this motivated the authors of this thesis to propose the shading detection technique, as discussed in section 3.2. The change in velocity of each particle of the PSO GMPPT algorithms is shown in Figure 3.9. With conventional PSO based GMPPT, global peak can be reached, but during tracking, when the velocity of particles is not limited, the position of particles may go outside the search space, and it takes ten iterations to converge. In the ELPSO GMPPT technique, the leader is updated in any of three mutations. Hence global peak is found without any premature convergence. The ELPSO algorithm takes a tracking time T_{mp} = 0.4018 sec, which is more than that of the conventional PSO algorithm. This is due to the fact that the number of population applied in each iteration is more, and the velocity of the particles is not limited. With the AVPSO algorithm, GMPP is reached in time T_{mp} = 0.2111 sec, and within five iterations, all particles converge, and the velocity is limited to vel_{max} = 0.16 which helps to avoid the skipping of any local MPP and thus avoid the premature convergence.

The proposed ELAVPSO algorithm takes advantage of both ELPSO and AVPSO algorithms as it takes less time to converge in both cases of irradiance conditions. Even under PSC also ELAVPSO algorithm takes tracking time of T_{mp} = 0.1578 sec, and in steady-state, it operates at global peak P_{mp} = 34.58 W and V_{mp} = 21.96 V.

Case (3): When weather conditions are dynamic, changing from uniform to PSC, the proposed shading detection technique is simulated, and the result is shown in Figure 3.10. Time instants

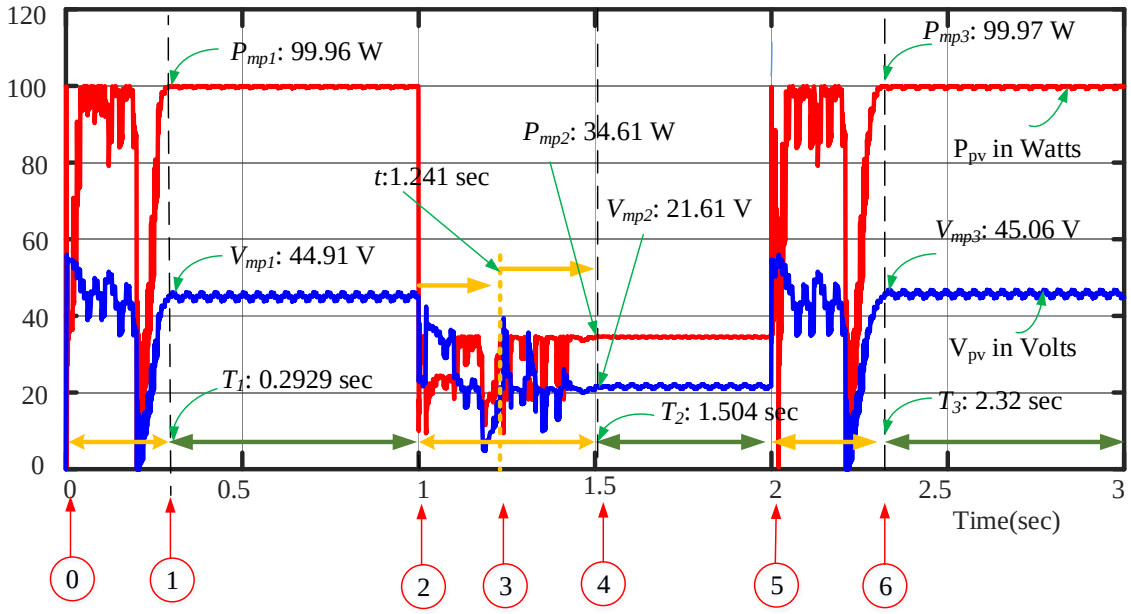

Figure 3.10: Simulation results of proposed shading detection technique.

0 to 6 indicates a sequence of algorithms applied to change in irradiance conditions. At instant 0 shading detection is started and VS-P&O algorithm uses three duty ratios $d_1 = 0.1$,$d_2 = 0.5$ and $d_3 = 0.9$ for scanning P-V curve.

At instant 1 based on (3.15) a single-peak is detected and a fixed-step P&O algorithm with a small value of perturbation Δd= 0.001 is used for tracking MPP from initial duty ratio d_{im_final} where d_{im_final} is the duty ratio which gives maximum power during the scanning of P-V curve among d_{i_final}. At instant 2, irradiance change is detected, and the algorithm changed from fixed-step P&O algorithm to VS-P&O algorithm for scanning P-V curve. At instant 3, multi-peak P-V curve is detected, and ELAVPSO GMPPT technique is activated with the initial population as given in (3.16). After reaching convergence criteria, GMPP is found, and at instant 4, a fixed-step P&O algorithm is activated to continue tracking of GMPP. At instant 5, again irradiance changes from PSC to uniform and VS-P&O algorithm is activated to detect the type of P-V curve. Since, uniform irradiance is applied after instant 5 onwards, at instant 6, the proposed shading detection finds a single-peak P-V and then fixed-step P&O algorithm is activated. Therefore, with this proposed shading detection technique, the GMPPT algorithm is used for tracking GMPP under PSC, in uniform irradiance conditions, conventional P&O algorithm is applied.

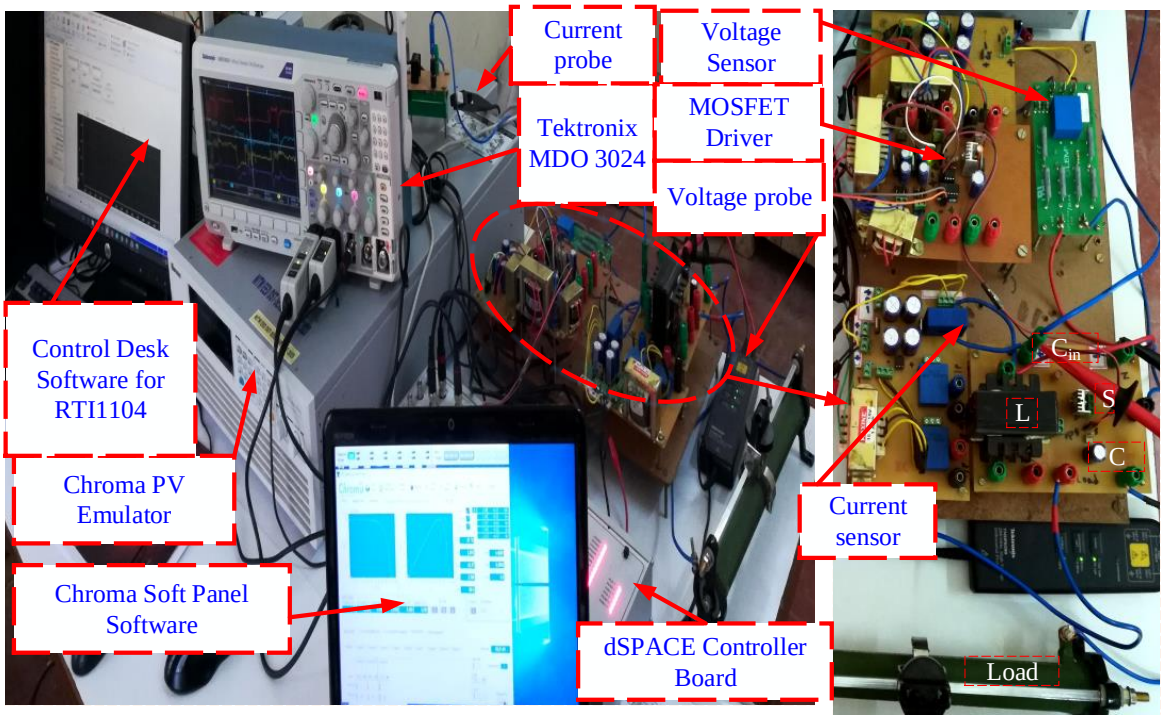

Figure 3.11: Experimental setup.

3.2.6.2 Hardware prototype and experimental validation of proposed algorithms

To validate the proposed algorithms experimentally, a laboratory prototype of the Dc-DC boost converter shown in Figure 3.11 is used as an MPPT converter. The details of the prototype are

Table 3.4: Details of the prototype used for experimental validation.

S.No	Component	Specifications
1	PV Simulator	Each Module Rating $V_{OC} = 14\ V$, $I_{SC} = 2.5\ A, V_{MPP} = 11.25\ V$, $P_{MPP} = 25\ W$.
2	dSPACE Control Control Board	RTI platform support RTI1104
3	Power Switch	MOSFET IRF840
4	Power Diode	MUR1560
5	Inductor	7 mH
6	Buffer Capacitor	22 μF
7	Output Capacitor	22 μF
8	Resistive Load	100 Ω
9	Switching Frequency	20 KHz

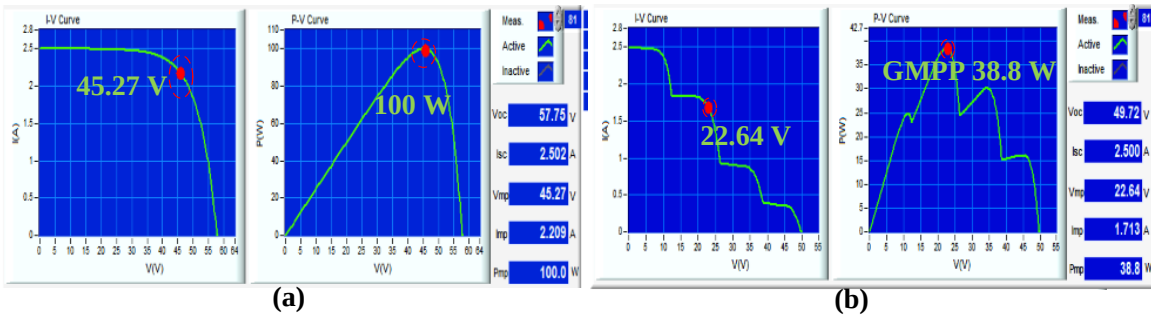

Figure 3.12: *I-V* and *P-V* curves used for emulating a) uniform irradiance, b) PSC.

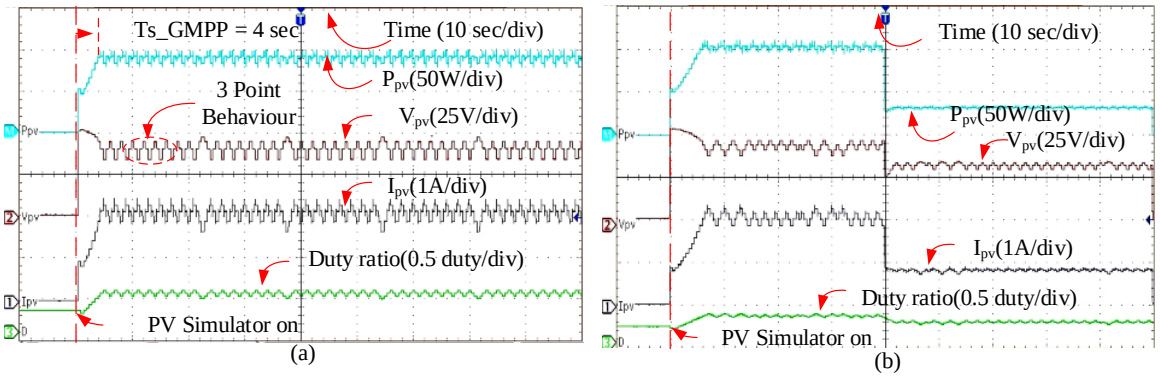

Figure 3.13: Experimentally obtained results of P&O MPPT algorithm under a) uniform irradiance, b) PSC.

given in Table 3.4. The behavior of the PV string under uniform and PSC are emulated with I-V and P-V curves shown in Figure. 3.12 by using a Chroma made 62100H-600S PV simulator.

A) Experimental validation under uniform irradiance

Experimental validation of uniform irradiance conditions is done with emulation of single-peak P-V curve and MPP is at $(P_{mp} = 100\ W, V_{mp} = 45.27\ V)$. All the algorithms are made to run with the same sample time $T_s = 0.5\ sec$. P&O algorithm is made to run with initial duty $d = 0.3\ and\ \Delta d = 0.05$. From the results shown in Figure 3.13.a), the P&O algorithm tracks the MPP in 4 sec and the results obtained are $(P_{mp} = 97\ W, V_{mp} = 45.54\ V)$. All the PSO algorithms are made to run under the same constraints and results are shown in Figure 3.14. Conventional PSO GMPPT technique tracks GMPP within 20 sec and the results obtained are $(P_{mp} = 99.92\ W, V_{mp} = 45.34\ V)$. Duty ratio oscillations are more in the initial stage of tracking, and all particles converge in steady-state, which results in zero

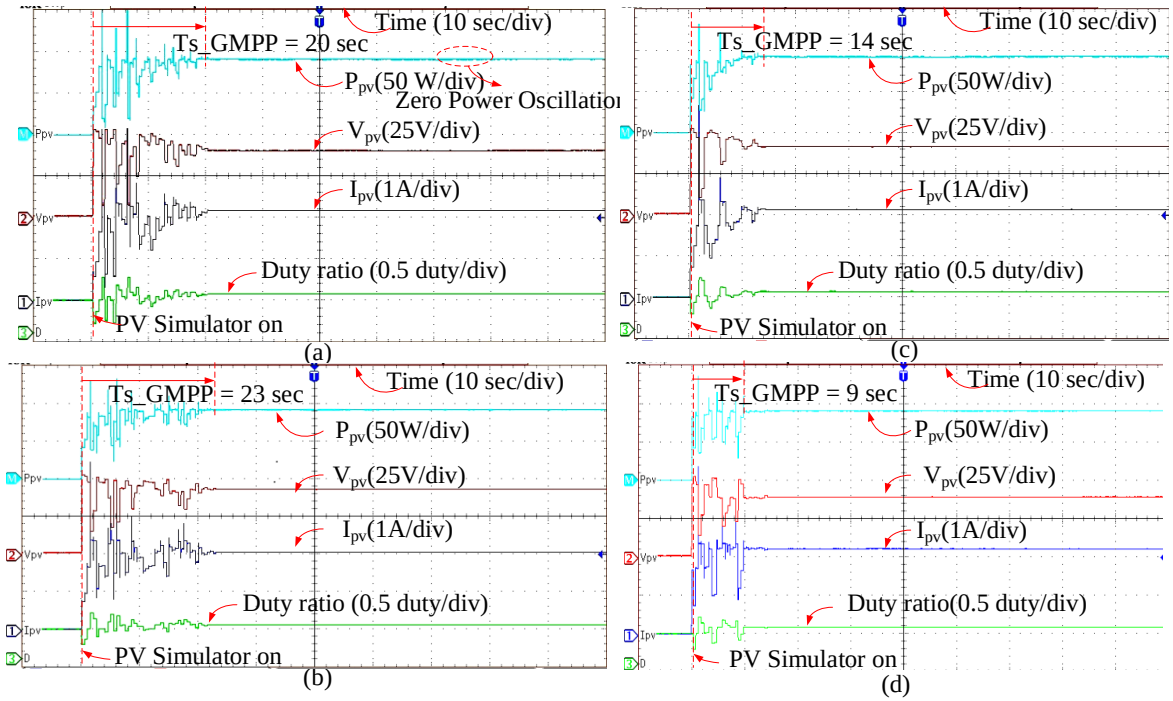

Figure 3.14: Experimentally obtained results of PSO based GMPPT algorithms under uniform irradiance a) PSO, b) ELPSO, c) AVPSO, d) ELAVPSO.

steady-state power oscillations. ELPSO algorithm uses the mutations to avoid premature convergence and takes more time to converge because of more particles in each iteration. The results obtained with ELPSO GMPPT technique are $(P_{mp} = 99.95\ W, V_{mp} = 45.21\ V)$, and reach the GMPP in 23 sec. The AVPSO GMPPT technique results in less voltage variations during tracking than PSO and ELPSO algorithms and takes less time to converge due to its adaptive velocity nature. The results obtained with AVPSO GMPPT technique are $(P_{mp} = 99.98\ W, V_{mp} = 45.22\ V)$, and it reaches GMPP in 14 sec.

The proposed ELAVPSO GMPPT technique reaches GMPP faster than conventional PSO, ELPSO, and AVPSO GMPPT techniques because of its superior leader enhancement capability and adaptive velocity. The results obtained with ELAVPSO GMPPT technique are $(P_{mp} = 99.99\ W, V_{mp} = 45.21\ V)$, and it takes 9 sec to reach GMPP.

B) Experimental validation under irradiance changes

Irradiance changes are emulated with two conditions: first, a 40-sec single-peak P-V curve is applied and after that multi-peak P-V curve is applied. Irradiance change is detected with

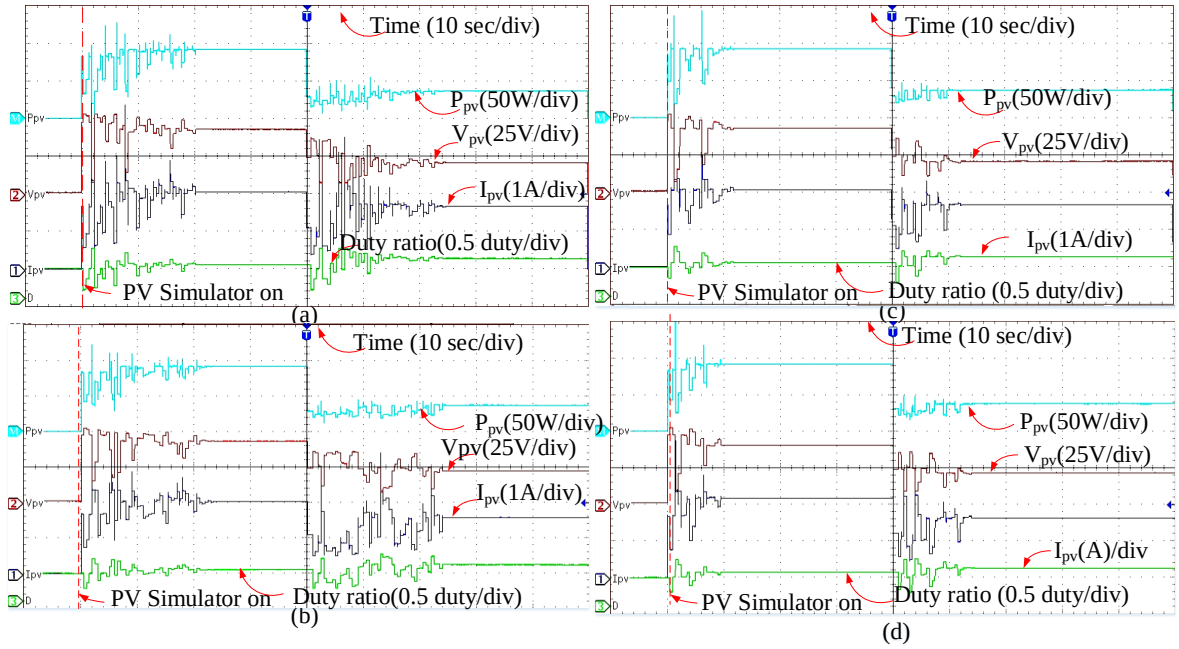

Figure 3.15: Experimentally obtained results of PSO based GMPPT algorithms under irradiance changes a) PSO, b) ELPSO, c) AVPSO, d) ELAVPSO.

Table 3.5: Experimentally obtained results of MPPT techniques.

	P&O			PSO			ELPSO			AVPSO			Proposed		
	T_{mp} (sec)	P_{mpp}(W)	$\%\eta_{static}$	T_{mp}(sec)	P_{mpp}(W)	$\%\eta_{static}$	T_{mp}(sec)	P_{mpp}(W)	$\%\eta_{static}$	T_{mp}(sec)	P_{mpp}(W)	$\%\eta_{static}$	T_{mp}(sec)	P_{mpp}(W)	$\%\eta_{static}$
Uniform (GMPP=100 W)	6	99.5	99.5	20	99.9	99.9	21	99.9	99.9	12	99.8	99.8	9	99.9	99.9
PSC (GMPP=38.8 W)	1	30.2	77.83	22	30.3	78.09	24	38.6	99.48	12	38.7	99.74	12	38.7	99.74

(3.17) and (3.18). From the Figure 3.13.b), P&O algorithm is not able to track GMPP, and the operating point under PSC is $(P_{mp} = 30.2\ W, V_{mp} = 31.57\ V)$, and it operates at LMPP3. Thus, PSO algorithms are tested for achieving GMPP and results are shown in Figure 3.15 and Table 3.5. Conventional PSO algorithm takes more time to converge under PSC due to oscillations of particles before convergence which may lead to premature convergence. Hence, ELPSO algorithm is tested for irradiance changes, and it is able to reach GMPP without any tendency of premature convergence, but it takes more time for convergence because of increased particles in the form of mutations. AVPSO algorithm results in almost the same tracking time for both the irradiance conditions.

But, as discussed in section 3.2.4, ELAVPSO algorithm results in faster convergence and from the observations in simulation and experimental results, performance comparison be-

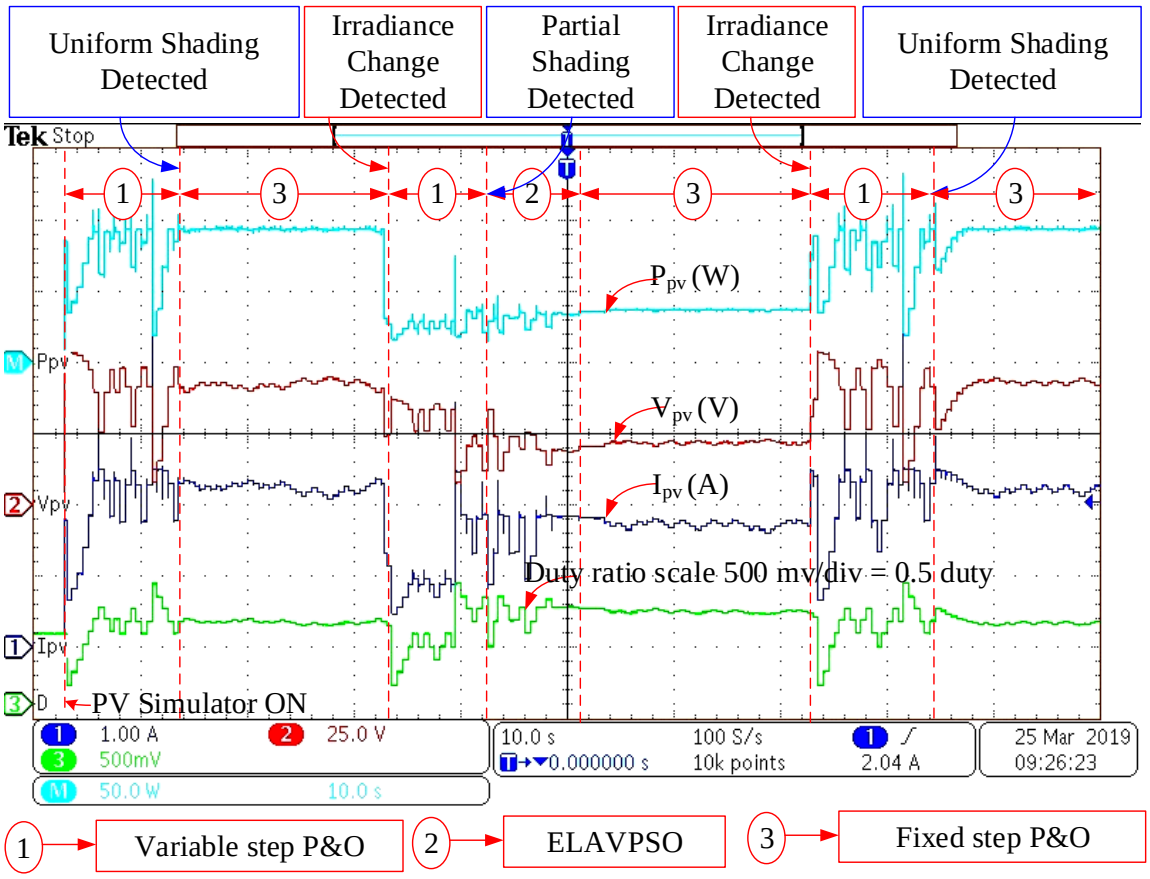

Figure 3.16: Experimentally obtained results of the proposed shading detection technique.

tween PSO algorithms is given in Table 3.6. Since ELAVPSO algorithm results in faster tracking, it is used as GMPPT algorithm in the proposed shading detection technique.

C) Experimental validation of proposed shading detection technique

The proposed shading technique is verified under three irradiance changes. For the first 30-sec uniform irradiance is emulated with a single-peak P-V curve, for the next 40 sec PSC

Table 3.6: Performance comparison between PSO algorithms.

S.No	Algorithm	Parameter Control	Mutations to Global Best	Convergence Speed
1	PSO	Remains constant	-	slow
2	ELPSO	Remains constant	Three mutations	slow
3	AVPSO	Adaptive	-	fast
4	ELAVPSO	Adaptive	Three mutations	faster

is emulated with multi-peak P-V curve, and in the last 30 sec uniform irradiance is applied as shown in Figure 3.16. After the PV simulator is on, shading detection is done with VS-P&O algorithm. It detects uniform shading because of which fixed-step P&O algorithm is activated with perturbation $\Delta d = 0.01$. When irradiance change is found at $t = 30$ *sec*, shading detection is activated, and multi-peak P-V curve due to PSC is found. Thus the proposed GMPPT technique ELAVPSO is activated to detect GMPP. Once the global peak is found, fixed-step P&O algorithm is operated until irradiance change is detected. At $t = 70$ *sec*, uniform shading is introduced, and the proposed shading detection algorithm finds the single-peak, and tracking is continued with fixed-step P&O algorithm. From the results, it is evident that the necessity of GMPPT technique is to find GMPP only when PSC occurs. During uniform shading, the conventional algorithm is able to track MPP.

3.3 Proposed hybrid GMPPT technique based on adaptive butterfly PSO and P&O algorithms

In the proposed ELAVPSO based GMPPT technique discussed in the previous section. 3.2, mainly premature convergence and complexity of parameter tuning are minimized. However, the other drawback of PSO-based GMPPT technique, i.e., high power oscillations during the exploration phase, remains when ELAVPSO is used alone without shading detection. This is mainly due to full tracking of GMPP is done only with the PSO technique under PSC, which involves unnecessary exploration of search space even after reaching the GP region. Since MPPT is an on-line/hardware-based search process, the five mutations applied to global best are nothing but increasing population size, and it causes more tracking time as well as high power oscillations. Hence to solve the problem of high power oscillations in PSO-based GMPPT techniques, the solutions found in the literature are: 1) reducing exploration phase, and 2) distribution of particles in the limited search space.

Hence, in this chapter, a new hybrid PSO-based GMPPT technique is proposed to get accurate and faster GMPP tracking with reduced power oscillations. To reduce the exploration phase of the SC technique, it is used only to identify the GP region and in that region gradient based technique (P&O) is used to track exact GMPP. Since GP region identification is the most important in this hybrid method, for switching between two algorithms, sensitivity feature of BF-PSO helps to identify the vicinity of GP region accurately, and BF-PSO is the best

alternative to ELPSO which improve the exploration capability of PSO algorithm without increasing the population size of the search in on-line-PV MPPT. Hence, BF-PSO is selected as SC technique in the proposed hybrid GMPPT technique.

3.3.1 Butterfly PSO algorithm

The butterfly PSO algorithm is derived from the basic PSO algorithm. It uses the butterfly swarm intelligence to find the optimal location based on the sensitivity of the flower, and the probability of nectar. The location of nectar (food source) represents the global best and the amount of nectar (food) is represented with fitness [30]. Hence, new parameters sensitivity and probability are added in the velocity and particle update equations of the basic PSO algorithm. Sensitivity is expressed using a mathematical function:

$$s_k = exp^{-\frac{(ITR_{max}-ITR_k)}{ITR_{max}}} \tag{3.20}$$

where s_k is the sensitivity of k^{th} iteration, ITR_{max} is the maximum iteration count for convergence, and ITR_k is the k^{th} iteration count. The probability is expressed as:

$$p_k = \frac{fitness(gbest_k)}{\sum(fitness(lbest_k))} \tag{3.21}$$

where p_k is the probability of k^{th} iteration, $fitness(gbest_k)$ is the fitness of global best in the k^{th} iteration, and $fitness(lbest_k)$ is the fitness of local best in the k^{th} iteration. The values of acceleration coefficients c_1 and c_2 are kept constant and same as the PSO algorithm. Weight factor w is expressed as

$$w_k = \frac{(ITR_{max} - ITR_k)}{ITR_{max}} \tag{3.22}$$

where w_k is the weight factor of k^{th} iteration, ITR_{max} is the maximum iteration count for convergence, and ITR_k is the k^{th} iteration count. Therefore, the velocity and particle update equations

of BF-PSO algorithm are given as:

$$vel_i^{k+1} = w_k \times vel_i^k + s_k \times (1 - p_k) \times c_1 \times r_1 \times \left(X_{lb\_i} - X_i^k\right) + c_2 \times r_2 \times \left(X_{gb} - X_i^k\right) \quad (3.23)$$

$$X_i^{k+1} = X_i^k + \alpha_k \times vel_i^{k+1} \quad (3.24)$$

where i indicates particle number, k indicates the present iteration, w is weight factor which ranges from 0.4 to 0.9, c_1 is cognitive factor which ranges from 0.1 to 2, c_2 is social factor which ranges from 0.1 to 2, r_1 and r_2 are random numbers $\varepsilon R(0,1)$, s_k is the sensitivity of k^{th} iteration, p_k is the probability of k^{th} iteration and α_k is the time-varying probability coefficient given in (3.25).

$$\alpha_k = rand \times p_k \quad (3.25)$$

where *rand* is the random number and ranges [0-1].

The sensitivity and probability in (3.23) lead to faster convergence and more accurate solutions. But these are tuned deterministically and depend on maximum iteration count. In the case of the PV MPPT problem, each particle is applied to the MPPT controller for a fixed sample time to evaluate the fitness. Hence, the convergence speed depends on the number of population in each iteration and maximum iterations required for convergence. At the beginning of the search process, estimating the maximum iterations required is difficult. If maximum iteration count considered is large, it affects the convergence speed because of oscillations of weight factor even after reaching the GP region and causes slower convergence. If it is small, the optimum solution may not be reached and causes premature convergence. In the standard PSO algorithm, the convergence occurs after a large number of iterations due to the improper setting of algorithm parameters. Hence, in the proposed technique, conventional BF-PSO algorithm parameters are tuned adaptively and are independent of the maximum number of iterations. The adaptive sensitivity parameter is used to detect the global region accurately.

3.3.2 Adaptive butterfly PSO algorithm

In this thesis, adaptive parameter control is used to avoid the time-dependent nature of deterministic parameter control of the BF-PSO algorithm. The sensitivity and weight factors are made adaptive based on feedback from the search process.

3.3.2.1 Adaptive sensitivity

Sensitivity and probability are the main features of the BF-PSO algorithm, which controls exploration and exploitation. Sensitivity varies from [0-1], and its value is low during the starting of exploration and high during exploitation. Hence in this thesis, adaptive sensitivity is derived based on the distance between maximum and minimum particle positions in each iteration. The distance between randomly distributed particles is more during the beginning of exploration, and it reduces as exploitation is reached,i.e., when all the particles come to the GP region. Hence, the proposed adaptive parameter control inherits the sensitivity parameter control of the basic BF-PSO algorithm, and it makes the parameter control independent of the maximum iteration count. The adaptive sensitivity in the proposed adaptive BF-PSO (ABF-PSO) algorithm is given by (3.26).

$$s_k = exp^{-\frac{(X^k_{max} - X^k_{min})}{ub}} \tag{3.26}$$

where X^k_{max} is the maximum value of particle position in k^{th} iteration, X^k_{min} is the minimum value of particle position in k^{th} iteration, and ub is the upper bound of search space.

3.3.2.2 Adaptive weight factor

The weight factor of the BF-PSO algorithm is given in (3.22) and varies with respect to the iteration count. At the beginning of exploration, value is high and decreases as the exploitation reaches. An adaptive weight factor is proposed in this chapter to avoid unnecessary oscillations of weight factor even after reaching the GP region, as given in (3.27).

$$w_k = \frac{(X^k_{max} - X^k_{min})}{ub} \tag{3.27}$$

where X^k_{max} is the maximum value of particle position in k^{th} iteration, X^k_{min} is the minimum value of particle position in k^{th} iteration. The adaptive weight factor inherits the features of (3.22), and its value becomes smaller as the global peak region is reached. Hence, the deterministic parameter control of the BF-PSO algorithm can be replaced with adaptive parameter control proposed in the ABF-PSO algorithm for the PV MPPT problem.

3.3.3 Hybrid GMPPT technique based on adaptive butterfly PSO and P&O algorithms

Even though the ABF-PSO algorithm avoids the deterministically tuned parameters in the BF-PSO algorithm, it cannot stop the exploration until all the particles meet the given convergence criterion. Even though the optimum solution is found before exploitation, because of lower fitness particle, convergence is delayed. Hence, it results in the unnecessary exploration of search space even after reaching the GP region, which leads to slower tracking of GMPP. Hence, in the proposed hybrid GMPPT technique ABF-PSO and P&O, first GP region is identified with the adaptive control parameter sensitivity (s), which depends on the distance between the maximum and minimum position of the particles in each iteration. Since the adaptive sensitivity factor in the ABF-PSO algorithm is derived based on the distance between particle positions in the search space, it can guarantee a global peak region based on the condition that its value is more than a threshold value. When s reaches a threshold value (=0.7), the solution obtained, which may be a complete or partial solution, is given to the variable step P&O (VS-P&O) by which unnecessary power oscillations in the GP region are avoided, and faster tracking can be achieved. The threshold value of s is important in identifying the GP region; a large value results in complete exploitation of the ABF-PSO algorithm, while a small value results in the inclusion of both local peak and GP regions. Hence, Based on the threshold value of s, the solution obtained, which may be the complete or partial solution, is given to the VS-P&O by which unnecessary power oscillations in the GP region are avoided, and faster tracking can be achieved. If complete tracking of GMPP is done with ABF-PSO only, it causes unnecessary exploration of search even after reaching the GP region by which tracking time is increased. Hence, in the proposed hybrid GMPPT technique, the ABF-PSO GMPPT technique is used only for identifying the GP region. The GP region can be identified with the adaptive sensi-

tivity factor, and in that region, tracking GMPP is continued with a variable step P&O MPPT algorithm.

The perturbation in variable step size of P&O algorithm [53–55] is calculated by (3.13). Because of the smaller value of $\frac{dP}{dV}$ as the peak is reached, it leads to a smaller step size because of which there are smaller power oscillations in the steady-state tracking by P&O as compared to fixed-step size [13]. Since the steady-state tracking is continued with the P&O algorithm and ABF-PSO stops exploration when the GP region is identified, to start the exploration of search space to find the new GMPP due to irradiance change, particles of ABF-PSO GMPPT technique should be reinitialized to find the new GMPP.

3.3.3.1 Reinitialization of particles under irradiance changes

In the algorithm point of view, choosing the initial position of particles based on the estimated knowledge of global best helps in finding accurate optimum value without premature convergence. Hence, there should be proper initialization of particles at the beginning of the exploration of search space for identifying an accurate GP region.

In PV MPPT, when Irradiance changes, i.e., either increase or decrease in irradiance, result in shifting of GMPP to the right or left of the present GMPP [51]. In PSO-based MPPT algorithms, the operating point is fixed at the global best after reaching the convergence criteria. Hence, to find the change in GMPP due to change in irradiance, the reinitialization of particles of PSO-based algorithms is necessary. The shift in the global peak depends on the previous irradiance value and magnitude of irradiance change. By considering medium irradiance changes, the new GMPP for the next irradiance change may be nearer to the present GMPP. In the case of severe non-uniformity in the irradiance pattern during irradiance change, it may result in new GMPP, which could be far from the previous GMPP. By considering both the possible cases of irradiance, i.e., medium and severe non-uniformity in the irradiance change, a novel reinitialization method is proposed in this hybrid GMPPT technique.

Since in the proposed hybrid GMPPT technique, ABF-PSO GMPPT technique is used only for identifying GP region and at the end of this identification stage, all the particles lie in the vicinity of GP region and the best solution obtained so far will be given to the P&O algorithm, which will continue further tracking. Hence, the knowledge of particles in the last

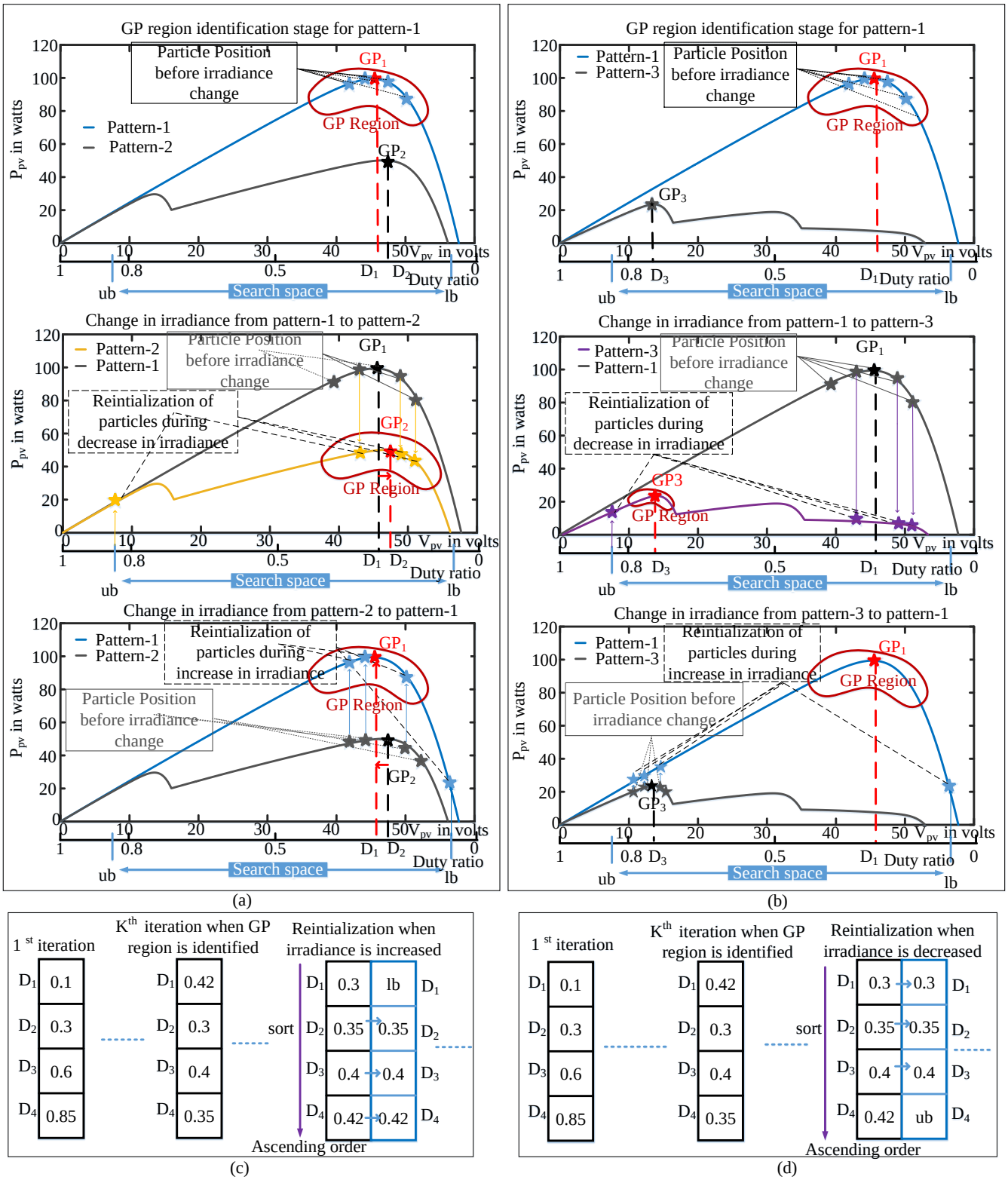

Figure 3.17: Proposed reinitialization method during a) medium irradiance change, b) severe non-uniformity in irradiance change, c) irradiance increase, d) irradiance decrease.

iteration of identifying the GP region stage for the previous irradiance conditions can be used as initial values in the reinitialization process for starting exploration of search space for identifying the new GMPP after irradiance change by considering both the GMPPS are nearer. In the case, if the new GMPP is far from the present GP region where most of the particles are distributed as per the proposed reinitialization, to cover the other parts of the search space, one of the particles in the list is kept at the boundary of search space based on increase or decrease in irradiance. Irradiance change can be identified with a change in power. If N is the number of particles or search agents and k is the iteration count of the GP region identification stage, during reinitialization of particles, first particles of k^{th} iteration are sorted in ascending order. Either maximum or minimum particle position, which is N^{th} or first particle in the sorted list is kept at the boundary of search space based on the change in irradiance condition, i.e., either increase or decrease as shown in Figure 3.17. The remaining (N-1) particles are in the same position as the previous GP region identification stage. The change in irradiance patterns from pattern-1 to pattern-2, pattern-1 to pattern-3, which can be used to explain the proposed reinitialization when the new GMPP after irradiance change is nearer and far to previous GMPP as shown in Figure 3.17. In Figure 3.17.a), when irradiance decreases from pattern-1 to pattern-2, maximum duty ratio particle will be kept at the upper boundary of search space, and the three remaining particles are kept in the same position as they are in the GP region of pattern-1. During irradiance increase from pattern-2 to pattern-1, minimum value duty ratio is kept at lower bound of the search space, and remaining particles are kept in the same position as they are in the GP region of pattern-2. Since both the GMPPS are nearer due to medium irradiance change, the proposed reinitialization of particles covers the GP region of both the changes of irradiance, and it helps in identifying an accurate GP region. In the case if the GMPPS are far as shown in Figure 3.17.b), when irradiance decrease from pattern-1 to pattern-3 which is considered as severe non-uniformity in irradiance, the maximum value of duty ratio is kept at upper bound and the remaining particles are kept in the same position as they are in the GP region of pattern-1. Since both the GMPPS are far away, the particles kept at boundaries help to explore the search space, which includes new GMPP. Hence, the proposed reinitialization helps in identifying the GP region accurately for any irradiance changes.

3.3.3.2 Steps to implement the proposed GMPPT technique

The sequential process of the proposed hybrid GMPPT technique is indicated from stages 1 to 20, which are marked in the flowchart shown in Figure 3.18. Steps to implement the proposed hybrid GMPPT technique are:

I) Initialize four particles dc[i] which are uniformly distributed in the search space limited from ub=0.85 to lb=0.1, set particle count u=1. Set fitness of particles p[i] and their best positions $P_{best}[i]$ to zero.

II) Apply each particle from u=1 – 4 to the MPPT converter to find their fitness as shown in flowchart stages 2 to 6. If any particle has the better fitness in the present iteration, update

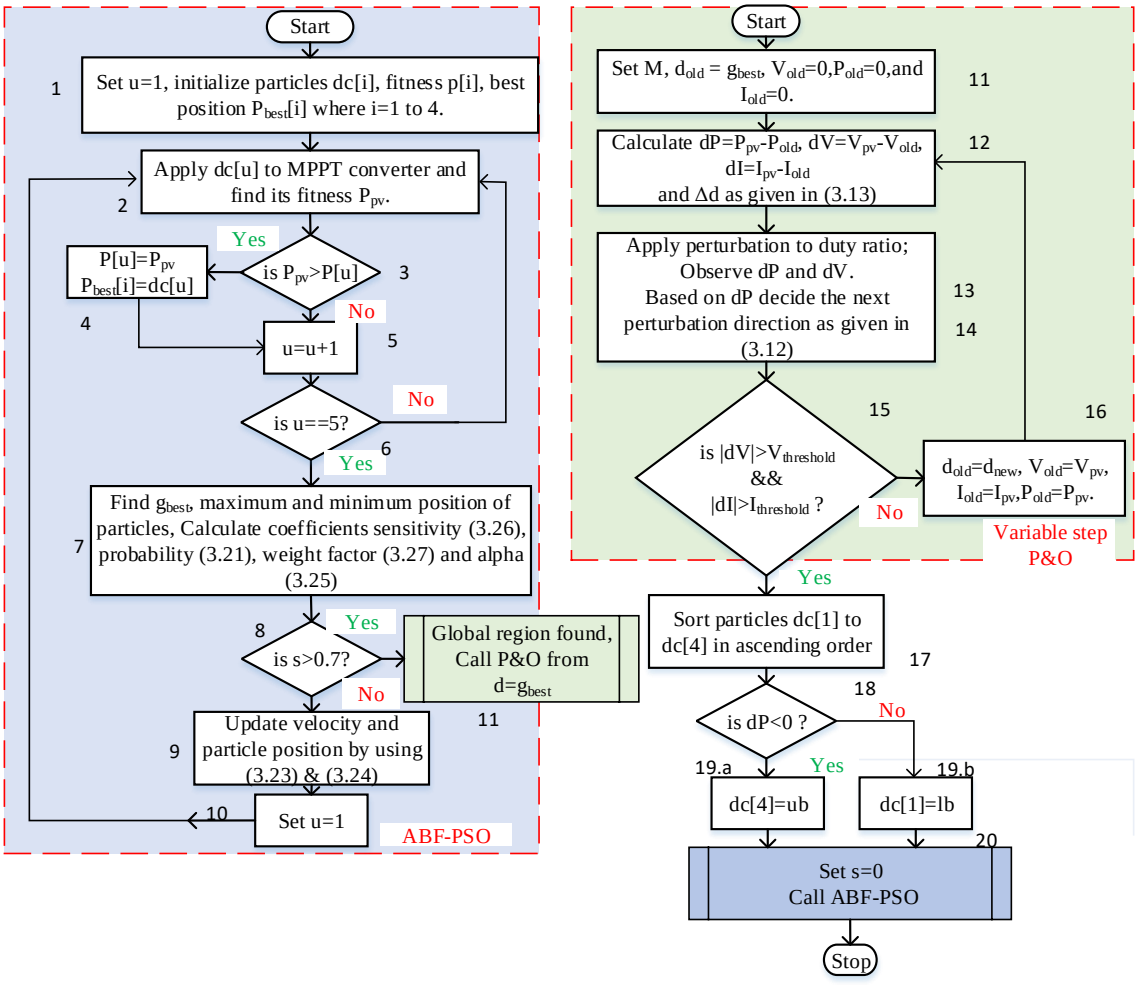

Figure 3.18: Flowchart of the proposed hybrid GMPPT technique based on ABF-PSO and P&O algorithms.

the particle fitness and its best position as given in stage 4.

III) Find better fitness particle g_{best} among the four particles, maximum and minimum position of particles, and calculate coefficients sensitivity as given in (3.26), probability as given in (3.21), weight factor as given in (3.27) and alpha as given in (3.25)

IV) Check for convergence criteria: is sensitivity 's' greater than the threshold or not? if

[i] No, Update velocity and particle position by using (3.23) & (3.24). Set u=1 to start next iteration and repeat the steps I to IV.

[ii] Yes, the global region is identified and calls the variable step P&O to start tracking GMPP from the best solution obtained in the ABF-PSO. Initialize the variables in P&O as given in stage 11.

V) Calculate M from the change in power dP, dV, and find dI. Calculate the perturbation step size by using (3.13).

VI) Apply perturbation to duty ratio based on the change in power as given in (3.12).

VII) Check for irradiance change. if

[i] No change is identified; save the present value of duty ratio, voltage, and power as given in stage 16 and repeat steps V and VII.

[ii] Change in irradiance identified; apply proposed reinitialization of particles as shown in stages 17-20. First, sort the particles in ascending order: if irradiance decrease is identified through the change in power; set the last particle in the list dc[4]=ub, if irradiance increase is identified; set the first particle in the list dc[1]=lb. Repeat the steps I to VII.

3.3.4 Simulation and experimental results

3.3.4.1 Simulation results

The proposed hybrid GMPPT technique and other conventional MPPT techniques are tested with MATLAB/ Simulink model of PV string connected to a DC-DC boost converter, which is used as MPPT converter, as shown in Figure 3.19. The details of the PV system and boost converter are given in Table 3.7. The uniform and complex partially shaded conditions are emulated with different irradiance patterns of 3S-1P short string and 6S-1P long string arrangement shown in Figure 3.19. a) and their P-V characteristics are shown in Figure 3.20 and details of ir-

Table 3.7: Details of the PV system and ratings of boost DC-DC converter used in the simulation.

S.No	Parameter	Specifications
1	Number of modules in the string	Short string-3 Long string-6
2	Each module rating	V_{oc} = 19.25 V, I_{sc} = 2.502 A, V_{mpp} = 14.97 V, P_{mpp} =33.3 W.
3	Inductance, L	7 mH
4	Output capacitance, C_{out}	22 μF
5	Input buffer capacitance, C_{in}	22 μF
6	Load Resistance, R_L	185 ohm
7	Switching Frequency, f_s	50 KHz

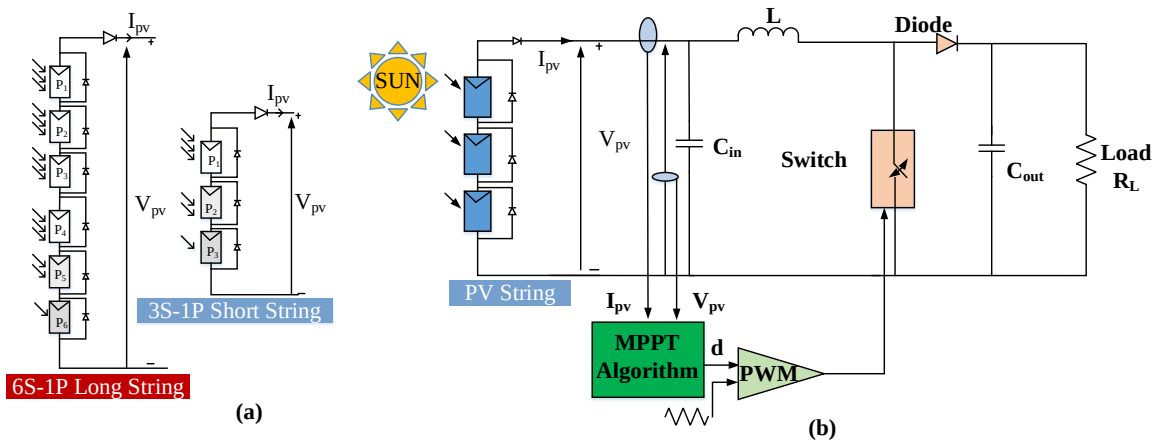

Figure 3.19: a) PV string arrangement, b) PV string connected to DC-DC boost MPPT converter.

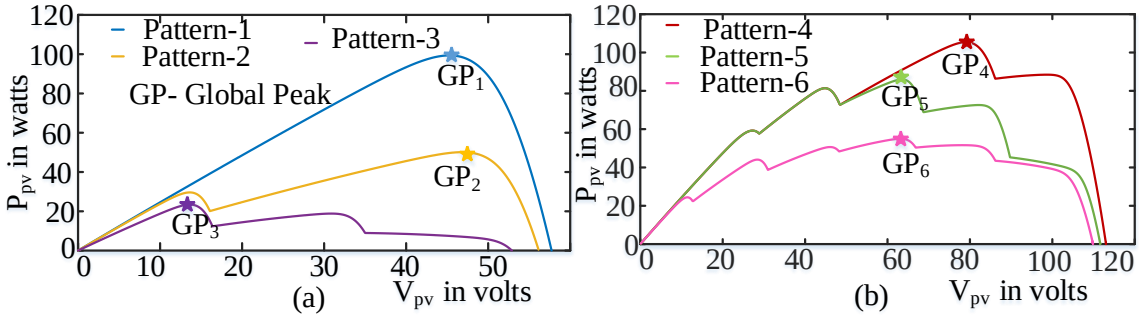

Figure 3.20: P-V curves under different patterns a) 3S-1P short string, b) 6S-1P long string.

Table 3.8: Details of irradiance patterns used for simulation and hardware.

String Type	Irradiance Pattern	Irradiance profile (KW/sq.mt)						Number of Peaks	Global Peak		
		P_1	P_2	P_3	P_4	P_5	P_6		V_{gp} (V)	I_{gp}(A)	P_{gp}(W)
3S-1P Short String	Pattern-1	1	1	1	–	–	–	1	45.6	2.18	99.4
	Pattern-2	1	0.5	0.5	–	–	–	2	47.4	1.05	50.01
	Pattern-3	0.8	0.3	0.1	–	–	–	3	13.64	1.71	23.42
6S-1P Long String	Pattern-4	1	1	0.8	0.6	0.6	0.4	4	79.59	1.32	105.4
	Pattern-5	1	1	0.8	0.6	0.4	0.2	5	63.54	1.35	85.96
	Pattern-6	1	0.7	0.5	0.4	0.3	0.2	6	63.12	0.87	54.98

radiance patterns are given in Table 3.8. Temperature of each module is considered constant and same ($T = 25^oC$). All the MPPT algorithms are simulated with the same constraints; sample time T_s = 15 msec, population count = 4, search space limits ub=0.85 & lb=0.1, and remaining parameters are given in Table 3.9.

Results shown in Figure 3.21 are used to verify the performance improvement of the proposed hybrid GMPPT technique in terms of faster tracking over its counterpart BF-PSO GMPPT techniques. From the simulation results, it is observed that all three GMPPT tech-

Table 3.9: Details of algorithm parameters used for simulation and hardware.

S.NO	Algorithm	Parameters
1	P&O	$\Delta d = 0.03$, $d\_init = 0.1$
2	PSO	$w = 0.4$, $c_1 = 1.2$, $c_2 = 2$, $vel\_max = 0.18$
3	PSO P&O	$w = [0.1\ 1]$, $c_1 = [1\ 2]$,$c_2 = [1\ 2]$ $vel\_max = 0.18$, $itr\_max = 20$, $\Delta d = 0.01$
4	GWO P&O	$itr\_max = 20$, $\Delta d = 0.01$
5	BF-PSO	$c_1 = c_2 = 2$, $itr\_max = 20$, $vel\_max = 0.18$
6	ABF-PSO P&O	M = 0.01, $\Delta dmax = 0.03$, $\Delta dmin = 0.001$, $vel\_max = 0.18$

niques can reach GMPP of the single-peak curve resulting from pattern-1, i.e., due to uniform irradiance conditions. In BF-PSO GMPPT technique, tracking is continued until the given convergence criteria (maximum iteration count = 10) is reached and algorithm control parameters are time-varying and highly dependent on the maximum iteration count, The results obtained in the steady-state are $P_{mpp} = 99.33\ W$, $V_{mpp} = 45.69\ V$, $I_{mpp} = 2.174\ A$, $d_{mpp} = 0.6526$, and $T_{mpp} = 0.6\ sec$. Slow tracking is mainly due to wrongly estimated maximum iteration count, and it may take a longer time for convergence or tracking GMPP with a large iteration count.

In the ABF-PSO GMPPT technique, the dependency of control parameters on unknown maximum iteration count required for convergence is avoided by the adaptive weight factor and sensitivity as given in (3.27) & (3.26). These adaptive parameters can influence the exploration and exploitation of ABF-PSO and result in a faster tracking time of $T_{mpp} = 0.408\ sec$ shown in Figure. 3.21. (b). Even though the ABF-PSO GMPPT technique can give faster tracking than the conventional BF-PSO GMPPT technique, tracking speed can be further improved with

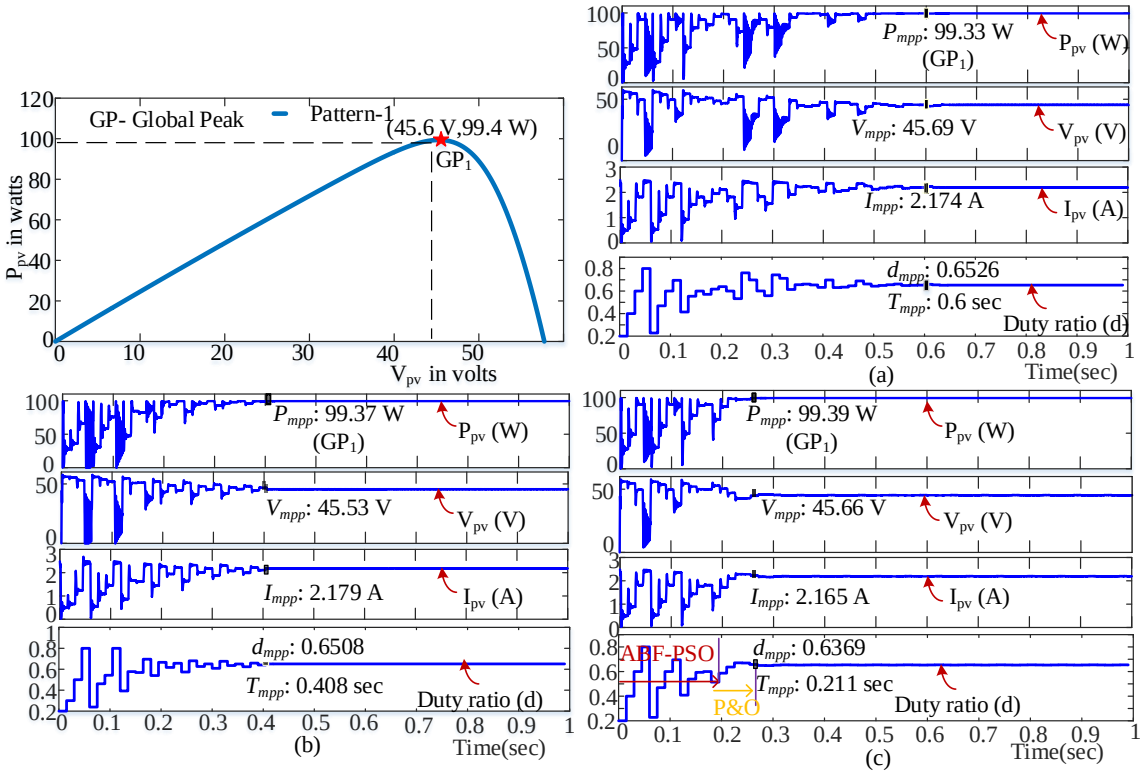

Figure 3.21: Simulation results of GMPPT techniques a) BF-PSO, b) ABF-PSO, c) Proposed hybrid GMPPT technique.

the integration of the ABF-PSO and P&O. From simulation result shown in Figure 3.21. (c), ABF-PSO gives a partial solution to VS-P&O, and tracking GMPP is achieved within a short time $T_{mpp} = 0.211\ sec$. From the simulation results obtained, it is observed that the proposed hybrid GMPPT technique is much faster than conventional BF-PSO and ABF-PSO GMPPT techniques. The variation of parameters of the BF-PSO and ABF-PSO GMPPT technique during the search process is shown in Figure 3.22. From the simulation result, it is verified that the adaptive sensitivity factor which uses feedback from search, i.e., the distance of maximum and minimum particle positions, helps in faster convergence. It also helps in identifying the GP region.

The performance of the proposed hybrid GMPPT technique under uniform and shading conditions is compared with both conventional and hybrid techniques shown in Figure 3.23, and the results are tabulated in Table 3.10. To measure the accuracy of tracking, static MPPT efficiency η_{static} can be used which is given by (3.28)

$$\%\eta_{static} = \frac{P_{pv}}{P_{mp}} \times 100 \tag{3.28}$$

where P_{PV} is the power measured at steady-state, P_{mp} is the actual maximum power. Since the uniform irradiance pattern (pattern-1) results in a single-peak P-V curve, all the five MPPT techniques can reach GMPP. However, for the multi-peak P-V curve, which is due to partially shaded conditions (Pattern-3), the conventional P&O MPPT technique can track the immediate peak just after the irradiance change and in this case, it tracks only local peak LP_{31} due

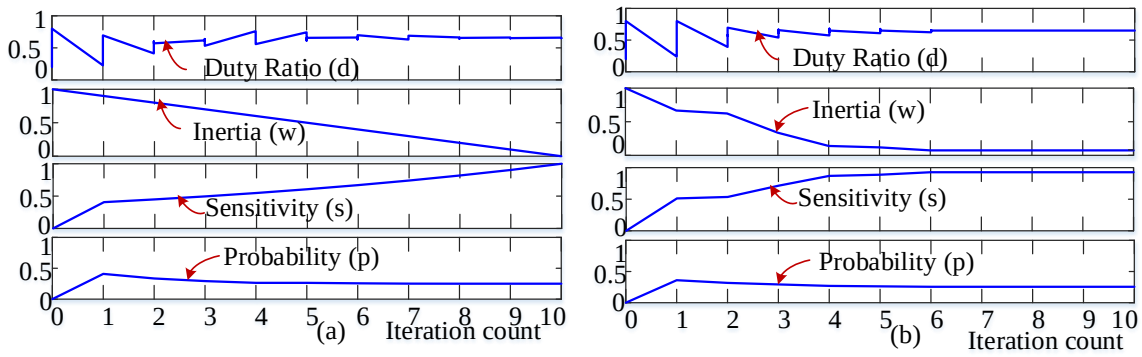

Figure 3.22: Simulation results of parameter variation of GMPPT techniques a) BF-PSO, b) ABF-PSO.

Table 3.10: Simulation results of the conventional and hybrid MPPT techniques.

	P&O			PSO			PSO-P&O [37]			GWO-P&O [38]			Proposed	
	T_{mpp} (sec)	P_{mpp}(W)	$\%\eta_{static}$	T_{mpp}(sec)	P_{mpp}(W)	$\%\eta_{static}$	T_{mpp}(sec)	P_{mpp}(W)	$\%\eta_{static}$	T_{mpp}(sec)	P_{mpp}(W)	$\%\eta_{static}$	T_{mpp}(sec)	P_{mpp}(W)	$\%\eta_{static}$
Pattern-1 (GMPP=99.4W)	0.28	98.77	99.36	0.683	99.4	100	0.618	99.37	99.96	0.36	99.36	99.96	0.264	99.39	99.98
Pattern-3 (GMPP=23.42W)	0.075	18.28	78.05	0.767	23.41	99.95	0.46	23.27	99.36	0.68	23.31	99.53	0.198	23.31	99.53

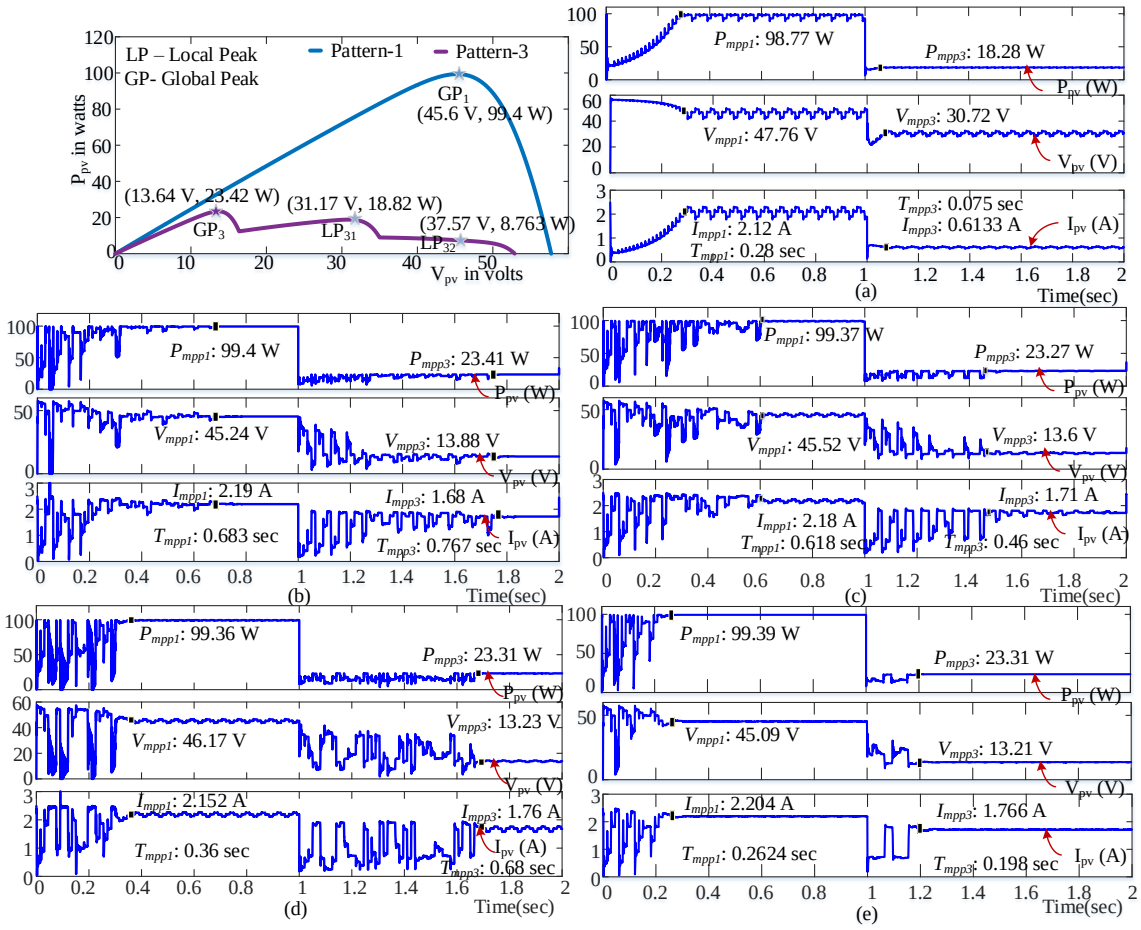

Figure 3.23: Simulation results of MPPT techniques a) P&O, b) PSO, c) PSO-P&O, d) GWO-P&O, e) Proposed hybrid GMPPT technique.

to its hill-climbing nature. Whereas the remaining swarm intelligence (SI) based techniques; conventional PSO, and hybrid GMPPT techniques: PSO-P&O [37], GWO-P&O [38], and the proposed hybrid GMPPT technique can track the global peak. Because of fixed control parameters in conventional PSO-based GMPPT technique, there are unnecessary oscillations even after reaching the GP region, and it results in slow tracking (T_{mpp1} = 0.683 sec and T_{mpp3} = 0.767 sec). Even though the parameters in PSO-P&O based hybrid GMPPT technique [37] are deterministically tuned, the over estimated maximum iteration count (= 20) causes for slow convergence (T_{mpp1} = 0.618 sec and T_{mpp3} = 0.46 sec) to identify the GP region and fixed-step P&O in steady-state results in constant power oscillations. Even in GWO assisted P&O based MPPT technique [38] also slow tracking (T_{mpp1} = 0.36 sec and T_{mpp1} = 0.68 sec) is due to the dependency of parameters on maximum iteration count. The proposed hybrid method achieves

fast-tracking (T_{mpp1} = 0.2624 sec and T_{mpp3} = 0.198 sec) over the other methods with the help of adaptive sensitivity and weight factor, which depends on the feedback of distance between particles. The power oscillations in the steady-state are minimized by using variable step P&O which has the small step size after reaching GMPP over the fixed-step P&O. From the results obtained, it is evident that the proposed hybrid GMPPT method tracks the GMPP in less time under both cases of irradiance when compared with other MPPT techniques.

Simulation results shown in Figure 3.24 are used to verify the concept of the reinitialization of particles under irradiance changes. The shift in GMPP may be nearer or far to the present GMPP after irradiance change due to medium and severe nonuniformity in irradiance, which are simulated with the change in irradiance patterns from pattern-1 to pattern-2 and from pattern-2 to pattern-3 respectively. In the conventional PSO GMPPT technique, when irradiance change is identified, particles need to be reinitialized in the search space without the knowledge of shift in GMPP due to irradiance change. Hence, in the Figure 3.24.a), it causes the slow tracking $T_{mpp1} = 0.453\ sec, T_{mpp2} = 0.247\ sec$, and $T_{mpp3} = 0.318\ sec$ respectively for three irradiance patterns. Apart from the slow tracking, the selection of same initial particles during reinitialization for all irradiance changes along with improper parameter setting may cause premature convergence. In this case, the conventional PSO-based MPPT technique tracks the local peak $LP_{31} = 18.84W$, whereas GMPP for the pattern-3 is $GP_3 = 23.42W$. The results obtained with the ABF-PSO and P&O GMPPT technique with and without proposed reinitialization are compared with the help of results obtained in Figure 3.24.b) and Figure 3.24.c) to know the effectiveness of proposed reinitialization technique. When irradiance changes from pattern-1 to pattern-2, which is considered as medium irradiance change, GMPP of pattern-2 after irradiance change is nearer to GMPP of pattern-1. Hence, based on the proposed reinitialization of particles, when same particles which are at the last stage of previous GP region identification stage of pattern-1 is used for the reinitialization of particles in pattern-2, it results in fast-tracking of GMPP, i.e., $T_{mpp2} = 0.102\ sec$ whereas without the proposed reinitialization it takes $T_{mpp2} = 0.27\ sec$. When the shift in GMPP far from present GMPP of pattern-2 after irradiance changes to pattern-3, because of the extreme particles in the sorted list which are kept at boundaries of search space allows the exploration of new GMPP without restricting the exploratory nature of proposed PSO-based algorithm only to the small region, i.e., previous GP region in the search space. Because of the proposed adaptive parameter setting and added

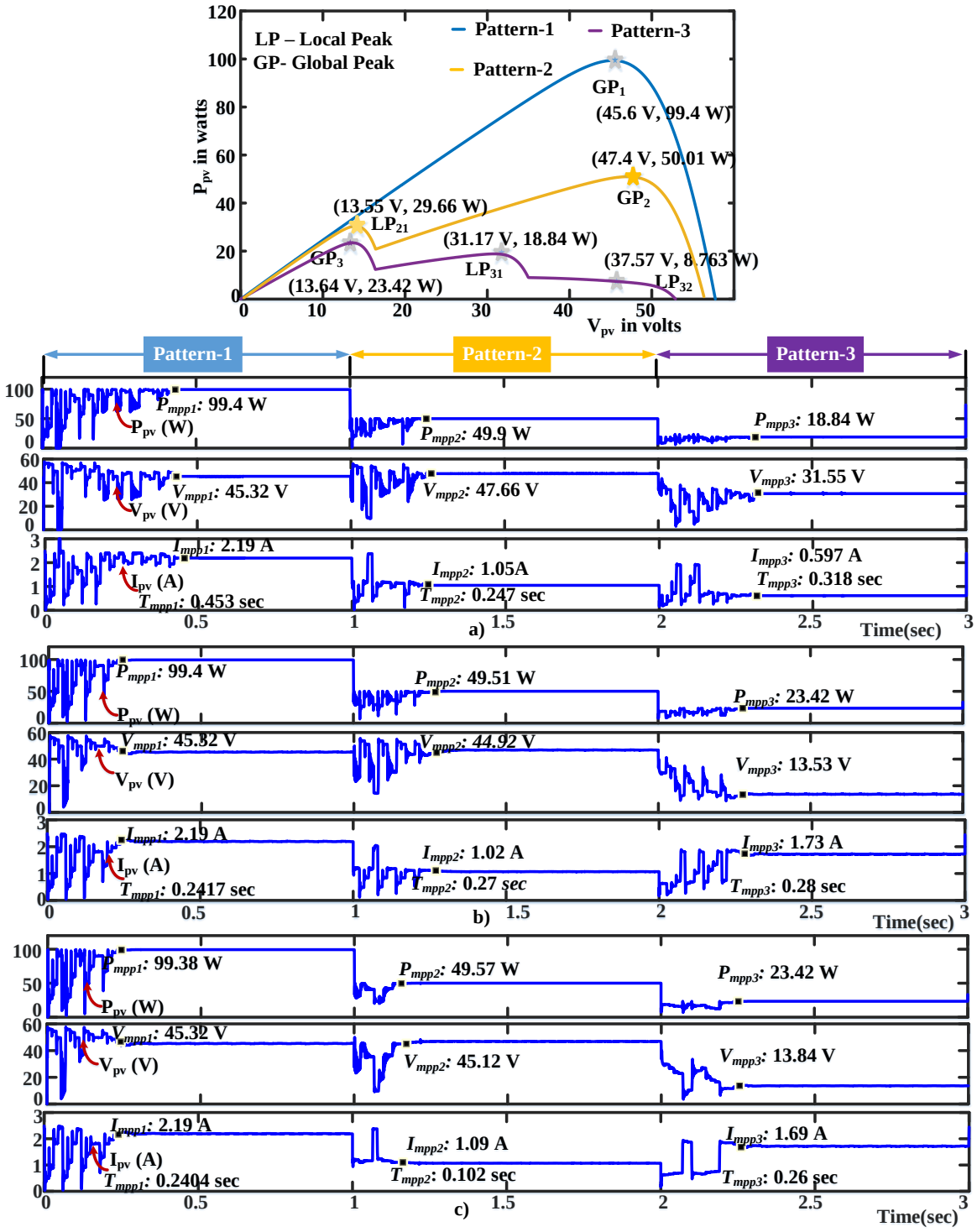

Figure 3.24: Simulation results of GMPPT technique under irradiance changes a) PSO, b) ABF-PSO and P&O without proposed reinitialization, c) ABF-PSO and P&O with the proposed reinitialization.

features of BF-PSO like sensitivity and probability, the proposed GMPPT tracks the GMPP accurately, and results obtained are $P_{mpp3} = 23.42\ W$, and $T_{mpp3} = 0.26\ sec$. Hence, from the simulation results, it is evident that the proposed reinitialization of particles gives faster tracking of GMPP in the case of medium irradiance changes when the shift in GMPP after irradiance change is nearer to previous GMPP.

Since the PSO-based MPPT techniques are population-based GMPPT techniques, where the particles explore the entire search space because of which there are oscillations in the waveforms. Whereas SI technique (ABF-PSO) used only for identifying GP region in the proposed hybrid GMPPT technique and small step size of variable step P&O algorithm after reaching steady-state, power oscillations in the proposed hybrid GMPPT technique, during GP region identification stage and steady-state tracking are minimized. Whereas in conventional PSO technique, these oscillations are high due to long exploration and high velocity of particles during the initial stage of exploration. Hybrid GMPPT methods: PSO-P&O [37] and GWO-P&O [38] are also suffered from oscillations in the power, voltage, and current due to fixed control parameters during the GP region identification stage and fixed-step P&O in stead-state. Even these steady-state oscillations may further increase if the large step size is selected. Hence, as compared to the conventional and hybrid GMPPT methods given in this chapter, the proposed GMPPT method has low power oscillations.

3.3.4.2 Experimental results

A laboratory prototype of a boost converter, which is used as an MPPT converter, is developed, and the experimental setup is shown in Figure 3.25 to test the performance of the proposed hybrid GMPPT method. The details of the experimental setup are given in Tables 3.7 and 3.11.

Chroma make programmable DC power supply model 62100H-600S is used as a solar PV array simulator to emulate different irradiance conditions by inserting corresponding P-V curves. Voltage and current at the input of converter are sensed with LEM made hall effect sensors and measured signals are given as analog input to the analog to digital converter (ADC) of the digital controller. Implementing an MPPT algorithm in real-time requires a digital controller with sufficient computational capability. To implement conventional MPPT algorithms,

Table 3.11: Details of the experimental setup.

S.No	Component	Specifications
1	PV Simulator	Chroma make programmable DC power supply 62100H-600S model
2	Digital Controller	ARDUINO UNO Rev3 board, Micro-controller-ATmega328P, 14 Digital I/O pins
3	Voltage sensor	LEM LV-25-P
4	Current sensor	LEM LA-55-P
5	Power MOSFET	47N60C3 N Channel MOSFET
6	Power Diode	MUR 1560

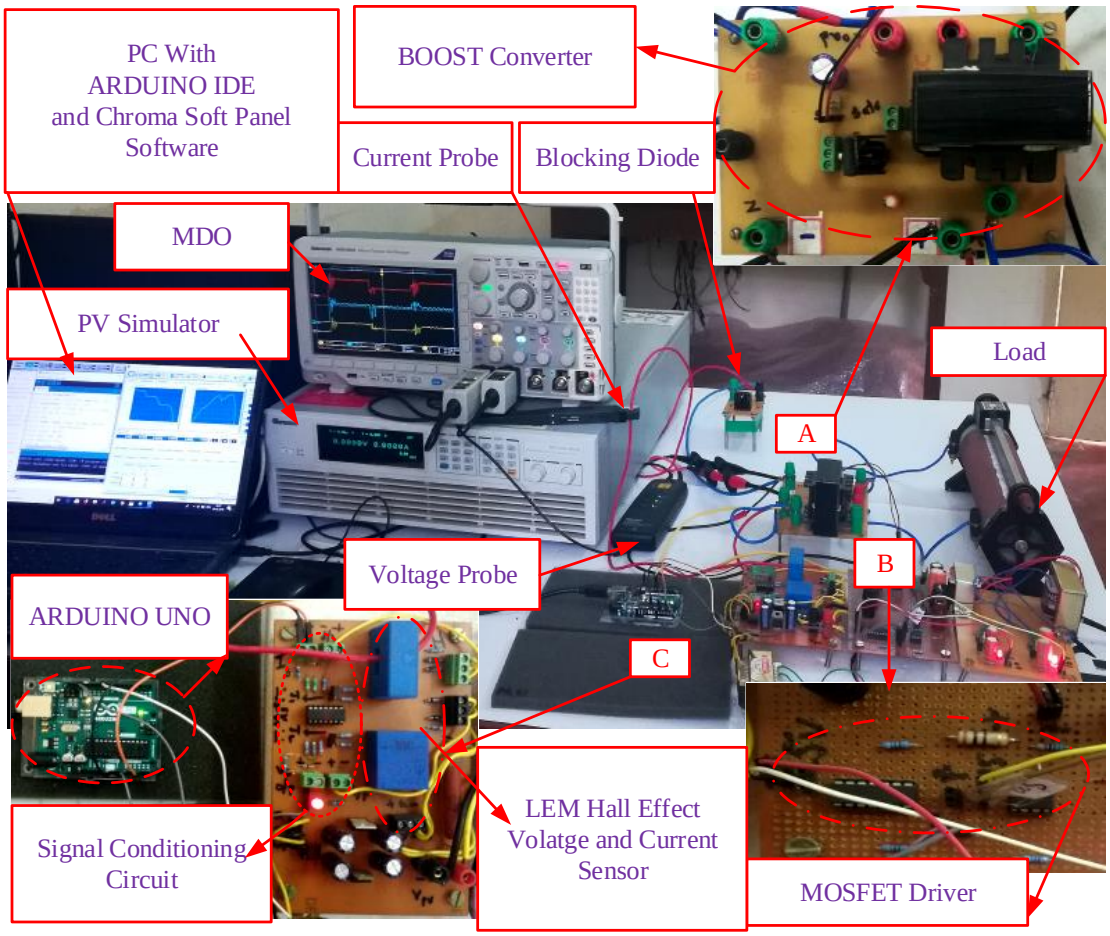

Figure 3.25: Experimental setup of the MPPT controller.

even though low-cost micro-controllers are used for reducing the cost of the system, low-speed microcontrollers that can handle low computational burden can not be used for fast MPP tracking with algorithms like PSO having mathematical operations. The Minimum requirements for the digital controller to implement MPPT techniques based on soft computing techniques are; to sample the voltage and current signals, two ADCs with a minimum speed of 10 ksps [56], to do the mathematical operations of PSO-based algorithms and to store the algorithm variables, a minimum 8-bit microcontroller with 16 KB memory is required. Hence, in the present hardware setup, ARDUINO UNO Rev3 board with an 8-bit micro-controller: Atmega-328P with

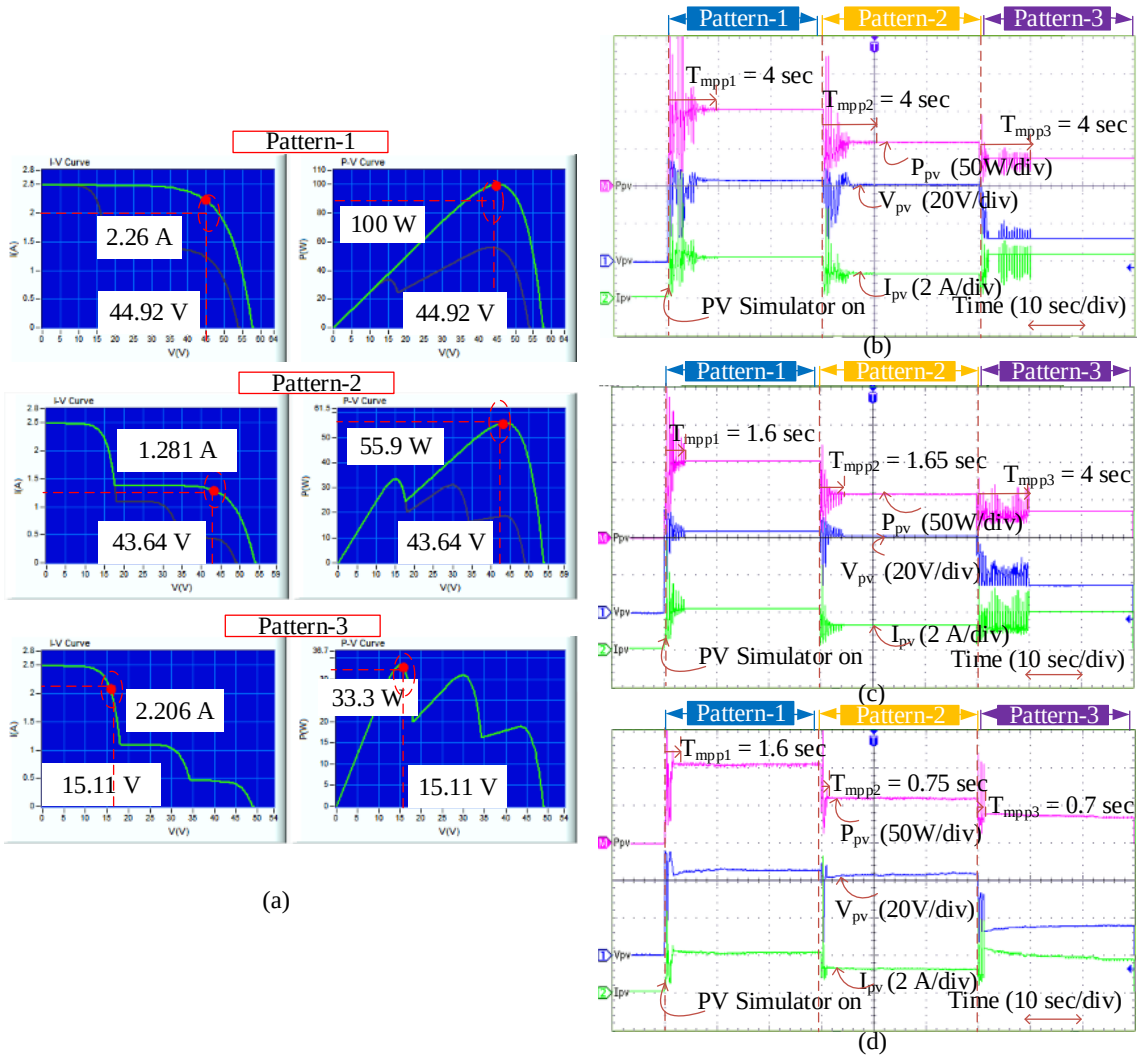

Figure 3.26: Experimentally obtained results of the GMPPT techniques a) Irradiance profiles b) BF-PSO, c) ABF-PSO, d) Proposed.

16MHZ clock is used as a digital controller to generate a 50 KHz gate pulses. The PV voltage and current are sensed with hall effect sensors and are given as inputs to the analog pins of the controller through a signal conditioning circuit. The MPPT algorithm uses voltage, current and generates a pulse width modulated (PWM) signal, which is given to the MOSFET driver circuit of the boost converter. The sample time for the digital controller is taken as Ts= 50 msec for all the algorithms.

Three irradiance patterns (pattern-1, pattern-2, and pattern-3) of a 3S-1P short string are used to test the performance improvement of the proposed hybrid GMPPT method over conventional BF-PSO GMPPT technique. Each pattern is emulated for 12 sec. The results obtained are shown in Figure 3.26. Experimental results obtained with the BF-PSO GMPPT technique are $T_{mpp1} = T_{mpp2} = T_{mpp3} = 4sec$. Since the maximum iteration count taken for convergence is 20, it takes $T_{mpp} = 4$ sec to reach GMPP of three patterns, and it may increases if the maximum iteration count is increased. More tracking time in the BF-PSO GMPPT technique is due to unnecessary exploration even after reaching the GP region and dependency of algorithm parameters on maximum iteration count. ABF-PSO GMPPT technique is proposed with adaptive sensitivity and weight factor to avoid the time-dependent nature of the deterministically tuned BF-PSO-based GMPPT technique. The experimental results of ABF-PSO GMPPT technique are $T_{mpp1} = 1.6sec, T_{mpp2} = 1.65sec$, and $T_{mpp3} = 4sec$. ABF-PSO GMPPT technique reaches GMPP faster than the BF-PSO GMPPT technique for the first two irradiance patterns, and it takes same time ($T_{mpp3} = 4$ sec) as BF-PSO to reach GMPP of pattern-3. Even though parameters of ABF-PSO are adaptively tuned, unnecessary exploration of particles even after reaching the GP region is not avoided because of which ABF-PSO results in slow tracking of GMPP. Further, to improve the tracking time, a hybrid GMPPT technique based on ABF-PSO and P&O is proposed. Experimental results of the proposed hybrid GMPPT technique are $T_{mpp1} = 1.6sec, T_{mpp2} = 0.75sec$, and $T_{mpp3} = 0.7sec$. The proposed hybrid GMPPT technique takes less than 1.6 sec for tracking the GMPP. Further, with the proposed reinitialization method, much faster tracking for medium irradiance changes is achieved. Hence, from the experimental results, it is evident that the proposed hybrid GMPPT is much faster than the conventional BF-PSO GMPPT technique by using added features of adaptive parameter control, GP region identification using adaptive sensitivity, and proposed reinitialization method.

Further to test the performance of proposed technique ABF-PSO and P&O under com-

plex shading conditions, which consist of more than three peaks (4, 5, and 6 peaks) of 6S-1P long string are used. Each irradiance pattern is applied for 12 sec, and results are shown in Figure 3.27. The results obtained are $T_{mpp4} = 2.4sec, T_{mpp5} = 1.6sec$, and $T_{mpp6} = 0.8sec$ and static MPPT efficiency obtained are 99.51 %, 99.50%, and 99.31% for the three irradiance patterns. In the hybrid GMPPT method, the GP region is identified with the ABF-PSO GMPPT technique and in the region identified, the variable step P&O algorithm can reach GMPP accurately. The GP region is easily identified using the adaptive sensitivity parameter of the ABF-PSO GMPPT technique. Hence, unnecessary exploration even after reaching the GP region can be avoided, which results in faster tracking. From these experimental results, it is evident that the proposed hybrid GMPPT method guarantees faster and accurate GMPP tracking even under complex shading conditions.

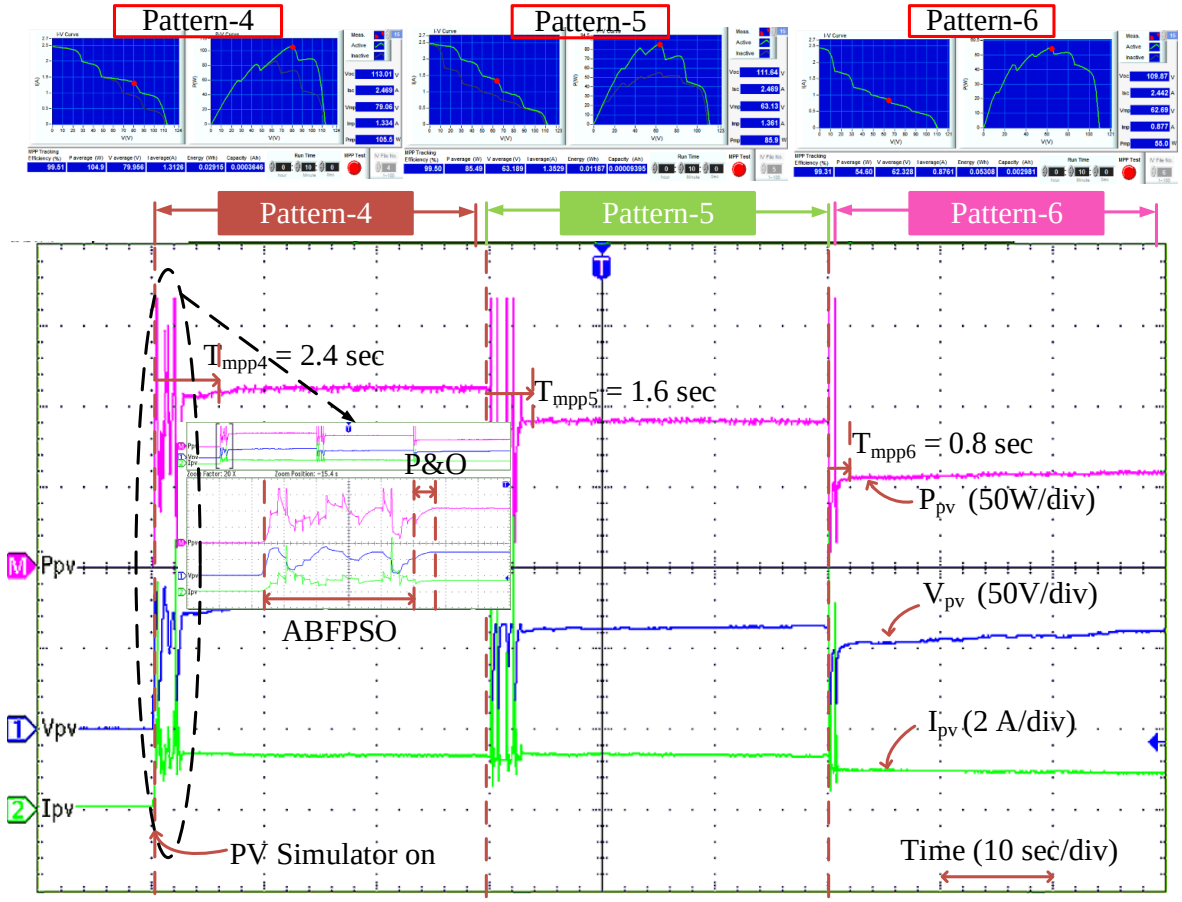

Figure 3.27: Experimentally obtained results of the proposed GMPPT technique under complex shading conditions of 6S-1P long string.

Table 3.12: Experimentally obtained results of conventional and hybrid MPPT techniques.

	P&O			PSO			PSO-P&O [37]			GWO-P&O [38]			Proposed	
	T_{mpp} (sec)	P_{mpp}(W)	$\%\eta_{static}$	T_{mpp}(sec)	P_{mpp}(W)	$\%\eta_{static}$	T_{mpp}(sec)	P_{mpp}(W)	$\%\eta_{static}$	T_{mpp}(sec)	P_{mpp}(W)	$\%\eta_{static}$	T_{mpp}(sec)	P_{mpp}(W)	$\%\eta_{static}$
Pattern-1 (GMPP=100W)	4	98.4	98.4	4	98.3	98.3	3.2	99.78	99.78	3.8	99.51	99.51	1.6	99.39	99.39
Pattern-2 (GMPP=55.9W)	0.8	55.5	99.14	4	55.76	99.75	3.2	55.7	99.27	3.3	54.1	97.95	0.75	55.7	99.7
Pattern-3 (GMPP=33.3W)	0.8	30.8	92.35	4	32.2	96.71	4	33.03	99.2	3.2	33.04	99.21	0.7	33.04	99.21

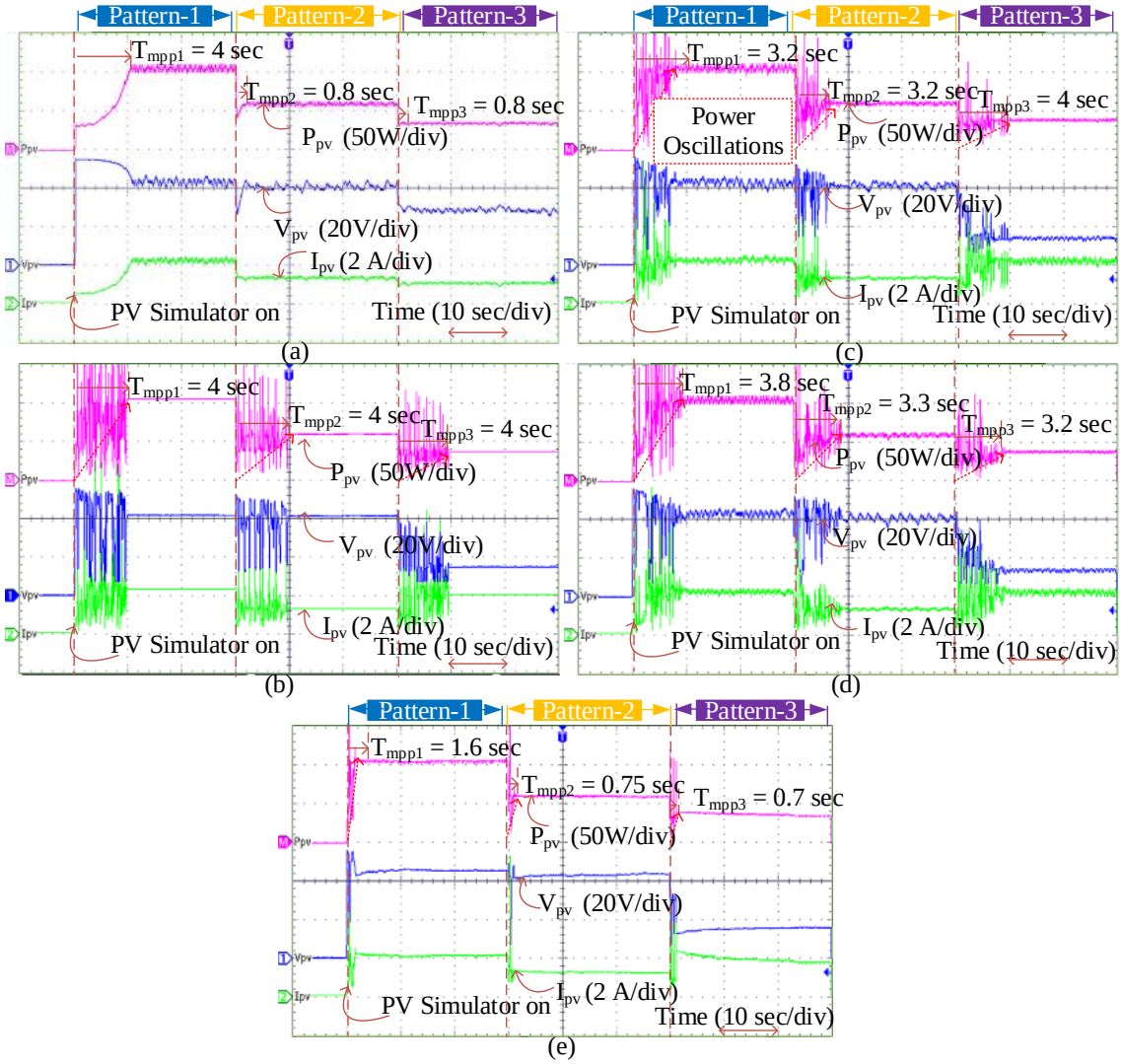

Figure 3.28: Experimentally obtained results of the MPPT techniques a) P&O, b) PSO, c) PSO-P&O, d) GWO-P&O, e) Proposed hybrid GMPPT technique.

The performance of the hybrid GMPPT technique is compared with conventional and hybrid MPPT techniques shown in Figure 3.28, and the results are given in Table 3.12. For the first 12 seconds, uniform irradiance is applied by emulating a single-peak P-V curve of pattern-1 and in the next 24 seconds, PSC is emulated with a multi-peak P-V curve of pattern-2 and pattern-3 (each for 12 sec). From the results obtained with P&O MPPT technique under uniform irradiance condition, it is evident that conventional P&O can track the MPP of a single-peak P-V curve, but for a multi-peak P-V curve, i.e., under PSC, it may be struck at a local peak or tracks the GMPP based on the immediate peak after the transition due to irradiance change. In

this case, the P&O MPPT technique can track only $P_{mpp3} = 30.8W$ for irradiance change form pattern-2 to 3, while GMPP of pattern-3 is 33.3 W. The power oscillations in the steady-state are dependent on the step size [17] and are large in this case due to the large and fixed-step size ($\Delta d = 0.01$). Even though PSO GMPPT technique can reach GMPP under uniform and PSC, slow tracking of GMPP ($T_{mpp1} = T_{mpp2} = T_{mpp3} = 4sec$) is due to the fixed control parameters and unnecessary exploration in the search space even after reaching the GP region. From the experimental results shown in Figure 3.28. b), it is evident that the conventional PSO takes more time (4 sec) for tracking, and accuracy of the solution obtained is less (less than 99 % in some cases), and oscillations of the waveform are high due to the fixed control parameters and unnecessary exploration of the search space even after reaching GP region.

In the case of hybrid GMPPT techniques; PSO-P&O [37], GWO-P&O [38], and proposed hybrid GMPPT technique, unnecessary exploration of search space even after reaching GP region is avoided by identifying GP region by SI technique and in that region identified tracking is continued with the P&O technique. Because of parameters dependency on maximum iteration count in PSO-P&O [37], and GWO-P&O [38] GMPPT techniques, these are resulted in slow tracking and in the steady-state because of fixed-step P&O, power oscillations are more. The proposed hybrid GMPPT method can track the GMPP within a time less than 2.4 sec for all the tested patterns, and the average static tracking efficiency of this technique is 99.43 %. The proposed hybrid GMPPT technique results in faster and more accurate tracking of GMPP as compared to given conventional and hybrid techniques because of adaptively tuned parameters, proper identification of GP region with adaptive sensitivity factor, and a further improvement in tracking speed under irradiance changes due to the proposed reinitialization method. Since the PSO-based MPPT techniques are population-based GMPPT techniques where the particles explore the entire search space because of which there are oscillations in the waveforms. However, in the proposed GMPPT technique, the power oscillations during the GP region identification stage and steady-state tracking are minimized with the help of fast and accurate tracking of GP region with adaptive sensitivity and smaller step size of the variable step P&O in the stead-state. Further, the proposed reinitialization method also helps reducing power oscillations as compared to the particle-initialization randomly in the search space. Whereas in the case of conventional PSO technique, it is observed that the waveform oscillations are high due to fixed parameters and long exploration process. In the experimental results shown

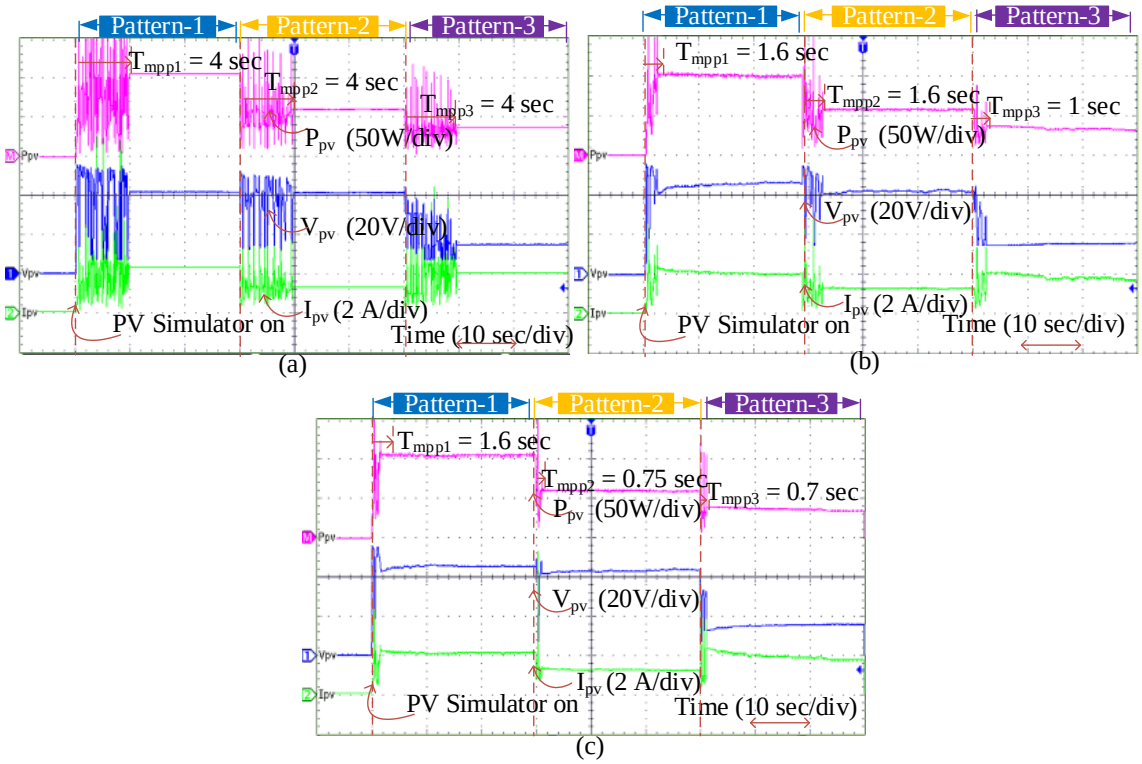

Figure 3.29: Experimentally obtained result of the GMPPT technique under irradiance changes a) PSO, b) ABF-PSO and P&O without proposed reinitialization, c) ABF-PSO and P&O with proposed reinitialization.

in Figure 3.28, the power oscillations during the GP region identification stage are marked with a red line. From the experimental results, it is evident that the power oscillations during the GP region identification stage and steady-state tracking are minimized in the proposed hybrid GMPPT method.

Pattern-1, patten-2, and pattern-3, which include moderate and severe nonuniformity in the irradiance changes, are used to verify the proposed reinitialization of particles during irradiance changes. For the first 12 seconds, pattern-1 is applied, as shown in Figure 3.29. Four particles are uniformly distributed in the search space without the knowledge of GP for pattern-1 to start the exploration of the ABF-PSO GMPPT technique. After finding the GP region, the algorithm is shifted to the variable step P&O algorithm, which continues tracking of GMPP. At the time of algorithm shifting, all the particles of ABF-PSO are present in the GP region of pattern-1 and are stored for use in the reinitialization of particles when the next irradiance change (pattern-1 to pattern2) is identified. The time taken for tracking GMPP, in

this case, is $T_{mpp1} = 1.6\ sec$. After 12 seconds, the irradiance pattern is changed to pattern-2 which is identified with variable step P&O algorithm. To start the exploration for new GP region, particles of ABF-PSO GMPPT technique are reinitialized with the help of the previous history of tracking GP region and based on the decrease in irradiance. In this case, two GMPPS are nearer, and the time taken to reach GMPP is $T_{mpp2} = 0.75\ sec$ which is less than the case when particles are initialized without the knowledge of GP region ($T_{mpp2} = 1.6\ sec$) shown in Figure 3.29. b). Again, after 12 seconds, irradiance is decreased to pattern-3. In this case, two GMPPS are far due to severe nonuniformity in the irradiance; particles are reinitialized as given in section 2.3.1 which results in faster and accurate tracking of GMPP without losing exploration capability. The time taken to reach the GMPP of pattern-3 is $T_{mpp3} = 0.7\ sec$. In all the other four MPPT methods, particles should be reinitialized without any knowledge of the GP position, and it results in more tracking time. In Figure 3.29. a), reinitialization in the conventional PSO technique is shown. Hence from the experimental results, it is evident that the proposed reinitialization method further improves the tracking speed of the ABF-PSO and P&O GMPPT technique.

3.4 Conclusion

In this work, a new modified PSO, ELAVPSO GMPPT technique is proposed with adaptive velocity and enhanced leader capability. Both simulation and experimental results show that the convergence speed of the proposed algorithm is faster without problems associated with premature convergence. The proposed shading detection would help in predict the type of shading, i.e., uniform and partial shading, under dynamic weather conditions. VS-P&O algorithm is used for detecting multi-peak and single-peak of the P-V curve. The proposed technique has the advantage of applying conventional algorithms for tracking GMPP under uniform irradiance conditions; in the case of PSC, GMPPT technique is used for finding GMPP and from that point onwards fixed-step P&O algorithm is used for tracking. Further, to reduce power oscillations during GMPP tracking, a new hybrid GMPPT technique is proposed based on adaptive butterfly PSO and P&O algorithms. The proposed GMPPT technique is compared with existing popular MPPT techniques in the literature to find the superiority of the proposed technique in terms of fast and accurate tracking of GMPP. From the simulation and experimental results analysis, the following detailed conclusions can be made:

1) The proposed ABF-PSO algorithm avoids the time-dependent nature of the butterfly PSO algorithm by using adaptive sensitivity and weight factor, which avoids the unnecessary exploration due to the high value of maximum iteration count. With adaptive parameters of the ABF-PSO algorithm, tracking speed and convergence rate are improved.

2) To get faster tracking of GMPP by avoiding unnecessary exploration even after reaching the GP region, the ABF-PSO GMPPT technique is only used to identify the GP region, and in the region identified, tracking is continued using variable step P&O algorithm. Identifying the global peak region is easily done with only one parameter, i.e., adaptive sensitivity of the ABF-PSO GMPPT technique.

3) The variable step size derived in the P&O algorithm results in smaller perturbation as the steady-state is reached, because of which there are smaller power oscillations in the steady-state tracking as compared to other techniques that use the fixed-step P&O algorithm. Hence in the proposed hybrid GMPPT technique, power oscillations in the steady-state are reduced drastically as compared to existing benchmark hybrid GMPPT techniques: PSO-P&O and GWO-P&O.

4) The power oscillations during the GP region identification stage and steady-state tracking are minimized with the help of fast and accurate tracking of GP region with adaptive sensitivity and smaller step size of the variable step P&O in the steady-state. Further, the proposed reinitialization method also helps reducing power oscillations as compared to the particle-initialization randomly in the search space.

Hence, from the simulation and experimental validation of the proposed PSO-based GMPPT techniques, it is evident that ABF-PSO and P&O GMPPT technique guarantees faster and accurate GMPP tracking with less power oscillations even under complex shading conditions.

Chapter 4

Hybrid GMPPT techniques based on adaptive salp swarm algorithm

Chapter 4

Hybrid GMPPT techniques based on adaptive salp swarm algorithm

4.1 Introduction

Among all swarm intelligence techniques, PSO is most popular in solving MPPT problems. From the modified PSO-based GMPPT techniques discussed in previous chapter 3, it is evident that the conventional PSO algorithm needs to be modified to match the requirements of the MPPT problem [39]. So, parameter tuning is essential for better performance of any soft computing technique, and these are known as adaptive techniques. In any soft computing technique, if few control parameters are involved, the complexity of parameter tuning reduces.

In an on-line or hardware-based search process, the population size of the swarm intelligence algorithms should be small for faster convergence [57]. But smaller population size may cause premature convergence. Performance of these techniques in terms of tracking speed, power oscillations during tracking, avoiding premature convergence depends on the selection of initial agents in the search space, and communication between them during exploration should be improved [34]. In ELAVPSO and ABFPSO-P&O GMPPT techniques, control parameters are tuned adaptively. However, there are more control parameters (three) that need to be tuned.

With the advantages and disadvantages of swarm intelligence methods mentioned above, a new integrated method based on a salp swarm inspired algorithm and P&O is used for finding GMPP with fewer control parameters, low power oscillations, and limited search space during irradiance changes. Fewer control parameters help in the easy design and implementation of the proposed technique. In [31], a bio-inspired optimizer for engineering design problems, a salp swarm algorithm is proposed. It is simple and easy to implement as compared to PSO. However, the single control parameter in SSA is dependent on the maximum iteration count; it results in the unnecessary exploration of search space even after reaching the GP region in an on-line search process like PV MPPT. It also results in slow convergence of conventional SSA-

based MPPT technique. A memetic salp swarm algorithm (MSSA) based MPPT is proposed in [33], which improves the searching ability and convergence stability by using multiple salp chains. Even this technique also suffers from slow convergence or slow tracking of GMPP due to dependency of control parameter on maximum iteration count. In [32], different metaheuristic techniques are proposed for mitigating partial shading conditions of PV systems in which SSA is simple and easy, which also motivated the authors of this thesis to propose a GMPPT method based on SSA. As per authors in [32], the superiority of SSA over other methods lies in the efficiency of extracting GMPP. However, the convergence speed and tracking time of conventional SSA-based MPPT technique is poor as compared to other MPPT methods based on grey wolf optimizer (GWO), hybrid method (PSO-GSA). The slow convergence or tracking GMPP is primarily due to the dependence of the deterministically tuned control parameter, which depends on the maximum iteration count. In an on-line search process like PV MPPT, the wrongly estimated maximum iteration count results in the unnecessary exploration of the search process even after reaching the GP region, which delays the convergence. Hence, there is a necessity of deriving the control parameter, which is independent of the iteration count and avoiding unnecessary exploration of search space in the GP region to get faster tracking with SSA-based MPPT technique.

Hence, in this chapter, a new GMPPT technique is proposed in which SSA is modified with an adaptive control parameter, adaptive SSA is used only to identify the GP region. Hence, unnecessary exploration in the GP region can be eliminated. In that GP region, tracking is continued with variable step P&O for the faster tracking of GMPP accurately with low power oscillations in the steady-state. The main objective of this chapter is to propose a simple, easy, and fast-tracking GMPP technique by using adaptive SSA and P&O algorithms for a PV string under partially shaded conditions and has a better performance than conventional and already existing modified SSA-based MPPT techniques. The novelty of the presented work lies in: 1) adaptive parameter tuning of the control parameter in the conventional SSA-based MPPT technique. 2) GP region identification with ASSA and in that region identified tracking is continued with a variable step size of the P&O algorithm. These two features help in achieving faster GMPP tracking by the proposed GMPPT technique. With a single control parameter that is adaptively tuned, the proposed GMPPT technique is becoming simpler than conventional PSO, where three control parameters need to be optimized. The performance of the proposed method

is compared with conventional P&O, PSO, SSA, and memetic SSA-based MPPT techniques under uniform and partial shading conditions.

Contributions of this chapter are

- To overcome the more number of parameters, i.e., three to be tuned in PSO based MPPT techniques, simple SI technique SSA based MPPT with one control parameter is proposed.
- To get the better accuracy and performance under load changes in off-drid PV system, a novel hybrid SI technique is proposed by using ASSA and DE.

4.2 Salp swarm algorithm

The salp swarm algorithm is derived from the biological nature of salps hunting food in the sea. Salps make the largest swarm in nature. These swarms are known as salp chains [31]. The population in the salp chain is divided into two parts. One is the leader, while the remaining are followers. The leader is at the beginning of the chain, and the follower follows the leader. During hunting for food source F in the search space, the leader guides the swarm, and food source may be stationary or moving. The leader position update is based on the food source, and it is given by (4.1).

$$X^1 = \begin{cases} F + C_1 \times ((ub - lb) \times C_2 + lb), if \;\; C_3 > 0.5 \\ F - C_1 \times ((ub - lb) \times C_2 + lb), if \;\; C_3 < 0.5 \end{cases} \tag{4.1}$$

where X^1 is the position of the first salp, F is the position of the food source, ub upper bound of search space, lb lower bound of search space, C_2, and C_3 random numbers $\in$ [0,1]. C_1 is the most crucial parameter in SSA. It balances exploration and exploitation.

$$C_1 = 2 \times e^{-\left(\frac{4l}{L}\right)^2} \tag{4.2}$$

where l is the current iteration number, and L is the maximum iteration number. (4.1) can be rewritten as

$$X^1 = \begin{cases} F + V_1, if \;\; C_3 > 0.5 \\ F - V_1, if \;\; C_3 < 0.5 \end{cases} \tag{4.3}$$

where V_1 is the velocity of leader and $V_1 = C_1 \times ((ub - lb) \times C_2 + lb)$. To update the position of follower salps X^i, (4.4) is used.

$$X^i = \frac{1}{2} \times \left(X^i + X^{(i+1)} \right) \tag{4.4}$$

In the PV MPPT problem, GMPP is the food source that is unknown initially [33]. In this case, the best solution obtained so far is the food source. In the first iteration, a uniformly distributed population or salps in the search space is considered. In this case, the salps position is nothing but the duty ratio. Based on the fitness values of the population, they are sorted in descending order. The first one in the list becomes the food source for the next iteration. In the next iteration, the position of the first salp is updated using (4.1), and if evaluated fitness is more than the fitness of food source, the food source is updated with the first particle. Otherwise, the first salp's position and fitness remain the same as that of the food source. The remaining salps in the salp chain are updated based on the adjacent higher fitness salp in the chain, as given in (4.4). Hence it can be observed that in the first iteration itself, the salp chain is formed, and the food source is updated with better fitness value in the exploration process. It can be seen that only the leader salp may go out of search space at the time of starting iterations when C_1 is large. In this case, the leader can be brought back to boundaries, and the possibility of salps going out of search space is very low because all follower salps move toward the food source. The main features of the SSA algorithm which are suitable for MPPT problem:

1) SSA algorithm updates the position of the leader with respect to a food source, so the leader always explores and exploits the global best region. It is similar to enhancing the leader in PSO. It inherits the feature of a dynamic leader and avoids stagnation at a local peak.

2) SSA algorithm updates the position of follower salps with respect to each other, so they move gradually towards the leading salp. It results in better voltage regulation during tracking.

3) Sorting PSO in [25], uses sorting of particles to eliminate random movement of particles and results in low power fluctuations during tracking, whereas SSA inherits this feature naturally.

4) SSA algorithm has only one main controlling parameter C_1.

4.3 Proposed GMPP tracking based on adaptive salp swarm algorithm and P&O

Controlling parameter C_1 in the exploration and exploitation process of the leader in the salp chain, and it depends on maximum iteration count [31]. Initially, C_1 value is high, so that leader explores the search space. As the iteration number l increases, C_1 becomes low and allows the leader to exploit. But for the MPPT problem, even the maximum number of iterations for convergence is low and is an unknown value. The maximum number of iterations for convergence is considered 10. From (4.2), after five iterations, the value of C_1 becomes very small, which leads to the exploitation of the leader. C_1 equation is modified to balance the exploration and exploitation of the leader.

$$C_1 = 2 \times e^{-\left(4\times\left(1-\left(\frac{d_{max}-d_{min}}{ub}\right)\right)\right)^2} \tag{4.5}$$

where d_{max} is the maximum value of duty ratio in the present iteration, and d_{min} is the minimum value of duty ratio in the present iteration, and ub is the upper bound of search space. From (4.5) control parameter C_1 changes with respect to the length of the salp chain. The length of the salp chain is nothing but the difference between maximum salp position and minimum salp position. In the first iteration, the length of the salp chain is large, and based on (4.5), C_1 becomes high, and it allows exploration of the leader in the search space. As the number of iterations increases, the population changes its position gradually and moves towards the food source. When all the population comes to the global peak region, the length of the salp chain decreases, which results in a minimal value of C_1, and it allows the leader to exploit. When C_1 is less than some critical value, the velocity of the food source becomes very small, and the salp position of the leader is not changed.

From the above discussion, it is evident that C_1 can be used for knowing the global peak region. So, in the proposed hybrid method ASSA P&O, based on C_1 value global peak region, is identified, and the food source identified so far is the starting point of the variable step P&O

algorithm. From thereon, P&O efficiently tracks the global peak. Hence, from the above discussion, it is evident that there is smooth switching between ASSA and P&O. The advantage of continuous tracking with P&O after reaching a global peak region is faster convergence in finding a global peak with lesser power oscillations. After finding the global peak region by ASSA, tracking of GP is continued with P&O until irradiance change is detected. When irradi-

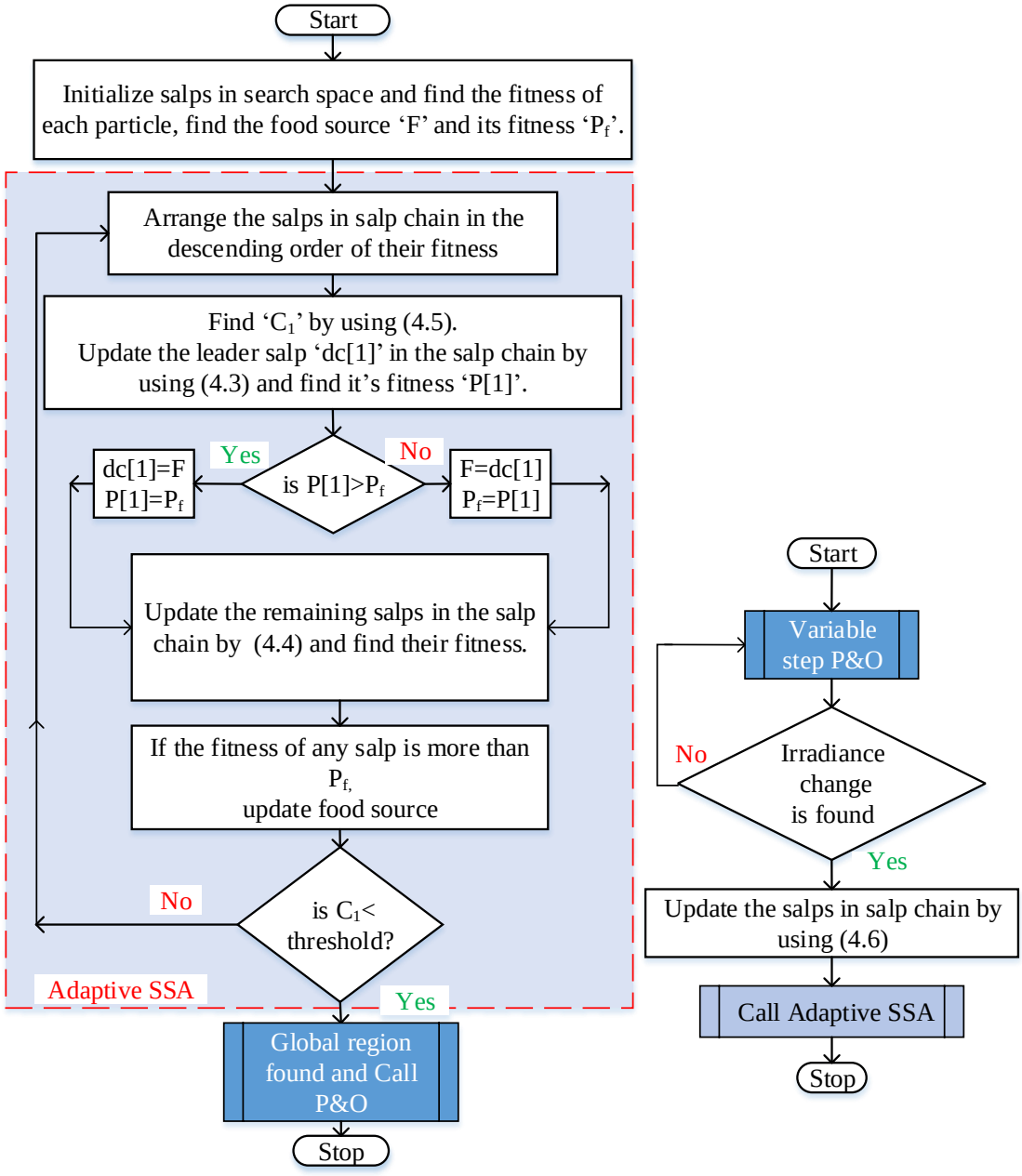

Figure 4.1: Flowchart of adaptive salp swarm algorithm with P&O.

ance is changed, it results in a change in the P-V curve, and global peak shifts from the previous value. If the irradiance change results in a multi-peak curve, the P&O algorithm may not be able to find the new GMPP, and it is stuck at any one local peak. Hence the ASSA algorithm is re-triggered to find the new global region. If the irradiance change is a result of partial shading, the shift of global peak is nearer to the previous operating point. The reinitialization of ASSA requires only the change in food source for starting the exploration. In the first iteration, after irradiance change is detected, the first particle is chosen based on the knowledge of previous global peak and change in power due to irradiance change. From [51], $F_{new} = F_{prev} \mp k$ where - sign denotes an increase in power, + sign denotes a decrease in power, and k is constant. Hence the salp chain for the first iteration after irradiance change must be formed between the previous food source and any one of the search space boundaries ub or lb to reduce the search space, which results in a decrease of power oscillations during tracking and faster convergence. Only one population either at the beginning or ending in the previous salp chain is modified as given in (4.6), and the remaining particles are unchanged. The values are the same as before the P&O algorithm was activated.

$$\begin{aligned} dc_1 &= ub, if \;\; dP < 0 \\ dc_n &= lb, if \;\; dP > 0 \end{aligned} \tag{4.6}$$

where dc_1 is the first salp in salp chain, dc_n is the last salp in salp chain, and dP is the change in power at the time of irradiance change. Therefore, the history of exploring the global peak region for previous irradiance conditions helps in limiting the search space of the next irradiance conditions. Hence, the search space is limited for identifying the global peak region with ASSA-P&O for irradiance changes. The process of identifying a global region for new irradiance conditions and switching between ASSA and P&O is the same as discussed above. The proposed methodology under irradiance changes results in low power oscillations during tracking, and only at the start of the system, there is a need for exploring the entire search space, i.e., ub to lb. So, the number of times there occurs a change of power from zero to rated value during tracking is reduced, which is the main drawback of all GMPPT methods. The flowchart of the proposed GMPPT method is given in Figure 4.1.

4.3.1 Simulation results of the proposed GMPPT technique

Performance of ASSA P&O algorithm and other algorithms is tested with the Simulink model of a PV system, which is described in Table 3.7 by using MATLAB/Simulink software and string arrangement of PV panels to study the different partial shading conditions is given in Figure 4.2. Boost converter with input buffer capacitor connected to resistive load is used as MPPT controller. Direct duty ratio control is used to generate the pulse width modulated gate signals to trigger the controlled switch used in a boost converter, as shown in Figure 3.19. All the MPPT algorithms shown are simulated with proper same sample time $T_s = 15$ *msec*.

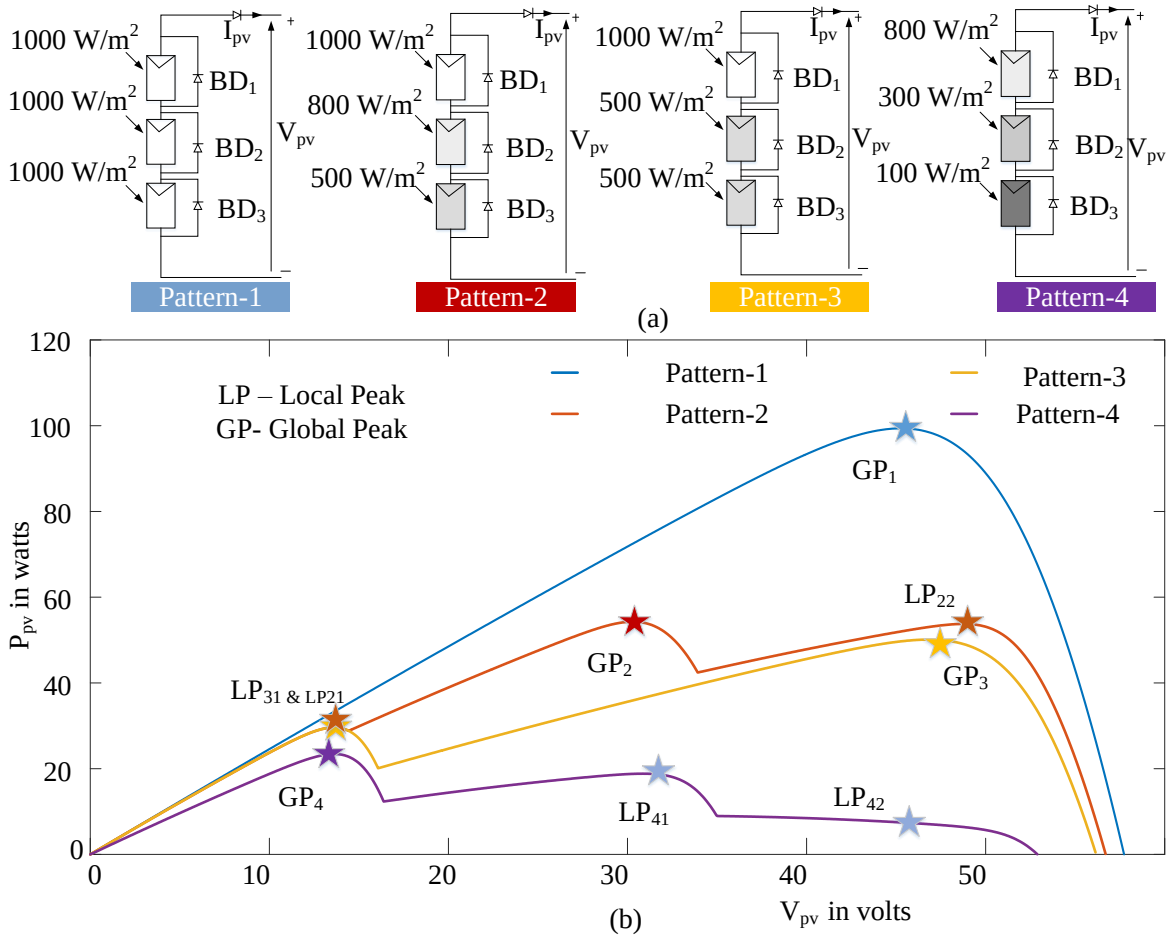

Figure 4.2: a) Different shading patterns on PV string, b) P-V curves under the given shading patterns.

Case (1): First, to know the performance improvement of ASSA-P&O over its conventional counterpart SSA, both are simulated with a single-peak P-V curve with pattern-1, as shown in

Figure 4.2 b). Since all three panels are under the same irradiance conditions, it resulted in a single-peak P-V curve with pattern-1, and $GP_1 = 100\ w$ is the global peak. Simulated results of SSA, ASSA, and ASSA-P&O are given in Figure 4.3. The maximum number of iterations

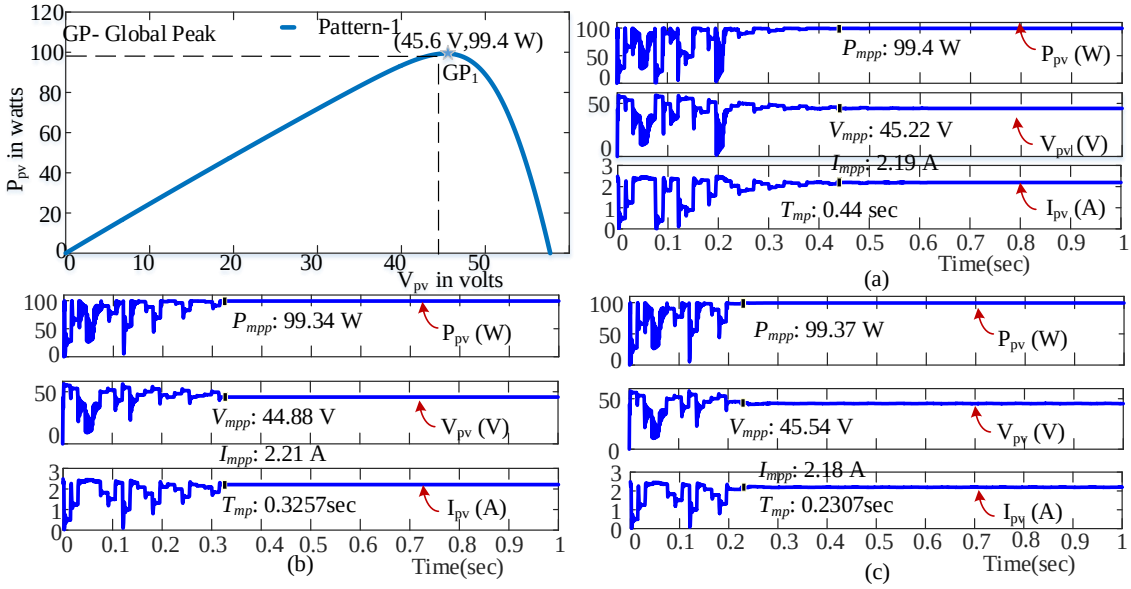

Figure 4.3: Simulation results of MPPT techniques under the shading pattern-1 a) SSA, b) ASSA, c) ASSA-P&O.

considered in SSA for simulation is 10. Four populations or salps are involved in the exploration of a given search space, and initially, these salps are uniformly distributed in the search space [0.1 0.85]. From the simulation results of proposed SSA algorithms, with the same initial population, all three algorithms can reach the global peak. From Figure 4.3.a), it is evident that the SSA algorithm track GP_1, which is the food source in the 10 th iteration. The maximum number of iterations required for an on-line/hardware search process like MPPT is not known initially. However, the SSA algorithm can find the global best solution before maximum iteration, and it continues exploring search space until the maximum number of iterations is reached. As discussed in section 4.2, the exploration and exploitation of the SSA algorithm is dependent on a single parameter C_1 and from Figure 4.4.a), it is evident that when C_1 is smaller, the food source is unaltered in further iterations and salp chain length becomes small. From the result, C_1 and salp chain length are related, and (4.5) is derived. With the proposed equation for C_1, the variation of C_1 in each iteration of ASSA is shown in Figure 4.4.b). ASSA GMPPT can find

a global peak in a fewer number of iterations and faster than SSA GMPPT, as shown in Figure 4.4.b). Even in ASSA-based GMPPT also, the exploration of search space is continued until the given convergence criteria are satisfied. Since all the salps come closer when exploration is completed, the convergence criteria used for ASSA GMPPT is

$$(dc_{max} - dc_{min}) \leq 0.05 \tag{4.7}$$

where dc_{max} is the maximum value of duty ratio in salp chain, and dc_{min} is the minimum value of duty ratio in salp chain. In ASSA-P&O, the exploration of search space is stopped when the global peak region is found. The convergence criteria used to find a global peak region is based on the length of the salp chain, which influences C_1. In this case, the convergence criterion is:

$$(dc_{max} - dc_{min}) \leq 0.2 \tag{4.8}$$

From Figure 4.5.c), it is evident that the exploration of search space is completed if the global region is found, and variable step P&O [55] with step size given in (3.13) can continue tracking GMPP with any small change in irradiance also. From the above simulation result analysis among three SSA algorithms, the ASSA-P&O GMPPT technique can track GMPP within a short time $T_{mp} = 0.2307$ sec. Since the exploration is stopped when the global region is found, oscillations of power and voltage during the transient part of MPP tracking are minimized. Further, the variable step P&O with small step size is used during steady-state operation of MPP tracking results in low power oscillations.

Case(2): When partial Shading occurs, the performance of the proposed ASSA-P&O GMPPT technique is compared with conventional P&O and PSO-based GMPPT techniques. Dynamic

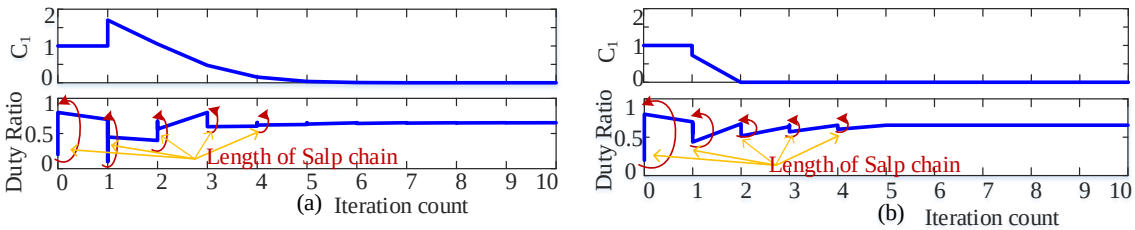

Figure 4.4: Simulation results of variation of C_1 in a) SSA, b) ASSA.

shading conditions are simulated with the help of pattern-1 and pattern-4 P-V curves of Figure 4.2.b), and simulated results are shown in Figure 4.5. The parameters of tested MPPT algorithms are given in Table 4.1. As discussed in [13, 53], P&O MPPT technique tracking time depends on sample time and perturbation step size, and in the present simulation, $\Delta d = 0.03$ and $T_s = 15$ *msec* are considered, which result in stable three-point behavior around MPP. Under uniform irradiance conditions, P&O can reach the global peak GP_1 on a single-peak P-V curve of pattern-1 within a time $T_{mp} = 0.28$ *sec*. But when irradiance is changed to pattern-4,i.e., partial shading condition, the conventional P&O algorithm with fixed perturbation step size tracks local peak LP_{41}, and it becomes stuck at that local peak of multi-peak P-V curve of pattern-4. Hence P&O algorithm may fail to track the global peak on the multi-peak P-V curve and able to track the only GP of a single-peak curve. Therefore, to track the global peak in both cases, soft computing techniques are used. In this case, the proposed ASSA-P&O is compared with the popular GMPPT technique PSO GMPPT and from the results obtained, ASSA P&O is seen to give better performance. Both techniques are simulated with the same initial population and sample time. PSO can reach the GP in $T_{mp} = 0.4317$ *sec* and 0.408 *sec* under uniform irradiation and PSC, respectively, with the convergence criteria in (4.8). Because of low adaptiveness in the velocity equation of PSO, the particle movement is large at the beginning of exploration, and it results in long tracking time and more power oscillations during tracking of GMPP.

In order to see the contribution of modifications done to original SSA in the proposed GMPPT technique, it is compared with conventional SSA [31], and memetic SSA [33] under PSC. Since memetic SSA presented in [33] is an off-line process that requires temperature and irradiation data at each panel. The remaining MPPT techniques presented in this chapter, including the proposed GMPPT technique, are an on-line process that requires only instantaneous PV voltage and current at the string terminals. For the fair comparison between all the MPPT techniques, memetic SSA in [33] is implemented as an on-line process in which two salp chains, each having two salps, are considered because of total salps in all three SSA algorithms are same. Regrouping of salps in two chains after each iteration is done in the same way as discussed in [33]. From the simulation results shown in Figure 4.5.c), it is evident that conventional SSA can track the GMPP of both pattern-1 and pattern-4, i.e., uniform and PSC. However, the slow-tracking of GMPP ($T_{mp1} = 0.3668sec$ and $T_{mp4} = 0.504sec$) in both the cases is due to the unnecessary exploration of search space even after reaching GP region.

Table 4.1: Parameters of MPPT algorithms in the simulation and hardware.

S.No	Algorithm	Parameters
1	P&O	$\Delta d = 0.03$
2	PSO	Population size = 4, Inertia constant $w = 0.4$ Acceleration constants $C_1 = 1.2, C_2 = 2$, Maximum Iteration count $itr_{max} = 10$ Limits of search space $[lb \;\; ub] = [0.1 \;\; 0.85]$
3	SSA	Population size = 4, Maximum Iteration count $itr_{max} = 10$ Limits of search space $[lb \;\; ub] = [0.1 \;\; 0.85]$
4	Memetic SSA	Population size in each chain = 2, salp chains = 2 Maximum Iteration count itr_{max}=10, Limits of search space $[lb \;\; ub] = [0.1 \;\; 0.85]$

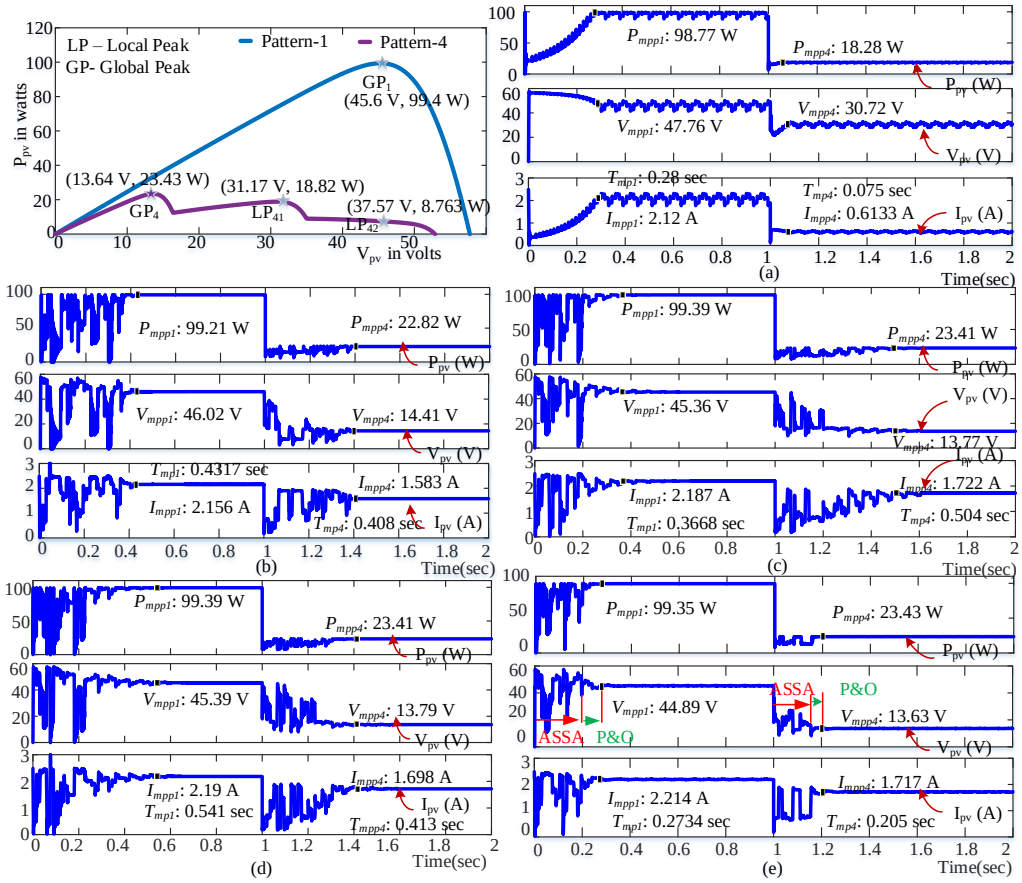

Figure 4.5: Simulation results of MPPT algorithms under PSC a) P&O, b) PSO, c) SSA, d) Memetic SSA, e) ASSA-P&O.

This unnecessary exploration is mainly due to the dependency of the control parameter C_1 on the maximum iteration count (=10). Whereas in the case of memetic SSA, the results obtained

Table 4.2: Simulation results of MPPT techniques.

	P&O			PSO			SSA			Memtic SSA			Proposed		
	T_{mp} (sec)	P_{mpp}(W)	$\%\eta_{static}$	T_{mp}(sec)	P_{mpp}(W)	$\%\eta_{static}$	T_{mp}(sec)	P_{mpp}(W)	$\%\eta_{static}$	T_{mp}(sec)	P_{mpp}(W)	$\%\eta_{static}$	T_{mp}(sec)	P_{mpp}(W)	$\%\eta_{static}$
Uniform Pattern-1 (GMPP=99.4W)	0.28	98.77	99.36	0.4317	99.21	99.8	0.3688	99.39	99.98	0.541	99.39	99.98	0.2734	99.35	99.94
PSC Pattern-4 (GMPP=23.43W)	0.075	18.28	78.02	0.4 08	22.82	97.39	0.504	23.41	99.91	0.413	23.41	99.91	0.205	23.42	99.95

under PSC shown in Figure 4.5.d) are better than the conventional SSA in terms of tracking speed ($T_{mp4} = 0.413sec$). However, the dependency of the control parameter C_1 on the maximum iteration count (=10) resulted in the unnecessary exploration of search space even after reaching the GP region, which delays the convergence. Hence, memetic SSA resulted in slow tracking of GMPP as compared with the proposed GMPPT technique. With the proposed hybrid GMPPT algorithm, unnecessary exploration in the GP region is reduced due to the soft computing technique is used only for identifying global peak region in the limited search space. At the same time, a variable step P&O can track the global peak in a short time.

As discussed in the case (1), with a single control parameter (C_1), the ASSA-P&O GMPPT technique can reach the global peak as shown in Figure 4.5.e) within a short time $T_{mp} = 0.2734$ *sec* and 0.205 *sec* under uniform irradiation and PSC, respectively. From the simulation result analysis, it is evident that the proposed GMPPT technique is much faster than other conventional and memetic SSA-based MPPT techniques. In the worst case, i.e., under pattern-1, the proposed GMPPT technique is 1.34 times faster than conventional SSA-based MPPT technique. Whereas under PSC, the proposed GMPPT technique is 2.45 times faster

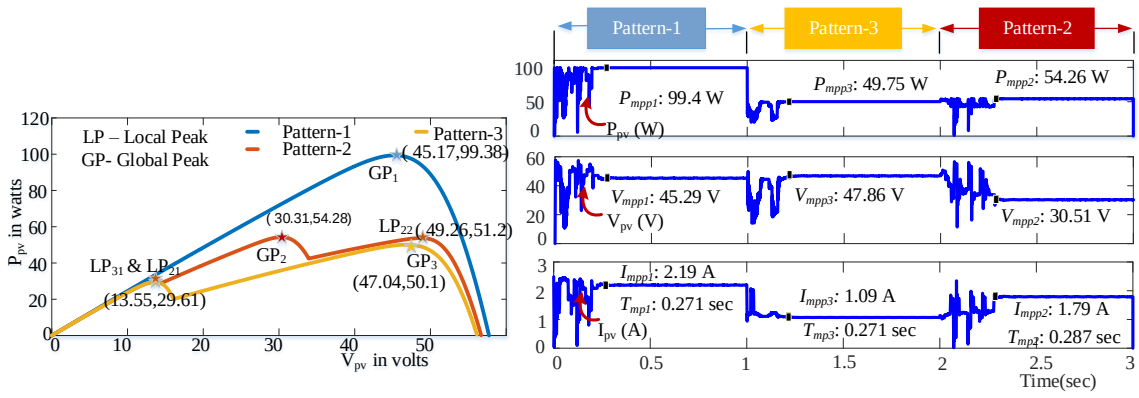

Figure 4.6: Simulation results of the proposed GMPPT technique under irradiance change.

than conventional SSA-based MPPT technique.

Case (3): Under irradiance changes, the global peak obtained so far is not fixed, and its position is changed based on the irradiance pattern. This change in irradiance is easily identified with a P&O algorithm with a change in power or with changes in voltage and current operating points. In this case, both an increase in irradiance and a decrease in irradiance are simulated with pattern-1,pattern-3, and pattern-2, respectively. When pattern-1 is applied first, GP is found, and variable step P&O can find the irradiance changes with the help of (4.9).

$$\begin{aligned} \left|\frac{V_k - V_{k-1}}{V_k}\right| &\geq 0.2 \\ \left|\frac{I_k - I_{k-1}}{I_k}\right| &\geq 0.1 \end{aligned} \tag{4.9}$$

where V_k and I_k are PV voltage, and current in the present perturbation, and V_{k-1} and I_{k-1} are PV voltage and current in the previous perturbation. From the simulation results, it is evident that the proposed ASSA-P&O GMPPT technique with limited search space can track GP under irradiance changes, as shown in Figure 4.6.

4.3.2 Hardware prototype and experimental validation of the proposed GMPPT technique

A laboratory prototype of the boost converter, as shown in Figure. 3.25 is used as an MPPT converter to validate the proposed GMPPT technique experimentally. The different shading patterns 1 to 4 are emulated by using chroma soft panel software of the PV simulator. The proposed hybrid algorithm and other algorithms are run with the same sample time $T_s = 300\ msec$. In a hardware implementation, the sample time is more than the simulation sample time because of the slow response time of the PV simulator.

4.3.2.1 Experimental validation of the proposed ASSA-P&O GMPPT technique

To validate the superiority of the proposed ASSA-P&O GMPPT algorithm over the SSA GMPPT technique, both are tested with pattern-1, and the experimentally obtained results are shown in Figure 4.7. The maximum number of iterations in the SSA GMPPT technique is considered as

10, and the results obtained are $P_{mpp} = 99.9\ W, V_{mpp} = 44.47\ V, I_{mpp} = 2.24\ A$ and $T_{mp} = 13\ sec$. Even though SSA GMPPT reaches GP around 9 sec, exploration is continued till ten iterations are completed, which causes unnecessary oscillations in power and requires more time for steady tracking of GMPP.

The proposed ASSA GMPPT technique with an adaptive C_1 equation, as given in (4.5), results in faster tracking and avoids unnecessary exploration due to the dependence of C_1 on maximum iteration count. The results obtained are $P_{mpp} = 99.9\ W, V_{mpp} = 44.45\ V, I_{mpp} = 2.24\ A$ and $T_{mp} = 8.7\ sec$. The performance of ASSA GMPPT is further improved with a combination of ASSA and P&O, and it is verified with results shown in Figure 4.7.c). The results obtained are $P_{mpp} = 99.9\ W, V_{mpp} = 44.47\ V, I_{mpp} = 2.24\ A$ and $T_{mp} = 5\ sec$. The time taken for tracking GP is significantly reduced in the proposed ASSA-P&O, and it is 2.6 times faster than the conventional SSA GMPPT technique.

The performance of the proposed GMPPT technique under PSC is compared with the conventional P&O MPPT technique and PSO GMPPT technique. Uniform irradiance condi-

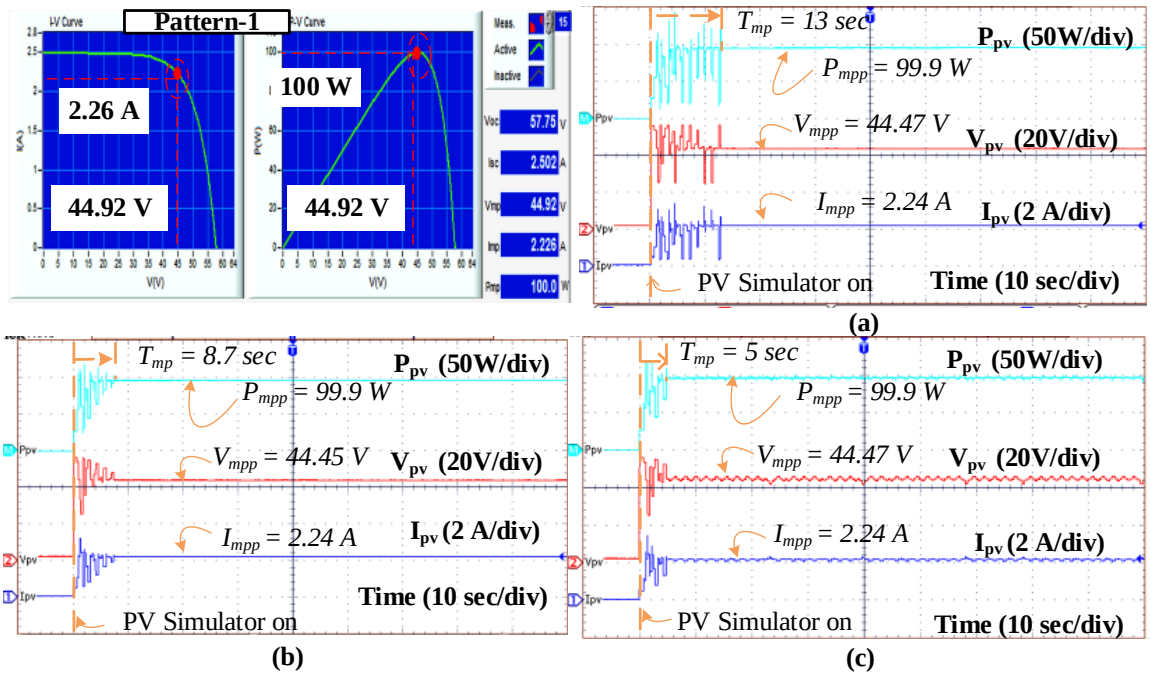

Figure 4.7: Experimentally obtained results of MPPT algorithms under uniform irradiance conditions a) SSA, b) ASSA, c) ASSA-P&O.

tions are emulated with pattern-1 for 40 sec, and then the next 50 sec PSC is emulated with pattern-4. The results obtained are shown in Figure 4.8. Conventional P&O is run with a step size $\Delta d = 0.05$, and the three-point behavior of P&O in steady operation is clearly observed in Figure 4.8.a). Under PSC, the results obtained are: $P_{mpp4} = 30.4\ W, V_{mpp4} = 29.82\ V, I_{mpp4} = 1.02\ A$ and $T_{mp4} = 1\ sec$. From this result, it is evident that P&O is not able to track GP, and in this case, GP for pattern-4 is 33.35 W. Soft computing techniques like PSO can reach GP, but it results in more time to track GP with large power oscillations during exploration. The results obtained with PSO GMPPT are $P_{mpp4} = 33.2\ W, V_{mpp4} = 15.1\ V, I_{mpp4} = 2.2\ A$ and $T_{mp4} = 11.2\ sec$. The slow-tracking of the PSO GMPPT technique is fixed control parameters and unnecessary exploration of search space even after reaching the GP region. Whereas the SSA-based MPPT technique is easy to implement with a single control parameter. Because of the wrongly estimated maximum iteration count (10), which affects the control parameter and results in slow-convergence. The experimentally obtained results with conventional SSA under PSC are $P_{mpp4} = 33.2\ W, V_{mpp4} = 15.02\ V, I_{mpp4} = 2.21\ A$ and $T_{mp4} = 11\ sec$.

For the fair comparison of Memetic SSA with other on-line methods presented in this chapter, memetic SSA also designed for the on-line search process. The results obtained with this technique under PSC are $P_{mpp4} = 33.25\ W, V_{mpp4} = 15.11\ V, I_{mpp4} = 2.2\ A$, and $T_{mp4} = 12\ sec$. The slow-tracking of memetic SSA is due to the same reason as conventional SSA, i.e., the dependency of control parameter on maximum iteration count. Even though memetic SSA results better in MPPT based on the off-line search process, in the case of on-line/ hardware-based search, it results in slow-tracking ($T_{mp1} = T_{mp4} = 12\ sec$) due to more salps in the form of salp chains and deterministic control parameter.

From the experimentally obtained results of ASSA-P&O, as shown in Figure 4.8.e), it is evident that the proposed algorithm tracks GP quickly with less power oscillations during irradiance changes or PSC due to limited search space. The results obtained are $P_{mpp4} = 33.1\ W, V_{mpp4} = 15.5\ V, I_{mpp4} = 2.13\ A$ and $T_{mp4} = 4\ sec$. From the experimental results, it is evident that the proposed GMPPT technique is faster (approximately 2.5 times) than the conventional SSA-based GMPPT technique.

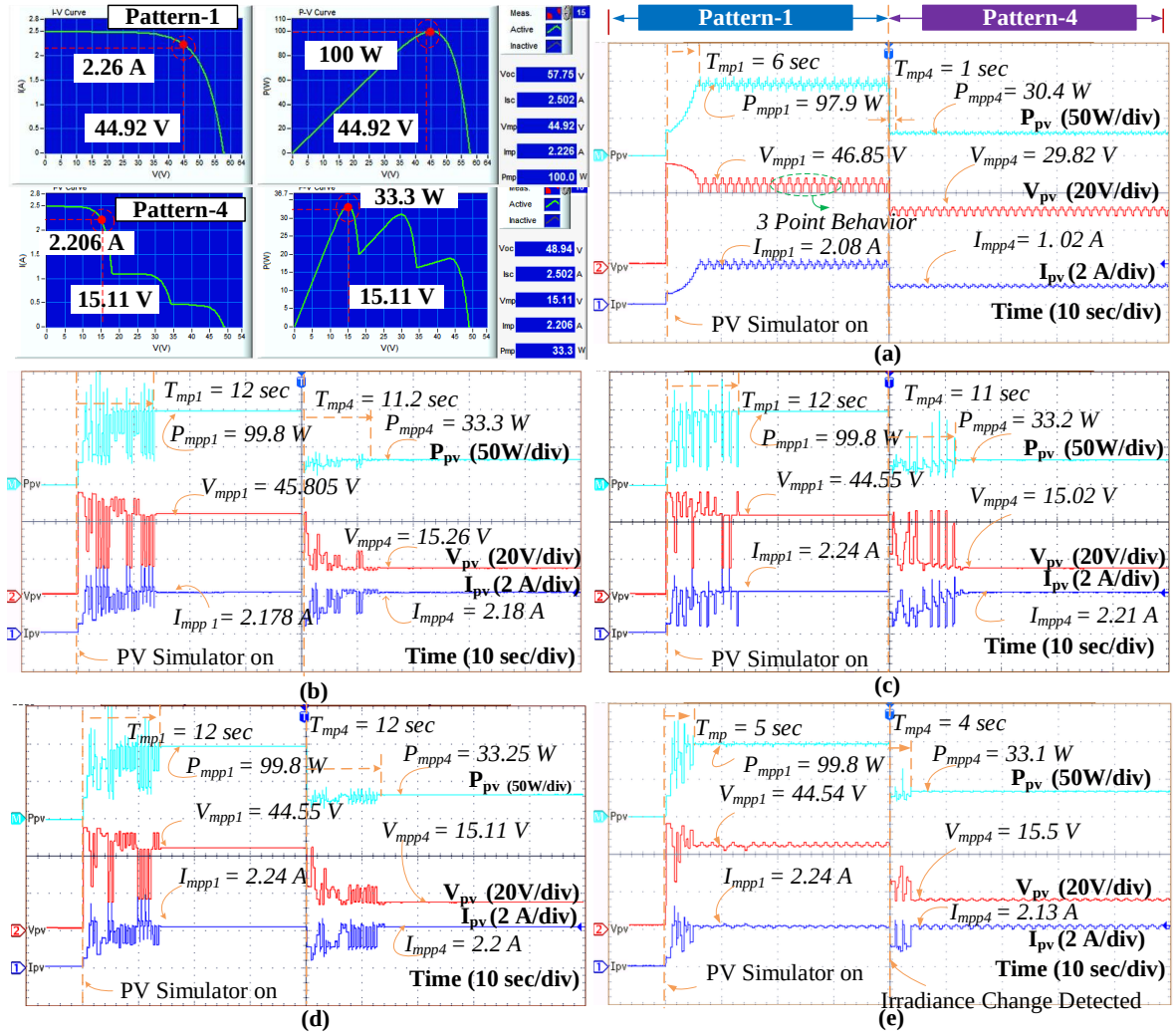

Figure 4.8: Experimentally obtained results of MPPT algorithms under PSC a) P&O, b) PSO, c) SSA, d) Memetic SSA, e) ASSA-P&O.

4.3.2.2 Experimental validation of the proposed ASSA-P&O GMPPT technique under irradiance changes

Under irradiance changes, the method proposed to reduce the search space discussed in section III is verified with a decrease and increase in irradiance with the help of transitions from pattern-

Table 4.3: Experimentally obtained results of MPPT techniques.

	P&O			PSO			SSA			Memtic SSA			Proposed		
	T_{mp} (sec)	P_{mpp}(W)	$\%\eta_{static}$	T_{mp}(sec)	P_{mpp}(W)	$\%\eta_{static}$	T_{mp}(sec)	P_{mpp}(W)	$\%\eta_{static}$	T_{mp}(sec)	P_{mpp}(W)	$\%\eta_{static}$	T_{mp}(sec)	P_{mpp}(W)	$\%\eta_{static}$
Uniform Pattern-1 (GMPP=100W)	6	97.9	97.9	12	99.8	99.8	12	99.8	99.8	12	99.8	99.8	5	99.8	99.8
PSC Pattern-4 (GMPP=33.35W)	1	30.4	91.15	11.2	33.3	99.85	11	33.2	99.55	12	33.25	99.7	4	33.1	99.25

1 to pattern-3 and pattern-3 to pattern-1. Each pattern is applied for 30 sec, as shown in Figure 4.9, and the results obtained with pattern-1 are $P_{mpp1} = 99.8\ W, V_{mpp1} = 44.5\ V, I_{mpp1} = 2.24\ A$ and $T_{mp1} = 6\ sec$. After 30 sec, when irradiance changes from pattern-1 to pattern-3, the results obtained are $P_{mpp3} = 55.5\ W, V_{mpp3} = 43.41\ V, I_{mpp3} = 1.28\ A$and $T_{mp3} = 4.2\ sec$.In this case, faster convergence and low power oscillations are due to reduced search space. After a 30-sec increase in irradiance is emulated with a change in pattern-3 to again pattern-1 and the results obtained are $P_{mpp1} = 99.9\ W, V_{mpp1} = 44.4\ V, I_{mpp1} = 2.24\ A$ and $T_{mp1} = 7\ sec$. In this case, it is observed that the power oscillations during tracking GP are minimized compared to the previous occurrence of pattern-1 at the beginning.

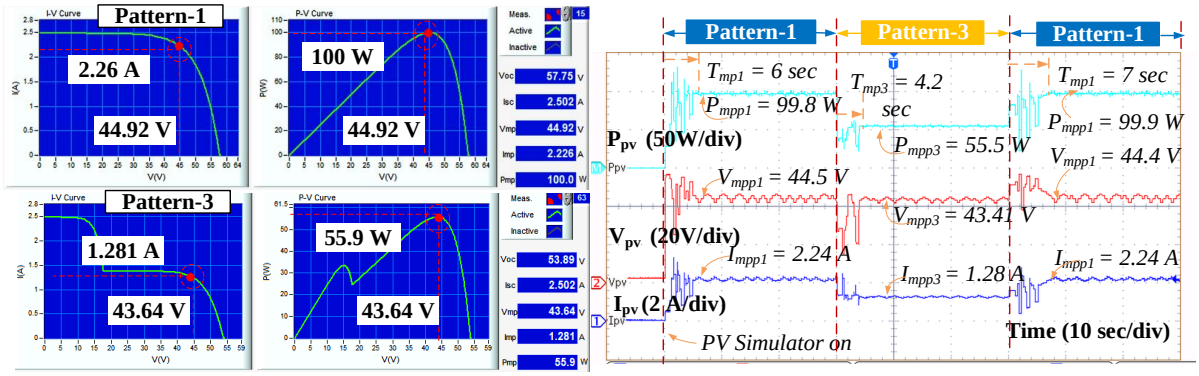

Figure 4.9: Experimentally obtained results of ASSA P&O under irradiance changes.

4.4 Proposed hybrid GMPPT technique: ASSADE-P&O

In ASSA-P&O, the number of parameters to be tuned and power oscillations during tracking are minimized. However, slower tracking of GP region identification in hybrid MPPT techniques (formed with SC and gradient MPPT techniques) is mainly due to the least fitness particles. When these techniques are applied to off-grid PV systems, reinitialization of GP region identification stage for load changes degrades the performance of the GMPPT technique. Hence, the least fitness particles should be accelerated more towards the leader to get faster GP region identification. To get the better accuracy, leader salp should be enhanced in the food source region. Hence, in this chapter, to get accurate and fast-tracking of GMPP, a hybrid GMPPT method ASSADE-P&O is proposed. The overview of each part of the proposed method is discussed in detail below.

4.4.1 Overview of DE

DE is an evolutionary algorithm to search for an optimal solution in the defined region by using mutation, crossover, selection operators [41,58]. Differential evolution starts from the selection of three target or parent vectors $D_{i1}(G)$, $D_{i2}(G)$and $D_{i3}(G)$, while trail vectors $U_i(G)$ are generated by mutation (4.10). The scale factor of mutation ξ is important to generate the trail vector, which varies from $[0.1\ \ 1]$.

$$U_i(G) = D_{i1}(G) + \xi \times (D_{i2}(G) - D_{i3}(G)) \tag{4.10}$$

where i is the population number. During crossover (4.10), child vector $D_i^{'}(G)$ is selected from trial vector $U_i(G)$ and best parent $D_{i1}(G)$ by using a random number and crossover probability ρ, which range from 0 to 1.

$$D_i^{'}(G) = \begin{cases} U_i(G), & if \ \ rand \leq \rho \\ D_{i1}(G), & if \ \ rand > \rho \end{cases} \tag{4.11}$$

Finally, DE selects the best solution $D_i(G+1)$ for the next generation based on the fitness value f of child and parent vectors given in (4.12).

$$D_i(G+1) = \begin{cases} D_i^{'}(G), & if \ \ f(D_i^{'}(G)) > f(D_i(G)) \\ D_{i1}(G), & if \ \ f(D_i^{'}(G)) < f(D_i(G)) \end{cases} \tag{4.12}$$

4.4.2 Details of the Proposed ASSADE–P&O GMPPT technique

In SSA, all salp positions depends on leader position. Whereas leader position is influenced by control parameter C_1. In conventional SSA, C_1 value is a time varying and depends on the maximum iteration count required for convergence which is an unknown value. If a large value of iteration count is considered, the leader position will be updated even after reaching optimum solution and causes for unnecessary exploration. Whereas a smaller value of iter-

ation count results in premature convergence. Therefore, the control parameter needs to be independent of maximum iteration count. Hence, in this proposed hybrid GMPPT technique, a time-independent adaptive control parameter is derived. C_1 in (4.2) is modified as (4.13) in adaptive SSA (ASSA)

$$C_1^i = 2 \times e^{-\left(4\times\left(1-\left(\frac{d_{max}^i - d_{min}^i}{ub}\right)\right)\right)^2} \tag{4.13}$$

where d_{max}^i is the duty ratio maximum in the current iteration and d_{min}^i is the duty ratio minimum in the current iteration, and ub is the upper boundary of search space. Control parameter C_1^i in (4.13) changes w.r.t. to salp chain length. Salp chain length is nothing but distance between maximum and minimum salp positions. In the first iteration, this distance is large since all the salps are distributed uniformly throughout the search space. Based on (4.13), a high value of C_1 allows exploration of leader in the search space. As the iterations proceeds, there is a gradual change in salp position and moves closer to the food source, i.e., GP in the k^{th} iteration. When all the salps enter into GP region, the salp chain length decreases, and C_1 becomes very small, which allows the leader to exploit. Even though ASSA avoids the dependence of algorithm performance on an unknown maximum iteration count, with few salps both SSA and ASSA can not guarantee optimum solution under all dynamic conditions. Hence ASSA algorithm is integrated with DE.

To get the fast-tracking by satisfying the defined convergence criteria other than maximum iteration count like the distance between each particle is lower than some threshold value, the least fitness particles should be accelerated more towards the leader. Hence in the proposed method, DE is applied on both food source as well as least salp in salp chain to reach the best solution to achieve faster tracking of GMPP, as shown in Figure 4.10. Applying DE on leader salp helps in finding a better solution without stagnation at local peak. Hence, the integration of ASSA with DE helps obtain a better solution with few salps in the ASSA. In the proposed method ASSA and DE are in series. The solutions obtained with ASSA are given to the DE in each iteration to get a better solution. For the food source, the mutation is defined as (4.14), while (4.15) is for the least fitness salp.

$$U_1(G) = D_1(G) + \xi \times |(D_2(G) - D_3(G))| \tag{4.14}$$

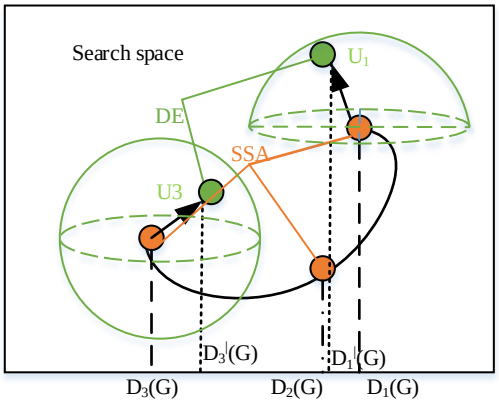

Figure 4.10: Salp movements in SSA-DE.

$$U_3(G) = \begin{cases} D_3(G) + \xi \times |(D_1(G) - D_2(G))|, \\ \qquad if \;\; D_3(G) \leq D_1(G) \\ D_3(G) - \xi \times |(D_1(G) - D_2(G))|, \\ \qquad if \;\; D_3(G) > D_1(G) \end{cases} \tag{4.15}$$

where $U_1(G)$ is the trail vector of leader salp, $U_3(G)$ is the trail vector of least fitness salp in salp chain, D_1, D_2, D_3 are solutions obtained in ASSA in each iteration, D_1 is the leader salp and D_3 is least fitness salp in the chain. The scale factor of mutation increases linearly from ξ_{min}=0.1 to ξ_{max}=0.6 as given in (4.16).

$$\xi = \xi_{min} + \left(\frac{it}{itr_{max}}\right) \times (\xi_{max} - \xi_{min}) \tag{4.16}$$

where it is the present iteration and itr_{max} is the iteration count maximum. Since MPPT is a on-line process in which each duty should be applied to the MPPT converter to find the fitness, there is a delay of tracking time if the same duty ratio is applied to find fitness in the form of target vector in the crossover as per [58]. Hence, without increasing tracking time in the form of DE, in crossover stage, selection of child vector for leader salp or least fitness salp is provided instead of choosing the same target vector. Hence, either DE on leader salp or DE on least fitness salp is executed in each iteration. Therefore, the crossover of the proposed method is

given in (4.17)

$$\begin{aligned} D_1^{'}(G) &= U_1(G), \;\; if \;\; rand \leq \rho \\ D_3^{'}(G) &= U_3(G), \;\; if \;\; rand > \rho \end{aligned} \tag{4.17}$$

where ρ is crossover probability constant varies from 0 to 1, and in the proposed method, 0.67 is considered as crossover probability constant. In conventional DE, selection of child or parent is based on the fitness $f(D_1^{'}(G))$. Without affecting the sorting order of salp chain, the selection of next-generation salps are based on (4.18).

$$\begin{aligned} D_1(G+1) &= \begin{cases} D_i^{'}(G), \;\; if \;\; f(D_1^{'}(G)) > f(D_1(G)) \\ D_1(G), \;\; if \;\; f(D_1^{'}(G)) < f(D_1(G)) \end{cases} \\ D_3(G+1) &= \begin{cases} D_3^{'}(G), \;\; if \;\; f(D_3^{'}(G)) > f(D_3(G)) \& \\ \qquad\qquad\qquad f(D_3^{'}(G)) < f(D_2(G)) \\ D_3(G), \;\; if \;\; f(D_3^{'}(G)) < f(D_3(G)) \end{cases} \\ D_2(G+1) &= \begin{cases} D_3^{'}(G), \;\; if \;\; f(D_3^{'}(G)) > f(D_2(G)) \& \\ \qquad\qquad\qquad f(D_3^{'}(G)) < f(D_1(G)) \\ D_2(G), \;\; if \;\; f(D_3^{'}(G)) < f(D_2(G)) \end{cases} \end{aligned} \tag{4.18}$$

After reaching the global peak region by ASSADE, to avoid unnecessary power oscillations due to exploration process of ASSA, in the proposed algorithm, tracking is shifted to P&O algorithm with variable steps. In variable step P&O, tuning M value is tedious. Hence M is automatically tuned by (4.19) before starting the perturbations.

$$M = \frac{\Delta D_{max}}{\frac{dp}{dv}|_{\Delta D_{max}}} \tag{4.19}$$

where ΔD_{max} is the maximum value of step size in fixed-step P&O. Partial solution obtained during identification of GP region is used as starting point of variable step P&O algorithm

Table 4.4: Change in voltage and current during insolation change and load variation.

Change Due to	dV Sign	dI Sign
Insolation Increase	Positive	Positive
Insolation Decrease	Negative	Negative
Load Increase	Positive	Negative
Load Decrease	Negative	Positive

which leads to a more accurate solution in steady-state with reduced power oscillations. The convergence criteria used for finding the GP region is given by the distance between each salp which is less than one percent.

After reaching steady-state, the output power changes due to either change in insolation or load variation. With the change insolation, GMPP shifts from the previous position, and due to load variation, GMPP is fixed at the same position just as it was before the load variation occurs [59], but the operating point changes and may lead to operating at any local peak in both the cases due to nature of P&O. Hence reinitialization of ASSADE is required for finding new GMPP due to shifting in GMPP when insolation change occurs; but for the same GMPP in the case of load change, reinitialization may result in unnecessary initial power oscillations during the exploration of ASSADE. To avoid initial power oscillations during this process, direct duty ratio is calculated for the load change based on the history of PV resistance at MPP and present load value. Direct duty ratio calculation for the load change results in rapid tracking of MPP for new load without facing power oscillations due to reinitialization of ASSADE. Resistance value at MPP (R_{mp}) is calculated using (4.20)

$$R_{mp} = V_{mp}/I_{mp}; \tag{4.20}$$

where V_{mp} is the voltage at MPP and I_{mp} is the current at MPP. Load resistance R_{load} of boost converter in terms of input resistance R_{in} where $R_{in} = V_{pv}/I_{pv}$ is

$$R_{load} = \frac{R_{in}}{(1-D_{mp})^2} \tag{4.21}$$

where D_{mp} is the duty ratio at MPP. Once load change is identified, the new duty ratio D_{new} is

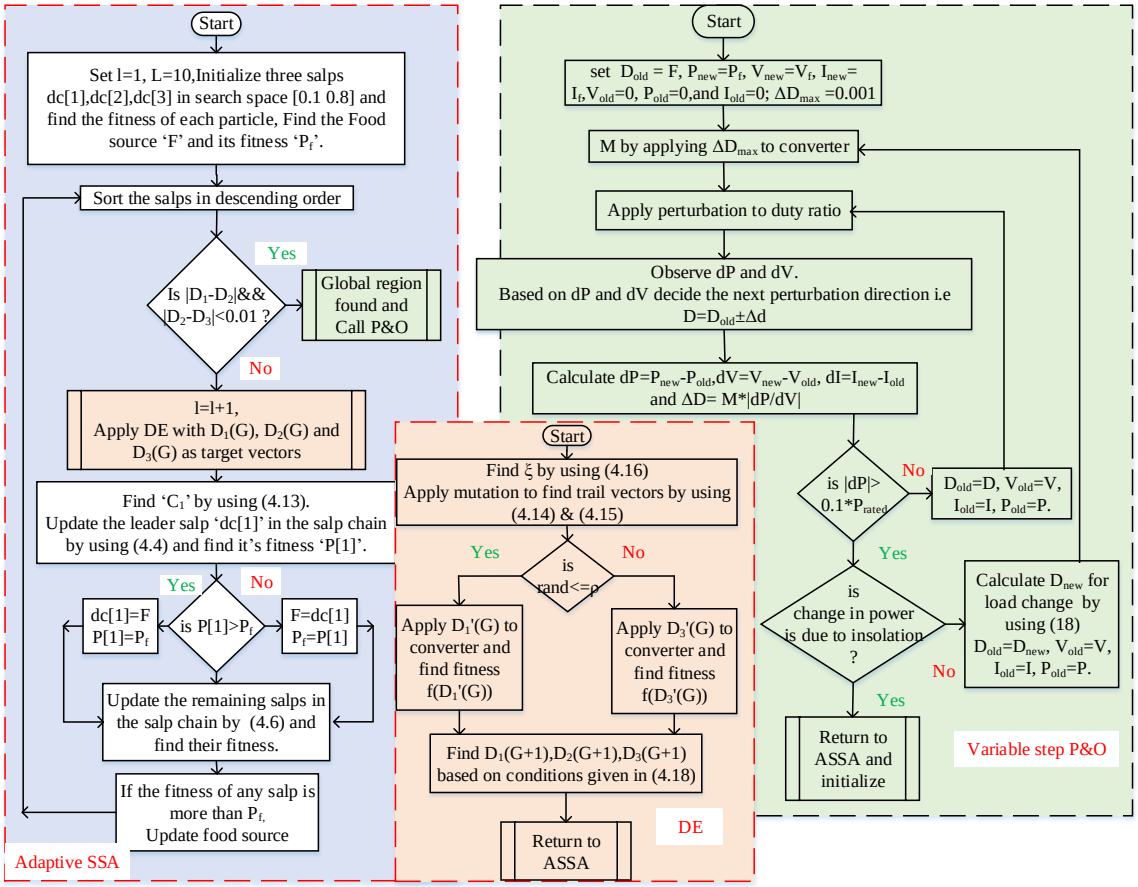

Figure 4.11: Flowchart of the proposed algorithm ASSADE-P&O.

calculated as (4.22).

$$D_{new} = 1 - \sqrt{\frac{R_{mp}}{R_{load}}} \tag{4.22}$$

The difference in the load change and insolation change is identified with the change in voltage and current direction as given in Table 4.4. The change in steady-state of the system is identified with change in power given by (4.23)

$$dP > P_{rated} * 0.1 \tag{4.23}$$

where dP is the change in power in one sample time.

Steps to implement the proposed ASSADE–P&O method as given in Figure 4.11 are:

1) Apply three salps, i.e., duty ratios D_1, D_2, and D_3 uniformly in the search space in the first iteration and calculate the fitness of each salp, i.e., power. Sort the salps in descending order

of their fitness. Find the food source F, i.e., first salp in the salp chain which is formed by sorting.

2) Apply DE on the food source or least fitness salp in the chain formed after the first iteration of ASSA.

3) Update the position of leader based on (4.4) with adaptive control parameter in (4.13). If the fitness of leader is more than food source, update the food source with leader; otherwise, keep the leader as food source.

4) Update the positions of the remaining salps in the chain by using (4.6). If the fitness of any salp is more than food source fitness, update food source with that salp.

5) Sort the salps given to DE. Find the fitness of evaluated particles in DE. If the fitness of evaluated particles of food source or the least fitness salp is more than the fitness obtained in ASSA, update the corresponding salp with the solution obtained in DE. Repeat steps 3, 4, and 5 until convergence criteria are reached, i.e., the distance between each salp is less than 1%.

6) Apply VS-P&O with the partial solution obtained in ASSADE. In the starting find M using (4.19).

7) Find step size using (3.13) and Repeat this step until change in power is identified either due to change in load or insulation.If

   [i] the load change is identified, calculate the new value of duty directly using (4.20) – (4.22) and repeat steps 6 and 7 until insolation change is identified.

   [ii] the insolation change is identified, repeat steps 1 to 7.

4.4.3 Simulation case studies

To test the performance of the proposed method, MATLAB/Simulink model of DC-DC converter and with short string and long string arrangement of PV panels are used as shown in Figure 4.12. In this simulation study, a 300 W PV system is studied with six panels connected in either six series one parallel (6S-1P long String) or two 3-panel strings connected in parallel

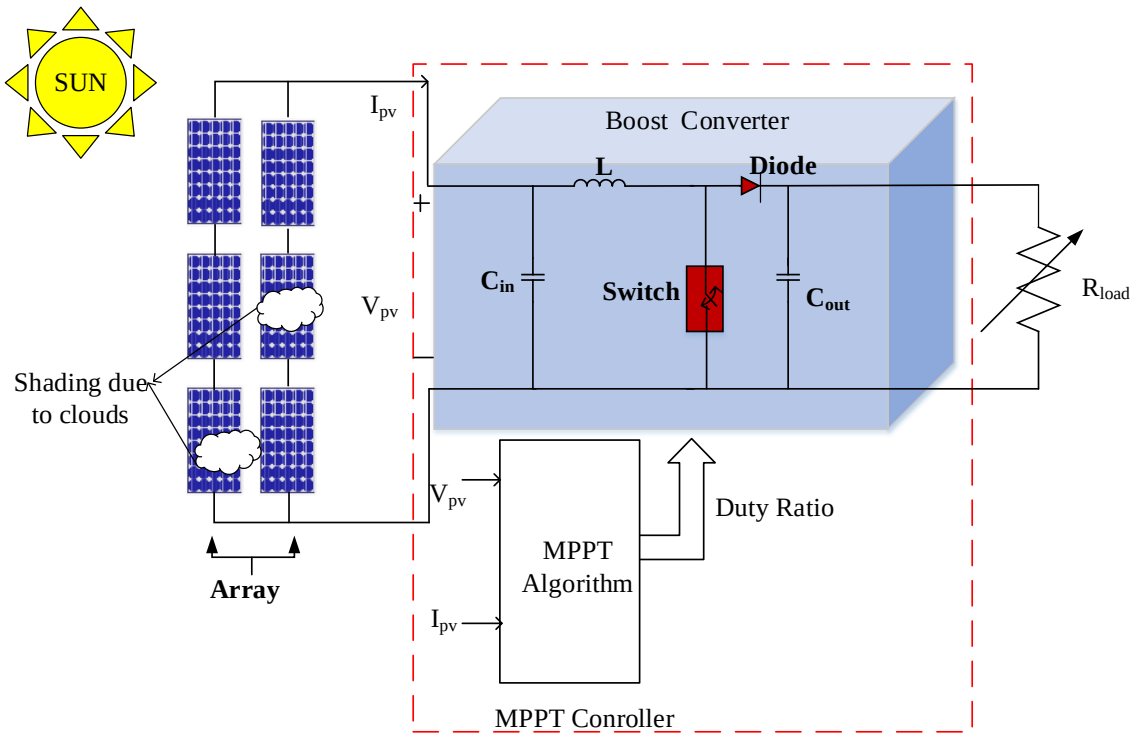

Figure 4.12: Block diagram of PV system under partially shaded conditions.

(3S-2P short string) as shown in Figure 4.13. A 50 W solar panels manufactured by solar power mart SPM-50M model are used. Its electrical equivalent circuit parameters are extracted as given in the appendix. With the insolation profiles from PSC-1 to PSC–6 shown in Figure 4.14, multi-peak P–V curves from 1–6 peaks as given in Table 4.6 can be simulated.

The dependence of tracking time on maximum iteration count for various conventional SI techniques is studied with the same number of population (=4). From the simulation results

Table 4.5: Parameters of boost converter used in the simulation and hardware.

S.NO	Parameter	Value
1	Inductance L	1.5 mH
2	Output capacitance C_{out}	22 μF
3	Input capacitance C_{in}	4.7 μF
4	Load R_L	100 Ω
5	Switching frequency f_s	50 KHz

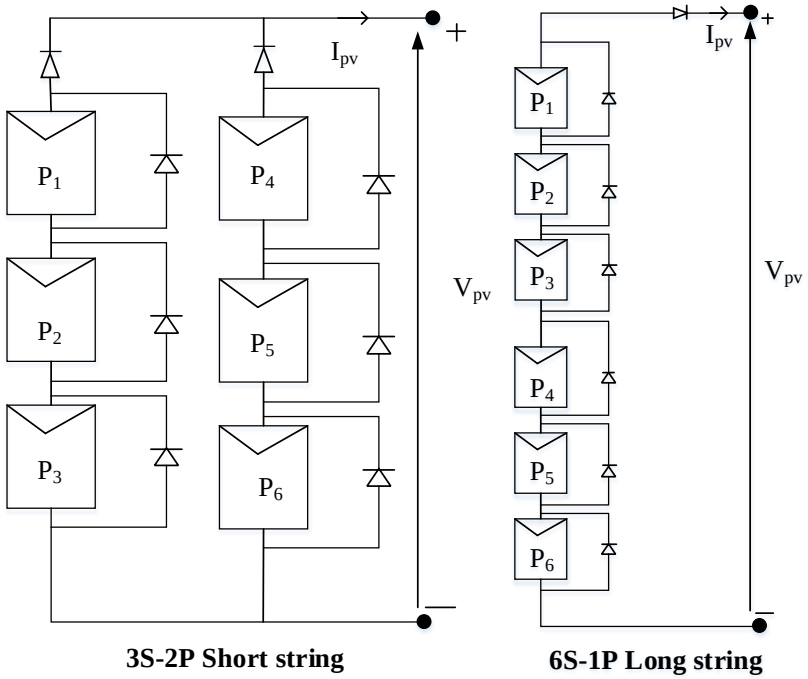

Figure 4.13: PV panels P1-P6 connected in string arrangment.

Table 4.6: Details of irradiance profiles used for simulation and hardware.

String Type	Irradiance Pattern	Irradiance profile (KW/sq.mt)						Number of Peaks	Global Peak		
		P_1	P_2	P_3	P_4	P_5	P_6		V_{GP} (V)	I_{GP}(A)	P_{GP}(W)
3S-2P Short String	PSC-1	1	1	1	1	1	1	1	55.87	5.38	300.6
	PSC-2	1	1	0.5	1	1	0.5	2	36.07	5.434	196.01
	PSC-3	0.8	0.5	0.2	0.8	0.5	0.2	3	37.19	2.77	102.9
6S-1P Long String	PSC-4	0.5	0.5	0.4	0.4	0.2	0.1	4	73.12	1.08	79.09
	PSC-5	1	1	0.6	0.4	0.3	0.2	5	56.69	1.663	94.26
	PSC-6	0.7	0.5	0.4	0.3	1	0.2	6	77.19	0.91	85.07

shown in Figure 4.15, it is evident that in all the presented algorithms, convergence time is directly related with iteration count under the same insolation conditions in an on-line search process like PV MPPT, and it leads to unnecessary exploration even after finding optimum value because of which power oscillations before reaching steady-state and tracking time are increased. The convergence time of three popular SI techniques for the PV MPPT in the literature PSO, GWO, and WOA are highly dependent on maximum iteration count, which is not known initially. In the case of SSA, even though the dependence of SSA on maximum iteration count is lower compared to the other three techniques. A large value of maximum iteration

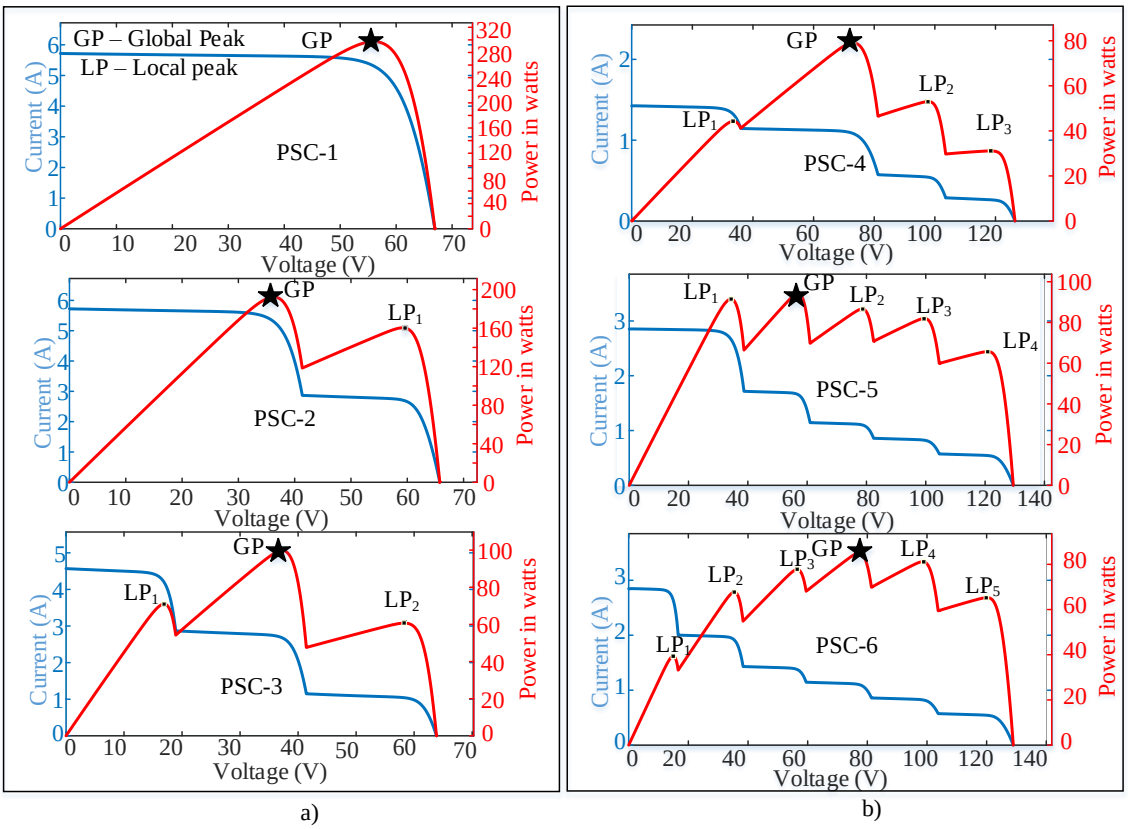

Figure 4.14: PSC profiles used for simulation and hardware a) 3S-2P short string, b) 6S-1P long string.

count (30) results in unnecessary power oscillations in the GP region even after optimum solution is reached. It causes slow tracking of MPP, i.e., 0.26 sec for PSC1, 0.2494 sec for PSC2, and 0.216 for PSC3. In the case a small value of iteration count (10), even though convergence speed is fast (0.144 sec for PSC1), it may cause convergence before reaching optimum solution with few salps. Hence, it is better to avoid the dependency of control parameter on maximum iteration count. In this work , self-adaptive parameter tuning based on the feedback of position of search agents during each iteration is proposed, which is also best suited for identifying GP region accurately.

The simulation results of the MPPT techniques are shown in Figure 4.16 and results are tabulated in Table 4.7, 4.8, and 4.9. In Figure 4.16.a), even though WOA results in better accuracy in the case of PSC1, i.e., P_{mp}=300.6 W than the other three SI techniques, but convergence largely depends upon the maximum iteration count, and takes more time to track the MPP

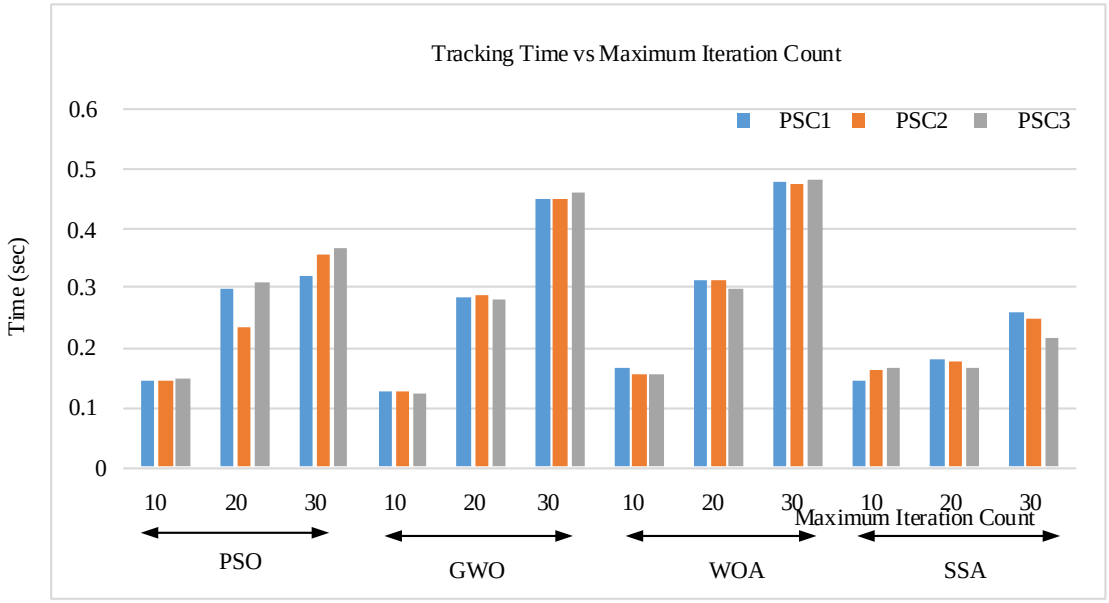

Figure 4.15: Barchart of maximum iteration count vs tracking time of conventional SI techniques.

T_{mp}=0.48 sec for PSC1. The three SI techniques, PSO, GWO, and WOA, suffers from more number of parameters tuned for dynamic changes in irradiance. Whereas for SSA, accuracy of tracking is less (P_{mp}=299 W in the case of PSC1). Even though SSA is faster (T_{mp}=0.268 sec in the case of PSC1) than the other three algorithms, it also faces the same problem of power oscillations in the GP region due to he wrong value of maximum iteration count chosen. Hence, in the proposed method, an adaptive control parameter is proposed which is not dependent on maximum iteration count, and depends on the distance between the salp position. In Figure 4.16.b) shows, gradual improvement of the proposed method, while deriving it from conventional SSA and integrating with DE and P&O. From the result, it is evident that the proposed method is superior to conventional SSA technique and takes less time to track the GMPP in all the three cases of shading with the convergence criteria as distance between the salps is less than 0.01. The conventional SSA takes T_{mp}= 0.26 sec to reach GMPP with P_{mp}=298.8 W for PSC1. Under the same insolation condition, whereas the proposed method takes T_{mp}= 0.16 sec to reach GMPP with P_{mp}=300.3 W. The proposed hybrid method is approximately 1.6 times much faster than its conventional SSA technique. The control parameter of conventional SSA is tuned adaptively in ASSA. However, the complete tracking of GMPP with ASSA only results in

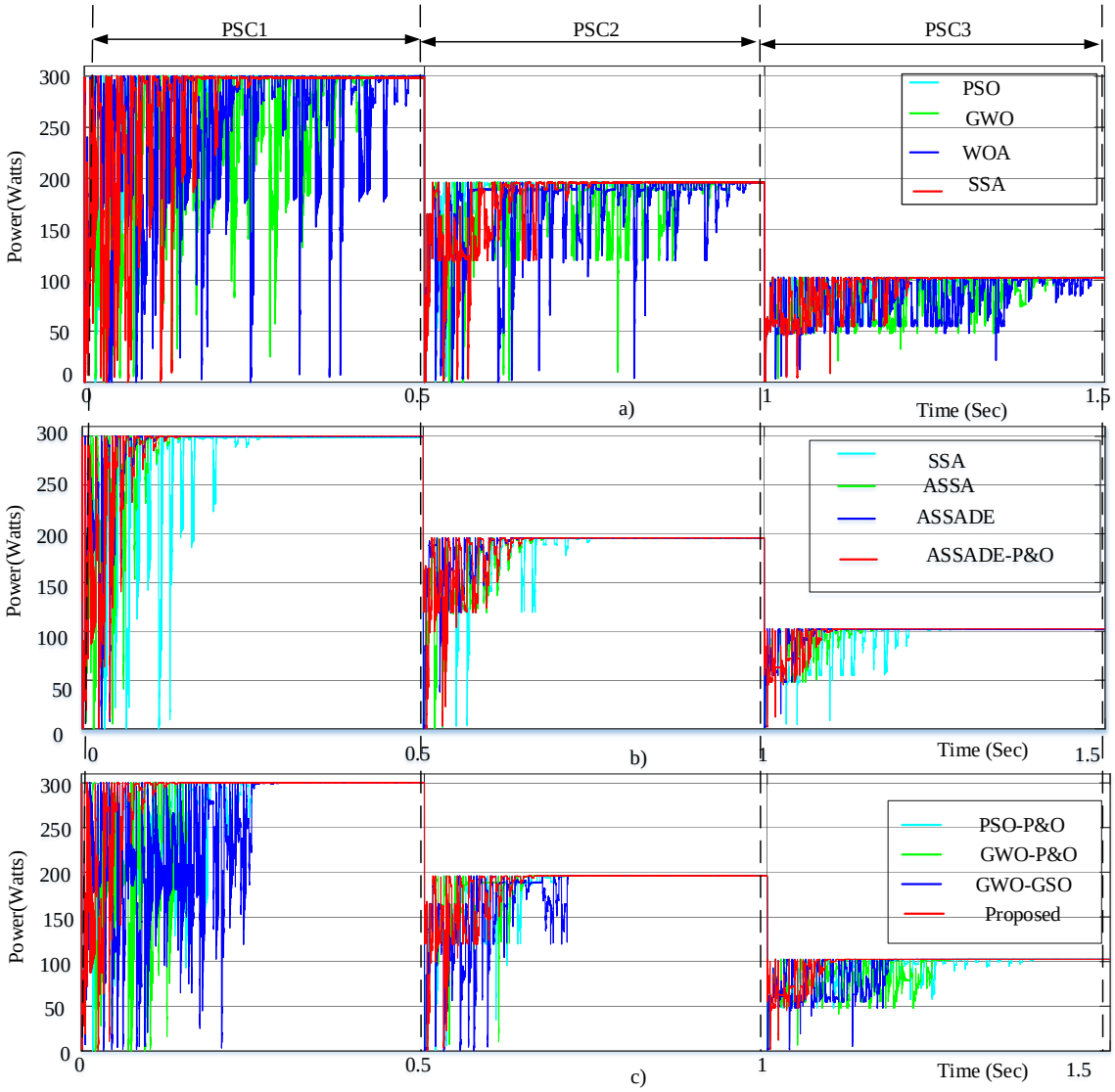

Figure 4.16: Simulation results under irradiance changes a) SI techniques, b) Gradual improvement of the proposed technique, c) Hybrid GMPPT techniques.

Table 4.7: Simulation results of the SI based GMPPT techniques.

	PSO			GWO			WOA			SSA		
	T_{mp} (sec)	P_{mp}(W)	$\%\eta_{static}$	T_{mp}(sec)	P_{mp}(W)	$\%\eta_{static}$	T_{mp}(sec)	P_{mp}(W)	$\%\eta_{static}$	T_{mp}(sec)	P_{mp}(W)	$\%\eta_{static}$
PSC1 (GMPP=300.6W)	0.398	300.2	99.86	0.45	300.2	99.86	0.49	300.2	99.86	0.272	299.3	99.57
PSC2 (GMPP=196.01W)	0.46	195.9	99.94	0.454	195.6	99.79	0.485	195.8	99.89	0.289	195.9	99.94
PSC3 (GMPP=102.9W)	0.404	102.5	99.61	0.436	102.5	99.61	0.483	102.5	99.61	0.285	102.2	99.32

unnecessary power oscillations even after finding the optimum value and slower convergence.

Table 4.8: Simulation results of the SSA based GMPPT techniques.

	SSA			ASSA			ASSADE			Proposed		
	T_{mp} (sec)	P_{mp}(W)	$\%\eta_{static}$	T_{mp}(sec)	P_{mp}(W)	$\%\eta_{static}$	T_{mp}(sec)	P_{mp}(W)	$\%\eta_{static}$	T_{mp}(sec)	P_{mp}(W)	$\%\eta_{static}$
PSC1 (GMPP=300.6W)	0.272	299.3	99.27	0.164	300.3	99.9	0.128	300.3	99.9	0.14	300.3	99.9
PSC2 (GMPP=196.01W)	0.289	195.9	99.84	0.28	195.9	99.94	0.145	195.9	99.94	0.17	195.9	99.94
PSC3 (GMPP=102.9W)	0.285	102.2	99.32	0.164	102.4	99.51	0.13	102.5	99.61	0.12	102.5	99.61

Table 4.9: Simulation results of the hybrid GMPPT techniques.

	PSO-P&O [35]			GWO-P&O [36]			GWO_GSO [41]			Proposed		
	T_{mp} (sec)	P_{mp}(W)	$\%\eta_{static}$	T_{mp}(sec)	P_{mp}(W)	$\%\eta_{static}$	T_{mp}(sec)	P_{mp}(W)	$\%\eta_{static}$	T_{mp}(sec)	P_{mp}(W)	$\%\eta_{static}$
PSC1 (GMPP=300.6W)	0.25	300.2	99.87	0.17	300.1	99.83	0.27	299.6	99.67	0.14	300.3	99.9
PSC2 (GMPP=196.01W)	0.7	195.9	99.94	0.16	195.8	99.89	0.21	195.7	99.84	0.17	195.9	99.94
PSC3 (GMPP=102.9W)	0.398	102.5	99.61	0.26	102.2	99.32	0.2	102.5	99.61	0.12	102.5	99.61

The main reasons for slower convergence of ASSA for on-line search process of PV MPPT are more number of search agents and unnecessary exploration of search space even after reaching GP region or optimum is found. If less number of salps is selected, it may cause premature convergence. Hence, with minimum number of search agents in ASSA, to avoid the premature convergence and to increase the convergence rate by accelerating the least fitness salp and enhancing the leader salp, DE is cascaded with ASSA. The number of salps selected in ASSADE are three in ASSA, and one more salp is generated in DE based on the history of three salps in ASSA exploration. Even though ASSADE results in accurate tracking of GMPP, the tracking time can be further improved by limiting the ASSADE only for GP region identification stage and in that region tracking is continued with P&O. The fastness of the proposed method in the tracking GMPP is due to integration of DE in series with ASSA which can improve the solution obtained in the each iteration of ASSA, where a more accurate solution is obtained with integration of P&O with variable step. From the simulation results shown in Figure 4.16.b) it is evident that the proposed hybrid GMPPT technique shows the gradual improvement in terms of accuracy and speed of tracking.

To know the superiority of the proposed method in terms of fast, accurate tracking and robustness, the proposed method is compared with existing hybrid algorithms PSO–P&O [37], GWO–P&O [38], GWO–GSO [43] based MPPT techniques. From the Figure 4.16.c), it is

evident that the proposed method is much faster and more accurate than other three hybrid methods. The results obtained with PSO-P&O hybrid GMPPT technique proposed in [37] are $T_{mp} = 0.2536\ sec,\ P_{mp} = 300.3\ W$ for PSC1. Since the velocity of particles is not limited, the parameters of the algorithm are dependent on the maximum iteration count and P&O used in the steady-state are with fixed-step, the PSO–P&O algorithm results in slow tracking. In the case of GWO-P&O GMPPT technique proposed in [38], the fixed control parameters and fixed-step size in P&O algorithm result in $T_{mp} = 0.16\ sec,\ P_{mp} = 300.2\ W$ for PSC1. The GWO-GSO base MPPT technique proposed in [43] results in $T_{mp} = 0.2721\ sec,\ P_{mp} = 300.2\ W$ with zero steady-state oscillations for PSC1. Whereas the proposed method results in $T_{mp} = 0.14\ sec,\ P_{mp} = 300.3\ W$ for PSC1 with fewer power oscillations during GP region identification as well as steady-state tracking. The power oscillations are reduced due to gradual change in salp positions, and the adaptive control parameter avoids the unnecessary power oscillations in GP region. In steady-state, the power oscillations are reduced with variable step P&O, which operates with a very small step size after reaching peak.

Further, the performance of proposed hybrid GMPPT method is optimized with the direct duty ratio calculation under load changes in an off-grid PV system. From the simulation result shown in Figure 4.17, it is evident that the proposed hybrid GMPPT technique is able to track the GMPP rapidly within a time $T_{Lmp1} = T_{Lmp2} = T_{Lmp3} = 12\ msec$ due to the direct duty ratio calculation for load changes from 100 Ω to 50 Ω vice versa. With the change in the direction of voltage and current change, insolation and load change can be easily identified. Only during the insolation change, ASSADE is reinitialized, and in the case of load change, direct duty ratio calculation is adapted by which unnecessary GP region identification can be avoided during the load change where GP is unaltered. Whereas in the case of the other three hybrid GMPPT techniques, PSO–P&O [37], GWO–P&O [38], and GWO–GSO [43], even for load changes also GP region identification stage has to be reinitialized for the load changes. Hence, direct duty ratio calculation in the proposed hybrid GMPPT technique results in rapid tracking of GMPP under load changes without the large power oscillations due to reinitialization of ASSADE. Hence, the performance of the proposed hybrid GMPPT technique is optimized for the load changes in off-grid PV system.

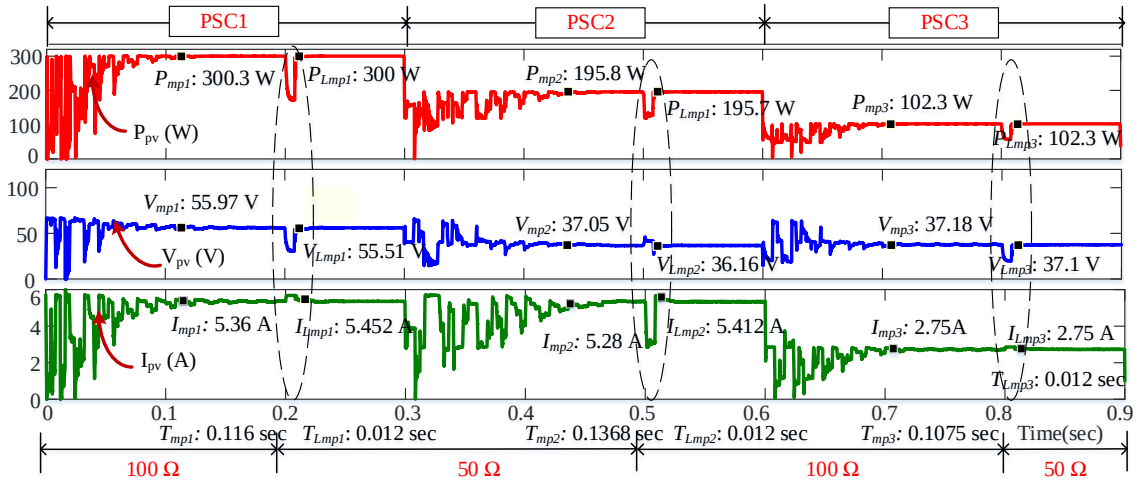

Figure 4.17: Simulation result of proposed hybrid GMPPT method under irradiance and load changes.

4.4.4 Experimental results and discussions

To test the performance of the proposed method during different irradiance conditions and load variation, the experimental setup shown in Figure 4.18 is used. To emulate the different shading conditions of 3S-2P short string and 6S-1P long string, chroma make programmable solar array simulator is used. PSC-1 to PSC-6 are emulated by using chroma soft panel software in which 128 data points of the *I-V* curves are imported. Test bench supports the real-time shad-

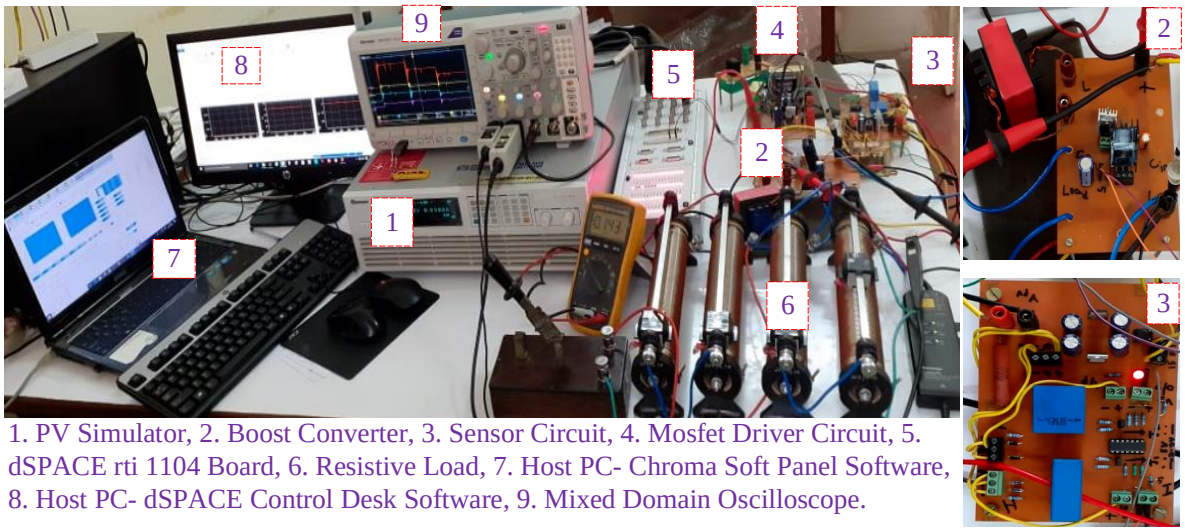

1. PV Simulator, 2. Boost Converter, 3. Sensor Circuit, 4. Mosfet Driver Circuit, 5. dSPACE rti 1104 Board, 6. Resistive Load, 7. Host PC- Chroma Soft Panel Software, 8. Host PC- dSPACE Control Desk Software, 9. Mixed Domain Oscilloscope.

Figure 4.18: Experimental setup.

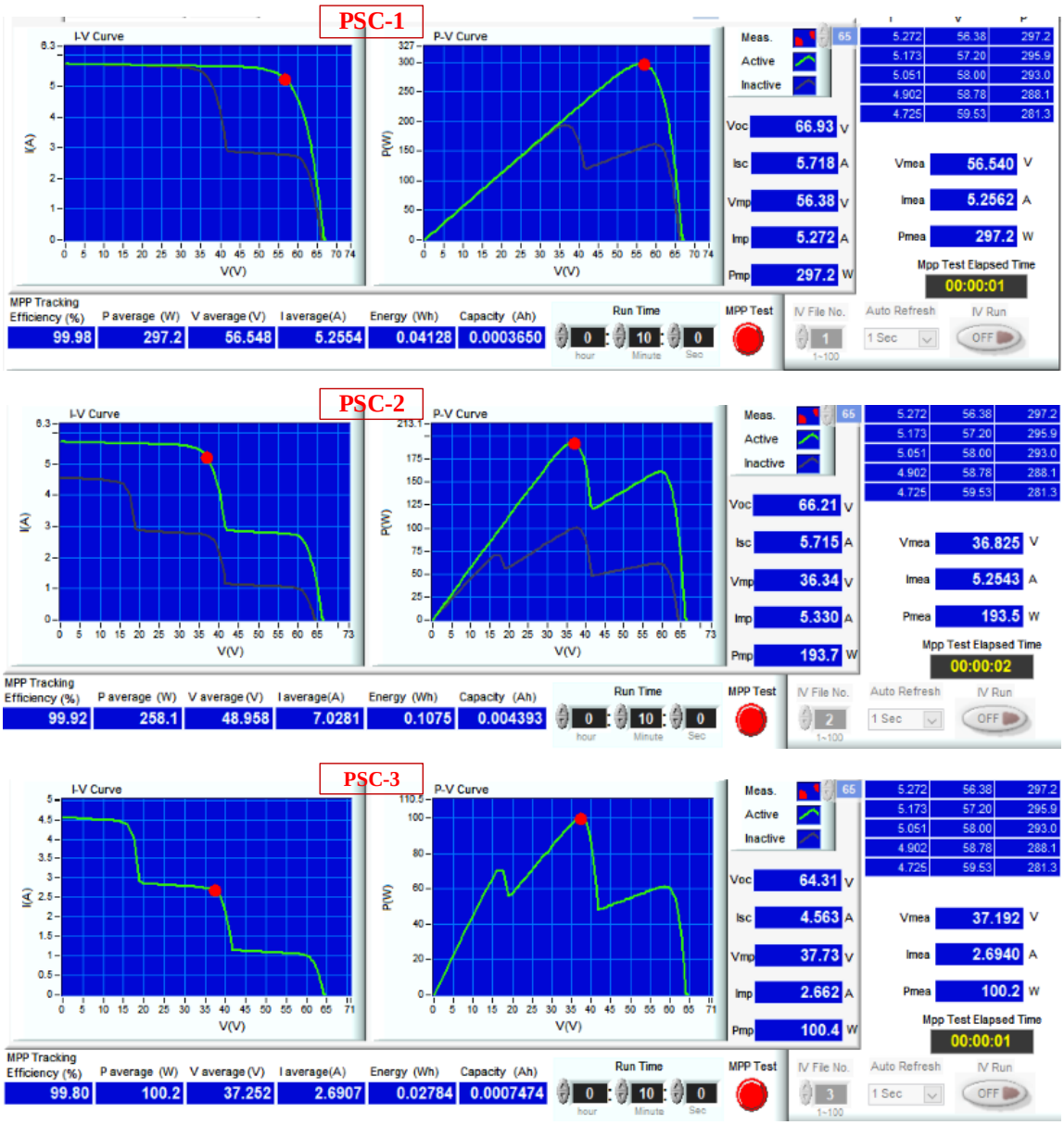

Figure 4.19: *I-V* and *P-V* curves emulated by using solar array simulator.

ing due to clouds, and calculates the static and dynamic MPPT efficiency of MPPT techniques. The parameters of DC-DC converter for both simulation and hardware are same as given in Table 4.5. In view of the slow response of the PV simulator and to observe the output clearly, proper sample time $T_s = 0.05$ *sec* is used for implementing all the algorithms by using dSPACE digital controller board. dSPACE rti 1104 digital controller board has the slave DSP for generating high frequency (50 KHz) PWM switching signals. LEM-made hall effect sensors are

used for sensing the voltage and current at the input of converter. These measured voltage and current signals are given as input to the MPPT algorithm through analog to digital converter (ADC) ports of digital controller board. The MPPT algorithm uses PV voltage, current and generates a pulse width modulated (PWM) signal, which is amplified by the MOSFET driver circuit made with HCPL A3120 and applied to the power MOSFET (IRFP-460) of the boost converter. Rheostats bank is used as variable resistance load connected to the boost converter, which is used for creating load changes as in the off-grid PV system.

4.4.4.1 Experimental results under partially shaded conditions

Complex shading conditions are emulated using P-V profiles from PSC-1 to PSC-6, which are multi-peak P-V curves up to 6 peaks with the help of chroma soft panel software, as shown in Figure 4.19. The results of the hybrid MPPT methods are tabulated in Table 4.10. To study the performance of presented algorithms, shading conditions PSC1,PSC2 and PSC3 (each one for 12 sec) are applied as shown in Figure 4.20. Even though all the algorithms track the GMPP with the same number of searching agents(=4) and convergence criteria, PSO–P&O and GWO–P&O results in large power oscillations during GP region identification stage as well as in the steady-state tracking. The large power oscillations in the steady-state are due to the large step size of the fixed-step P&O. GWO–GSO results in faster convergence and lower steady-state power oscillations than PSO–P&O and GWO–P&O, but it also suffers from large power oscillations during tracking GP region. The conventional SI techniques: PSO and GWO algorithms used in these hybrid GMPPT techniques are fixed and best suited for only few irradiance condi-

Table 4.10: Experimentally obtained results of the hybrid GMPPT techniques.

	PSO-P&O [35]			GWO-P&O [36]			GWO_GSO [41]			Proposed		
	T_{mp} (sec)	P_{mp}(W)	$\%\eta_{static}$	T_{mp}(sec)	P_{mp}(W)	$\%\eta_{static}$	T_{mp}(sec)	P_{mp}(W)	$\%\eta_{static}$	T_{mp}(sec)	P_{mp}(W)	$\%\eta_{static}$
PSC1 (GMPP=297.2W)	3	294.7	99.16	3.6	295.1	99.29	3.6	297.2	100	1.58	297.14	99.98
PSC2 (GMPP=193.7W)	1.4	190.31	98.25	1.2	188.35	97.24	1	193.19	99.74	1.6	193.5	99.89
PSC3 (GMPP=100.4W)	2.4	99.83	99.43	3.2	99.48	99.08	2	99.31	98.91	1.58	100.2	99.8
PSC4 (GMPP=79.1W)	3.4	73.88	93.4	3.6	71.1	89.89	2	64.78	81.9	1.2	78.6	99.37
PSC5 (GMPP=93.6W)	3.6	92.34	98.65	3.6	92.53	98.86	3.8	93.52	99.91	1.2	93.3	99.68
PSC6 (GMPP=85W)	5.6	76.29	89.75	3.4	75.38	88.68	2.6	77.59	91.28	1	84.4	99.29
Average	3.2	–	96.44	3.1	–	95.5	2.5	–	95.29	1.36	–	99.67

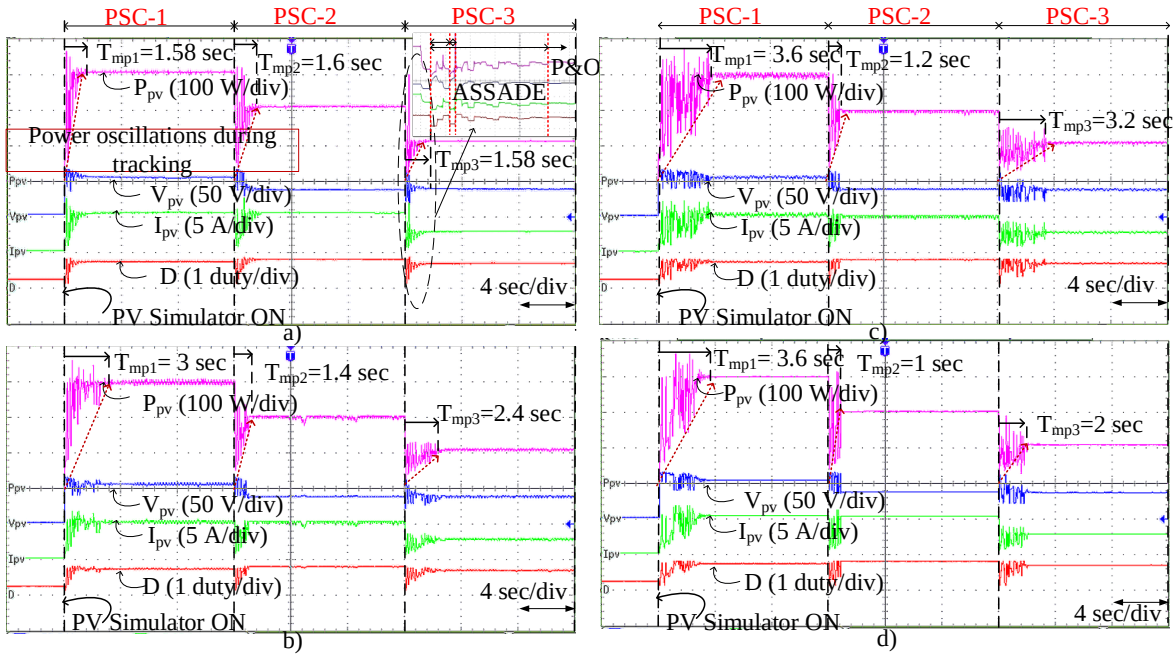

Figure 4.20: Experimentally obtained results of hybrid GMPPT techniques a) proposed, b) PSO–P&O, c) GWO–P&O, d) GWO–GSO.

tions and may cause premature convergence. On the other hand, the proposed hybrid GMPPT technique takes very little time to track GMPP, which is less than 1.6 sec due to the cascaded effect of ASSA and DE along with variable step P&O, which also results in accurate tracking of GMPP. Power oscillations during tracking are reduced due to gradual movement of salps and in steady-state oscillations are minimized due to the effect of reduced step size of VS-P&O. From the results obtained for six shading conditions, it is evident that the proposed method is faster than the other three with average tracking time of T_{mp}=1.36 sec. The merit order of GMPPT techniques based on speed of tracking is ASSADE-P&O, GWO-GSO, GWO-P&O and PSO-P&O. The slow tracking of the remaining techniques is mainly due to the fixed control parameters. Static MPPT efficiency can be calculated by

$$\%\eta_{static} = \frac{P_{pv}}{P_{mp}} \times 100 \tag{4.24}$$

where P_{pv} is the power measured at steady-state, P_{mp} is the actual maximum power. The average static MPPT efficiency of the proposed method is 99.68 % which shows that the proposed method is more accurate than other three presented.

4.4.4.2 Experimental results under Load variations

The load changes in off-grid PV system are experimentally verified by suddenly changing the load resistance. To optimize the performance of proposed hybrid GMPPT technique, reinitialization of GP region identification by SI technique is done only for irradiance change and direct duty ratio is calculated based on the information of MPP for the given irradiance conditions. The direction of voltage and current change is used for identifying the change in power is due to load or insolation. Hence, in the proposed method, when load changes, there is no need of reinitialization to identify GP region. Based on the method discussed in section III, direct duty ratio calculation results in rapid tracking of GMPP for any load change, as shown in Figure 4.21. The proposed method takes T_{mpL}=0.1 sec for load changes from either 100 Ω to 60 Ω or vice versa. Hence, the proposed method avoids tracking GMPP again from the beginning, which results in power oscillations and calculates the duty directly by using (4.22) for the new value of load after load change occurs. In the proposed method, reinitialization is required only for insolation changes. Whereas the remaining three hybrid algorithms, it requires reinitialization

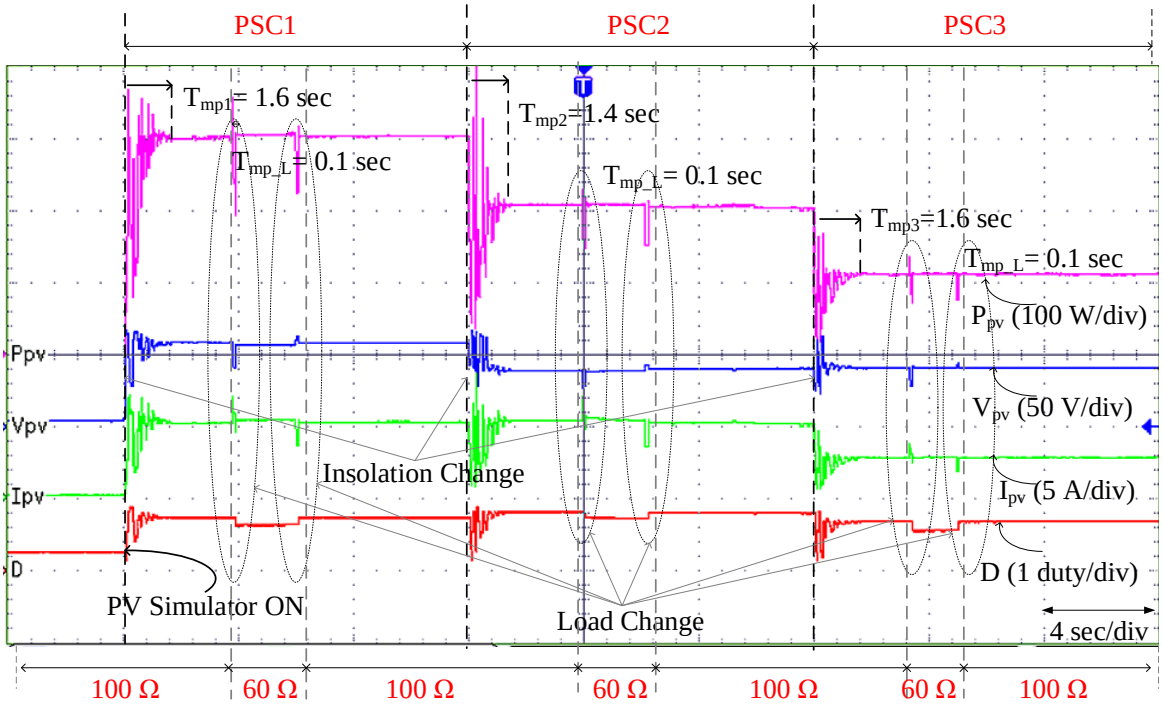

Figure 4.21: Experimentally obtained result of the proposed method under insolation and load variation.

of GMPP stage for both insolation and load changes. When a change in power is identified for change in insolation, all hybrid GMPPT techniques presented are reinitialized, as shown in Figure 4.21. Hence, from the experimental results, it is evident that the proposed hybrid GMPPT technique results in faster and accurate GMPPT tracking with low power oscillations under load changes, and the methodology used for load change is best suited for an off-grid PV system.

4.4.4.3 Experimental results under dynamic shading

Dynamic shading is a common phenomenon in residential and large-scale PV installations due to clouds. Dynamic shading due to clouds is tested by using a shadowed I-V curve simulation panel of chroma solar array simulator. The direction of cloud movement on the top of the panels chosen for testing the dynamic shading is from left to right, as shown in Figure 4.22. The cloud position changes from SP-0 to SP-3. SP-0 is the unshaded condition applied before initializing the dynamic shading where irradiance profile is same as PSC-1. SP-1 and SP-2 are the shadow positions due to clouds gradual movement, which creates the PSC. Whereas SP-3 is unshaded shadow position after passing of clouds. The cloud moment initialized after 10 seconds and resulted in multi-peak P-V curves due to shading, and the proposed method tracks the GMPP in each condition accurately and gives a total tracking efficiency of 98.1%.

$$\%\eta_{tracking} = \frac{1}{P_{mp} \times T_M} \sum V_{pv} \times I_{pv} \times \Delta T \times 100 \tag{4.25}$$

where P_{mp} is the global peak set by the PV simulator, T_M is the total measurement time, V_{pv} voltage at the terminals of PV simulator, I_{pv} is the current through the PV simulator, ΔT is the time step size. Hence from the experimental results, it is evident that the proposed method is robust and guarantees global convergence for insolation and load changes with less tracking time and reduced power oscillations.

4.5 Conclusion

In this work, an adaptive salp swarm algorithm based GMPPT technique is proposed with only one control parameter to be tuned. From the simulation results, the effect of adaptive control parameter C_1 on exploration and exploitation of the ASSA GMPPT technique is studied, and it results in faster convergence than the SSA GMPPT technique with maximum

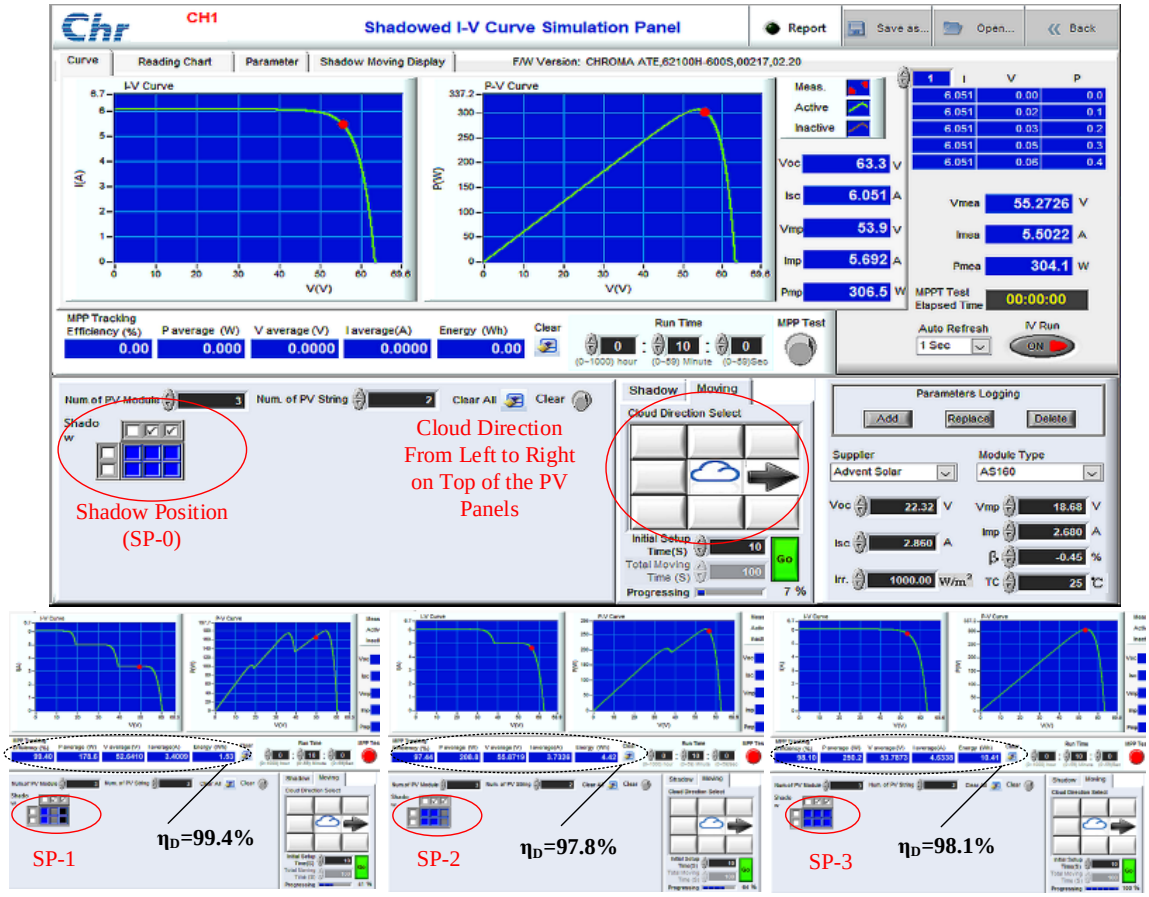

(a)

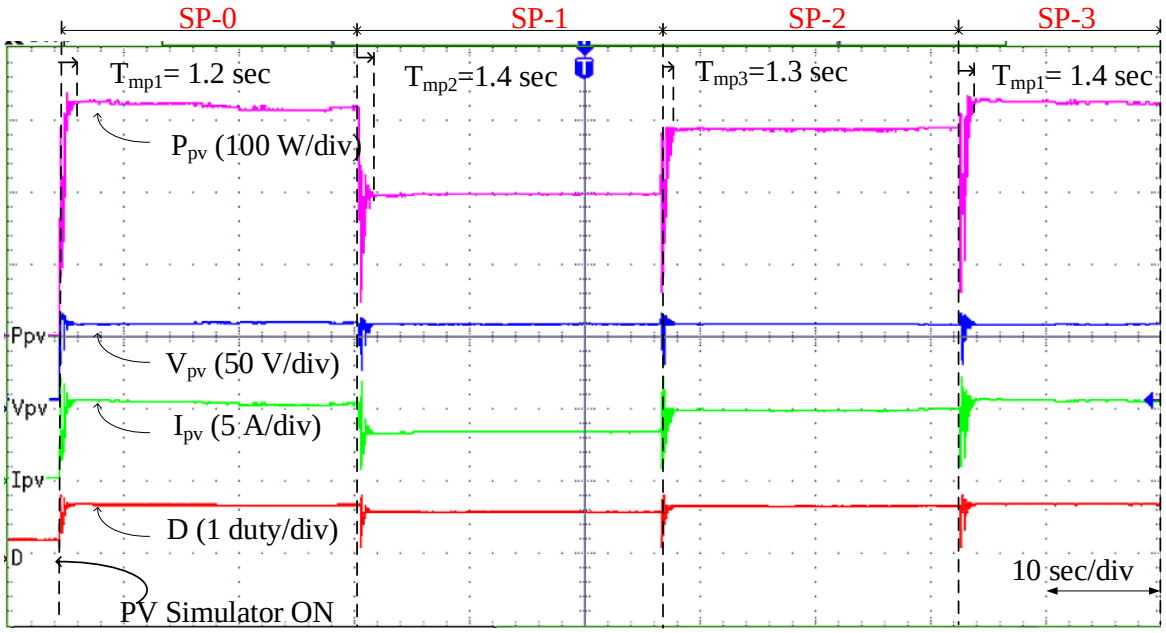

(b)

Figure 4.22: a) Shadowed I-V curve simulation panel, b) Experimentally obtained result of the proposed method under dynamic shading by clouds.

iterations dependent control parameter C_1. The hybrid method proposed with ASSA and P&O is easy to implement with the proposed switching between ASSA and P&O algorithms. The global peak region is identified with only one parameter C_1 in ASSA, and from there on the tracking of GMPP in the GP region is continued with variable step P&O. Both the simulation and experimental results show that the proposed hybrid method gives faster convergence, less tracking time, and reduced power oscillations during tracking.

Further, integration of ASSA and DE results in more accurate tracking of GP region with few searching agents in ASSA. Cascaded operation of DE with ASSA is best suitable for MPPT operation and applying DE on leader and least fitness salp of ASSA results in fast and accurate tracking of maximum power point. Further integration of ASSADE with variable step size P&O results in more accurate tracking of GMPP with fewer power oscillations in steady-state. The proposed direct duty ratio calculation under load changes results in rapid tracking of GMPP within 0.1 sec for any load change, which avoids the unnecessary power oscillations due to reinitialization of GP region identification stage. The superiority of the proposed method in terms of tracking time and accuracy is compared with three popular hybrid MPPT methods which exist in the literature. The proposed method guarantees less tracking time and more accuracy under complex partial shading conditions as well as load changes. The proposed method, ASSADE-P&O based GMPPT technique with direct duty ratio calculation under load changes, has been established as a favorable method for an off-grid PV system.

Chapter 5

Performance optimization of hybrid tracking techniques for an on-grid PV system.

Chapter 5

Performance optimization of hybrid tracking techniques for an on-grid PV system.

5.1 Introduction

In the literature, several hybrid tracking techniques are proposed for PV systems under PSC, classified as follows. In the first category, conventional gradient-based methods are used to find all LMPP in the first-stage, and in the second-stage, these MPPs are sorted to get GMPP [4, 29]. These two-stage techniques guarantee an accurate GMPP. However, traversing all the curve peaks imposes a long tracking time, which is not a good feature of an efficient, fast-tracking MPPT technique. In the second-category, the SC technique is used to identify the GP region in the first-stage, and in the second-stage, the tracking is continued with the conventional P&O technique [37, 38]. These techniques can track the GMPP much faster than the first-category. However, the exact GP region identification with SC technique and power oscillations in the steady-state are major challenges of these methods. In most of these methods found in the literature, the GP region identification is made with an unjustified predetermined number of iterations.

To avoid the power oscillations due to the irregular searching of the SC technique, tracking MPP with P&O in the UIC and SC technique during PSC is ideal. The second-category methods should rely on the SC technique for tracking MPP of both UIC and PSC due to a lack of partial shading identification methodology. In the third-category, two or more soft computing techniques are combined to enhance the exploration and exploitation of the main SC technique [41–43]. In this category, the optimum solution obtained in each iteration of the main SC technique is enhanced by another SC technique, which may be evolutionary or swarm-based. Accuracy of the solution obtained will be more than the case of a single SC technique is used. However, the number of algorithm parameters to be tuned is more and complex. In the fourth-category, shade detection is enabled in the first-stage to find a uniform or PSC. In the

second-stage, the SC technique is used only to identify the GP region of the PSC, and P&O is used in the steady-state and the UIC so that the use of the SC technique can be limited to PSC only. An accurate shade detection helps to improve the performance of these hybrid tracking technologies. The main challenges of fourth-category methods that need to be investigated more are fast and accurate tracking of maximum power point, accurate shade detection, low power oscillations in the steady-state tracking, easy parameter tuning, and proper shifting of algorithms, which comes under optimizing the performance of the hybrid tracking techniques [44]. Hence, performance optimization of the hybrid tracking technique is most important and challenging for researchers in the field of PV MPPT.

With the increase in rooftop grid-connected solar PV systems, penetration of medium and high rated PV systems connected to the grid are increased. With the high penetration of PV systems, the power injected into the grid may become more than the demand during sunny or peak production periods, which may cause instability and overload [45]. Therefore, the grid-connected PV system should have the flexibility to deliver the active power within the power limit known as flexible power point tracking (FPPT) [60]. The new grid codes impose MPPT for all grid-connected systems to get maximum energy yield and active power limit control to maintain stability under peak power production periods. Hence, the MPPT tracking algorithm should have maximum power point tracking under all dynamic weather conditions and active power limit control in the form of FPPT, which is a cost-effective solution for active power control [46]. Hence, when these hybrid tracking technologies are used for grid-connected PV systems, FPPT should be included as part of the MPPT algorithm to meet new grid code standards. Since partial shading is quite a common phenomenon in the grid-connected system and grid code also demands active power control, MPPT with flexible and global maximum power point tracking with hybrid tracking technology and shade detection is vital. The combined study of FPPT, GMPPT, and shade detection have not been investigated in the literature.

Hence, in this chapter, a steady-output P&O algorithm (SO-P&O) and a hybrid GMPPT technique using a self-adaptive salp swarm algorithm and differential evaluation (ASSA-DE) are proposed. In the proposed hybrid tracking technology framework, the new SO-P&O is used for a curve scan, which can accurately identify both shade and active power limit. Hybrid SC technique: self-adaptive SSA-DE algorithm is used only to determine the GP region in PSC. In the steady-state tracking of both the UIC and PSC, SO-P&O is used, which gives zero steady-

state oscillations. The proposed curve scan is used to identify both types of shading, i.e., either uniform or partial shading and active power limit. If the power available is more than the active power limit during a sunny day, the proposed curve scan with SO-P&O can find the flexible power point in the MPP left. This chapter's main objective is: to optimize the fourth-category hybrid tracking technology's overall performance; an exact shade & active power limit detection scheme, and FPPT along with a hybrid GMPPT algorithm are proposed for a grid-connected PV system under varying atmospheric conditions.

This work's main contributions are: 1) Proposed an accurate and unique shade detection with a new SO-P&O, which can detect both types of shading and active power limit. 2) Proposed a fast and accurate hybrid self-adaptive GMPPT technique, ASSA-DE, to identify the exact GP region under PSC. 3) Proposed a hybrid tracking technique that uses the above shade and active power limit detection, FPPT, and GMPPT. The main achievements of the proposed hybrid tracking technology are accurate shade and active power limit detection, fast and accurate maximum and flexible power point tracking, and zero steady-state oscillations under all dynamic weather conditions.

Contributions of this chapter are

- Flexible and global maximum power point tracking with hybrid tracking technology and shade detection.
- Performance optimization of the hybrid tracking technique in a grid connected PV system.

5.2 Hybrid self-adaptive salp swarm algorithm and differential evolution

The main aim of any GMPPT technique is to find the global peak among the multiple local peaks of the multi-peak P-V curve under PSC, which is the possible operating point for a PV system to yield maximum energy for the given irradiance conditions. The accuracy and speed of the GMPPT algorithm depend on the strength of the search process, i.e., balance between the exploration and exploitation of search space. Since the GMPPT algorithm converges to a solution after search process is completed, these techniques require a proper re-initialization for identifying the new GMPP due to irradiance change. The performance of meta-heuristic based on-line GMPPT technique depends on several algorithm parameters like number of search agents, pop-

ulation initialization, and algorithm parameters selection, etc. The GMPPT technique used in this chapter is the self-adaptive SSA-DE algorithm which is a hybrid optimization algorithm designed with the best features of the swarm and evolutionary algorithms. The main aim of hybridization is to get faster and accurate GP region identification with fewer population and self-tuned algorithm parameters for any complex irradiance conditions.

In the proposed hybrid GMPPT technique, DE is cascaded with SSA, and a total of three algorithm control parameters are self-adaptive, as discussed below. To optimize the performance of the proposed hybrid tracking technique, ASSA-DE is used only to identify the GP region during the onset of PSC. The convergence criterion used to find the GP region is given by the distance between each salp, less than one percent. Once the convergence is reached, the optimum, i.e., food source found inside the GP region, is the starting point for the SO-P&O, and further tracking is continued with the SO-P&O until GMPP is found. After reaching the global maximum, the duty ratio is fixed. Voltage and current at GMPP are stored, which can be used for identifying irradiance change accurately. The proposed global region identification with ASSA-DE and GMPP tracking with SO-P&O are given in the flowchart as shown in Figure 5.1.

Even though ASSA avoids the dependence of algorithm performance on unknown maximum iteration count, with few salps, both SSA and ASSA can not guarantee optimum solutions under all dynamic conditions. Hence ASSA is integrated with DE.

5.2.1 Self-adaptive differential evaluation

GP region can be identified when all the search agents come closer during the exploration phase. Hence, in order to get the fast-tracking of GP region by satisfying the given convergence criteria other than maximum iteration count like the distance between each particle is lower than some threshold value, the least fitness particles should be accelerated more towards the leader without skipping the any possible optimum value. Hence, in the proposed method, DE is applied on both food source as well as least salp in salp chain to enhance the best solution and to achieve faster tracking of GP region.

In the proposed hybrid GMPPT technique, ASSA and DE are in series. The solutions obtained with ASSA are given to the DE in each iteration to get a better solution. The conven-

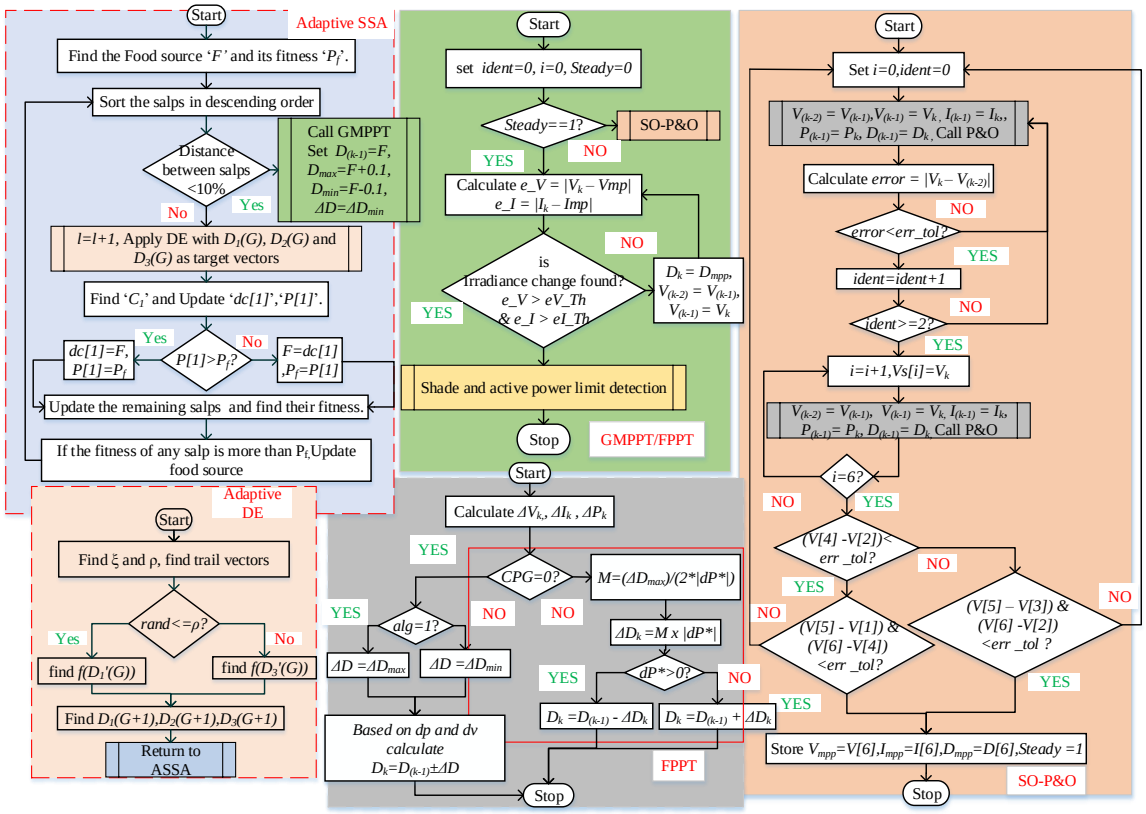

Figure 5.1: Flowchart of the proposed hybrid GMPPT algorithm self-adaptive SSA-DE and GMPP tracking with SO-P&O.

tional DE mutation operator is modified as (5.1) and (5.2). For the food source, the mutation is defined as (5.1), and (5.2) is for the least fitness salp.

$$U_1(G) = D_1(G) + \xi \times |(D_2(G) - D_3(G))| \tag{5.1}$$

$$U_3(G) = \begin{cases} D_3(G) + \xi \times |(D_1(G) - D_2(G))|, \\ \qquad\qquad if \;\; D_3(G) \leq D_1(G) \\ D_3(G) - \xi \times |(D_1(G) - D_2(G))|, \\ \qquad\qquad if \;\; D_3(G) > D_1(G) \end{cases} \tag{5.2}$$

where $U_1(G)$ is the trail vector of leader salp, $U_3(G)$ is the trail vector of least fitness salp in salp chain, D_1, D_2, and D_3 are solutions obtained in the ASSA in each iteration, D_1 is the leader salp and D_3 is least fitness salp in the chain.

Since MPPT is an on-line process in which each duty should be applied to MPPT converter to find the fitness, there is a delay of tracking time if the same duty ratio is applied to find fitness in the form of target vector in the crossover as per [58]. Hence, without increasing tracking time in the form of DE, in crossover stage, selection of child vector for leader salp or least fitness salp is provided instead of choosing same target vector. Hence, in each iteration, either DE on leader salp or DE on least fitness salp is executed. Therefore, The crossover of the proposed method is given in (5.3)

$$\begin{aligned} D_1^{'}(G) &= U_1(G), \;\; if \;\; rand \leq \rho \\ D_3^{'}(G) &= U_3(G), \;\; if \;\; rand > \rho \end{aligned} \tag{5.3}$$

where ρ is crossover probability constant varies from 0 to 1. The DE parameters ξ and ρ are essential to get the better food source or least fitness salp and it is difficult to tune these parameters manually for most uncertain irradiance conditions. Hence, In this work, the DE algorithm uses self-adaptive parameter control based on the successive history of parameters. First, a memory M of size H is created with index $i = 1,2,..,H$. In the first iteration ρ_i, ξ_i are initialized to 0.5. random index r_i is selected randomly from 1 to H. The scaling factor and crossover rate are selected by using,

$$\xi_i = randn_i\left(M_{\xi_{r_i}}, \sigma^2\right) \tag{5.4}$$

$$\rho_i = randc_i\left(M_{\rho_{r_i}}, \sigma^2\right) \tag{5.5}$$

where $randn_i$ is the normal distribution, $randc_i$ is the Cauchy distribution, and σ^2 is the variance. If ρ_i is greater than one or less than 0, it is kept at the corresponding boundary. If ξ_i is greater than 1, it is limited to 1. When ξ_i is less than zero, (5.4) is repeated until it is not zero and valid. A child vector is generated by using mutation, crossover, and selection. If the generated parameters ξ_i, and ρ_i produces a better child than the parent, present values are stored in the variables S_ξ and S_ρ. M_{ξ_k}, and M_{ρ_k} are updated by using weighted Lehmer mean [61]. Where $k = 1\ to\ H$. If the generated parameters are not producing a better child, memory M is not updated.

5.2.2 Hybrid self-adaptive SSA-DE algorithm

In the proposed hybrid GMPPT technique, DE is cascaded with SSA, and a total of three algorithm control parameters are self-adaptive, as discussed above. To optimize the performance of the proposed hybrid tracking technique, SSA-DE is used only to identify the GP region during the onset of PSC. The convergence criteria used for finding the GP region is given by the distance between each salp, which is less than one percent. Once the convergence is reached, the optimum, i.e., food source found inside the GP region is the starting point for the SO-P&O and further tracking is continued with the SO-P&O until GMPP is found. After reaching the global maximum, the duty ratio is fixed. Voltage and current at GMPP are stored, which can be used for identifying irradiance change accurately. Steps to implement the proposed GMPPT technique:

1) Initialize the variables of SSA and DE

   Number of salps N=3, select uniformly distributed initial salp positions dc[1],dc[2] and dc[3] in the search space ub=0.85, lb=0.1, and their fitness values Ps[1],Ps[2], and Ps[3] respectively, iteration count l=1.

   Memory size of successive history DE = 5, History count H=0, $M_{\xi_k} = 0.5,\ M_{\rho_k} = 0.5$, and $S_{\xi_k} = S_{\rho_k} = 0$ where k=1 to H.

2) Apply each salp to the MPPT converter to find the fitness in the first iteration and find the food source. Finally, sort the salps based on fitness values to form the salp chain.

3) Apply DE on food source or least fitness salp.

   First, calculate ξ_i and ρ_i values by using (5.4), and (5.5). Apply mutation operator to find trail vectors $U_1(G)$ and $U_3(G)$ as given in (5.1) and (5.2).

   Selected Child vectors as given in (5.3) are applied to the MPPT converter to find fitness. Update the salp chain if better fitness salps are found in the DE and increase the iteration count by 1.

4) In the next iteration, first calculate C_1 by using (4.13), and update the food source and remaining salps by using (4.1) & (4.4).

5) Sort the salps based on their fitness values and check the convergence criteria is met or not

If no, repeat the step 3 and step 4 until convergence is met.

If yes, apply a final optimum value until irradiance change is found; if any irradiance change occurs, reinitialize the SSA as given in step 1 and repeat steps 1 to 5.

5.3 Steady-output perturb and observe (SO-P&O) algorithm

Perturb and Observe algorithm is simple to design and easy to implement, ideal for single-peak P-V curves of the uniform irradiance conditions. However, the performance of the P&O method, i.e., tracking time and power oscillations in the steady-state depends upon the perturbation step-size [62]. If a large value of step-size is selected, it results in faster tracking of MPP and power oscillations in the steady-state are high due to large continuous perturbations even after reaching MPP. Hence, if a constant duty ratio, i.e., duty ratio at MPP is maintained in the steady-state, power oscillations can be avoided [21]. Hence, in this chapter, repetitive behavior of the voltage magnitude due to duty ratio perturbation in the steady-state is used to identify the steady-state duty ratio, and this method named as SO-P&O. Three-point and five-point behavior can be identified with, repetitive behavior in the stead-state can be observed in

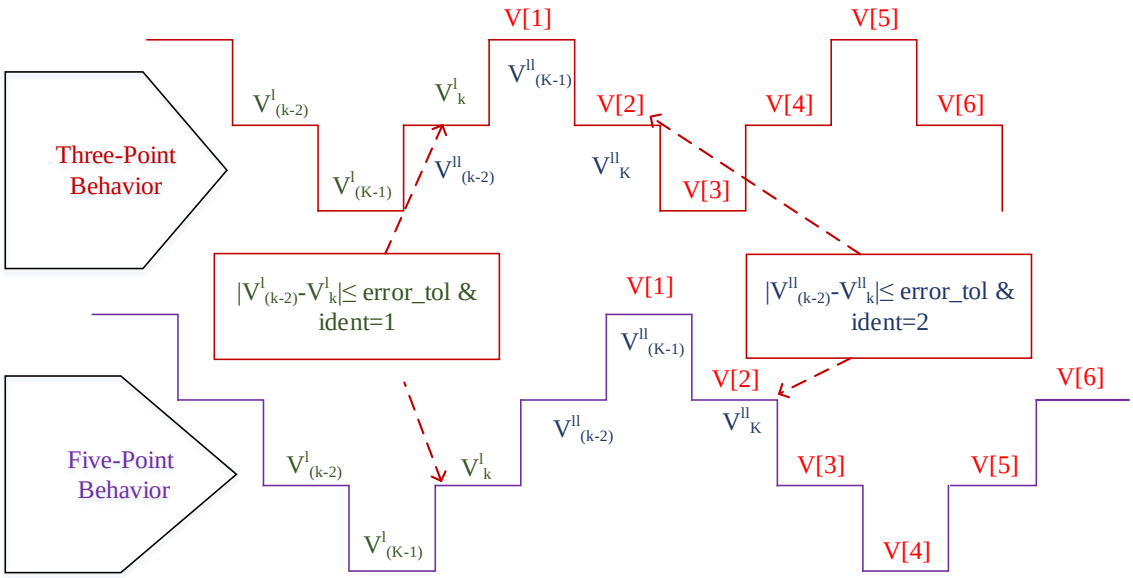

Figure 5.2: Three and five-point behavior of the P&O in the steady-state.

the form of two or more stepped voltage and current waveform in the steady-state. Three and five steps are most commonly found which depends upon the selected perturbation step size and irradiance. When these steps are observed continuously, the duty ratio oscillates around a fixed value which is the duty ratio at MPP. Hence, the fixed value of duty is selected as steady-state duty ratio in the SO-P&O. Error between two consecutive voltage magnitudes are selected to identify the steady-state. If the error is less than threshold value for two times, the voltage magnitudes in the six perturbations are stored starting form the previous duty ratio when the steady-state identified.

$$\begin{aligned} (V[4]-V[2])\ \&\ (V[5]-V[1])\ \&\ (V[6]-V[4]) \leq err\_tol, \\ if\ three-point \\ (V[4]-V[2]) > err\_tol\ \&\ ((V[5]-V[3])\ \&(V[6]-V[2])) \leq err\_tol \\ if\ five-point \end{aligned} \tag{5.6}$$

where $V[1]$ to $V[6]$ are voltages at six perturbations after identifying steady-state is reached, as shown in Figure 5.2, and err_tol is the error tolerance threshold of voltages in two consecutive perturbations. From these stored duty ratios the steady-state duty ratio is identified as given in (5.7).

$$D_{mpp} = \begin{cases} D[6] & if\ three-point \\ \\ \frac{(D[5]+D[6])}{2} & if\ five-point \end{cases} \tag{5.7}$$

where D_{mpp} is the steady-state duty ratio, $D[5],\ D[6]$ are duty ratios in 5^{th} and 6^{th} perturbation, starting from previous duty ratio of steady-state identification $ident$=2.

5.4 Shade and active power limit detection

Even though the proposed hybrid GMPPT technique is able to find MPP of both UIC and PSC, the SO-P&O is ideal for UIC, to avoid initial random power oscillations during the uneven searching process of the SC technique. The optimum use of the hybrid SC technique, i.e., ASS-DE, is needed for the performance optimization of the proposed hybrid tracking technique for

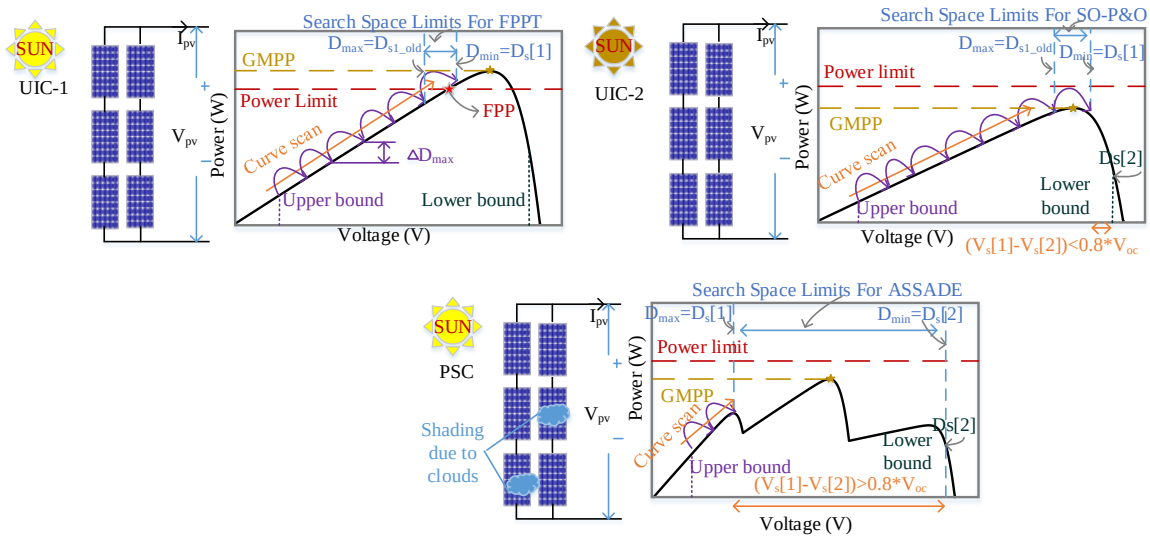

Figure 5.3: Proposed shade and active power limit detection.

the grid-connected PV system. Hence, in the proposed hybrid tracking technology, identifying the type of shading is essential to choose a proper tracking technique,i.e., either SO-P&O during UIC or ASSA during PSC. After studying the P-V curves of both UIC and PSC shown in Figure 5.3, the following important conclusions are made, which are crucial for deriving an efficient shade detection technique.

1) P-V curves of the UIC and PSC are distinct, and in the case of PSC, multiple peaks occurred due to the bypassing of the shaded module through an external bypass diode.

2) To cover MPP of any irradiance with the possible operating region of the boost converter as MPPT converter, the lower bound should be right of the MPP, and the upper bound should be left of the MPP.

3) Distance between any two peaks is more than the $0.8 * V_{oc}$, where V_{oc} is the open-circuit voltage of one panel in the string. Distance between the first peak of the UIC,.i.e.,$V_s[1]$, and operating point of the lower bound duty ratio $V_s[2]$ is much closer and it is less than $0.8 * V_{oc}$, whereas it is more than $0.8 * V_{oc}$ for PSC.

From the above last conclusion, when the curve scan is started from upper bound duty ratio with larger step size ΔD_{max} of SO-P&O, the occurrence of the first peak from the upper bound can be found and corresponding voltage $V_s[1]$ and duty ratio $D_s[1]$ are stored. To distinguish

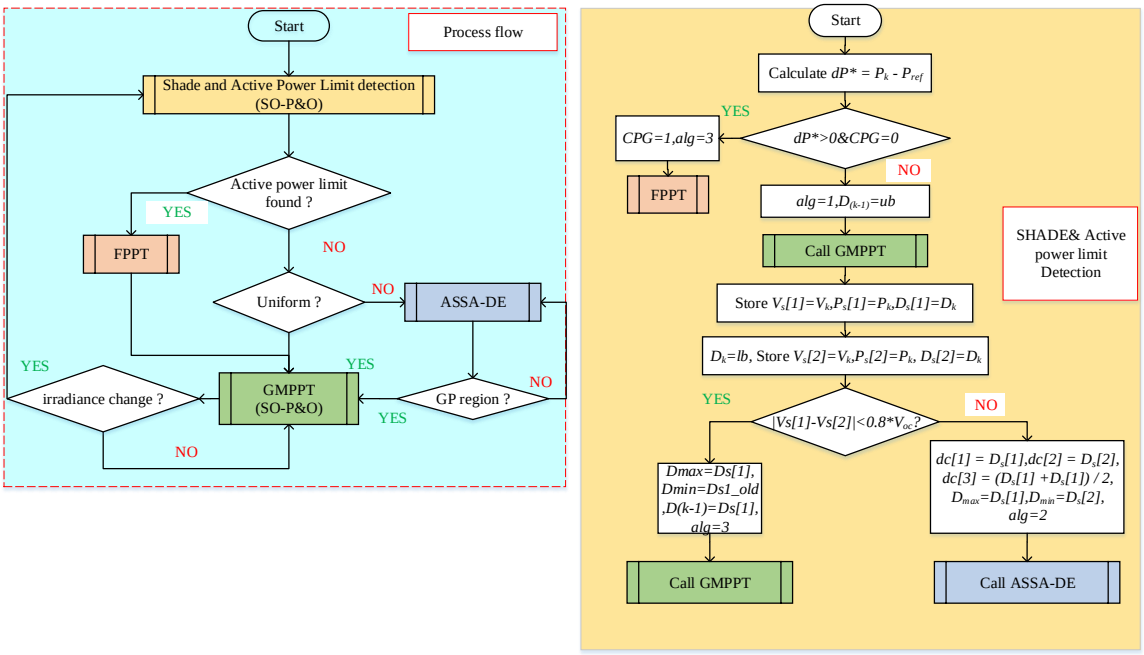

Figure 5.4: Flowchart of the proposed shade and active power limit detection.

the UIC and PSC, another duty ratio is applied which is the lower bound of the search space, and corresponding voltage $V_s[2]$ and duty ratio $D_s[2]$ are stored. Based on the voltage difference between $V_s[1]$ and $V_s[2]$, as shown in Figure 5.3, a uniform or PSC can be found.

In any case, if the first peak is more than the active power limit, it is possible to detect the active power limit in left of the MPP, which is the added advantage of the proposed curve scan, start from the upper bound of the search space, i.e., left side of the GMPP. Further, search space limits for the FPPT and GMPPT can be found and are limited to D_{max} to D_{min}, as shown in Figure 5.3. A flowchart of the proposed shade and active power limit detection is shown in Figure 5.4. With the proposed shade detection, it is possible to identify the type of shading with only curve scanning of the first peak from the upper bound of the search space and another duty ratio at the lower search space. Hence, a complete curve scan or scan from both sides is not necessary which reduces the shade detection time as well as GMPP or FPP tracking time. Further, search space limits can be defined for FPPT and GMPPT.

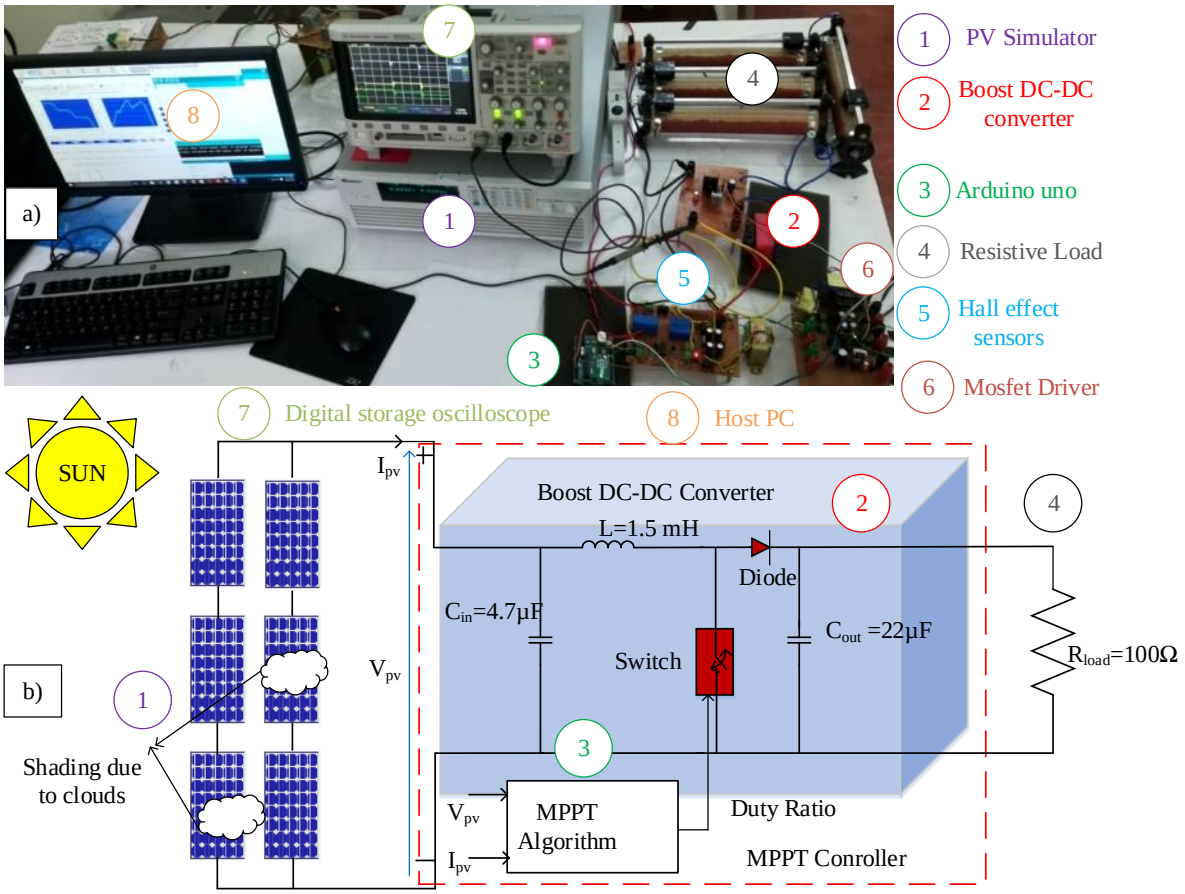

Figure 5.5: a) Experimental setup, b) Block diagram of a PV system under partially shaded conditions.

5.5 Simulation and experimental results

A 300 Watt PV system is designed in the PSIM simulation software, and Chroma programmable solar array simulator in laboratory prototype developed as shown in Figure 5.5 are used to verify the performance of the proposed hybrid tracking technique. Three solar power mart SPM-050M model, 50 WP PV panels in series form the string and two such strings are connected in parallel to form a 3S-2P PV array.

The boost converter is used as an MPPT converter connected to a restive load, which can be used for testing the proposed hybrid tracking technique in the case of a grid-connected PV system. Parameters of the boost converter are designed optimally to get continuous conduction mode [63]. A simple direct duty ratio method is used for MPPT control. Hence the complexity of tuning gains of the closed-loop controllers can be avoided. Since the proposed MPPT

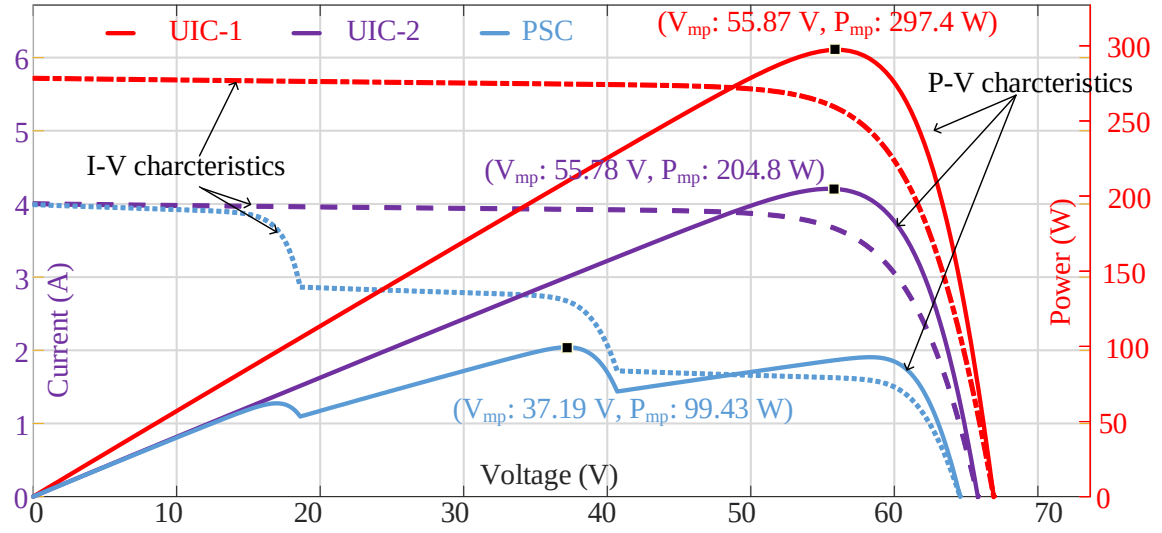

Figure 5.6: I-V and P-V characteristics of the 3S-2P PV array used for simulation and hardware.

technique is an on-line search method, only two parameters, PV voltage and current, which are sensed with hall-effect sensors are given as input to the ATMEGA328P micro-controller through the analog to digital converter pins of the ARDUINO UNO board. A 50 KHz PWM signal is generated based on the duty ratio calculated by the control algorithm and applied to the MOSFET IRFP460 through the gate driver circuit. Both the simulation and experimentation are carried with an optimum sample time Ts=40 msec, which is required to sense the exact PV input voltage and current in each duty ratio after the transients are over. Even though practical irradiance levels on the PV panels are most uncertain and dynamically changes, three irradiance profiles as shown in Figure 5.6, UIC-1: $1000\ W/m^2, 1000\ W/m^2, 1000\ W/m^2$, UIC-2: $700\ W/m^2, 700\ W/m^2, 700\ W/m^2$, and PSC: $500\ W/m^2, 300\ W/m^2, 700\ W/m^2$ at temperature $25^o\ C$ are used for verifying all features of the proposed hybrid tracking technique.

5.5.1 Experimental and simulation verification of hybrid GMPPT technique

ASSA-DE, along with SO-P&O, UIC-1, and PSC irradiance profiles are used to test the performance of the proposed hybrid GMPPT method, as shown in Figure 5.6, and the results are compared with the other third-category hybrid techniques found in the literature. Convergence criterion to reach GP region is the distance between search agents is less than 10%, $Max_{itr} = 15$,

and population count $N = 4$ for all hybrid GMPPT techniques. The simulation and experimental results of the MPPT techniques are shown in Figure 5.7 and Figure 5.8. PSO-P&O results in tracking time $T_{mpp} \leq 2.67\ sec$ and efficiency $\%\eta \geq 98.69$. Even though the hybrid method PSO-P&O [37] gives better accuracy, it fails to find the GP region faster, and more delay in GMPP tracking are due to three fixed control parameters. Similarly, in GWO-P&O [64] also fixed control parameters results in poor tracking time ($T_{mpp} \leq 2.34\ sec$) and efficiency ($\%\eta \geq 98.49$). In both PSO-P&O and GWO-P&O, fixed duty ratio $D = 1\%$ is used, which results in constant power and voltage oscillations in the steady-state tracking. Whereas in GWO-GSO [43], GSO gives the fixed duty ratio. Hence, the oscillations in the steady-state tracking are zero. However, it is also suffering from slower tracking time ($T_{mpp} \leq 1.88\ sec$) and less accuracy ($\%\eta \geq 92.62$) due to the fixed control parameters. Even though adaptive parameter tuning is used in ASSA-P&O [65], fixed duty ratio P&O results in steady-state power oscillations. From the bar chart of the tracking time and efficiency curves of the various MPPT techniques shown in Figure 5.9, it is evident that the proposed hybrid GMPPT technique has the best features, less tracking time, accurate tracking of GMPP, and zero power oscillations in the steady-state. The tracking delay of the proposed method is less due to the application of DE on both the least and best salp of SSA. Hence, slower GMPP tracking and unnecessary power oscillations in the GP are avoided. From both simulation and experimental results shown in Figure 5.7, 5.8, and Figure 5.9, it is evident that the proposed GMPPT technique self-adaptive SSA-DE along with the SO-P&O results in faster (less than 1 sec) and accurate tracking of GMPP (more than 99.16%) and these features are best suited for fourth category hybrid tracking technology as discussed in the introduction section of this chapter.

5.5.2 Experimental and simulation verification of the proposed shade and active power limit detection

Irradiance profiles UIC-1, UIC-2, and PSC are used to test the proposed shade and active power limit detection, and results are shown in Figure 5.10, and Figure 5.11 . Since UIC-1 emulates the sunny day irradiance profile, the grid-connected PV system should operate at a predefined active power limit or flexible power point on the curve. In this case, 85 % of $P_{MPP} = 300\ W$, i.e., $P_{ref} = 255\ W$ is selected as active power limit. First, curve scan with

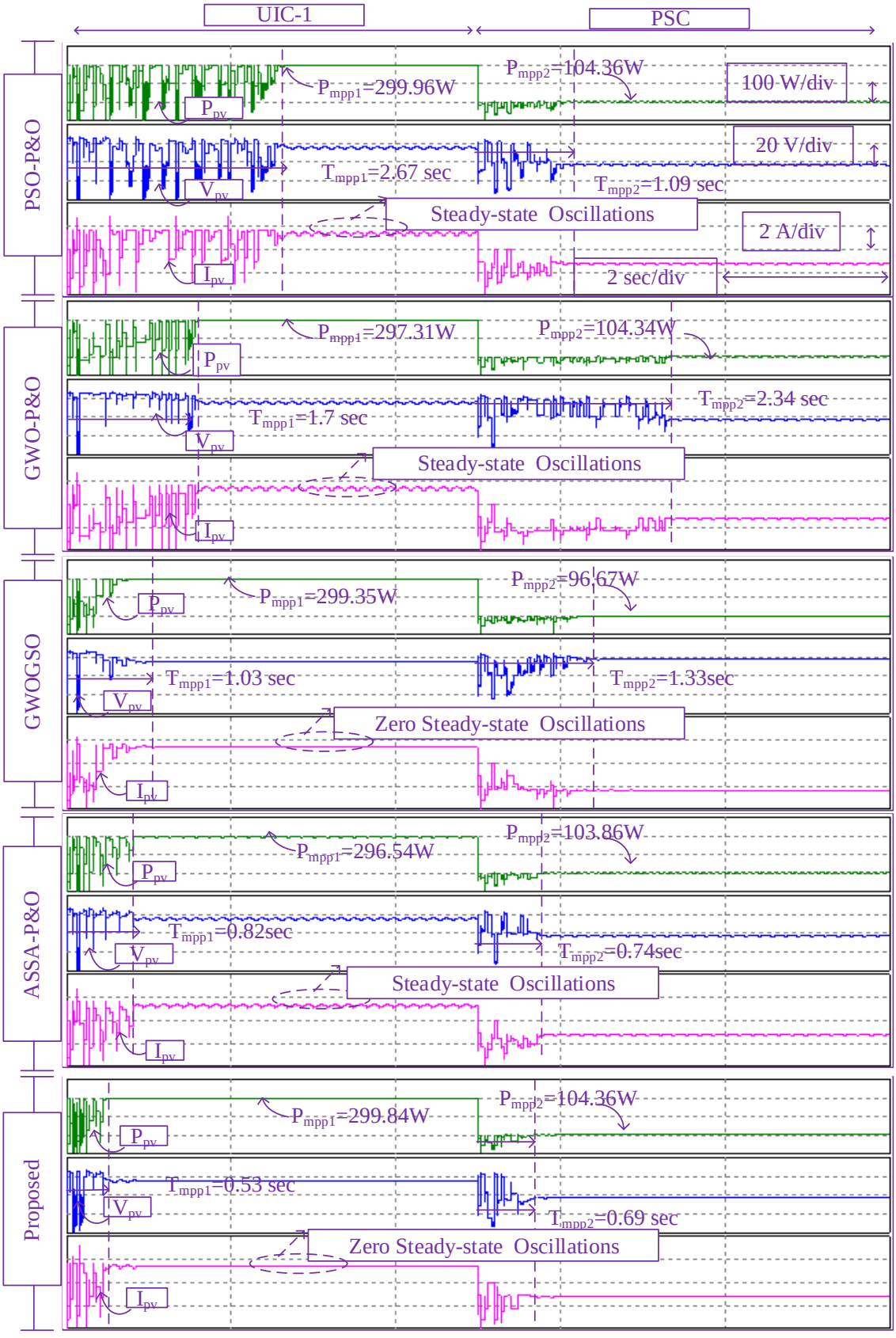

Figure 5.7: Simulation results of the hybrid GMPPT techniques.

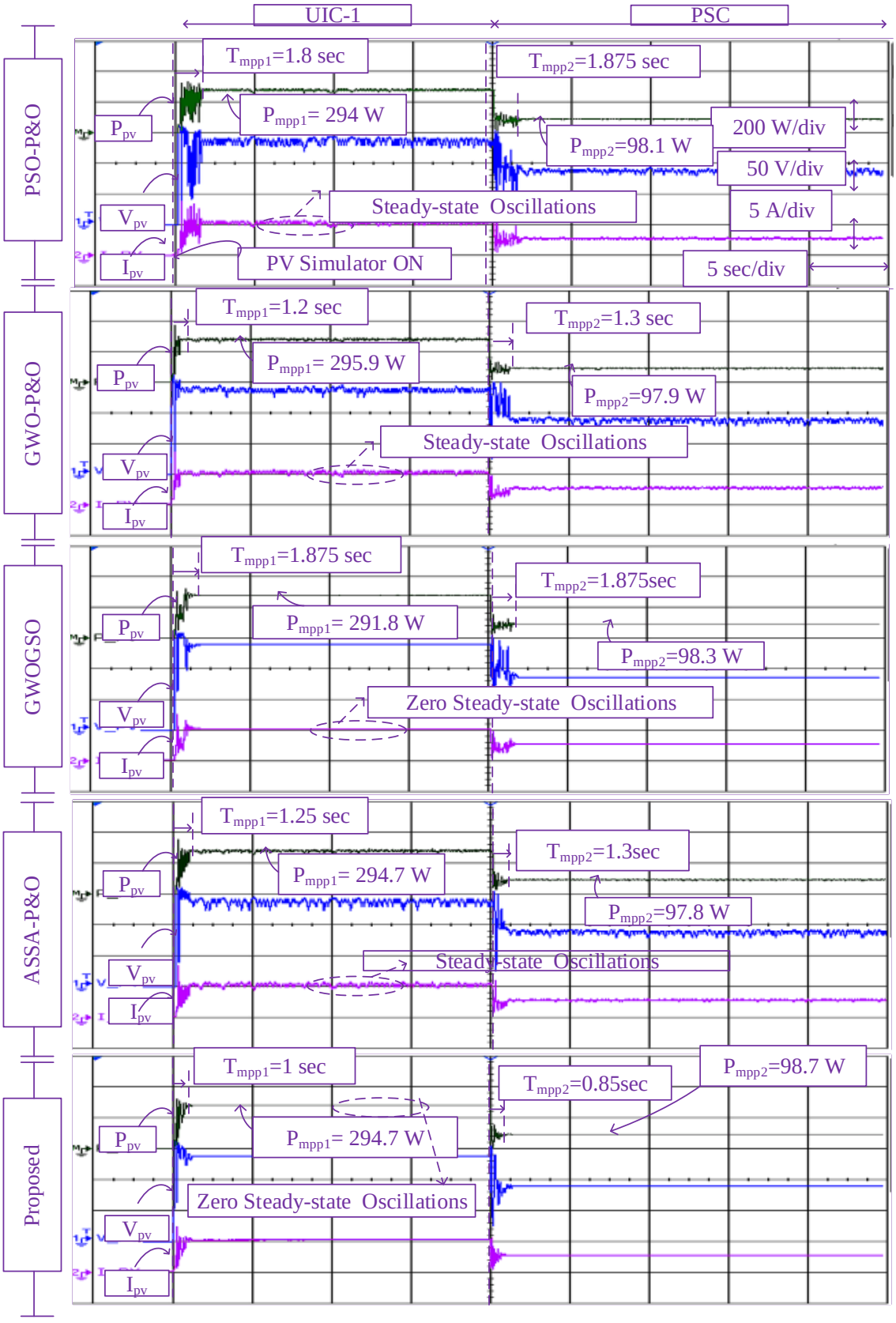

Figure 5.8: Experimental verification of the hybrid GMPPT techniques.

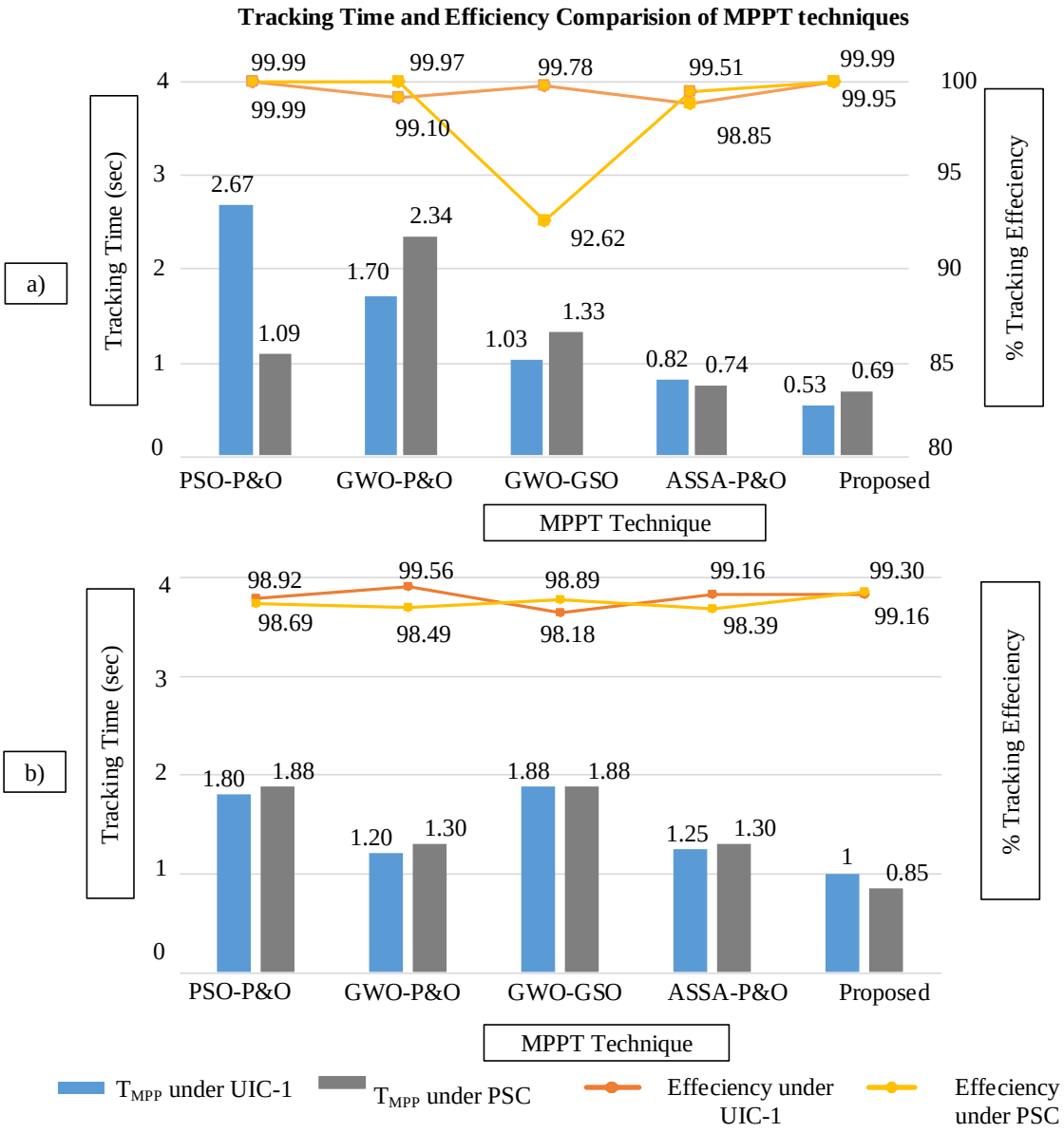

Figure 5.9: Bar-chart of the tracking time and efficiency of MPPT techniques for a) Simulation results, b) Experimentally obtained results.

SO-P&O from the upper bound ub=0.85 with higher perturbation step size $\Delta D_{max} = 5\%$ is started , in simulation at $t = 0.11\ sec$, $P_1 = 286\ W > P_{ref}$ is found. Hence, FPPT control is activated within the limited search space, and multiplication constant M is calculated. The duty ratio is adjusted with the proposed adaptive FPPT control. Since, steady-state duty ratio is found with SO-P&O, FPPT control's accuracy is more with tracking error less than 0.3%. The tracking time of FPP is $T_{FPP} \leq 0.375 sec$. When irradiance changes to UIC-2, i.e., single-peak

curve with P_{MPP} less than P_{ref}, curve scan with SO-P&O from the upper bound ub=0.85 with larger perturbation step-size $\Delta D_{max} = 5\%$ is started. In the simulation, at t=0.36 sec, the first peak $P_{LLP1} = 204.24W$ from the upper bound is found, and the corresponding voltage is stored in $V_s[1] = 57.13V$. when second duty ratio $D = lb = 0.1$ is applied corresponding voltage $V_s[2] = 64.51V$ is stored. Since the difference in two voltages is less than $0.8 * V_{oc}$, uniform detection is found and SO-P&O is activated from $Ds[1]$ with a smaller duty ratio $\Delta D_{min} = 1\%$ within the limited search space. Hence, an accurate GMPP is found with zero oscillations in the steady-state. When irradiance changes to partial shading irradiance profile PSC, shade detection activated and a first peak $P_{LLP1} = 62.9W$ from the upper bound is found, and the corresponding voltage is stored in $V_s[1] = 15.82V$. When second duty ratio $D = lb = 0.1$ is applied corresponding voltage $V_s[2] = 62.48V$ is stored. Since the difference in two voltages is greater than $0.8 * V_{oc}$, partial shading is found, and the proposed hybrid GMPPT technique,

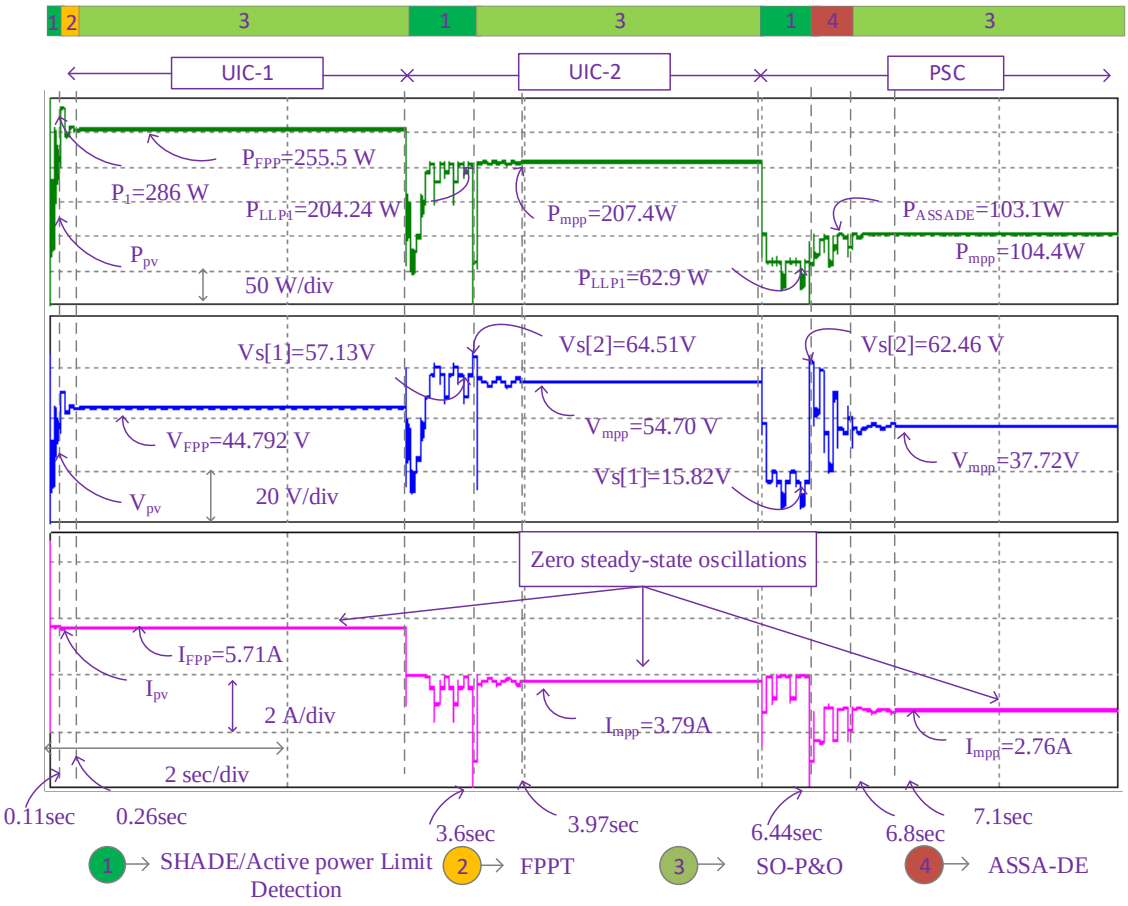

Figure 5.10: Simulation results of the proposed shade and active power limit detection.

ASSA-DE, is activated within the limited search space from $D_{max} = Ds[1]$ to $D_{min} = Ds[2]$. When the GP region is found, tracking is shifted to SO-P&O from the food source found in the GP region. Hence, an accurate GMPP is found with zero oscillations in the steady-state.

From both experimental and simulation results, it is evident that the proposed hybrid tracking technology results in accurate shade detection less than 0.8 sec, accurate FPP tracking with smaller tracking error less than 0.3%, and faster and accurate GMPP tracking within ($T_{mpp} \leq 1.2\ sec$) with zero steady-state oscillations. These features are best suited for the grid-connected PV system under varying weather conditions. Hence, the proposed hybrid tracking technology guarantees both faster and exact FPP and GMPP tracking with zero steady-state oscillations.

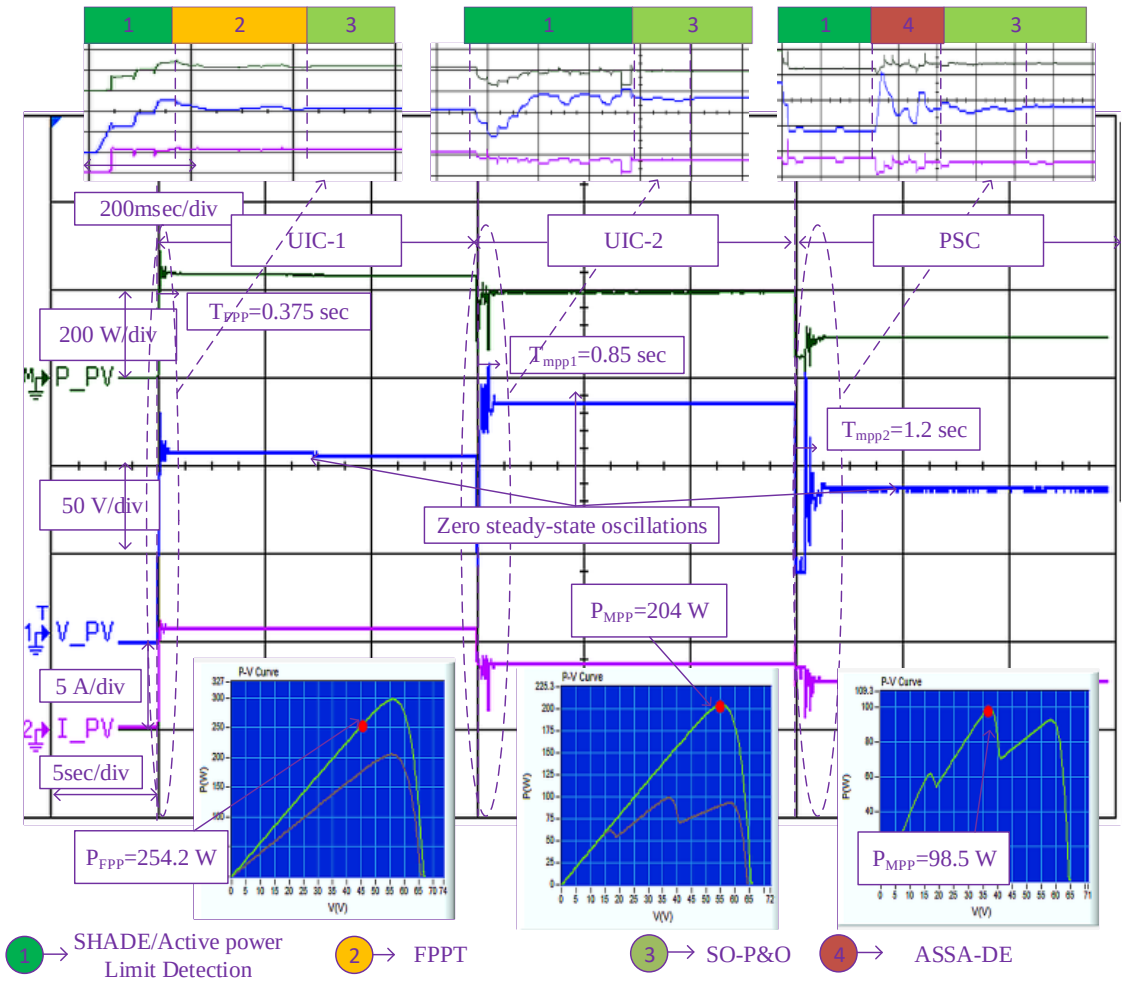

Figure 5.11: Experimentally obtained results of the proposed shade and active power limit detection.

5.6 Conclusion

The simulation and experimental results discussion shows that the proposed hybrid GMPPT technique has the best features; less tracking time, fast and accurate tracking of GMPP and FPP, and zero power oscillations in the steady-state. Further, with the proposed shade detection, it is possible to identify the type of shading with only scanning of the first peak from the search space's upper bound and another duty ratio at a lower search space. Hence, a complete curve scan or scan from both sides is unnecessary, which reduces the shade detection time as well as GMPP or FPP tracking time. Further, search space limits can be defined for FPPT and GMPPT. These features are best suited for the grid-connected PV system under varying weather conditions. Hence, the proposed optimal performance of hybrid tracking technique guarantees both faster and exact FPP and GMPP tracking with zero steady-state oscillations.

Chapter 6

Performance comparison of MPPT techniques

Chapter 6

Performance comparison of MPPT techniques

6.1 Introduction

The main focus of the all the proposed MPPT techniques is to get faster and accurate tracking of MPP under all dynamic weather conditions. However, the other functionalities like shading detection, particle reinitalization, direct duty ratio calculation for the load changes in off grid PV system and flexible power point tracking techniques in grid connected PV system are added to the proposed algorithms wherever necessary. Three different hardware prototypes are designed to test the corresponding functionalities also. Therefore, the proposed algorithms are compared with simulation and experimental results of the state of art techniques in the Chapter 3, 4, and 5. However, the comparison among the five proposed algorithms is missing. In practice, to compare the performance of several MPPT techniques, the constraints used for implementing MPPT techniques, i.e., PV system, irradiance profiles, and algorithm parameters (perturbation step size, number of population, and convergence criteria, etc.) should be common for all the MPPT techniques. Hence, in this chapter, to compare the proposed MPPT techniques with state-of-art MPPT techniques, a model of a 300 Watt PV system as shown in Figure 6.1 is used, which is same as the PV system used in chapter 4 and 5. The details of the MPPT controller are given in Table. 4.5. Three irradiance profiles of the 3S-2P short string are given in Table. 6.1. These are used to study the performance of MPPT techniques under both uniform irradiance and partially shaded conditions. P-V and I-V curves of the given irradiance profiles are shown in the Figure 6.2.

Sample time for simulation is $T_s = 10\ msec$, and the switching frequency of the boost converter is $f_s = 50\ KHz$. From the simulation results, the performance parameters, tracking time, static tracking accuracy and average static tracking accuracy, power oscillations, net energy yield, and percentage energy loss are evaluated for all the MPPT techniques. Net energy yield and percentage energy losses are calculated by using (6.1) and (6.3)

$$E_{net} = \int_0^t P_{pv}(t)\, dt \tag{6.1}$$

$$E_{max} = \int_0^t P_{mp}(t)\, dt \tag{6.2}$$

$$\%E_{loss} = \frac{E_{max} - E_{net}}{E_{max}} \times 100 \tag{6.3}$$

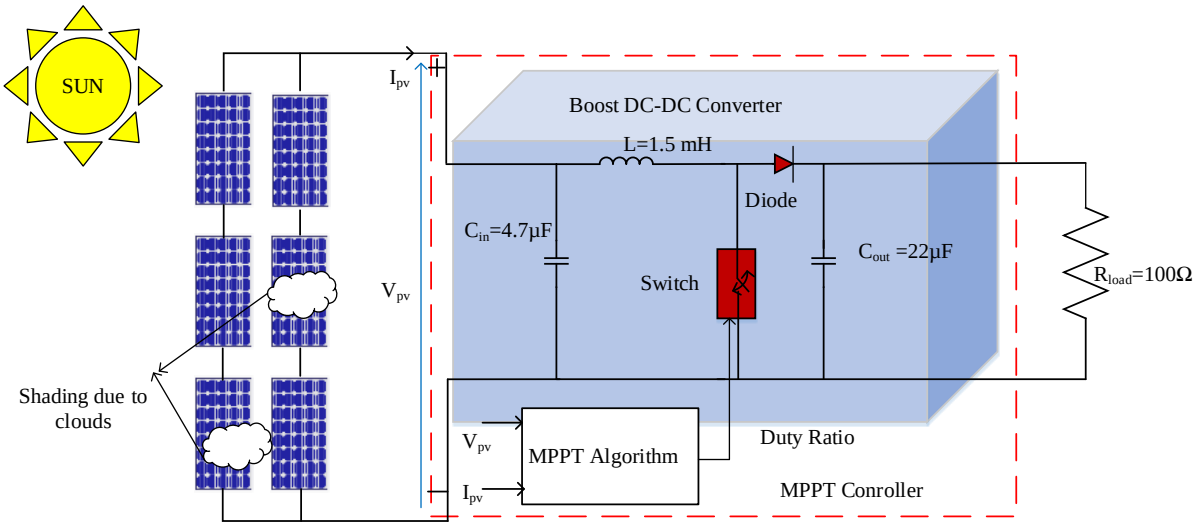

Figure 6.1: PV system used for comparing the performance of MPPT techniques.

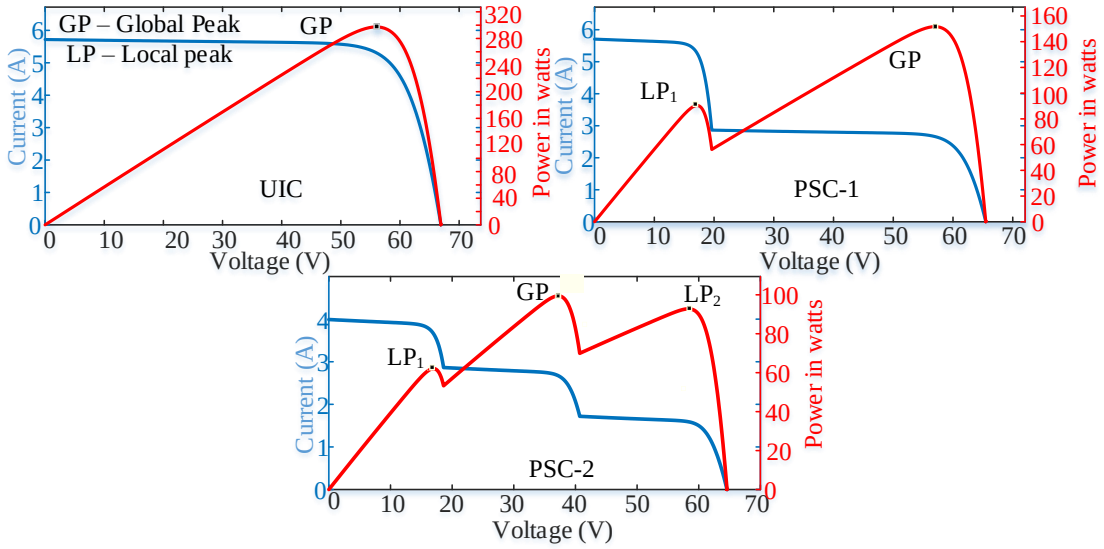

Figure 6.2: *P-V* and *I-V* curves for the given irradiance profiles.

Table 6.1: Details of irradiance profiles.

String Type	Irradiance Pattern	Irradiance profile (KW/sq.mt)						Number of Peaks	Global Peak		
		P_1	P_2	P_3	P_4	P_5	P_6		V_{GP} (V)	I_{GP}(A)	P_{GP}(W)
3S-2P Short String	UIC	1	1	1	1	1	1	1	55.87	5.38	300
	PSC-1	1	0.5	0.5	1	0.5	0.5	2	57.02	2.72	155.5
	PSC-2	0.8	0.5	0.2	0.7	0.3	0.5	3	37.19	2.81	104.5

6.2 Performance comparison of gradient-based MPPT techniques

In this chapter, mainly three gradient-based techniques, i.e., perturb and observe (P&O), variable step P&O (VS-P&O), and steady output P&O (SO-P&O) are investigated. The proposed gradient-based MPPT technique, SO-P&O is compared with the variable step P&O under the same constraints and irradiance conditions. The algorithm parameters used for simulation are given in the Table. 6.2. The simulation results of the gradient-based MPPT techniques are shown in Figure 6.3 and corresponding results are tabulated in Table 6.3.

The main drawback of the conventional P&O MPPT technique is power oscillations in the steady-state due to continuous perturbations even after reaching MPP is eliminated with steady output P&O. From the simulation results in the Figure 6.3, it is evident that the tracking time and power oscillations in the steady-state are improved with the the proposed gradient-based technique (SO-P&O). However, the static efficiency of the three gradient-based MPPT techniques in the PSC case is poor due to the tracking of local peak. Hence, average static tracking efficiency of the gradient-based techniques is low (less than 86.81%) and it leads to high energy loss (more than 8.83 %). The overall performance parameters of the gradient-based

Table 6.2: Parameters of gradient-based MPPT techniques used in the simulation.

S.No	Algorithm	Parameters
1	P&O	$\Delta d = 0.01$, d_{start}=0.8
		duty ratio limits $[lb \;\; ub] = [0.1 \;\; 0.85]$
2	VS-P&O	Multiplying factor $M = 0.005$, $\Delta d_{max} = 0.05$, $\Delta d_{min} = 0.001$
		d_{start}=0.8, duty ratio limits $[lb \;\; ub] = [0.1 \;\; 0.85]$
3	SO-P&O	$\Delta d_{max} = 0.05$, $\Delta d_{min} = 0.001$
		d_{start}=0.8, duty ratio limits $[lb \;\; ub] = [0.1 \;\; 0.85]$

Table 6.3: Simulation results of gradient-based MPPT techniques.

S.NO	Algorithm	Pattren-1 (300 W)			Pattren-2 (155.5 W)			Pattren-3(104.5 W)		
		T_{mp} (sec)	P_{mp} (W)	$\%\eta_{static}$	T_{mp} (sec)	P_{mp} (W)	$\%\eta_{static}$	T_{mp} (sec)	P_{mp} (W)	$\%\eta_{static}$
1	P&O	0.10	299.70	99.90	0.12	155.22	99.82	0.02	63.19	60.47
2	VS-P&O	0.05	299.97	99.99	0.08	155.36	99.91	0.01	63.20	60.48
3	SO-P&O	0.15	300.00	100.00	0.04	155.35	99.90	0.08	63.24	60.52

Table 6.4: Performance evaluation of gradient-based MPPT techniques.

S.NO	Algorithm	Avg. $\%\eta_{static}$	Power oscillations		Net Energy yield(J)	% Energy loss
			Transient	Steady-State		
1	P&O	86.73	low	high	502.57	10.26
2	VS-P&O	86.79	low	low	510.54	8.83
3	SO-P&O	86.81	low	zero	508.23	9.24

MPPT techniques are given in Table 6.4.

6.3 Performance comparison of PSO-based MPPT techniques

In this chapter, mainly five PSO-based MPPT techniques, i.e., particle swarm optimization (PSO), enhanced leader PSO (ELPSO), adaptive velocity PSO (AVPSO), and two proposed techniques: enhanced leader adaptive velocity PSO (ELAVPSO), and adaptive butterfly PSO - P&O (ABFPSO-P&O) are investigated. The presented PSO-based MPPT techniques are compared under the same constraints and irradiance conditions. The algorithm parameters used

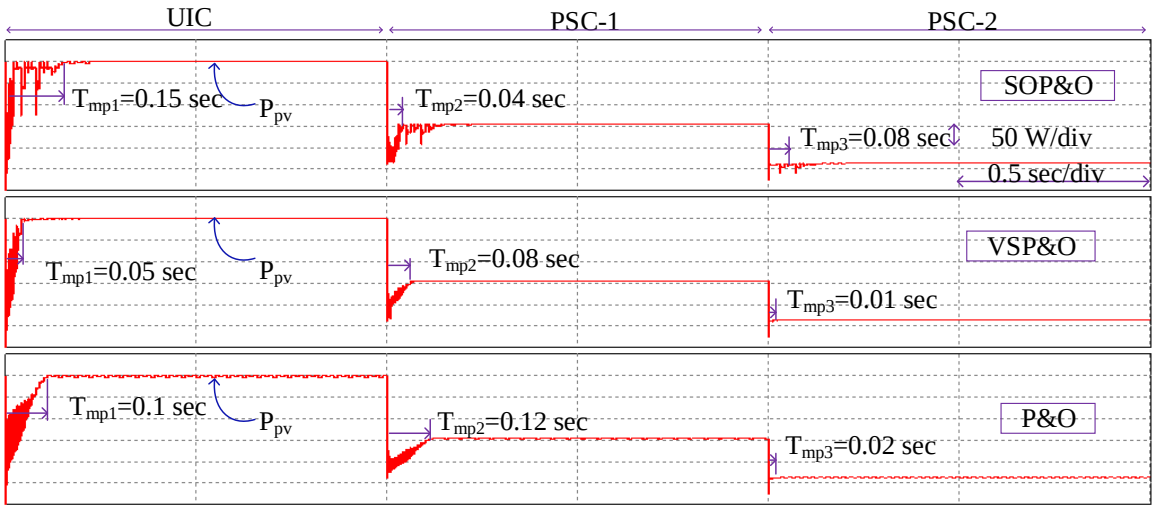

Figure 6.3: Simulation results of gradient-based MPPT techniques.

Table 6.5: Parameters of PSO-based MPPT algorithms in the simulation.

S.No	Algorithm	Parameters
1	PSO	Population size = 4, Inertia constant $w = 1$ Acceleration constants $C_1 = 2, C_2 = 2$, $vel_{max} = 0.15$ Maximum Iteration count $itr_{max} = 15$ Limits of search space $[lb \;\; ub] = [0.1 \;\; 0.85]$
2	ELPSO	Population size = 4, Inertia constant $w = 1$ Acceleration constants $C_1 = 2, C_2 = 2$, $vel_{max} = 0.15$ mutation constants h=0.02, s=0.01, F=0.5 Maximum Iteration count $itr_{max} = 15$ Limits of search space $[lb \;\; ub] = [0.1 \;\; 0.85]$
3	AVPSO	Population size = 4, Acceleration constant $C_2 = 2$ Maximum Iteration count $itr_{max} = 15$ Limits of search space $[lb \;\; ub] = [0.1 \;\; 0.85]$
4	ELAVPSO	Population size = 3, Acceleration constant $C_2 = 2$ mutation constants h=0.02, s=0.01, F=0.5 Limits of search space $[lb \;\; ub] = [0.1 \;\; 0.85]$
5	ABFPSO-P&O	Population size = 4, Acceleration constant $C_1 = C_2 = 2$ Multiplying factor $M = 0.005$, $\Delta d_{max} = 0.05$, $\Delta d_{min} = 0.001$ Limits of search space $[lb \;\; ub] = [0.1 \;\; 0.85]$

Table 6.6: Simulation results of PSO-based MPPT techniques.

S.NO	Algorithm	Pattren-1 (300 W)			Pattren-2 (155.5 W)			Pattren-3(104.5 W)		
		T_{mp} (sec)	P_{mp} (W)	$\%\eta_{static}$	T_{mp} (sec)	P_{mp} (W)	$\%\eta_{static}$	T_{mp} (sec)	P_{mp} (W)	$\%\eta_{static}$
1	PSO	0.61	300.00	100.00	0.62	155.40	99.94	0.61	104.36	99.87
2	ELPSO	0.59	299.92	99.97	0.60	155.17	99.79	0.59	104.45	99.95
3	AVPSO	0.47	298.31	99.44	0.26	155.37	99.92	0.21	104.40	99.90
4	ELAVPSO	0.30	300.00	100.00	0.37	154.51	99.36	0.30	104.46	99.96
5	ABFPSO-P&O	0.28	299.04	99.68	0.21	155.35	99.90	0.18	104.39	99.89

Table 6.7: Performance evaluation of PSO-based MPPT techniques.

S.NO	Algorithm	Avg. $\%\eta_{static}$	Power oscillations		Net Energy yield(J)	% Energy loss
			Transient	Steady-State		
1	PSO	99.93	high	zero	502.57	10.26
2	ELPSO	99.90	high	zero	473.68	15.41
3	AVPSO	99.75	medium	zero	510.17	8.90
4	ELAVPSO	99.78	low	low	512.68	8.45
5	ABFPSO-P&O	99.83	medium	low	516.35	7.79

for simulation are given in the Table. 6.5. The simulation results of the PSO-based MPPT techniques are shown in Figure 6.4 and corresponding results are tabulated in Table 6.6.

The main drawbacks of PSO-based MPPT techniques, parameter tuning, slower con-

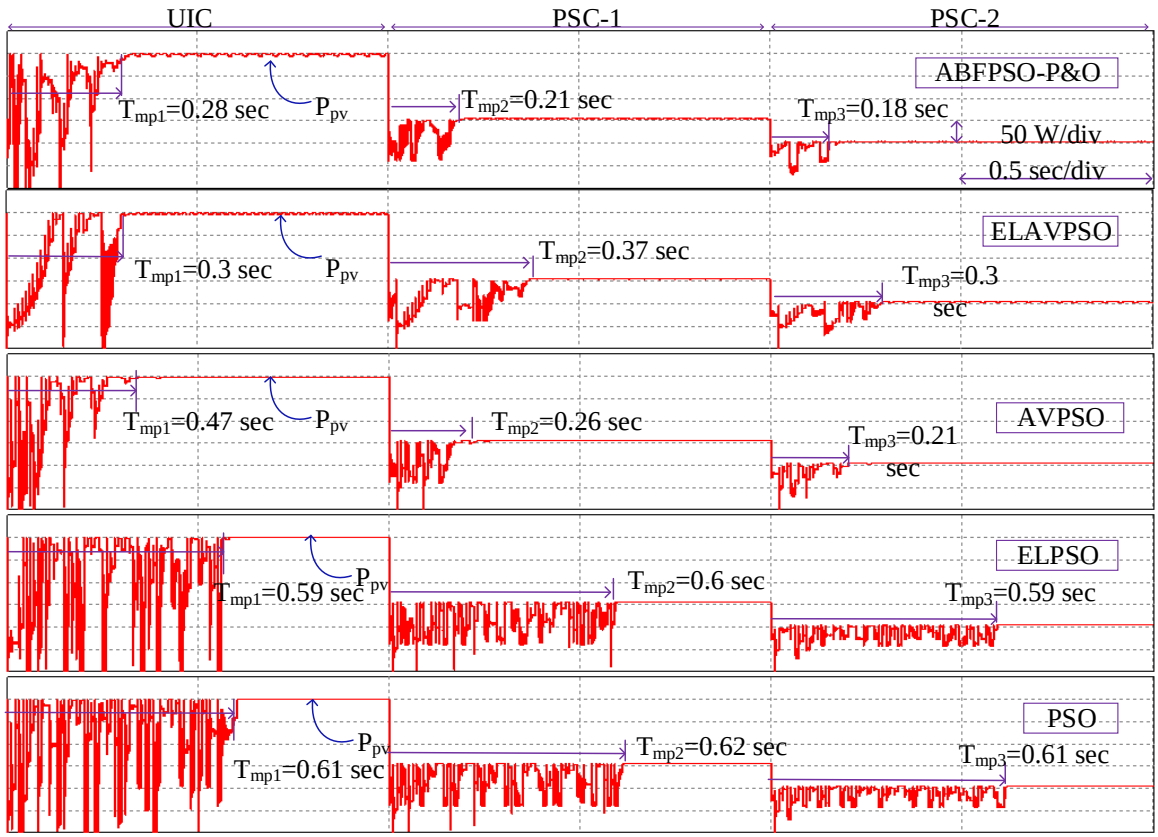

Figure 6.4: Simulation results of PSO-based MPPT techniques.

vergence, premature convergence, and power oscillations in the transient and steady-state are minimized with proposed techniques ELAVPSO along with shade detection and ABFPSO-P&O with the proposed reinitialization technique. From the simulation results in the Figure 6.4, it is evident that the tracking time and power oscillations of the proposed hybrid MPPT technique ABFPSO-P&O is low, which leads to high energy yield (516.35 J) and low energy loss (7.79%). The overall performance parameters of the PSO-based MPPT techniques are given in the Table 6.7.

6.4 Performance comparison of SSA-based MPPT techniques

In this chapter, mainly four SSA-based MPPT techniques, i.e., salp swarm algorithm (SSA), memetic SSA), and two proposed hybrid techniques: adaptive SSA-P&O (ASSA-P&O), and self-adaptive SSADE- P&O (ASSADE-P&O) are investigated. The presented SSA-based MPPT techniques are compared under the same constraints and irradiance conditions. The

Table 6.8: Parameters of SSA-based MPPT algorithms in the simulation.

S.No	Algorithm	Parameters
1	SSA	Population size = 4, Maximum Iteration count $itr_{max} = 15$ Limits of search space $[lb \;\; ub] = [0.1 \;\; 0.85]$
2	Memetic SSA	Population size in each chain = 2, salp chains = 2 Maximum Iteration count itr_{max}=15, Limits of search space $[lb \;\; ub] = [0.1 \;\; 0.85]$
3	ASSA-P&O	Population size = 4 Multiplying factor $M = 0.005$, $\Delta d_{max} = 0.05$, $\Delta d_{min} = 0.01$ Limits of search space $[lb \;\; ub] = [0.1 \;\; 0.85]$
4	ASSADE-P&O	Population size = 4, $\Delta d = 0.01$ Limits of search space $[lb \;\; ub] = [0.1 \;\; 0.85]$

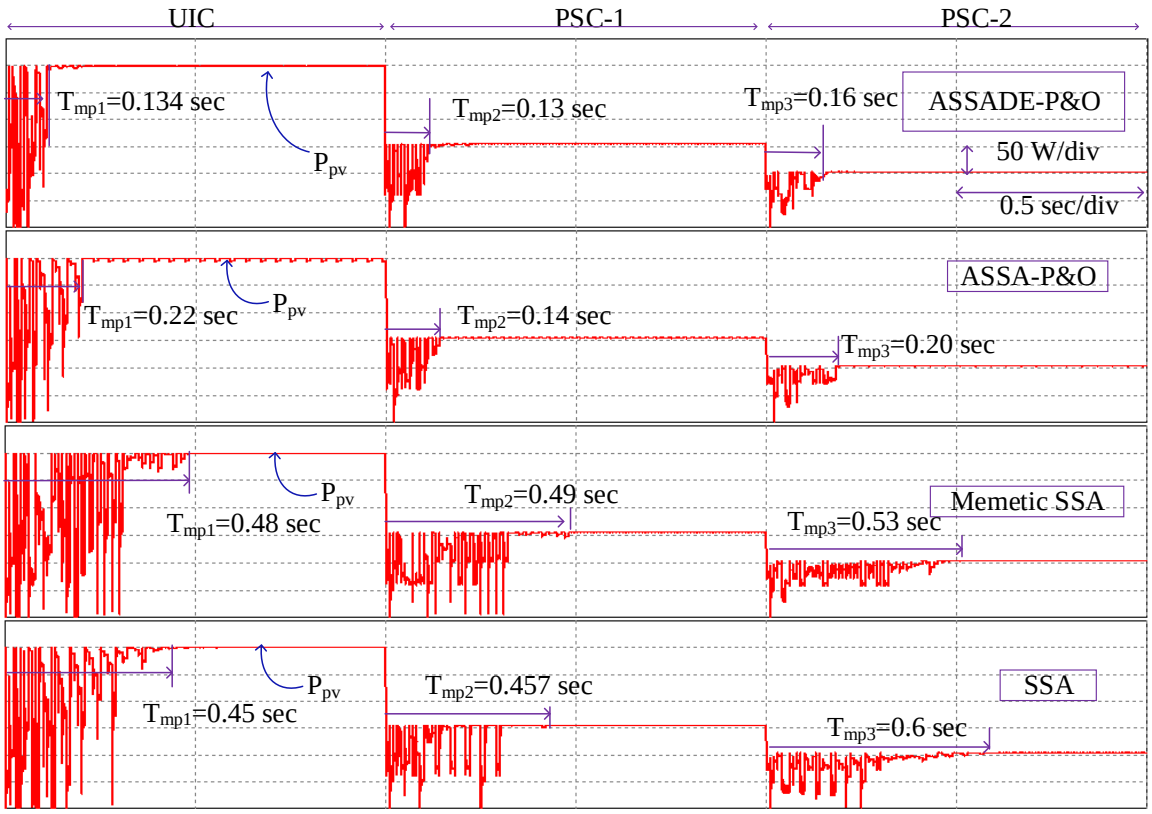

Figure 6.5: Simulation results of SSA-based MPPT techniques.

algorithm parameters used for simulation are given in the Table. 6.8. The simulation results of the SSA-based MPPT techniques are shown in Figure 6.5 and corresponding results are tabulated in Table 6.9.

The main drawback of SSA-based MPPT techniques, parameter tuning, slower conver-

Table 6.9: Simulation results of SSA-based MPPT techniques.

S.NO	Algorithm	Pattren-1 (300 W)			Pattren-2 (155.5 W)			Pattren-3(104.5 W)		
		T_{mp} (sec)	P_{mp} (W)	$\%\eta_{static}$	T_{mp} (sec)	P_{mp} (W)	$\%\eta_{static}$	T_{mp} (sec)	P_{mp} (W)	$\%\eta_{static}$
1	SSA	0.45	299.87	99.96	0.457	155.40	99.94	0.6	104.45	99.95
2	Memetic SSA	0.48	299.80	99.93	0.49	155.46	99.97	0.53	104.25	99.76
3	ASSA-P&O	0.22	299.92	99.97	0.14	155.43	99.95	0.20	104.46	99.96
4	ASSADE-P&O	0.134	299.92	99.97	0.13	155.40	99.94	0.16	104.40	99.90

Table 6.10: Performance evaluation of SSA-based MPPT techniques.

S.NO	Algorithm	Avg. $\%\eta_{static}$	Power oscillations		Net Energy yield(J)	% Energy loss
			Transient	Steady-State		
1	SSA	99.95	high	zero	503.82	10.03
2	Memetic SSA	99.89	high	zero	497.31	11.19
3	ASSA-P&O	99.96	medium	low	529.95	5.37
4	ASSADE-P&O	99.94	medium	zero	532.13	4.98

gence, and power oscillations in the transient and steady-state are minimized with proposed hybrid techniques ASSA-P&O and ASSADE-P&O. From the simulation results in the Figure 6.5, it is evident that the tracking time and power oscillations of the proposed hybrid MPPT technique ASSADE-P&O is low, which leads to high energy yield (532.13 J) and low energy loss (4.98%). The overall performance parameters of the SSA-based MPPT techniques is given in the Table 6.10.

6.5 Performance comparison of hybrid MPPT techniques

In this chapter, mainly six hybrid MPPT techniques, i.e., PSO-P&O, GWO-P&O, GWO-GSO, and three proposed hybrid techniques: ABFPSO-P&O, ASSA-P&O, and ASSADE-P&O are investigated. The presented hybrid MPPT techniques are compared under same constraints and irradiance conditions. The algorithm parameters used for simulation are given in the Table. 6.11. The simulation results of the hybrid MPPT techniques are shown in Figure 6.6 and corresponding results are tabulated in Table 6.12.

The main challenges of hybrid MPPT techniques, slower GP region identification, switching between algorithms, and power oscillations in the transient and steady-state are minimized with proposed hybrid techniques, ABFPSO-P&O, ASSA-P&O and ASSADE-P&O. From the simulation results in the Figure 6.6, it is evident that the tracking time and power oscillations of the proposed hybrid MPPT technique ASSADE-P&O is low which leads to high energy yield

Table 6.11: Parameters of hybrid MPPT algorithms in the simulation.

S.No	Algorithm	Parameters
1	PSO-P&O	Population size = 4, $\Delta d = 0.01$ Limits of search space $[lb \;\; ub] = [0.1 \;\; 0.85]$
2	GWO-P&O	Population size = 4, $\Delta d = 0.01$ Maximum Iteration count itr_{max}=15, Limits of search space $[lb \;\; ub] = [0.1 \;\; 0.85]$
3	GWO-GSO	Population size = 4, golden ratio = 0.618 Maximum Iteration count itr_{max}=15, Limits of search space $[lb \;\; ub] = [0.1 \;\; 0.85]$
4	ABFPSO-P&O	Population size = 4, Acceleration constant $C_1 = C_2 = 2$ Multiplying factor $M = 0.005$, $\Delta d_{max} = 0.05$, $\Delta d_{min} = 0.01$ Limits of search space $[lb \;\; ub] = [0.1 \;\; 0.85]$
5	ASSA-P&O	Population size = 4 Multiplying factor $M = 0.005$, $\Delta d_{max} = 0.05$, $\Delta d_{min} = 0.01$ Limits of search space $[lb \;\; ub] = [0.1 \;\; 0.85]$
6	ASSADE-P&O	Population size = 4, $\Delta d = 0.01$ Limits of search space $[lb \;\; ub] = [0.1 \;\; 0.85]$

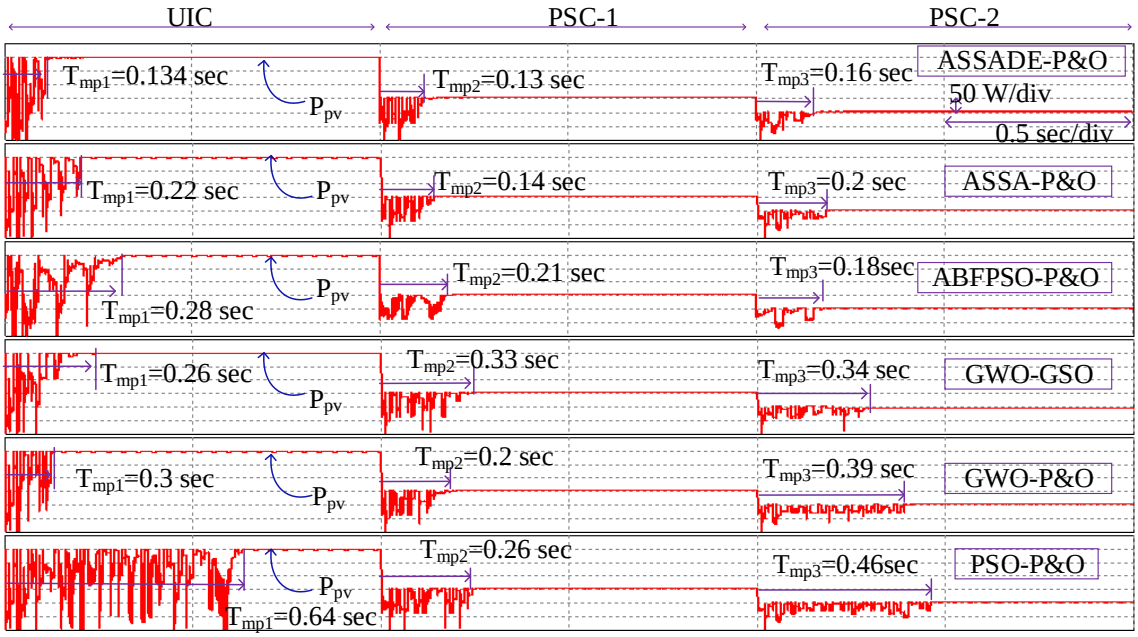

Figure 6.6: Simulation results of hybrid MPPT techniques.

(532.13 J) and low energy loss (4.98%) which is evolved as superior MPPT technique among all presented MPPT techniques. The overall performance parameters of the hybrid MPPT techniques are given in the Table 6.13.

Table 6.12: Simulation results of hybrid MPPT techniques.

S.NO	Algorithm	Pattren-1 (300 W)			Pattren-2 (155.5 W)			Pattren-3(104.5 W)		
		T_{mp} (sec)	P_{mp} (W)	$\%\eta_{static}$	T_{mp} (sec)	P_{mp} (W)	$\%\eta_{static}$	T_{mp} (sec)	P_{mp} (W)	$\%\eta_{static}$
1	PSO-P&O	0.64	298.80	99.60	0.26	153.81	98.91	0.46	104.28	99.79
2	GWO-P&O	0.3	300.00	100.00	0.2	154.83	99.57	0.39	103.93	99.45
3	GWO-GSO	0.26	299.94	99.98	0.33	155.42	99.95	0.34	97.43	93.23
4	ABFPSO-P&O	0.28	299.04	99.68	0.21	155.35	99.90	0.18	104.39	99.89
5	ASSA-P&O	0.22	299.92	99.97	0.14	155.43	99.95	0.20	104.46	99.96
6	ASSADE-P&O	0.134	299.92	99.97	0.13	155.40	99.94	0.16	104.40	99.90

Table 6.13: Performance evaluation of hybrid MPPT techniques.

S.NO	Algorithm	Avg. $\%\eta_{static}$	Power oscillations		Net Energy yield(J)	% Energy loss
			Transient	Steady-State		
1	PSO-P&O	99.43	high	high	489.30	12.63
2	GWO-P&O	99.67	high	high	523.46	6.52
3	GWO-GSO	97.72	high	zero	524.85	6.28
4	ABFPSO-P&O	99.83	medium	low	516.35	7.79
5	ASSA-P&O	99.96	medium	low	529.95	5.37
6	ASSADE-P&O	99.94	medium	zero	532.13	4.98

6.6 Conclusion

In this chapter, the performance of all the proposed gradient and SC-based MPPT techniques are compared with state-of-art MPPT techniques under common atmospheric conditions with same constraints. The main drawback of the conventional P&O MPPT technique is power oscillations in the steady-state due to continuous perturbations even after reaching MPP is eliminated with steady output P&O. The tracking time and power oscillations in the steady-state are improved with the proposed gradient-based technique (SO-P&O). All the proposed PSO and SSA-based MPPT techniques are evolved as efficient MPPT techniques with optimal performance for the PV systems under partial shading conditions. The superiority of the proposed methods over the state-of-art techniques is in terms of higher accuracy, low power oscillations, low energy loss. Hence, the proposed MPPT techniques guarantees maximum energy yield under all dynamic weather conditions.

Chapter 7

Conclusions and future scope of research

Chapter 7

Conclusions and future scope of research

7.1 Conlcusions of the proposed MPPT techniques for PV system under partially shaded conditions

The focus on the MPPT techniques for the PV system under partially shaded conditions increased with the need for maximum energy yield from the PV system under all dynamic conditions. The SC-based MPPT techniques are simple and model-independent to find the accurate GMPP. However, the main drawbacks of parameter tuning complexity, premature convergence, slow tracking, and large power oscillations are reduced with adaptive parameter tuning and with hybrid GMPPT techniques. In this thesis, various hybrid MPPT techniques for the PV system under PSC are proposed. These MPPT techniques display the capability of fast and accurate tracking of MPP with low power oscillations even under worst shading conditions which are discussed and presented using the simulation studies. The focus on the MPPT techniques for the PV system under partially shaded conditions increased with the need for maximum energy yield from the PV system under all dynamic conditions. Under PSC, the power loss due to tracking wrong MPP and mismatch losses causes a high energy losses. Hence, in this thesis, hybrid MPPT techniques are developed to overcome the power loss due to tracking wrong MPP of the multi-peak P-V curve under PSC. These MPPT techniques display the capability of fast and accurate tracking of MPP with low power oscillations even under worst shading conditions which are discussed and presented using the simulation studies in the chapters 3, 4, 5, and 6. The simulation results are verified with the experimental results obtained from the developed low scale laboratory prototypes. The main drawbacks of SI based MPPT techniques; parameter tuning complexity, premature convergence, slow tracking, and large power oscillations are reduced with adaptive parameter tuning and hybrid GMPPT techniques. Even though SI based techniques are effective in finding GMPP under PSC, because of the limitations like slow tracking of MPP and power oscillations during tracking as compared to gradient based

techniques, identifying the irradiance conditions and applying proper algorithm is vital. Therefore, in this thesis, the proposed shading detection in the chapter-1 allows the optimum use of GMPPT technique under dynamic partial shading conditions. The long exploration phase and large random moment of particles in SI based MPPT techniques results in the slow tracking with large power oscillations. Hence, the proposed hybridization of the P&O with SI technique results in efficient hybrid MPPT techniques to get faster tracking with reduced power oscillations. The detailed discussion of the proposed ABFPSO-P&O hybrid GMPPT technique is presented in the chapter-3 of this thesis. In the stand-alone PV system, to get maximum power under both irradiance and load changes, a new hybrid GMPPT technique, ASSADE-P&O along with direct duty ratio calculation is proposed in chapter-4 of this thesis. In grid connected PV systems, active power control is required as per the grid code and optimal performance of the MPPT controller is required to get the high energy yield under PSC. Therefore, in this thesis, an accurate power limit control and shade detection is proposed in t he chapter 5. The proposed optimal performance of the hybrid MPPT technique results faster tracking of FPP and MPP. The proposed MPPT techniques for PV system under partially shaded conditions are compared with the state-of-art techniques found in the literature. All the proposed PSO and SSA based MPPT techniques are evolved as efficient MPPT techniques with optimal performance for the PV systems under partial shading conditions. Hence, the maximum possible energy can be extracted from the solar PV system under partial shading conditions, which is the main objective of the proposed thesis work.

7.1.1 Summary of important findings

In this thesis, efficient MPPT techniques are proposed for the PV system under partial shading conditions. The important findings and highlights from this study are as follows:

- In ELAVPSO, mainly premature convergence and parameter tuning are minimized. However, the other drawback of PSO based GMPPT technique: high power oscillations during exploration phase is still remained when ELAVPSO is used alone without shading detection.

  In order to reduce power oscillations exploration phase should be limited to identify the GP region and particles should be more distributed in the one region instead of random

distribution.

- In ABF-PSO, mainly premature convergence, parameter tuning and power oscillations during tracking are minimized. Further, the reintialization of particles under irradiance changes improves the tracking speed as well as limits the power oscillations during tracking. However, there are more number of parameters, i.e., three to be tuned in PSO based MPPT techniques.

  To reduce the complexity of parameter tuning, simple SI technique with less control parameters needs to be used for PV MPPT.

- In ASSA-P&O, number of parameters to be tuned and power oscillations during tracking are minimized. However, slower tracking of GP region identification in hybrid MPPT techniques (formed with SC and gradient MPPT techniques) is mainly due to the least fitness particles. When these techniques are applied to off-grid PV systems, reintialization of GP region identification stage for load changes degrades the performance.

  To overcome these limitations, the least fitness particles should be accelerated more towards the leader to get faster GP region identification. To get the better accuracy, leader salp should be enhanced in the food source region. In off-grid PV system, reintialization of GP region identification only for irradiance change and direct duty ratio calculation for load change.

- ASSADE-P&O based GMPPT technique with direct duty ratio calculation under load changes has established as a favorable method for off-grid PV system. However, for grid-connected PV system, performance optimization of the hybrid tracking technique is required to meet the grid standards like active power limit control.

  Hence, MPPT with flexible and global maximum power point tracking with hybrid tracking technology and shade detection is vital.

- The proposed hybrid GMPPT technique self-adaptive ASSA-DE has the best features; less tracking time, fast and accurate tracking of GMPP and FPP, and zero power oscillations in the steady-state. The proposed optimal performance of hybrid tracking technique guarantees both faster and exact FPP and GMPP tracking with zero steady-state oscillations.

7.2 Future scope of research

The research work presented in this thesis can be further investigated as pointed below:

- Photovoltaic array reconfiguration, along with the proposed hybrid MPPT techniques, can increase the energy yield. Hence, dynamic PV array reconfiguration along with MPPT could be investigated with different meta-heuristic techniques.
- The proposed partial shading detection schemes could be investigated to identify the other faults in the PV system.
- Performance optimization of hybrid MPPT techniques could be investigated to perform ancillary services, such as reactive power control and harmonic current compensation in grid-connected PV systems.
- Further, different meta-heuristic techniques could be investigated to get the optimum energy from the PV system under partial shading conditions.

Appendix

Appendix A

Design of a 300 Watt PV system

PV System power rating = 300 Watts

PV panels selected for the given system: solar power mart SPM-050M model 50 WP PV panel

Each panel rating = 50 watts

Electrical characteristics of solar power mart SPM-050M model 50 WP PV panel are given in Table A.1.

Design of PV array:

Number of panels in array = $\frac{PV\ system\ rating}{each\ panel\ rating} = \frac{300}{50} = 6$.

Number of panels in series string = 3.

number of strings in parallel = 2.

PV input voltage at MPP = $V_{mp} * Number\ of\ panles\ in\ string$ = 18.68*3 = 56.04 Volts.

PV input current at MPP = $I_{mp} * Number\ of\ strings\ in\ array$ = 2.68* 2 = 5.36 Amperes.

Maximum PV input voltage= $V_{oc} * Number\ of\ panles\ in\ string$ = 22.32*3 = 66.96 Volts.

Maximum PV input current= $I_{sc} * Number\ of\ strings\ in\ array$ = 2.86*2 = 5.72 Amperes.

Table A.1: Electrical characteristics of solar power mart SPM-050M model 50 WP PV panel at standard test conditions AM 1.5.

S.NO	Parameter	Value
1	Maximum Power P_{mp}(W)	50
2	Voltage at Maximum Power V_{mp} (V)	18.68
3	Current at Maximum Power I_{mp} (A)	2.68
4	Open-Circuit Voltage V_{oc} (V)	22.32
5	Short-Circuit Current I_{sc} (A)	2.86
6	Temperature Coefficient of P_{mp} $(\%^{\circ}C)$	-0.45 ± 0.05

Derivation of single diode electrical equivalent circuit parameters of the PV panel: The electrical equivalent circuit parameters of the given solar panels are extracted using an analytical method proposed in [7]

MATLAB code for parameter extraction:

****

```
Vmp=18.68;
Imp=2.68;
Voc=22.32;
Isc=2.86;
a=1.1;
n=36;
k=1.38e-23;
T=298;
q=1.6e-19;
Vt=n*k*T/q;
A=a*Vt/Imp;
B=-Vmp*(2*Imp-Isc)/((Vmp*Isc)+Voc*(Imp-Isc));
C=(-1*(2*Vmp-Voc)/(a*Vt))+(((Vmp*Isc)-(Voc*Imp))/((Vmp*Isc)+Voc*(Imp-Isc)));
D=(Vmp-Voc)/(a*Vt);
Rs=A*(lambertw(-1,(B*exp(C)))-(D+C))
Rsh=(Vmp-Imp*Rs)*(Vmp-(Rs*(Isc-Imp))-(a*Vt))/(((Vmp-Imp*Rs)*(Isc-Imp))-(a*Vt*Imp))
I0=(((Rsh+Rs)*Isc)-Voc)/(Rsh*(exp(Voc/(a*Vt))))
Iph=((Rsh+Rs)*Isc)/Rsh
```

****

The values obtained are:

Series resistance $R_s = 0.24\ \Omega$.

Shunt resistance $R_{sh} = 613.6\ \Omega$.

Diode saturation current $I_0 = 8.46 \times 10^{-10}\ A$.

Dark current $I_{ph} = 2.8611\ A$.

Design of boost converter as MPPT converter:

The calculation of the components for the MPPT boost converter is based on the total resistance seen by the PV module, which is proposed in [63]. Parameters of the boost converter are designed optimally to get continuous conduction mode.

The MPP resistance $R_{mp} = \frac{V_{mp}}{I_{mp}}$.

At maximum irradiance, i.e., 1000 W/m^2, MPP resistance is minimum $R_{mp(min)} = 6.2\ ohms$.

At minimum irradiance , i.e., 100 W/m^2, MPP resistance is maximum $R_{mp(max)} = 68\ ohms$.

The desired operating limits of the boost converter:

Inductor current ripple $\gamma I_L(\%)$ = 25.

MPP voltage ripple $\gamma V_{mp}(\%)$ = 1.

Output voltage ripple factor $\gamma V_O(\%)$ = 1.

Maximum duty cycle limit, $D_{max}(\%)$ = 85.

Minimum duty cycle limit, $D_{min}(\%)$ = 10.

Switching frequency, f(KHz) = 50 kHz.

Maximum output resistance, $R_{O(max)}$ = 100 Ω.

Inductance $L = \frac{V_{mp}D}{I_{mp}\gamma I_L f} = \frac{R_{mp(max)}}{\gamma I_L f}\left(1 - \sqrt{\frac{R_{mp(max)}}{R_{O(max)}}}\right) = 1.5\ mH$.

Input buffer capacitor $C_i = \frac{D_{max}}{8L\gamma V_{mp} f^2} = 4.7\mu F$.

Output capacitor $C_O = \frac{D}{R_O \gamma V_O f} = \frac{4}{27 R_{mp(min)} \gamma V_O f} = 22\mu F$.

Bibliography

Bibliography

[1] S. K. Gupta and R. S. Anand, "Development of Solar Electricity Supply System in India: An Overview," *Journal of Solar Energy*, pp. 1–10, 2013.

[2] A. Urja, "Newsletter of the Ministry of New and Renewable Energy, Government of India," vol. 12, no. 5, apr 2019.

[3] T. V. Dixit, A. Yadav, and S. Gupta, "Experimental assessment of maximum power extraction from solar panel with different converter topologies," *International Transactions on Electrical Energy Systems*, vol. 29, no. 2, p. e2712, 2019.

[4] H. Patel and V. Agarwal, "Maximum power point tracking scheme for pv systems operating under partially shaded conditions," *IEEE Transactions on Industrial Electronics*, vol. 55, no. 4, pp. 1689–1698, April 2008.

[5] M. Balat, "Solar technological progress and use of solar energy in the world," *Energy Sources, Part A: Recovery, Utilization, and Environmental Effects*, vol. 28, no. 10, pp. 979–994, 2006.

[6] A. Mäki and S. Valkealahti, "Power losses in long string and parallel-connected short strings of series-connected silicon-based photovoltaic modules due to partial shading conditions," *IEEE Transactions on Energy Conversion*, vol. 27, no. 1, pp. 173–183, 2012.

[7] J. Cubas, S. Pindado, and C. D. Manuel, "Explicit Expressions for Solar Panel Equivalent Circuit Parameters Based on Analytical Formulation and the Lambert W-Function," *Energies*, vol. 7, no. 7, pp. 1–18, June 2014.

[8] E. A. Sweelem, F. H. Fahmy, M. M. A.-E. Aziz, P. Zacharias, and A. Mahmoudi, "Increased efficiency in the conversion of solar energy to electric power," *Energy Sources*, vol. 21, no. 5, pp. 367–377, 1999.

[9] A. Dadjé, N. Djongyang, J. D. Kana, and R. Tchinda, "Maximum power point tracking methods for photovoltaic systems operating under partially shaded or rapidly variable insolation conditions: a review paper," *International Journal of Sustainable Engineering*, vol. 9, no. 4, pp. 224–239, 2016.

[10] H. D. Tafti, A. I. Maswood, G. Konstantinou, J. Pou, and F. Blaabjerg, "A general constant power generation algorithm for photovoltaic systems," *IEEE Transactions on Power Electronics*, vol. 33, no. 5, pp. 4088–4101, 2018.

[11] B. Subudhi and R. Pradhan, "A comparative study on maximum power point tracking techniques for photovoltaic power systems," *IEEE Transactions on Sustainable Energy*, vol. 4, no. 1, pp. 89–98, Jan 2013.

[12] M. Abdel-Salam, M. T. EL-Mohandes, and M. Goda, "History of maximum power point tracking," *Green Energy and Technology*, pp. 1–29, 2020.

[13] N. Femia, G. Petrone, G. Spagnuolo, and M. Vitelli, "Optimization of perturb and observe maximum power point tracking method," *IEEE Transactions on Power Electronics*, vol. 20, no. 4, pp. 963–973, July 2005.

[14] M. F. N. Tajuddin, M. S. Arif, S. M. Ayob, and Z. Salam, "Erratum to the 'perturbative methods for maximum power point tracking (mppt) of photovoltaic (pv) systems: a review' international journal of energy research 2015; 39:1153–1178," *International Journal of Energy Research*, vol. 39, no. 12, pp. 1720–1720, 2015.

[15] R. Rawat and S. S. Chandel, "Review of maximum-power-point tracking techniques for solar-photovoltaic systems," *Energy Technology*, vol. 1, no. 8, pp. 438–448, 2013.

[16] M. Seyedmahmoudian, B. Horan, T. K. Soon, R. Rahmani, A. M. Than Oo, S. Mekhilef, and A. Stojcevski, "State of the art artificial intelligence-based mppt techniques for mitigating partial shading effects on pv systems – a review," *Renewable and Sustainable Energy Reviews*, vol. 64, no. C, pp. 435–455, 2016.

[17] T. Radjai, J. P. Gaubert, L. Rahmani, and S. Mekhilef, "Experimental verification of p&o mppt algorithm with direct control based on fuzzy logic control using cuk converter,"

International Transactions on Electrical Energy Systems, vol. 25, no. 12, pp. 3492–3508, 2015.

[18] M. Seyedmahmoudian, T. K. Soon, B. Horan, A. Ghandhari, S. Mekhilef, and A. Stojcevski, "New armo-based mppt technique to minimize tracking time and fluctuation at output of pv systems under rapidly changing shading conditions," *IEEE Transactions on Industrial Informatics*, pp. 1–1, 2019.

[19] A. Tavakoli and M. Forouzanfar, "A self-constructing lyapunov neural network controller to track global maximum power point in pv systems," *International Transactions on Electrical Energy Systems*, vol. n/a, no. n/a, p. e12391.

[20] E. Koutroulis and F. Blaabjerg, "Overview of maximum power point tracking techniques for photovoltaic energy production systems," *Electric Power Components and Systems*, vol. 43, no. 12, pp. 1329–1351, 2015.

[21] S. Bhattacharyya, D. S. K. Patnam, S. Samanta, and S. Mishra, "Steady output and fast tracking mppt (soft mppt) for p o and inc algorithms," *IEEE Transactions on Sustainable Energy*, pp. 1–1, 2020.

[22] S. Mohanty, B. Subudhi, and P. K. Ray, "A new mppt design using grey wolf optimization technique for photovoltaic system under partial shading conditions," *IEEE Transactions on Sustainable Energy*, vol. 7, no. 1, pp. 181–188, Jan 2016.

[23] Y. Liu, S. Huang, J. Huang, and W. Liang, "A particle swarm optimization-based maximum power point tracking algorithm for pv systems operating under partially shaded conditions," *IEEE Transactions on Energy Conversion*, vol. 27, no. 4, pp. 1027–1035, Dec 2012.

[24] R. Sridhar, S. Jeevananthan, and P. Vishnuram, "Particle swarm optimisation maximum power-tracking approach based on irradiation and temperature measurements for a partially shaded photovoltaic system," *International Journal of Ambient Energy*, vol. 38, no. 7, pp. 685–693, 2017.

[25] J. Zhang, K. Ding, R. Mei, and Y. Cai, "Global maximum power point tracking method based on sorting particle swarm optimizer," *International Journal of Green Energy*, vol. 15, no. 13, pp. 821–836, 2018.

[26] N. Pragallapati, T. Sen, and V. Agarwal, "Adaptive velocity pso for global maximum power control of a pv array under nonuniform irradiation conditions," *IEEE Journal of Photovoltaics*, vol. 7, no. 2, pp. 624–639, March 2017.

[27] J. P. Ram and N. Rajasekar, "A new robust, mutated and fast tracking lpso method for solar pv maximum power point tracking under partial shaded conditions," *Applied Energy*, vol. 201, pp. 45 – 59, 2017.

[28] K. Ishaque and Z. Salam, "A deterministic particle swarm optimization maximum power point tracker for photovoltaic system under partial shading condition," *IEEE Transactions on Industrial Electronics*, vol. 60, no. 8, pp. 3195–3206, Aug 2013.

[29] H. Li, D. Yang, W. Su, J. Lü, and X. Yu, "An overall distribution particle swarm optimization mppt algorithm for photovoltaic system under partial shading," *IEEE Transactions on Industrial Electronics*, vol. 66, no. 1, pp. 265–275, Jan 2019.

[30] A. K. Bohre, G. Agnihotri, and M. Dubey, "The Butterfly-Particle Swarm Optimization (Butterfly-PSO/BF-PSO) Technique and Its Variables," *International Journal of Soft Computing, Mathematics and Control*, vol. 4, no. 3, pp. 23–39, 2015.

[31] S. Mirjalili, A. H. Gandomi, S. Z. Mirjalili, S. Saremi, H. Faris, and S. M. Mirjalili, "Salp swarm algorithm: A bio-inspired optimizer for engineering design problems," *Advances in Engineering Software*, vol. 114, pp. 163 – 191, 2017.

[32] M. A. Mohamed, A. A. Z. Diab, and H. Rezk, "Partial shading mitigation of pv systems via different meta-heuristic techniques," *Renewable Energy*, vol. 130, pp. 1159 – 1175, 2019.

[33] B. Yang, L. Zhong, X. Zhang, H. Shu, T. Yu, H. Li, L. Jiang, and L. Sun, "Novel bio-inspired memetic salp swarm algorithm and application to mppt for pv systems considering partial shading condition," *Journal of Cleaner Production*, vol. 215, pp. 1203 – 1222, 2019.

[34] K. Aygül, M. Cikan, T. Demirdelen, and M. Tumay, "Butterfly optimization algorithm based maximum power point tracking of photovoltaic systems under partial shading condition," *Energy Sources, Part A: Recovery, Utilization, and Environmental Effects*, vol. 0, no. 0, pp. 1–19, 2019.

[35] A. Anurag, S. Bal, S. Sourav, and M. Nanda, "A review of maximum power-point tracking techniques for photovoltaic systems," *International Journal of Sustainable Energy*, vol. 35, no. 5, pp. 478–501, 2016.

[36] M. Chamanpira, M. Ghahremani, S. Dadfar, M. Khaksar, A. Rezvani, and K. Wakil, "A novel mppt technique to increase accuracy in photovoltaic systems under variable atmospheric conditions using fuzzy gain scheduling," *Energy Sources, Part A: Recovery, Utilization, and Environmental Effects*, vol. 0, no. 0, pp. 1–23, 2019.

[37] K. Sundareswaran, V. V. kumar, and S. Palani, "Application of a combined particle swarm optimization and perturb and observe method for mppt in pv systems under partial shading conditions," *Renewable Energy*, vol. 75, pp. 308 – 317, 2015.

[38] S. Mohanty, B. Subudhi, and P. K. Ray, "A grey wolf-assisted perturb observe mppt algorithm for a pv system," *IEEE Transactions on Energy Conversion*, vol. 32, no. 1, pp. 340–347, March 2017.

[39] C. Manickam, G. R. Raman, G. P. Raman, S. I. Ganesan, and C. Nagamani, "A hybrid algorithm for tracking of gmpp based on p o and pso with reduced power oscillation in string inverters," *IEEE Transactions on Industrial Electronics*, vol. 63, no. 10, pp. 6097–6106, Oct 2016.

[40] J. P. Ram, D. S. Pillai, N. Rajasekar, and S. M. Strachan, "Detection and identification of global maximum power point operation in solar pv applications using a hybrid elpso-p o tracking technique," *IEEE Journal of Emerging and Selected Topics in Power Electronics*, pp. 1–1, 2019.

[41] N. Kumar, I. Hussain, B. Singh, and B. K. Panigrahi, "Mppt in dynamic condition of partially shaded pv system by using wode technique," *IEEE Transactions on Sustainable Energy*, vol. 8, no. 3, pp. 1204–1214, July 2017.

[42] M. Seyedmahmoudian, R. Rahmani, S. Mekhilef, A. Maung Than Oo, A. Stojcevski, T. K. Soon, and A. S. Ghandhari, "Simulation and hardware implementation of new maximum power point tracking technique for partially shaded pv system using hybrid depso method," *IEEE Transactions on Sustainable Energy*, vol. 6, no. 3, pp. 850–862, July 2015.

[43] J. Y. Shi, D. Y. Zhang, L. T. Ling, F. Xue, Y. J. Li, Z. J. Qin, and T. Yang, "Dual-algorithm maximum power point tracking control method for photovoltaic systems based on grey wolf optimization and golden-section optimization," *Journal of Power Electronics*, vol. 18, no. 3, pp. 841–852, 2018.

[44] D. S. Pillai, J. P. Ram, A. M. Y. M. Ghias, M. A. Mahmud, and N. Rajasekar, "An accurate, shade detection-based hybrid maximum power point tracking approach for pv systems," *IEEE Transactions on Power Electronics*, vol. 35, no. 6, pp. 6594–6608, 2020.

[45] A. Sangwongwanich, Y. Yang, F. Blaabjerg, and H. Wang, "Benchmarking of constant power generation strategies for single-phase grid-connected photovoltaic systems," *IEEE Transactions on Industry Applications*, vol. 54, no. 1, pp. 447–457, 2018.

[46] H. D. Tafti, G. Konstantinou, C. D. Townsend, G. G. Farivar, A. Sangwongwanich, Y. Yang, J. Pou, and F. Blaabjerg, "Extended functionalities of photovoltaic systems with flexible power point tracking: Recent advances," *IEEE Transactions on Power Electronics*, vol. 35, no. 9, pp. 9342–9356, 2020.

[47] M. Lasheen, A. K. Abdel Rahman, M. Abdel-Salam, and S. Ookawara, "Adaptive reference voltage-based mppt technique for pv applications," *IET Renewable Power Generation*, vol. 11, no. 5, pp. 715–722, 2017.

[48] Z. Zhan, J. Zhang, Y. Li, and H. S. Chung, "Adaptive particle swarm optimization," *IEEE Transactions on Systems, Man, and Cybernetics, Part B (Cybernetics)*, vol. 39, no. 6, pp. 1362–1381, Dec 2009.

[49] J. Liu, J. Li, J. Wu, and W. Zhou, "Global mppt algorithm with coordinated control of pso and inc for rooftop pv array," *The Journal of Engineering*, vol. 2017, no. 13, pp. 778–782, 2017.

[50] M. E. Başoğlu and B. Çakır, "Hybrid global maximum power point tracking approach for photovoltaic power optimisers," *IET Renewable Power Generation*, vol. 12, no. 8, pp. 875–882, 2018.

[51] K. Ishaque, Z. Salam, M. Amjad, and S. Mekhilef, "An improved particle swarm optimization (pso)–based mppt for pv with reduced steady-state oscillation," *IEEE Transactions on Power Electronics*, vol. 27, no. 8, pp. 3627–3638, Aug 2012.

[52] T. Sen, N. Pragallapati, V. Agarwal, and R. Kumar, "Global maximum power point tracking of pv arrays under partial shading conditions using a modified particle velocity-based pso technique," *IET Renewable Power Generation*, vol. 12, no. 5, pp. 555–564, 2018.

[53] L. Tang, W. Xu, and C. Mu, "Analysis for step-size optimisation on mppt algorithm for photovoltaic systems," *IET Power Electronics*, vol. 10, no. 13, pp. 1647–1654, 2017.

[54] C. Hua, Y. Fang, and W. Chen, "Hybrid maximum power point tracking method with variable step size for photovoltaic systems," *IET Renewable Power Generation*, vol. 10, no. 2, pp. 127–132, 2016.

[55] S. A. Abuzed, M. P. Foster, and D. A. Stone, "Variable pwm step-size for modified hill climbing mppt pv converter," in *7th IET International Conference on Power Electronics, Machines and Drives (PEMD 2014)*, April 2014, pp. 1–6.

[56] S. Selvakumar, M. Madhusmita, C. Koodalsamy, S. P. Simon, and Y. R. Sood, "High-speed maximum power point tracking module for pv systems," *IEEE Transactions on Industrial Electronics*, vol. 66, no. 2, pp. 1119–1129, Feb 2019.

[57] J. P. Ram, T. S. Babu, and N. Rajasekar, "A comprehensive review on solar pv maximum power point tracking techniques," *Renewable and Sustainable Energy Reviews*, vol. 67, pp. 826 – 847, 2017.

[58] K. S. Tey, S. Mekhilef, M. Seyedmahmoudian, B. Horan, A. T. Oo, and A. Stojcevski, "Improved differential evolution-based mppt algorithm using sepic for pv systems under partial shading conditions and load variation," *IEEE Transactions on Industrial Informatics*, vol. 14, no. 10, pp. 4322–4333, Oct 2018.

[59] T. K. Soon and S. Mekhilef, "A fast-converging mppt technique for photovoltaic system under fast-varying solar irradiation and load resistance," *IEEE Transactions on Industrial Informatics*, vol. 11, no. 1, pp. 176–186, Feb 2015.

[60] H. D. Tafti, A. Sangwongwanich, Y. Yang, J. Pou, G. Konstantinou, and F. Blaabjerg, "An adaptive control scheme for flexible power point tracking in photovoltaic systems," *IEEE Transactions on Power Electronics*, vol. 34, no. 6, pp. 5451–5463, 2019.

[61] R. Tanabe and A. Fukunaga, "Success-history based parameter adaptation for differential evolution," in *2013 IEEE Congress on Evolutionary Computation*, 2013, pp. 71–78.

[62] S. K. Kollimalla and M. K. Mishra, "Variable perturbation size adaptive p o mppt algorithm for sudden changes in irradiance," *IEEE Transactions on Sustainable Energy*, vol. 5, no. 3, pp. 718–728, July 2014.

[63] R. Ayop and C. W. Tan, "Design of boost converter based on maximum power point resistance for photovoltaic applications," *Solar Energy*, vol. 160, pp. 322 – 335, 2018.

[64] S. Mohanty, B. Subudhi, and P. K. Ray, "A grey wolf-assisted perturb observe mppt algorithm for a pv system," *IEEE Transactions on Energy Conversion*, vol. 32, no. 1, pp. 340–347, March 2017.

[65] D. K. Mathi and R. Chinthamalla, "Global maximum power point tracking technique based on adaptive salp swarm algorithm and p&o techniques for a pv string under partially shaded conditions," *Energy Sources, Part A: Recovery, Utilization, and Environmental Effects*, vol. 0, no. 0, pp. 1–18, 2020.

List of publications

International journal publications:

[1] D. K. Mathi and R. Chinthamalla, "**Enhanced leader adaptive velocity particle swarm optimisation based global maximum power point tracking technique for a PV string under partially shaded conditions**," in *IET Renewable Power Generation*, vol. 14, no. 2, pp. 243-253, 3 2 2020, doi: 10.1049/iet-rpg.2019.0575.

[2] D. K. Mathi and R. Chinthamalla, " **Global maximum power point tracking technique based on adaptive salp swarm algorithm and P&O techniques for a PV string under partially shaded conditions.**," in *Taylor & Francis; Energy Sources, Part A: Recovery, Utilization, and Environmental Effects*, 2020,doi: 10.1080/15567036.2020.1755391.

[3] D. K. Mathi and R. Chinthamalla, "**A hybrid global maximum power point tracking method based on butterfly particle swarm optimization and perturb and observe algorithms for a photovoltaic system under partially shaded conditions.**," in *Wiley International Transactions on Electrical Energy Systems*, vol. 30, no. 10, e12543, 2020,doi.org/10.1002/2050-7038. 12543.

[4] D. K. Mathi and R. Chinthamalla, " **A Hybrid Global Maximum Power Point Tracking of Partially Shaded PV System under Load Variation by Using Adaptive Salp Swarm and Differential Evolution – Perturb & Observe Technique.**," in *Taylor & Francis; Energy Sources, Part A: Recovery, Utilization, and Environmental Effects*, 2020, doi:10.1080/15567036.2020.1850927.

Journals communicated:

[1] D. K. Mathi and R. Chinthamalla, " **Optimal Performance of Hybrid Tracking Technique for Maximum and Flexible Power Point Tracking of Grid-Connected PV System Under Partially Shaded Conditions**," in *Solar Energy*.